Evaluating how Auto-reactive T cells Promote the Progression of Colorectal Cancer

By

Amanda Ann Thomson (BSc Hons)

This thesis is submitted to Cardiff University in fulfilment of the requirements for the Degree of Doctor of Philosophy in the School of Medicine.

September 2018

Declaration

This work has not been submitted in substance for any other degree or award at this or any other university or place of learning, nor is being submitted concurrently in candidature for any degree or other award.

Signed …… (candidate) Date ……

STATEMENT 1

This thesis is being submitted in partial fulfillment of the requirements for the degree of ……(insert MCh, MD, MPhil, PhD etc, as appropriate)

Signed …… (candidate) Date ……

STATEMENT 2

This thesis is the result of my own independent work/investigation, except where otherwise stated, and the thesis has not been edited by a third party beyond what is permitted by Cardiff University's Policy on the Use of Third Party Editors by Research Degree Students. Other sources are acknowledged by explicit references. The views expressed are my own.

Signed …… (candidate) Date ……

STATEMENT 3

I hereby give consent for my thesis, if accepted, to be available online in the University's Open Access repository and for inter-library loan, and for the title and summary to be made available to outside organisations.

Signed …… (candidate) Date ……

STATEMENT 4: PREVIOUSLY APPROVED BAR ON ACCESS

I hereby give consent for my thesis, if accepted, to be available online in the University's Open Access repository and for inter-library loans **after expiry of a bar on access previously approved by the Academic Standards & Quality Committee.**

Signed …… (candidate) Date ……

Table of Contents

Acknowledgements

This thesis is dedicated to Javier Uceda Fernandez
(1992- 2018)
A great friend, a wonderful scientist and the happiest person I've ever known.

I am eternally grateful to have been given the opportunity to carry out my PhD in the laboratory of Professor Andrew Godkin and Professor Awen Gallimore. They are extraordinary people and as a young scientist it has been a privilege to learn from them both. Without their on-going support, guidance and remarkable scientific knowledge the completion of this thesis would not have been possible. I would like to thank them both for the time they have invested in me. I'd especially like to thank Andy for his encouraging talks when things weren't quite going as planned – "oh you're a worrier" was the most often used phrase I think! I would also like to thank Awen for showing that she had confidence in me to complete this project and for reading my thesis chapters so quickly. It made the whole process of writing much easier. Leaving home for the first time to move to Cardiff was daunting but I am truly thankful to have joined such a supportive lab family with such wonderful supervisors. To all of the Godkin/Gallimore lab members – thank you for all your support and advice - you lot are the best!!

I'd also like to thank Professor Ann Ager for providing me with the opportunity as an undergraduate student to carry out a summer project in her laboratory here in Cardiff. With her guidance and kindness I began to find my feet as a scientist, got a taste for academia and I also met Awen! I will be forever grateful, as without Ann I may never have been given the chance to do this PhD.

To my amazing office mates and good friends: Martin, Gau, Lauder and Alex, I couldn't have asked for a better place to be for the last 4 years. Our bizarre silly chats and laughs over the Scottish phrases I use will never be forgotten. Nor will the encouraging chats, advice on experiments/data/writing and awesome office Christmas decorating days. In particular, I'd like to thank Martin for helping me from day one. Probably without even realising, you became a mentor to me and without you I'd still be sterile filtering the cells out of my media! Thank you.

I'd also like to give a special thank you to Michelle and Kath – You both are crucial to the day-to-day workings of this lab I couldn't have wished for better technicians to work with. I'm immensely grateful for your help.

I have been blessed to have such wonderful friends in Cardiff. Katie, you have been my rock and I am so lucky to have shared a house with my best friend. Also thank you for becoming an honorary lab member when needed!
Diana and Ellyn, thank you for your support and of course all of those cups of tea. Even when in different countries you both managed to give me encouragement and advice. Without the help from all three of you, both in and out of work, I wouldn't have been able to finish this PhD.
I'd also like to thank my other friends for the brilliant memories I've made here in Cardiff: Ariadni, Javier, Jade, Stefan, Vincent, Ana, and Emma. Without you my PhD journey wouldn't have been the same.

I'd like to thank my family for their support, both mentally and financially. To my mum and dad, I am truly thankful that you gave me the courage to move to Cardiff to do this PhD and that you believed in me even when I didn't believe in myself. I will always be grateful for having such loving and generous parents.
Finally, to my fiancé Richard, without your support I wouldn't be where I am today. Thank you for travelling the country to visit me, putting up with the regular weekend days in the lab and of course for building/fixing our lab equipment. I am so thankful that you are supportive of my career and I am truly blessed to have you in my life.

Summary

Substantial evidence has been generated demonstrating that the immune system is important for controlling tumour development. This includes colorectal cancer (CRC).

Current dogma states that patients capable of mounting anti-tumour immune responses have increased survival. As a result, therapies to enhance anti-tumour immune responses are an attractive treatment strategy for cancer patients. However, the long-term effect of generating such responses is not fully understood. Our laboratory has previously shown that an IFN-γ response towards the tumour antigen Carcinoembryonic antigen (CEA) is associated with tumour recurrence in CRC patients. In contrast, a 5T4 IFN-γ response provided a protective advantage. In this thesis, reasons to explain this observation were explored.

Firstly, anti-CEA IL-17A and dual IFN-γ/IL-17A responses were investigated to determine if high frequencies of IL-17A could potentially outweigh a beneficial IFN-γ response. Infiltration of $CD4^+$ T cell subsets into tumours from CEA responding and non-responding patients was also examined. Results revealed that CEA specific IL-17A responses were not up-regulated in CRC patients compared to healthy donors, nor were they increased compared to IL-17A 5T4 specific responses. $IL\text{-}17A^+$ $CD4^+$ T cell infiltration was also not increased within patients harbouring a CEA T cell response. However, infiltration of other T helper subsets was reduced. These data imply that IL-17A release is not responsible for early tumour recurrence. Results also suggest that tumours developing within CEA responding patients may be less immunogenic and hence more aggressive.

Investigations were also made to assess if a blood CEA T cell response was associated with increased intestinal permeability. Data obtained via Ussing chamber experiments suggests that a high magnitude CEA response is associated with reduced gut integrity in the right side of the colon. Further experiments are required, but it is possible that increased permeability could allow translocation of microbial products, leading to an inflammatory environment that could aid tumour development.

It's hoped that such findings will help to explain the potential long-term effects of generating anti-tumour immune responses. This knowledge would be beneficial when selecting targets for immunotherapy.

List of Abbreviations

Ag/AgCl	Silver/silver chloride
ALDH	Aldehyde dehydrogenase
AOM	Azoxymethane
AP	Adenoma patient
APC	Antigen presenting cell
APC gene	Adenomatous polyposis coli
CAC	Cancer associated cachexia
CD	Cluster of differentiation
CEA	Carcinoembryonic antigen
CFTR	Cystic fibrosis transmembrane conductance regulator
CRC	Colorectal cancer
CTLA-4	Cytotoxic T-lymphocyte antigen 4
DAMP	Danger associated molecular patterns
DC	Dendritic cell
DSS	Dextran sodium sulphate
EGFR	epithelial growth factor receptor
ELISpot	Enzyme linked immunosorbent spot assay
EMT	Epithelial-mesenchymal transition
ENaC	Epithelial soidum channel
FACS	Fluorescence activated cell sorting
FAP	Familial adenomatous polyposis
FITC	Fluorescein isothiocyanate
fMLP	N-formyl-L-methionyl-L-leucyl-L-phenylalanine
FMO	Fluorescence minus one
FoxP3	Forkhead box P3
FSC	Forward scatter
GI	Gastrointestinal
HA	Haemagglutinin
HLA	Human leukocyte antigen
HSC	Hematopoietic stem cell
IBD	Inflammatory bowel disease
IDO	Indoleamine 2,3-dioxygenase
IFN-γ	Interferon-gamma
IL	Interleukin
IPEX	Immunodysregulation polyendocrinopathy enteropathy X-linked
Isc	Short circuit current
JAM-A	Junction adhesion molecule A
LAG-3	Lymphocyte activation gene
LN	Lymph node
LPS	Lipopolysaccharide
mAB	Monoclonal antibody
MAGE	Melanoma-associated antigen
MCA	Methylcholanthrene
MHC	Major histocompatibility complex
MMR	Miss match repair
MSI	Microsatellite instability
mTEC	Medullary thymic epithelial cells
MVA	Modified Vaccinia Virus Ankara
NBFS	Neutral buffer formalin solution
NSAID	Non-steroidal anti-inflammatory drugs
OS	Overall survival
PBMC	Peripheral blood mononuclear cell

PD	Potential difference
PFS	Progression free survival
PGE2	Prostaglandin E2
PHA	Phytohaemagglutinin
PMA	Phorbol Myristate Acetate
PP	Peptide pool
PPD	Purified protein derivative
PRR	Pattern recognition receptor
pTreg	Peripheral Treg
R	Resistance
RAG	Recombinant activating gene
SAA-1	Serum Amyloid A1
SFB	Segmented filamentous bacteria
SFC	Spot forming cell
SSC	Side scatter
STAT	Signal transducer and activator of transcription
TAA	Tumour associated antigen
TaCTiCC	Trovax and cyclophopsphamide treatment in colorectal cancer
TAM	Tumour associated macrophage
TAP-1	Transporter associated with Antigen Processing 1
Tg	Transgenic
TGF-β	Transforming growth factor beta
Th	T helper
TIL	Tumour infiltrating lymphocyte
TNF-α	Tumour necrosis factor-alpha
TRA	Tissue restricted antigen
Treg	T regulatory cell
TSA	Tumour specific antigen
TSLP	Thymic stromal lymphopoietin
tTreg	Thymic Treg
VEGF	Vascular endothelial growth factor
VELIPI	Vascular emboli, lymphatic invasion, and perineural invasion
WT	Wild type
ZO	Zonula occludens

List of Figures

List of Tables

Chapter 1. General Introduction

1.1 The gastrointestinal tract

The gastrointestinal (GI) tract is a hollow muscular tube. It starts at the oral cavity, continuing through the oesophagus, stomach, intestines and rectum to the anus, where waste is then expelled. The function of the GI tract is to absorb nutrients from the breakdown of food, with many organs including salivary glands, the pancreas and liver providing enzymes to aid digestion. Intake of food however makes it possible for exogenous organisms such as bacteria, fungi and viruses to also enter. In particular, microorganisms that symbiotically inhabit the intestine are termed the microbiota. They do not simply reside within the gut but rather can be beneficial to the host. Microbiota are capable of digesting fibre to generate short chain fatty acids (SCFA), which the host can use as an energy source (1). Moreover, they can synthesise vitamin B and K as well as metabolise bile acids derived from the liver (2-4). The microbiota can also influence host immunity through interactions with immune cells or by producing various metabolites. This host–microbiota relationship within the intestine is highly regulated by various mechanisms to maintain a healthy gut. Accordingly, examining dysregulation of this system and its impact on intestinal disease is a rapidly expanding field.

1.1.1 Intestinal Epithelial cells

Intestinal epithelial cells lie between the microbiota and the host, creating an important physical barrier. As well as being necessary to provide water and nutrient absorption, epithelial cells have two major roles to maintain gut health in relation to the microbiota: “segregation” and “mediation”. Segregation is defined as the separation of host cells in the lamina propria from the microbiota, while mediation describes the transmission of signals from the gut microbiota to

immune cells (5). Cytokine or chemokine signalling can induce immune responses or deliver antigens to antigen presenting cells (APCs) to promote tolerance (discussed later within this Chapter). However, the structure of epithelial cells themselves is critical for creating a barrier to maintain healthy intestinal function.

1.1.1.1 Tight Junctions

Tight junction (TJ) protein complexes link intestinal epithelial cells, sealing the paracellular space to regulate the permeability of ions, solutes and separate the microbiota from the host (Figure 1.1). Structurally, the TJ is composed of proteinaceous filaments termed “strands”, spanning the extracellular space to interact with adjacent cells. Crucially, the “tightness” of the TJ is determined by the protein composition within the strands themselves and not only by strand number. Farquhar and Palade first encapsulated the ultrastructure of the TJ in a seminal paper in 1963 (6). However, it was not until 1986 that the first TJ protein zonula occludens-1 (ZO-1) was identified by immune-electron microscopy (7). This was followed by the discovery of other peripheral “scaffolding” membrane proteins ZO-2 and ZO-3 that engage with actin filaments of the cell cytoskeleton (8). Interacting with ZO-1, the first transmembrane protein to be discovered was occludin, a member of the Tight Junction-Associated Marvel domain-containing protein (TAMP) family (9). *In vitro* work revealed that overexpression of occludin reduced paracellular permeability in Madin-Darby canine kidney cell lines. Meanwhile transfer of a terminally truncated occludin resulted in increased paracellular leakage of small molecule tracers (10). However, occludin deficient mice had normal levels of intestinal paracellular permeability compared to experimental controls. This indicated that other TJ proteins are present to maintain TJ structure and function.

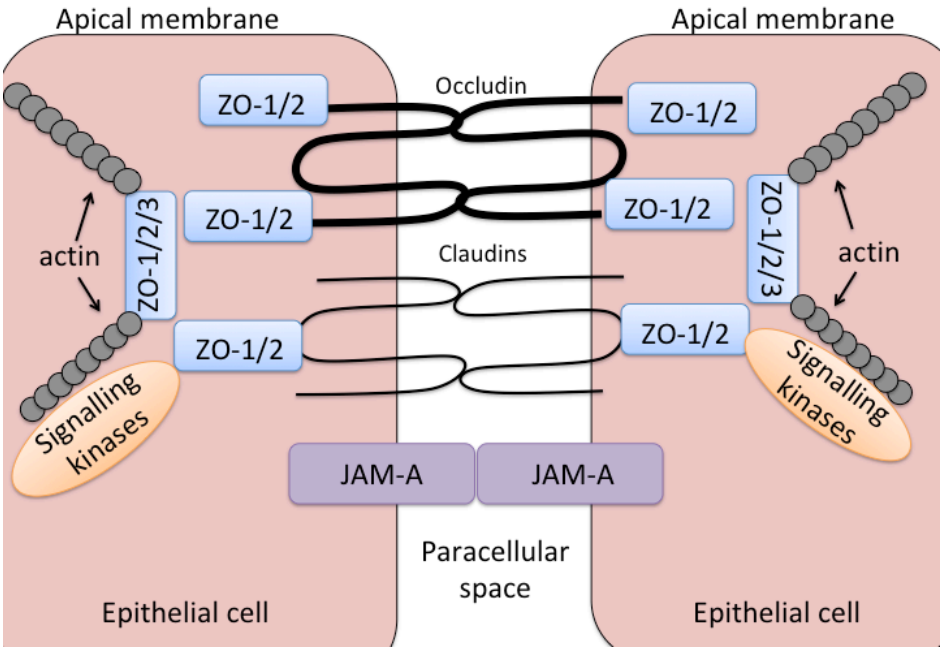

Figure 1.1 Structure of the TJ found between epithelial cells.
TJ strands are composed of various claudins, occludin and JAM proteins. This seals the paracellular space by associating with scaffolding proteins ZO-1/2/3 which are connected to the cell cytoskeleton.

1.1.1.2 Claudin molecules

Many studies have emphasised the importance of the large claudin family of TJ transmembrane proteins, which share no sequence homology with the TAMP family. There are twenty-seven known members of the claudin family (11), with morphological and functional studies proving that they are critical for effective barrier formation (12). Claudins are capable of forming pores within the TJ strand structure but also regulate strand number and complexity (13, 14). Moreover they are important for transmitting actomyosin tension across the TJ (15). In cells that naturally lack TJs, such as fibroblasts, Furuse and colleagues demonstrated that claudins are sufficient to reconstitute strand-like networks between cells. (13). In context with this, it is now thought that TJ structures undergo continuous remodelling in response to extracellular signals and stimuli, with claudin switching playing a key role (16).

Paracellular passage, between epithelial cells, can be classified by two mechanisms termed the “pore” and “leak” pathways (Figure 1.2). The leak pathway allows flux of large molecules in a non-selective manner. In contrast, the pore pathway is charge and size selective, allowing passage of small ions and uncharged molecules across the TJ. Studies show that claudins can function as paracellular pores and generally can be classified into two categories: “Tight” sealing claudins or “leaky” pore forming claudins. For example, claudin-2 was the first claudin found to increase permeability, by mediating selective passage of the cations Na^+ and K^+ as well as water (12). After stimulation of epithelial cells with inflammatory cytokines such as TNF-α and within inflammatory bowel disease (IBD) patients, claudin-2 is highly upregulated within the intestine (17). As a result, permeability to cations is increased, causing diarrhoea in patients. In contrast, claudin-1, which is widely expressed in the intestine, is known for its barrier-forming ability, reducing ionic passage along with claudin-3 and 4 (14). Expression of claudin-3 is higher within colonic epithelium compared the rest of the intestine (18). This is a common feature of claudin molecules, with distinct areas of the intestinal tract expressing various claudin proteins at different levels (Table 1) (19). Further to this, a crypt-lumen distribution of claudins has been identified. Claudins 2, 10 and 15 localise to the crypt base while claudins 3, 4, 7 and 8 are expressed on luminal epithelial cells (19). An alteration to claudin composition not only allows passage of ions but can also permit the translocation of bacterial products. Tsukita and colleagues investigated the role of claudin-7 in a conditional knockout mouse model. Results showed that claudin-7 deficiency allows for enhanced paracellular flux of the bacterial product N-formyl-L-methionyl-L-leucyl-L-phenylalanine (fMLP) (20). fMLP is released by intestinal bacteria and is a major chemotactic product known to drive intestinal inflammation. Transportation of

fMLP usually occurs transcellularly via the PepT1 receptor on colonic epithelial cells, a receptor that is abnormally over-expressed in IBD patients (21, 22). However, claudin-7 deficient mice have revealed it is possible for fMLP to translocate via the paracellular route, even when all other TJ proteins are present (20). This demonstrates a key function of claudin molecules within the TJ.

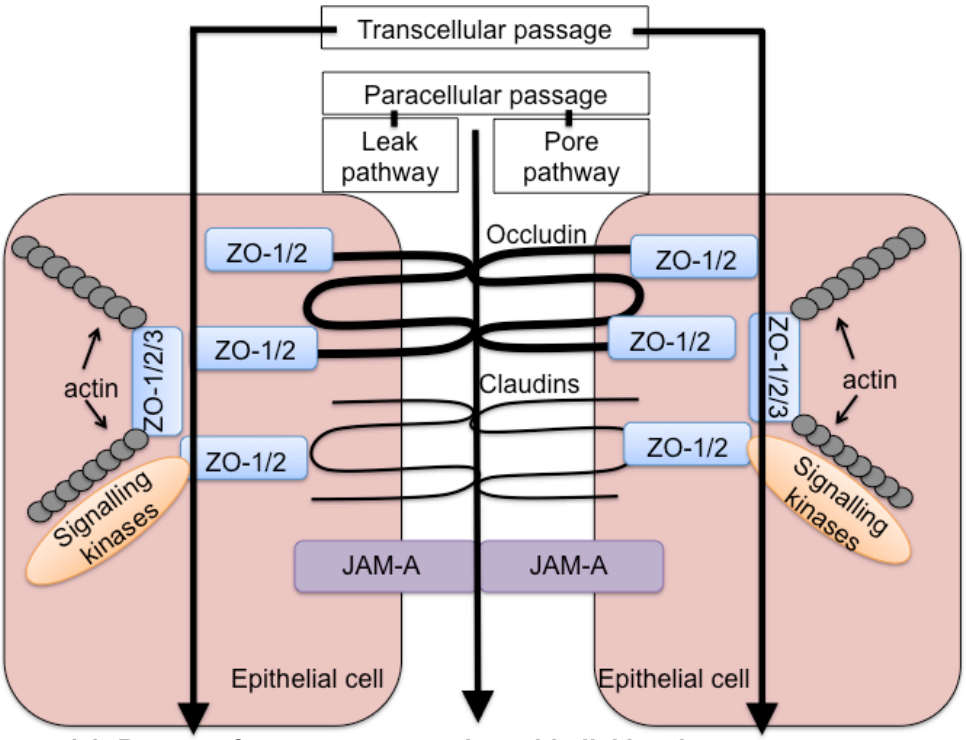

Figure 1.2. Routes of passage across the epithelial barrier
Paracellular passage describes the movement of substances between epithelial cells and is composed of pore and leak pathways. Transcellular passage describes the movement of molecules through the cell itself.

Table 1. Claudin expression in mammalian intestine

Intestinal Segment	**Claudin expression**
Duodenum	1, 2, 3, 4, 5, 7, 12, 15
Jejunum	1, 2, 7, 2, 15
Ileum	2, 7, 8, 12, 15
Large intestine	1, 3, 4, 7, 8, 12, 15

Adapted from Lu *et al.* (2013) and Garcia-Hernandez *et al.* (2017) (19, 23)

1.1.1.3 Junction Adhesion Molecules

Junction Adhesion Molecules (JAM) are another component of the TJ structure, belonging to the Ig superfamily. The JAM family consists mainly of three closely related proteins: JAM-A, B and C, which are widely expressed in many cell types. This includes neutrophils and monocytes as well as endothelial and epithelial cells (24). Current evidence indicates that mucosal epithelial cells of the intestine mostly express JAM-A, which is directly involved in TJ formation and maintenance (25). JAM-A has a key role in facilitating the recruitment of scaffolding proteins ZO-1, 2 and 3 and aids in the assembly of the TJ structure (26). Even though not directly involved in TJ strand formation, JAM-A depletion still results in increased permeability within human epithelial cell monolayers (25). This finding has been validated in JAM-A deficient mice, showing increased in paracellular flux of the 4 kD FITC dextran probe compared to wild type animals (27). In addition, JAM-A deficient mice are more susceptible to Dextran Sodium Sulfate (DSS)-induced colitis compared to controls. This indicates that JAM-A depletion facilitates at least in part the development of inflammatory conditions through the induction of a “leaky” mucosal barrier. Loss of JAM-A has also been implicated in the up-regulation of specific claudin molecules such as claudin-5 and claudin-10, suggesting that JAM-A can further regulate the molecular composition of the TJ and hence impact the permeability of small molecules (27, 28).

The proteins mentioned, as well as others, play key roles in the formation of the TJ structure to maintain close contact between individual epithelial cells. Therefore, it is easy to see that loss or change in function of such molecules can have detrimental effects on the integrity of the intestinal barrier.

1.1.1.4 Electrolyte transport

Intestinal epithelial cells have the major role of absorbing nutrients, including sugars, salt (NaCl) and water. This is achieved as epithelial cells are polarised structures, having a sophisticated system of ion pumps, channels and transporters at apical and basolateral epithelial membranes. Na^+ absorption is in fact the driving force for all other ionic movements across the cell. Na^+ absorption occurs by electroneutral transport via Na^+/H^+ exchangers (NHE) on the apical membrane (29). However, electrogenic Na^+ absorption via specific channels, such as ENaC channels, at the apical surface also takes place. Such channels allow Na^+ to diffuse down a concentration gradient into epithelial cells. At the baslolateral membrane active transport of Na^+ ions out of the cell is mediated by the electrogenic Na^+, K^+-ATPase pump. Each pump cycle results in the extrusion of three Na^+ ions in exchange for the basolateral uptake of two K^+ ions. This results in the net transfer of one positively charged Na^+ ion across the basolateral membrane (30). The movement of Na^+ alters the osmolarity of the extra cellular fluid, resulting in water accompanying the flow of Na^+ across the epithelial barrier into the body. Also present are channels to dissipate the K^+ uptake by the ATPase pump to maintain the membrane potential.

Cl^- movement across epithelial cells occurs in a passive manner. However, it can also occur by electroneutral pathways involving Na^+/H^+ and Cl^-/HCO_3^- exchange at the apical surface. A key Cl^- channel is the CFTR receptor, which is responsible for secreting Cl^- across the apical membrane (29). The CFTR is mutated within cystic fibrosis patients. This leads to insufficient Cl^- secretion, the development of thick intestinal mucus and an inability to properly absorb nutrients across the gut (31). Alterations in Cl^- secretion are also associated with excessive diarrhoea, such as that seen during cholera infection (32).

Transporters to absorb nutrients have also been identified and can utilise the mechanisms of Na^+ absorption. In particular SGLT1 located on the apical membrane is responsible for glucose and galactose uptake from the lumen. SGLT1 is electrogenic and uses the Na^+ gradient to transport Na^+ and sugar in a 2:1 ratio against a sugar gradient into the cell. Studies show that GLUT2, present on the basolateral membrane then facilitates movement of the sugars into the interstitium (33). Another key transporter identified is the monocarboxylate transporter 1 (MCT1). It functions as an H^+-coupled electro-neutral transporter and aids in the absorption of SCFAs. This includes butyrate and propionate, the products of bacterial fermentation, which the host can use as an energy source (29).

Studies investigating ionic movements have clearly demonstrated that efficient and continuous ionic transportation across epithelial cells is key to maintaining a healthy intestinal environment.

1.1.2 Mucus layer

Aside from TJs other physical barriers exist within the intestine to segregate the microbiota. The mucus layer and the glycocalyx, a meshwork of carbohydrate glycolipids able to trap organisms, form on top of intestinal epithelial cells (Figure 1.1). A study by J*ohansson* and colleagues shows that the mucus layer in the large intestine, produced by goblet cells, is extremely thick compared to the small intestine. Most likely this is in defence of the vast quantity of intestinal bacteria (~10^{13}) that reside within the colon (34). The mucus layer extends approximately 150μm above intestinal epithelial cells and is composed of an innermost firm layer and a looser outer layer. Identified by composite agarose-PAGE (AgPAGE) the major component of both layers was found to be the highly O-glycosylated mucin protein MUC-2, which forms gel-like structures (34). The

inner mucus layer is a stratified layer containing polymerised MUC-2 and is anchored to epithelial cells, efficiently excluding bacteria. Accordingly, it was found that MUC-2 deficient mice have bacteria in direct contact with epithelial cells (34). Proteolytic cleavage of MUC-2 results in a less condensed outer mucus layer, which is inhabited by intestinal microbes. It has been shown that the microbiota can use MUC-2 as an energy source. However, in the absence of dietary fibre numbers of mucin-degrading bacterial species increase, resulting in inner mucus layer degradation and risk of mucosal invasion (35).

1.1.3 Chemical barriers

Epithelial cells also provide a chemical barrier against microbial invasion (Figure 1.3). In the small intestine, paneth cells are able to secrete anti-microbial peptides such as defensins and cathelicidins (36). Both are capable of interacting with the negatively charged microbial cell membrane and cause damage by creating pore-like holes (37). In conjunction with this, epithelial cells secrete immunoglobulin A (IgA). IgA is the most abundant antibody within mucosal secretions and is released in a dimeric form (dIgA). dIgA is produced by plasma cells within lymphoid tissue and then trancytosed across epithelial cells, mediated by the polymeric immunoglobulin receptor (pIgR) (38). pIgR binds dIgA at the basolateral membrane of the epithelial cell and the complex is then displayed at the apical surface. Subsequently the complex undergoes proteolytic cleavage, resulting in secretion of dIgA at the mucosal surface. Secretory IgA (sIgA) is able to bind bacterial epitopes, preventing commensal bacteria from adhering to the mucosal surface. A small pIgR derived polypeptide remains within the sIgA structure after cleavage. Termed the secretory component it maintains stability of the antibody and helps anchor sIgA to the mucus layer. Furthermore, sIgA can inhibit microbial motility via unspecific

binding of bacteria through the presence of sticky glycan molecules. sIgA is able to neutralise pathogens not only within the lumen but also within intestinal epithelial cells themselves. Moreover, it can carry out its functions without activating complement, thus preventing any untoward inflammation within the gut (39). Antimicrobial peptides and IgA are thought to be extremely important in preventing invasion at the mucosal surface. However, within the large intestine there are no paneth cells present, therefore no anti-microbial peptides are produced. Recently, a study by Okumura *et al.* identified the molecule Lypd8 in the mouse colon (40). It was shown that this highly glycosylated protein is expressed in epithelial cells at the uppermost layer of the large intestinal gland and is secreted into the intestinal lumen. Lypd8 preferentially bound to flagellated bacteria, including those from the *Proteus*, *Helicobacter* and *Escherichia* genera. This binding inhibited bacterial motility and prevented invasion of the inner mucus layer (40). In the human colon Lypd8 was also present, however expression was reduced within samples obtained from IBD patients (40). *Proteus* and *Helicobacter* have both been associated with IBD pathogenesis (41-43). In relation to this, it was found that Lypd8 -/- mice had increased numbers of these bacteria invading the inner mucus layer and intestinal crypts of the large intestine. Furthermore Lypd8 -/- mice also had an amplified susceptibility to dextran sodium sulphate (DSS) induced inflammation (40). This data indicates that Lypd8 is important for segregation of intestinal bacteria within the colon to preserve gut homeostasis. Furthermore, loss of Lypd8 may be important within intestinal disease.

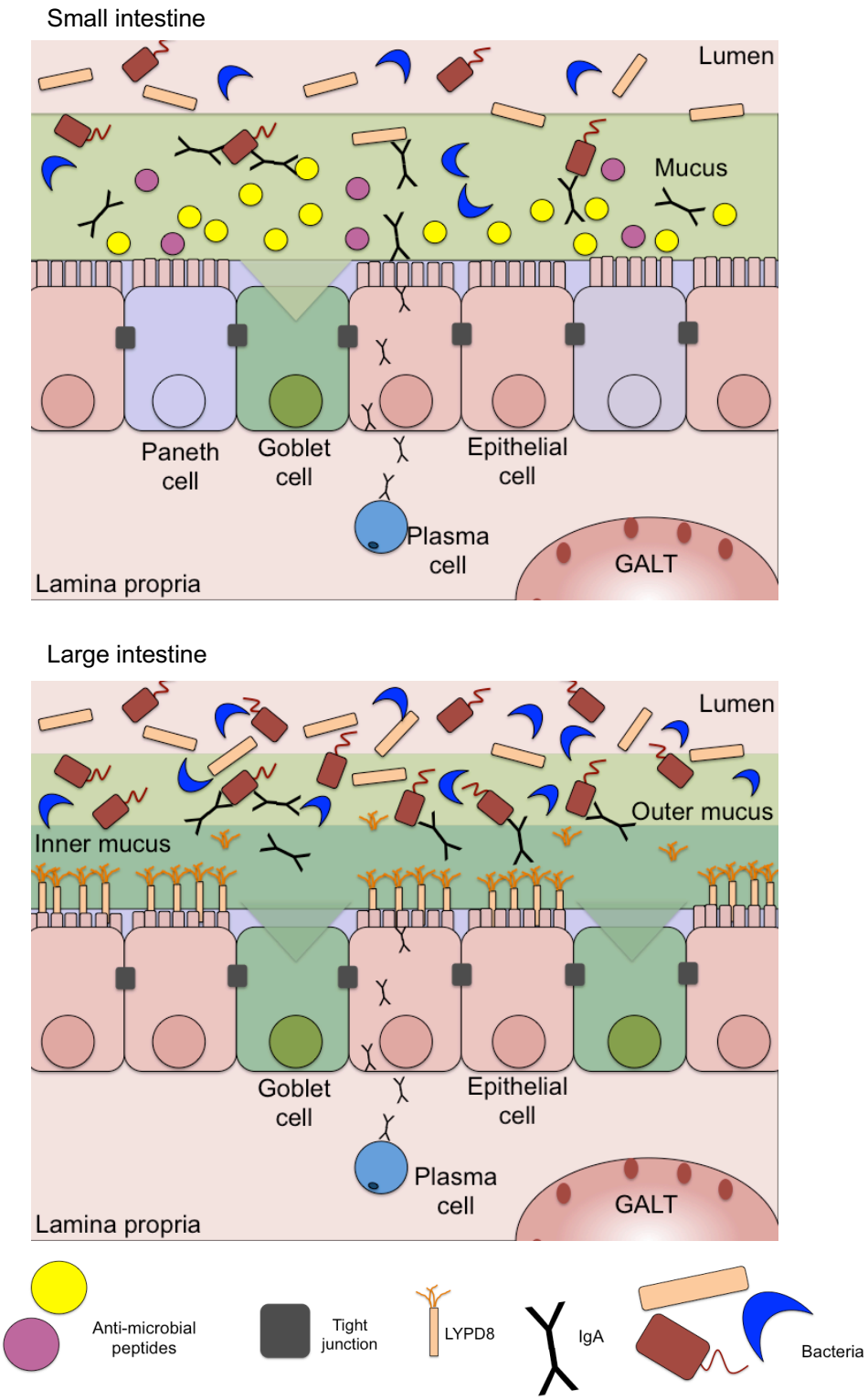

Figure 1.3 Representative diagram of the epithelial layer of the small and large intestine.
Epithelial cells form a barrier between the microbiota within the lumen and the lamina propria, joined together by tight junctions (TJs). Mucus layers are present to prevent bacterial invasion alongside the secretion of anti-microbial peptides and IgA. IgA is released from plasma cells that differentiate in gut associated lymphoid tissue (GALT) before travelling to the lamina propria. Lypd8 secretion occurs in the large intestine.

1.2 Immune responses

All leukocytes arise from hematopoietic stem cells (HSCs) residing within the bone marrow. Various growth factors such as IL-2, IL-4, GM-CSF and flt3 ligand are produced to support HSC differentiation into downstream lineages by bone marrow stromal cells. This includes cells of the innate arm of the immune system such as macrophages, neutrophils, eosinophils, basophils and dendritic cells. During pathogen invasion innate cells respond first, recognising foreign antigens in a non-specific manner via pattern recognition receptors (PRRs). Receptors such as TLRs or C-type lectins can recognise conserved features of foreign pathogens such as lipoteichoic acid on the cell wall of Gram-positive bacteria, LPS on the membrane of Gram-negative bacteria, flagellin, double stranded RNA or β-glucans found within fungal cell walls. Furthermore, molecules released by stressed or necrotic cells such as HMGB1 and IL-33 can trigger activation of innate cells via danger associated molecular pattern receptors (DAMPs). Activation of innate cells results in pathogens being engulfed and destroyed by the release of toxic chemicals (superoxide) and degradative enzymes (lysozyme).

Following initiation of the innate response an adaptive immune response is generated. This is a delayed but specific response, produced by T and B lymphocytes. Like innate cells, B cells develop within the bone marrow. However, T cell pre-cursors migrate from the bone marrow to mature within the thymus before being released into the circulation.

1.2.1 T cell development in thymus

It was work carried out by Miller and colleagues in the 1960s that first suggested that the thymus supported T cell development. Early studies showed that mice without a thymus from the time of birth were susceptible to infection, had

atrophic lymphoid structures and had low levels of circulating lymphocytes (44). Furthermore, Miller demonstrated that foreign skin grafts from rats were able to survive within athymic mice, while wild type mice showed rejection (44). Also observed was that removal of the thymus was associated with a marked reduction in the number of lymphocytes in lymphoid tissues. However, numbers were not as reduced in areas where antibody formation usually occurred. This led to investigations demonstrating that two distinct and separate lymphocyte lineages existed, one derived from the thymus: the T cell, and one responsible for antibody production: the B cell.

Mechanisms behind thymic T cell development are now better understood and have shown that education of T cells within the thymus is critical for the development of central tolerance. Reported by Owen *et al.*, lymphoid progenitor cells seed the thymus as early as embryonic day (ED) 11.5 in mice (45) and by the eighth week of gestation within humans (46). T cell precursor entry to the thymus initially occurs in a vasculature independent manner during embryogenesis, with CCL21 and CCL25 having a role. In plt/plt mice that naturally lack CCL21 and within CCR7 (the receptor for CCL21) deficient mice, numbers of thymocytes were lower compared to normal mice until ED 14.5 (47). Furthermore, mice deficient in CCR9, the receptor for CCL25 had a 3-fold decrease in the number of thymocytes until ED 17.5 (48). In the postnatal thymus progenitor cells are located in an area harbouring a well-developed blood supply, close to the medullary junction. This indicates that cells can transmigrate from the vasculature system into the thymus. Studies report this migration is regulated by the adhesive interaction of PSGL1 expressed on progenitor cells and P-selectin expressed by thymic endothelium (49).

Once in the thymus progenitor cells undergo development into T cells, however approximately only 1-3% of all thymocytes succeed survival and export into the circulation (50, 51). Upon entry thymocytes migrate to the outer subscapsular zone of the thymic cortex and generate a random TCR via VDJ recombination. It is thought that at this stage T cells commit to being an αβ or γδ T cell (52). Both T cell types are present within vertebrates but have key differences. γδ cells, unlike αβ T cells are located primarily at epithelial surfaces and are able to recognize and respond to a broad range of antigens. This includes non-classical MHC molecules, heat shock proteins, and lipids (52). In contrast, αβ T cells recognise antigens via classical MHC/peptide complexes and are found primarily within lymphoid tissue. Within the subcapsular zone of the thymus αβ T cells will also up-regulate the co-stimulatory molecules CD4 and CD8, to become double positive (DP) cells. DP cells will undergo a process of positive selection with cortical thymic epithelial cells expressing MHC/peptide complexes. Thymocytes able to recognise the MHC/peptide complex are provided with survival signals such Psmb11 and cathepsin, for the selection of $CD8^+$ and $CD4^+$ cells respectively (53, 54). The now single positive (SP) thymocytes undergo a process of negative selection within the thymic medulla, migrating there via CCR7 and CCL21/CCL19 chemokine interactions. Here $CD4^+$ and $CD8^+$ T cells interact with APCs such as medullary thymic epithelial cells (mTECs) and dendritic cells, leading to the deletion of auto-reactive T cells. mTECs are able to express many tissue restricted antigens (TRA), allowing for the deletion of T cells that are specific for antigens found within the periphery. Anderson and colleagues showed that expression of TRAs is regulated by the transcription factor Aire within mTECs. Insulin and casein are prime TRA examples (55). Aire deficient mice have an autoimmune phenotype with autoantibody production and inflammatory cell infiltration into multiple tissues (55). This is also seen within human Aire deficiency, which results in

autoimmune polyendocrinopathy syndrome type 1 (APS-1) (56). Another transcription factor, Fezf2, has been identified as a regulator of TRA expression (57). mTECs can be classified into $mTEC^{hi}$ and $mTEC^{lo}$ based on expression of MHC class II and CD80. It was found that approximately 30-40% of mTECs are $mTEC^{hi}$ and express Aire. Meanwhile 40-50% of mTECs are $mTEC^{lo}$, expressing Fezf2 and are Aire negative (58). A Fezf2 conditional knockout model showed upregulation of CCL2, secretion of autoantibodies and an increased number of activated T cells in secondary lymphoid organs. In addition, as with Aire deficiency, cellular infiltration into tissues was increased. However, the spectrum of autoimmunity did vary from Aire deficient mice, indicating that Fezf2 and Aire regulate different TRAs (58). This leads to deletion of different auto-reactive T cells and an altered autoimmune phenotype.

Once educated, mature thymocytes must leave the medulla and enter the circulation. Egress from the adult thymus requires the sphingosine-1-phosphate receptor 1 (SIP_1). This receptor is expressed by mature thymocytes and binds to the high concentration of circulating S1P in serum (59). Due to thymic education T cells now in circulation are governed by central tolerance to prevent auto-reactivity and autoimmunity.

The co-receptors CD4 and CD8 distinguish T helper and cytotoxic T cells, respectively. Cytotoxic T cells can kill their target in a cell-to-cell contact manner through the release of enzymes such as granzyme B and perforin. They are activated through the recognition of peptide/MHC class I on APCs. Helper $CD4^+$ T cells recognise peptide/MHC class II complexes. They coordinate the immune response through supporting cytotoxic T cell responses, macrophage activation, and aiding B cells to produce antibody. There are many different subtypes of $CD4^+$ T cells with Th1 and Th2 being the first identified. However, regulatory T

cells (Tregs), Th22, Th9, T follicular helper and Th17 cells have subsequently been discovered; all of which have various functions in order to maintain a broad response to infection and disease. Th1, Th17 and Treg cells are thought to be relevant to colorectal cancer, the disease focused on within this thesis.

1.3 T helper cell subsets

1.3.1 Th1 cells

It was formally shown in 1986 that mouse $CD4^+$ cells could be subdivided into two subsets, designated Th1 and Th2 on the basis of their pattern of cytokine production (60). This was made possible due to technical advances within the field; the ability to clone T cells and the development of cytokine assays. Mossman and Coffman were able to investigate the cytokine production of a stable panel of T cell clones, observing that cells stimulated with antigen could produce IL-2, IFN-γ, GM-CSF and IL-3. These cells are now known as Th1 cells which can also produce TNF-α and lymphotoxin-α (LT-α) to potentiate their effector functions (61). In contrast Th2 cells produce IL-4 and IL-5 (60). It was also noticed that Th1 and Th2 cells were associated with different classes of antibody production. Th2 cells enhance IgE synthesis while Th1 cells promote IgG2a release. This was in keeping with the finding that IL-4 controls class switching to IgE, and IFN-γ controls switching to IgG2a (62).

In the early 1990s the group of Romagnani identified Th1 and Th2 cells within human peripheral blood (63). This was achieved using large panels of $CD4^+$ T cell clones, specific for the intracellular bacterium *Mycobacterium tuberculosis* and for the extracellular helminth *Toxacara canis*. It was observed that *M.tuberculosis* mostly stimulated IFN-γ production while *Toxocara* clones were mainly IL-4/IL-5 producers (63).

1.3.1.2 Th1 cell development

Bacterial antigens drive dendritic cells and macrophages to produce IL-12, which is the key cytokine required to drive Th1 cell development. IL-12 stimulation promotes Th1 cell activation and expansion through transcription factors STAT-1 and STAT-4, required to induce the transcription factor T-bet (TBX21 in humans). T-bet is essential as it binds to the IFN-γ promoter to induce its secretion. On the other hand IL-4 is required to promote Th2 expansion through activation of the transcription factors STAT-6 and GATA-3.

1.3.1.3 Th1 cells in disease

Uncontrolled Th1 responses have been associated with many inflammatory diseases such as rheumatoid arthritis, multiple sclerosis and IBD. The hallmark of Th1 cell infiltration is increased levels of IFN-γ, as well as TNF-α, seen within all the aforementioned conditions. Treatments to reduce Th1 associated immunity have proved beneficial in some cases, such as anti-TNF-α, which can reduce inflammation in IBD. However, recent studies have revealed that the Th17 subtype of $CD4^+$ T cells also contribute to the pathogenesis of such diseases, inducing inflammation and autoimmunity alongside Th1 cells.

1.3.2 Th17 cells

Prior to the discovery of Th17 cells, studies had already suggested a role for the Th17 associated cytokine IL-17A, first described by Rouvier et al. (64), within inflammatory conditions. *In vitro* work demonstrated that IL-17A was associated with IL-8 secretion to recruit neutrophils to sites of inflammation. IL-17A deficient mice also showed resistance to the development of inflammatory arthritis (65). In 2005 Park and colleagues first described $CD4^+$ Th17 cells within mice, observing that they are capable of producing IL-17A (66). Further studies have

shown Th17 cells can also secrete IL-17F, IL-21 and IL-22. However, IL-17A is the most well studied Th17 associated cytokine. IL-17A is mainly produced by activated Th17 cells but can also be produced by γδ, NK T cells and ILC3s. Binding of IL-17A to its receptor, which is found on many cell types including neutrophils, macrophages and non-haematopoietic cells such as fibroblasts and epithelial cells, stimulates the transcription factor TRAF6 via the adapter protein ACT-1. This leads to the activation of NFκB and MAPK pathways. This results in increased activation of macrophages and endothelial cells to produce mediators such as IL-6, IL-8, TNF-α, IL-1β, GM-CSF, PGE2, nitric oxide and matrix metalloproteinases. Other important roles of IL-17A include the recruitment of granulocytes, upregulation of chemokine receptors and aiding in T cell proliferation (67) (68).

IL-17A secretion by Th17 cells is strongly induced by IL-23, which is released by macrophages and dendritic cells. IL-23 shares a subunit, called p40, with the Th1 promoting cytokine IL-12. *In vivo* studies demonstrated that IL-23 was important for the development of autoimmune brain inflammation within experimental autoimmune encephalomyelitis (EAE), the mouse model of multiple sclerosis (69). Until this discovery in 2003 it had been assumed that IL-12 and Th1 development was the main driver of this disease. To determine the involvement of IL-23, Cau and colleagues used a series of genetically modified mice: $p19^{-/-}$ mice that lack IL-23, $p35^{-/-}$ mice that lack IL-12 and $p40^{-/-}$ mice that lack both cytokines. It was found that only mice lacking both IL-23 and IL-12 were resistant to EAE development (69). Control animals showed that $p19^{+/-}$ mice and $p35^{-/-}$ mice had concentrated cellular infiltration of the spinal cord but this was not detected when IL-23 was absent, shown in $p19^{-/-}$ and $p40^{-/-}$ animals. The group also demonstrated that gene transfer of IL-23 into the CNS of $p19^{-/-}$

and p40$^{-/-}$ mice reconstituted EAE. Furthermore, by administering IL-12 and IL-23 to p40$^{-/-}$ mice it was observed that IL-12 alone was not sufficient to stimulate disease. However, IL-12 followed by IL-23 gave intense EAE comparable to that seen within WT control mice (69). This data provided evidence to show that IL-23 and not IL-12 signalling was key to EAE development. As IL-23 was associated with IL-17A producing cells such findings at the time supported the idea that a subset of T cells existed with particular IL-17A secreting functions.

1.3.2.1 Th17 cell maintenance

Reports show that IL-6, IL-21 and low doses of transforming growth factor-β (TGF-β) are required for the differentiation of naive T cells into Th17 cells (70). Up-regulation of the transcription factors STAT-3 and RORγt are also essential. RORC is the homologue for RORγt in humans. Yang and colleagues demonstrated the importance of STAT-3 using a cre-recombinase STAT-3 KO mouse, developed as STAT-3 knockdown is embryonically lethal (71). Investigations demonstrated that upon stimulation of STAT-3 deficient CD4^{+} cells, surrounded by a cocktail of Th17 promoting cytokines, RORγt expression and IL-17A secretion were reduced. Furthermore STAT-3 was required for up-regulation of the IL-23 receptor on Th17 cells, important for stabilisation of Th17 cells (71). In another study, Ivanov *et al.* showed that RORγt drives cytokine release from Th17 cells. Using RORγt deficient mice it was observed that IL-17A production from CD4^{+} T cells was drastically reduced compared to WT animals (72).

Th17 cells and Th1 cells express different chemokine receptors. Th1 cells circulate lymphoid tissues and gain entry into sites of inflammation, with CXCR3 and CCR5 being the main chemokine receptors expressed. CXCR3 and CCR5 bind a variety of chemokines such as CXCL9, CXCL10, CXCL11

and CCL3, CCL4 and CCL5, respectively. However, Th17 cells primarily home to mucosal sites such as the gut and skin, through expression of the chemokine receptor CCR6 that binds to CCL20 (73). One function of IL-17A is to promote chemokine expression, guiding Th17 cells to the intestine where there is a multitude of pathogens. This associates with findings showing the importance of Th17 cells in the defence against extracellular bacteria and fungi, where Th1 and Th2 cells are less effective. In particular Th17 cells are important for responses against the fungal pathogen *Candida albicans*. Patients failing to clear Candida infections suffer from chronic mucocutaneous candidiasis and have extremely low levels of IL-17A production (74). Mutations within the transcription factor STAT-3 are associated with autosomal dominant Hyper IgE syndrome, characterized by elevated IgE levels as well as recurrent skin and pulmonary infections (75). As STAT-3 induces Th17 cell differentiation and IL-17A signalling, which leads to neutrophil recruitment and enhanced survival of macrophages, patients present with impaired innate responses. Consequently, patients often suffer with recurrent infections.

Importantly IL-17 and IL-22 play a role in the expression of antimicrobial peptides such as defensins at mucosal sites. IL-22 is thought to defend against pathogens including bacteria within the intestine as its receptor is expressed on intestinal epithelial cells. In support of this, IL-22 deficient mice show increased susceptibility to infection with *Clostridium rodentium*, an enteric mouse pathogen compared to WT control mice (76).

1.3.2.2 Development of Th17 cells by the microbiota

As mentioned previously intestinal epithelial cells, as well as segregating bacteria, have the role of mediating the crosstalk between the microbiota and

host immune cells. A prime example comes from the development of Th17 cells in the intestine. Germ-free mice lack Th17 cells but they develop upon microbiota colonisation. In particular Ivanov and colleagues observed that experimental mice obtained from different vendors displayed marked differences in Th17 cell proportions within the gut (77). Furthermore, transfer of microbiota from one vendor but not the other into germ free mice resulted in Th17 cell development. The group were able to demonstrate that signals from a specific commensal microbe called segmented filamentous bacteria (SFB) transferred into germ free Swiss Webster mice resulted in robust accumulation of Th17 cells in the lamina propria of the small and large intestine. SFB, which are gram-positive, anaerobic, spore-forming bacteria, were sufficient to induce strong IL-17 and IL-22 production from $CD4^+$ T cells (77). Moreover, SFB did not affect IFN-γ secretion or alter other IL-17A secreting cells (NK or γδ T cells) indicating specificity for Th17 cell induction. A member of the acute phase response proteins called serum amyloid A (SAA-1), which is induced during infection and inflammation is also generated in response to SFB colonisation. SAA-1 can act as a cytokine, inducing IL-8 and TNF-α within neutrophils as well as IL-23 in monocytes and intestinal epithelial cells. Co-cultures of naïve $CD4^+$ T cells with intestinal lamina propria derived DCs demonstrated that through SAA-1 induction of IL-23, DCs stimulate a Th17 differentiation program with upregulation of effector cytokines and RORγt (77). In a follow up study in 2014 the group provided *in vivo* evidence that $CD11c^+$ DCs and macrophages can promote Th17 differentiation through MHC class II presentation of SFB antigens (78, 79) (Figure 1.4).

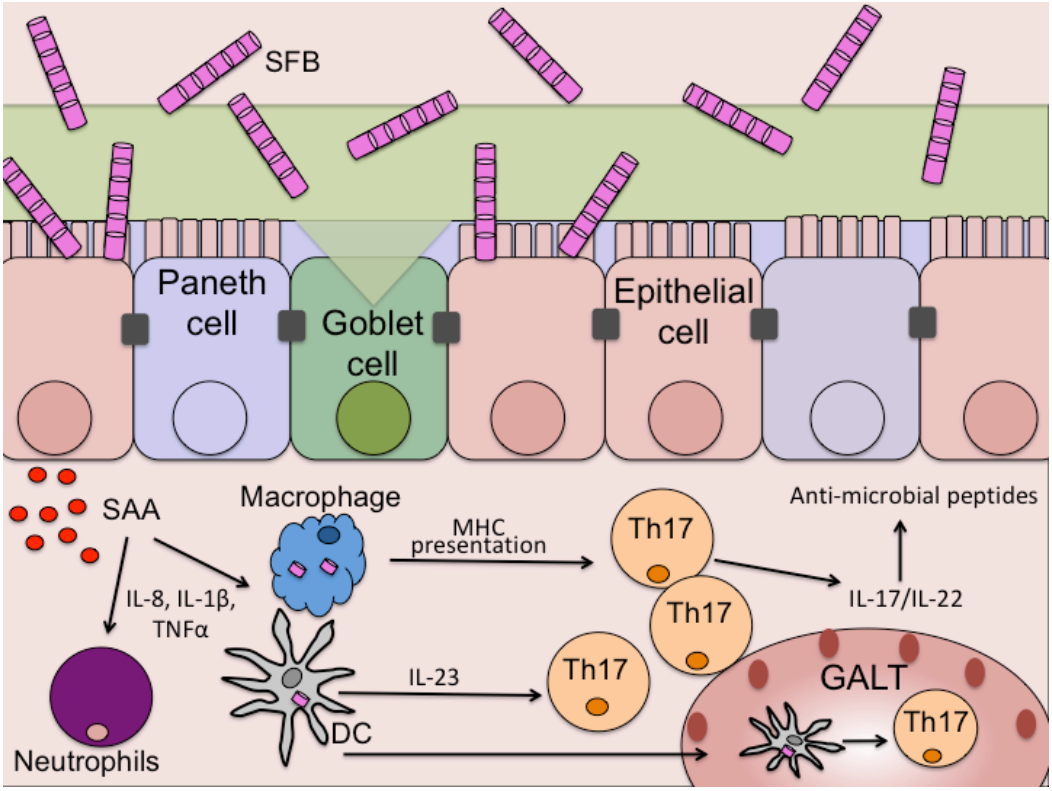

Figure 1.4. Colonisation with SFB induces Th17 cells.
SFB adhere to intestinal epithelial cells stimulating the release of SAA. SAA acts upon neutrophils and DC to express cytokines including IL-8, IL-1β, TNF-α and IL-23, respectively. IL-23 promotes Th17 cell development. SFB antigens are also presented by intestinal macrophages and DCs to induce Th17 cells. This leads to IL-17 and IL-22 production, stimulating antimicrobial peptide release by epithelial cells.

1.3.2.3 Th17 cells in inflammatory bowel Disease (IBD)

Th17 cells are protective at mucosal sites but their involvement in intestinal disease has been recognised by many groups. IBD describes mainly two conditions: Ulcerative colitis (UC) and Crohn's disease (CD). The pathologies are characterised by ulceration of the mucosal lining of the intestine, resulting in symptoms such as abdominal pain, chronic diarrhoea, fever and rectal bleeding. As well as Th1 cells, the inflamed gastrointestinal mucosa harbours a large infiltration of Th17 and IL-23 producing cells, accompanied by inflammatory cytokines (80). Moreover, increased expression of IL-17A mRNA can be detected in faecal content during active CD as well as within gut tissue (80). Genome wide association studies (GWAS) have reported that several polymorphisms in Th17 related genes, such as STAT-3 and the IL-23 receptor

associate with IBD susceptibility, supporting a role for Th17 cells in disease pathogenesis (81, 82). Shown by $CD4^+$ T cell transfer models, Th1 cells and their associated cytokine IL-12 promote IBD inflammation. This can be abrogated with an anti-IL-12 monoclonal antibody, a treatment shown to have some effectiveness in human CD trials (83). However, as within EAE studies, it was proven that anti-IL-12 was also blocking IL-23 function. A study by Hue *et al*. demonstrated using two complementary models of intestinal inflammation (*H. hepaticus* triggered innate immune model and adoptive transfer of naive $CD4^+$ T cells into C57BL/6 $p35^{-/-}$, $p19^{-/-}$ and $p40^{-/-}$ $RAG^{-/-}$ recipients) that IL-23 was key to the promotion of gut inflammation (84). However, a new member of the IL-12 family called IL-35 was identified relatively recently. IL-35 is comprised of the IL-12 associated alpha subunit IL-12p35 as well as an Ebl3 subunit. Therefore, mice deficient in p35 lack the IL-35 cytokine as well as IL-12. In light of this, it was suggested that IL-35 depletion might be masking the role of IL-12 in T cell mediated colitis. To clarify the contribution of IL-12 and IL-23 signalling Imamura and colleagues compared the efficacy of a monoclonal antibody against IL-12/IL-23p40 with that of an anti-IL-23 specific subunit antibody, within $CD4^+$ T cell transfer models in SCID mice. Results confirmed that IL-23 signalling is indeed essential for the development of intestinal inflammation with both IL-23R and IL-12/IL23p40 antibodies completely inhibiting the development of colitis (85). Furthermore, a study by Tang and colleagues has demonstrated that expression of SAA-1, the acute phase protein shown to drive Th17 responses, is associated with intestinal inflammation in IBD (86). Together this data suggests a link between Th17 cells, the microbial community and IBD pathogenesis.

On the other hand, some studies in experimental models of colitis have reported a tissue protective role for Th17 cells. For example, neutralisation of IL-17A within mice was found to aggravate dextran sodium sulphate (DSS) driven

intestinal inflammation (87). Furthermore, compared to WT mice, IL-22 deficient mice show increased inflammatory processes during DSS treatment also (88). It has been suggested that a reduction in Th17 cells actually reduces tissue protective responses, such as the release of anti-microbial peptides, efficient epithelial cell proliferation, goblet cell mucus production and claudin regulation within TJs (89). In agreement with this there has been little success in human trials aiming to target IL-17A. For example, even though the drug secukinumab demonstrated beneficial effects of IL-17A blockage in psoriasis and rheumatoid arthritis studies, there was no therapeutic effect of neutralising IL-17A in a study enrolling 59 CD patients (90). Secukinumab actually had higher rates of adverse events (fungal infections) than the placebo arm of the trial (90). In contrast promising data has emerged from a biological therapy called Ustekinumab. It targets both IL-12 and IL-23 cytokines, via blocking the shared p40 subunit (91). Data from phase 2 and 3 trials showed good induction and maintenance of clinical responses in CD patients. There were significant reductions in disease associated C-reactive protein and fecal calprotectin levels. Ustekinumab was recently been approved for used by the FDA in 2016 (91). Other IL-23 blocking antibodies are under investigation with the hope of inhibiting in part the development of pathogenic Th17 cells.

1.3.2.4 Th17 cell plasticity

It has been established that once a $CD4^+$ T cell commits to a Th1 or a Th2 lineage, conversion to any other lineage is not possible, thus resulting in stable phenotypes. However, Annunziato and colleagues reported that within the intestine of CD patients Th17 cells could secrete both IFN-γ and IL-17A (92). *In vitro* experiments using PMA/ionomycin demonstrated that incubation of Th17 cells with the Th1 promoting cytokine IL-12 led to the production of IFN-γ and IL-

17A (Th1/Th17 cells) or IFN-γ instead of IL-17A (non-classical Th17 cells). Furthermore, IL-12 stimulation upregulated the Th1 associated transcription factor T-bet and down regulated RORγt expression, indicating that Th17 cells can convert to a Th1 phenotype. Analysis of Th17 cell clones expanded *in vitro* showed selective expression of IL-23R, CCR6 and RORγt. Both Th17 and Th17/Th1 cells were able to aid in B cell antibody production and had low cytotoxic potential (92). Continuing with this work, Cosmi *et al.* observed that Th1 cells derived from Th17 cells express CD161, a Th17 cell progenitor marker, unlike conventional Th1 cells (93). This could make it possible to identify IFN-γ secreting cells that were originally Th17s.

The role of Th17/Th1 IFN-γ/IL-17A producing cells in disease is not understood. However it has been shown that IBD patients have increased numbers of these dual producing cells within peripheral blood and gut tissue compared to healthy controls (92). In a study by Harbour *et al.,* a Th17 transfer model was used to evaluate Th1/Th17 cells within colitis (94). Th17 polarized cells were generated from IL-17F$^{Thy1.1}$ mice, utilised as IL-17F is a dominant cytokine expressed early on during Th17 cell commitment. Transfer of IL-17F$^{Thy1.1}$ Th17 cells into Rag deficient recipients resulted in a faster onset of colitis but with a severity comparable with that seen by transfer of CD45RB^{hi} CD4^{+} naïve T cells. It was observed that three distinct subsets arose from the transferred cells: IL-17A only expressing, IL-17A/IFN-γ expressing and IFN-γ only expressing Th17 cells. Interestingly transfer of Th17 cells polarized from IFN-γ$^{-/-}$ mice into rag deficient recipients failed to induce intestinal inflammation, indicating that IFN-γ expression from Th17 cells is required for colitis development (94). It has been highlighted that pathogens can also influence cytokine production from Th17 cells. *In vitro* and *in vivo* evidence shows that naïve CD4^{+} T cell stimulation with *C.albicans* mostly resulted in Th17/Th1 cells, secreting both IFN-γ and IL-17A,

with upregulation of both T-bet and RORγt expression (95). In contrast stimulation with *S.aureus* resulted in IL-17A secretion from Th17 cells with no IFN-γ production and no T-bet expression. However, after re-stimulation with antigen pulsed APC or CD3/CD28 stimulation *C.albicans* and *S.aureus*-specific cells transiently downregulated IL-17A expression, regaining the original cytokine profile as cells reverted to the resting state. *S.aureus*-specific but not *C.albicans*-specific cells also were able to secrete IL-10, demonstrating regulated expression of IL-17A by certain microorganisms (95).

1.3.3 T regulatory cells (Tregs)

Tregs are a $CD4^+$ T helper subset capable of regulating the activity of other immune cells. T cell mediated immunosuppression was identified not long after it was discovered that the thymus was a key component of the immune system. Original studies by Nishizuka and Sakakura showed that thymectomy of day 3 neonatal mice resulted in autoimmunity, while thymectomy at 7 days did not. This indicated that suppressive cells are released from the thymus after conventional T cells (96, 97). In 1995, Sakaguchi and colleagues convincingly showed that $CD4^+$ suppressive cells migrating from the thymus after day 3 could be identified by expression of the IL-2 receptor, CD25 (98). Elimination of $CD4^+$ $CD25^+$ cells from BALB/c mice triggered the production of circulating autoantibodies and the generation of inflammatory lesions within a wide range of organs. The resulting histopathology was similar to that seen within human autoimmune diseases such as autoimmune-gastritis, systemic lupus erythematosus and rheumatoid arthritis (98). Restoring the $CD4^+$ $CD25^+$ cell population prevented autoimmune disease. Furthermore, $CD4^+$ $CD25^+$ cells could transfer tolerance to lymphopenic and thymectomy mice, indicating that CD25 expressing $CD4^+$ cells were important for maintaining peripheral tolerance

by T-cell mediated control of self-reactive T cells (98, 99). The discovery of the CD25 marker converged with a population of Tregs identified as $CD45RB^{lo}$, shown to prevent the generation of colitis upon transfer. However, subsequent studies showed that the majority of regulatory activity within the $CD45RB^{lo}$ group was restricted to $CD25^{+}$ cells, validating CD25 as a good marker for suppressive T cells (100). Due to their ability to suppress immune responses to both self and foreign antigen, now known as Tregs, these $CD4^{+}$ $CD25^{+}$ suppressive cells have not only been implicated in autoimmune disease but also in tolerance, allergy and anti-tumour immunity (discussed later).

Although initially CD25 was beneficial for identifying Tregs, the downside was that activated conventional T cells also transiently express CD25. Many investigations led to a number of markers being associated with Tregs, including expression of GITR, CTLA-4, LAG-3 and CD127 (101). Nonetheless, transient expression on other T cell subsets during activation was again an issue. However, discovery that the transcription factor Forkhead box 3 (FoxP3) is highly expressed in $CD4^{+}$ $CD25^{+}$ but not in $CD4^{+}$ $CD25^{-}$ cells fundamentally altered Treg characterisation (102) . Today, Tregs are typically identified using a combination of markers and are characterised as being $CD3^{+}$, $CD4^{+}$, $CD25^{+}$ $FoxP3^{+}$ and $CD127^{lo/-}$ (103). For experimental procedures surface markers remain crucial for Treg isolation. As Foxp3 is found intracellular, requiring permeabilisation of cells for staining, most often $CD4^{+}$ T cells are sorted based on high CD25 expression and low CD127 expression, a marker found to be down regulated on suppressive T cells in peripheral blood (104). Of note, $Foxp3^{+}$ $CD25^{-}$ cells do also exist (3-5% of PBMC) and in vitro studies have shown they can have suppressive abilities (104).

1.3.3.1 Identification of Foxp3

Observations of patients with the severe autoimmune condition immune dysregulation polyendocrinopathy X-linked syndrome (IPEX) led to the identification of FoxP3 as a marker for Tregs (105). Alongside this, the Brunkow group investigated the scurfy mouse, which was originally described by Godfrey *et al.* as having a general autoimmune phenotype, similar to that seen in IPEX patients (106). Brunkow and colleagues identified that the FoxP3 gene, part of the forkhead/winged-helix protein family of transcriptional regulators was defective due to a frame shift mutation within scurfy mice. This results in hyper-responsiveness of $CD4^+$ T cells and the onset of autoimmune disease, characterised by wasting and multi-organ-lymphocytic infiltrates (107). A study by Fontenot *et al.* then reported that FoxP3 is highly expressed in $CD4^+$ $CD25^+$ Tregs and that it is required for Treg cell development, with FoxP3 deficient mice lacking a Treg population (102). Furthermore, the authors showed that expression of FoxP3 is required to promote the suppressor functions of Tregs. $CD4^+$ $CD25^-$ T cells transduced with a retrovirus expressing FoxP3/GFP or GFP alone were injected into RAG deficient mice. Mice given the GFP-$CD4^+$ $CD25^-$ cells developed autoimmune wasting disease but animals receiving the $FoxP3^{+/}$GFP-$CD4^+$ CD25 cells displayed no signs of disease for the entire experimental period (102). The data highlighted that the lethal autoimmune syndromes seen in scurfy mice and IPEX result from Treg deficiency rather than a cell intrinsic defect of Tregs (102). In a follow-up study Fontenot and colleagues developed a $Foxp3^{GFP}$ reporter mouse to investigate $FoxP3^+$ Tregs during ontogeny. The group were able to demonstrate as originally suggested by Nishizuka and Sakakura and then by Asano *et al.*, that FoxP3 expressing Treg development is substantially delayed in the thymus relative to conventional thymocytes (96, 99, 108). In 2007 the same group developed a new mouse strain, engineered to express the diphtheria toxin receptor under the FoxP3

gene promoter. Therefore in this system selective depletion of FoxP3+ cells could be achieved upon injection with diphtheria toxin, resulting in an autoimmune phenotype similar to that seen in FoxP3 deficient mice (109).

1.3.3.2 Survival and maintenance of Tregs

Unlike conventional T cells, Treg survival and proliferation is strictly dependent on IL-2. IL-2 deficient mice are deficient in Tregs (110). Also shown to be necessary for Treg survival is TGF-β. TGF-β knockout mice are also deficient in Tregs. Marie and colleagues demonstrated that this is due to down regulation of FoxP3 within the periphery as thymic output of Tregs was normal (111). Also important are co-stimulatory molecules such as CD28 and ICOS, both of which provide survival and proliferation signals to Tregs.

1.3.3.3 Treg subsets

Several lines of evidence suggest that $FoxP3^+$ Tregs consist of two developmentally different subsets: thymus-derived Tregs (tTreg) and peripheral-derived Tregs (pTreg). tTregs develop from the thymus while pTregs arise from the thymus as conventional T cells but can convert to FoxP3 expressing Tregs in peripheral tissues.

1.3.3.3.1 tTregs

tTregs develop independently of environmental stimulation, subjected to positive and negative selection processes like conventional thymocytes in the thymus. It is thought that tTregs are generated as a result of thymocytes recognising self-MHC/peptide complexes with avidity higher than that of conventional T cells but not too high to avoid negative selection. A study by Jordan *et al.* took advantage of transgenic mice that have T cells bearing a high avidity TCR specific for the common influenza protein haemagglutinin (HA) (112). The mice were crossed

with transgenic animals expressing the HA protein. It was found that in double transgenic mice (expressing both TCR and antigen) the $CD4^+$ cells specific for HA were not clonally deleted but in fact a large proportion (30%) of the population were $CD25^+$ cells. In contrast only 13% of peripheral T cells were $CD25^+$ within HA transgenic animals. This indicates that specificity for self-peptide is important for directing the selection of tTregs (112). After leaving the thymus tTregs can be found in circulation but mostly reside within the gut and peripheral lymph nodes in a quiescent state until activation (113).

FoxP3 is not sufficient to distinguish tTregs from pTregs therefore a specific tTreg marker would be useful. In 2010 Shevach's group published that Helios, a member of the Ikaros transcription factor family, could be detected in all thymocytes but only within a proportion of $CD4^+$ $FoxP3^+$ cells in peripheral tissues (114). The group showed that neither mouse nor human naive T cells induced to express Foxp3 *in vitro* by TCR stimulation or antigen specific $FoxP3^+$ T cells induced in vivo expressed Helios. This suggested that Helios could be a specific marker for tTregs. However, further studies have disputed this, providing evidence that Helios expression can be induced in pTregs both *in vitro* and *in vivo*, possibly depending on APC derived influences (115). A second marker, neuropillin-1 has also been suggested as a tTreg marker(116), however again this has been disputed within the field (117).

1.3.3.3.2 pTregs

It is established that conventional $CD4^+$ T cells can be converted into Tregs within the periphery. pTregs are generated upon TCR stimulation with cognate antigen in the presence of TGF-β. The intestinal lamina propria is the best example of an environment where pTregs thrive. Accordingly, upon adoptive transfer of TCR transgenic naïve $FoxP3^-$ $CD4^+$ T cells, followed by oral exposure

to the cognate antigen an increased number of donor derived FoxP3$^+$ pTregs can be detected within the gut (118). Interestingly it has been demonstrated that the autoimmune pathology associated with FoxP3 deficiency cannot be completely rescued by transfer of FoxP3$^+$ tTregs alone. Co-transfer with FoxP3$^-$ CD4$^+$ cells was required, indicating an essential non-redundant role for pTregs (119). The intestinal microbiota can also affect the generation of Tregs in the colon. Both germ free and antibiotic-treated animals have reduced Treg numbers and decreased expression of activation markers such as CTLA-4 and ICOS compared to wild type controls (120). However, in the small intestine the microbiota does not affect Treg numbers to the same extent. Instead reports indicate that Tregs within the small intestine accumulate in response to dietary antigens (121). pTregs generation is also dependant on interactions and signals from intestinal epithelial cells, macrophages, innate lymphoid cells and importantly dendritic cells (DC). There are various subsets of intestinal DCs but CD103$^+$ DCs show the greatest ability to induce pTregs (122). In contrast CD103$^-$ DCs are not as effective. CD103$^+$ DCs are migratory, potent antigen-presenting cells that are able to sample luminal contents by extending dendrites across the intestinal epithelial barrier (123). pTreg generation by DCs relies on many factors. In particular the microbiota are capable of stimulating IECs to release of indoleamine 2,3-dioxygenase (IDO), thymic stromal lymphopoietin (TSLP) and WNT ligands. These condition DCs to express the receptor aldehyde dehydrogenase (ALDH) (124). ALDH is capable of metabolizing vitamin A from the gut into retinoic acid, which in combination with TGF-β promotes pTregs to differentiate (124). The gut homing markers CCR9 and $\alpha4\beta7$ are also upregulated by retinoic acid (125). The ability of intestinal DCs to induce pTregs makes them a key driver of oral tolerance within the gut.

1.3.3.4 Mechanisms of Treg suppression

Tregs have a multitude of mechanisms to suppress immune responses. This can be either direct by targeting effector T cells or indirect by targeting DCs to prevent immune activation of effector cells.

1.2.2.4.1 Metabolic disruption

Competition for IL-2 has been documented as a method of Treg suppression in many studies. Tregs express all components of the CD25 receptor, providing them with high affinity for IL-2 over conventional T cells that only express CD25 after TCR activation (126). This leads to local cytokine deprivation and inability of conventional cells to proliferate and survive. Borsellina and colleagues have also demonstrated that CD39 expressed on both $CD25^+$ and $CD25^-$ Tregs can disrupt effector cell function. Exogenous ATP is hydrolysed by CD39 into ADP and 5'AMP, which can be converted further by the ectonucleotidase CD73 (127). Treatment with adenosine inhibitors has been shown to reverse this suppression (127).

1.2.2.4.2 Suppressive cytokines

Tregs can exert their suppressive effects through the release of soluble factors such as TGF-β, IL-10 and IL-35 (128). Li *et al.* have shown that TGF-β deficient animals develop T cell mediated autoimmunity a few weeks after birth and mice that lack TGF-β responsiveness show a similar phenotype (129, 130). It has been repeatedly observed that TGF-β is required for Treg survival but there has been some controversy over whether membrane bound TGF-β can suppress target cells in a cell-to-cell contact manner. A study by Nakamura *et al.* suggested that membrane bound TGF-β on Tregs could be delivered to $CD25^-$ T cells where it can be converted into an active form (131). Further analyses indicated that no active or latent TGF-β could be detected on the cell surface of resting $FoxP3^+$ Tregs. However, after TCR activation a high number of Tregs did

show positive staining for LAP, presumably having expressed latent TGF-β. It is thought that release of TGF-β causes “infectious tolerance”, promoting further conversion of $FoxP3^-$ cells into $FoxP3^+$ cells (132).

Tregs also secrete the inhibitory cytokines IL-10 and IL-35. The use of IL-10 blocking antibodies or IL-10 deficient Tregs diminishes the protective effect Tregs normally have in transfer models of colitis (133). Furthermore the IL-10 locus was identified as a susceptibility region for the development of UC, highlighting an important role for IL-10 in abrogating intestinal inflammation (134). Collinson *et al.* have shown that IL-35 secretion by Tregs can directly inhibit the proliferation of conventional T cells (135). Further to this Wei *et al.* observed that IL-35 and IL-10 expressing Tregs have a distinct activation status, suggesting that IL-10 producing and IL-35 producing Tregs work in a co-operative manner to maintain immune tolerance (136).

1.2.2.4.3 Cytolysis

Tregs possess cytotoxic activity to kill target cells. As shown by Gondek and colleagues this is through the secretion of granzymes A and B (137). It has been demonstrated this is in a perforin-dependent manner, with activated human Tregs able to eliminate various autologous immune cells (138). This suppressive mechanism has been shown to drive susceptibility to tumour growth. A mouse model of B16 melanoma adoptive transfer in granzyme B deficient recipients showed that WT Treg cells, but not granzyme $B^{-/-}$ or $perforin^{-/-}$ Treg cells prevented tumour clearance via the inhibition of anti-tumour NK and $CD8^+$ T cell responses (139). Furthermore, engagement of Fas expressed on Tregs with FasL-bearing target cells results in the stimulation of a caspase-8 signalling pathway, capable of driving apoptosis of the target cell. Using cell lines, Janssens *et al.* observed that this mechanism could also kill antigen presenting B cells to down regulate immune responses (140).

1.2.2.4.4 Targeting dendritic cells

Tregs also target DCs to alleviate effector immune responses. One of the most widely studied molecules involved is CTLA-4, which is highly expressed on Tregs. CTLA-4 binds to co-stimulatory molecules CD80/86, in direct competition with CD28 expressed on effector cells. CTLA-4 deficient mice develop spontaneous autoimmunity that can be abrogated by the transfer of WT Tregs. Studies also show that anti-CTLA-4 blocking antibodies are capable of abrogating Treg mediated suppression (100). Tregs can suppress DC activation further through expression of LAG-3, the CD4 homolog. LAG-3 is capable of binding MHC class II on DCs. This reduces binding of CD28 found on effector cells to MHC class II (141).

1.4 Tumourgenesis

1.4.1 Immunosurveillance

Evidence arising from mouse and clinical observations show that the immune system plays an important role in surveying the body for transformed cells. Paul Ehrlich originally postulated that the host immune system could defend against nascent pre-malignant cells in the early 1900s. Sir Frank MacFarlane Burnet developed the theory of immunosurveillance further, hypothesising that antigens derived from tumours were capable of activating immune responses (142). This was following initial experiments by Foley in 1953, showing that tumours induced within mice by methylcholanthrene (MCA) were antigenic within the host (143).

Advances in genetics then led to the generation of RAG KO mice in the 1990s. This made it possible to deplete NKT, B and T cells within mice while non-lymphocyte linages remained. Shankaran and colleagues injected aged matched female RAG-2 deficient and WT mice with MCA, observing that RAG-2^{-}

$^{-/-}$ mice developed tumours faster and had a higher tumour burden compared to control mice. This indicated a role for the adaptive immune system in chemically induced tumours (144). To investigate the development of spontaneous tumours, untreated RAG-2$^{-/-}$ and WT mice were evaluated for fifteen months. It was observed that 12/12 RAG-2$^{-/-}$ mice developed intestinal lesions within the intestine as well as in other locations. In contrast, no WT mice developed cancer. The authors also took a transplantation approach to investigate whether the immune system influenced the immunogenic phenotype of tumours. When RAG-2$^{-/-}$ mice received tumours derived from RAG-2$^{-/-}$ or WT mice, tumours grew progressively and with similar kinetics. WT mouse-derived tumours transplanted into WT immunocompentent hosts resulted in the formation of tumours in all recipients (17//17). However, it was observed that transplantation of RAG-2$^{-/-}$ derived tumours into WT recipients were rejected 40% of the time. The authors inferred that tumours developing in lymphocyte deficient animals are more immunogenic than those developing in immunocompetent hosts. The fact that fewer immunogenic tumours developed in the presence of an intact immune system implies that the anti-tumour response drives immunoselection of tumour cells that are capable of surviving (144). Links between the immune system and prevention of cancer development also became apparent through studies involving transplant patients and those suffering with AIDS. Both patient groups are comprised of immune compromised individuals and both groups also presented with higher rates of mainly virus-induced tumours (145).

1.4.1.1 Immunoediting

In 2002 the Schreiber group presented the three-step model of “cancer immunoediting” (146). The three steps are termed the three E’s of cancer immunoediting and are as follows: elimination, equilibrium and escape (146). Elimination describes the classical concept of cancer immunesurveillance,

where tumour cells are eliminated by the immune system. Early experiments identified that IFN-γ has a key role in this prevention. MCA tumours unresponsive to IFN-γ, due to a truncated chain in the IFN-γ receptor, showed enhanced tumourigenicity. Rapidly progressing tumours were formed compared to WT MCA tumours when transplanted into syngeneic recipients. However in SCID mice, which lack lymphocytes, both WT and IFN-γ insensitive tumours grew with similar growth characteristics, indicating that IFN-γ production by lymphocytes was important (147). In a follow up study, the same group evaluated the role of IFN-γ in the development of spontaneous tumours as opposed to transplanted tumours. Mice lacking the tumour suppressor gene p53 were crossed with IFN-γ insensitive mice to create double KO animals. Compared to p53 single KO mice, double KO animals developed tumours significantly faster. Furthermore, unlike p53 single KO mice, double KO mice developed non-lymphoid tumours. Taken together the data demonstrated that IFN-γ does promote tumour surveillance (148). Other key immune molecules have been identified for being important for tumour surveillance including perforin and the TNF-related apoptosis-inducing ligand (TRAIL). Perforin is a cytolytic molecule, capable of making holes in target cells. Early studies showed that challenge with MCA in perforin$^{-/-}$ mice resulted in the formation of 2 - 3 times more tumours. Furthermore, ageing perforin$^{-/-}$ mice were found to spontaneously develop lymphomas at a much higher rate that WT mice.

Activation of the innate arm of the immune system is also important for immunosurveillance. Cui *et al*. described the generation of a naturally occurring germline trait that resulted in a BALB/C mouse being able to resist the development of ascites after injection with the aggressive S180 sarcoma cell line (149). Further investigations revealed that mice with this trait were able to kill a range of both syngeneic and allogeneic tumours. When the trait was bred into nude mice, which lack a thymus, the enhanced resistance to tumour

development remained, suggesting that the innate immune response was responsible for the phenotype. In keeping with this finding, experiments where the apoptosis inducing molecule TRAIL, which is constitutively expressed on NK cells and dendritic cells as well as $CD8^+$ T cells, is neutralised with mAbs, MCA tumour development is greatly increased (150).

The equilibrium stage of immunoediting refers to a situation when some nascent cells have survived the elimination phase but are still being kept under control by the immune system. This is often termed immune mediated tumour dormancy. In a key paper, Koebel and colleagues investigated whether the equilibrium phase occurred during primary tumourigenesis (151). WT mice were injected with low dose MCA and monitored for tumour development. Mice that developed stable masses after approximately 200 days were then treated with mABs against immunological components. Results indicated a particular role for the adaptive immune system in maintaining tumour dormancy. Treatment with anti-, anti-CD8 and anti-IL12p40 caused progressively growing sarcomas at the injection site within mice that originally had stable tumours (151). In contrast monoclonal antibody treatment to deplete NK cells or inhibit TRAIL did not result in tumour outgrowth (151). The balance between anti-tumour effector cells such as $CD4^+$/$CD8^+$ T cells and numbers of suppressive cells such as Tregs is important for maintaining tumours in the equilibrium phase, with an increase in suppressive cells being linked to tumour escape (152).

Ultimately the escape phase of immunoediting occurs when tumour cells proceed, unrestrained by the immune system and can form a clinically detectable mass. Studies have shown that tumour escape can be a direct result of alterations occurring in edited tumour targets themselves. In particular, loss of HLA class I antigens on tumour cells and other molecules in the antigen

presentation pathway such as TAP1 are frequently deficient in an effort to evade the immune system. Tumour cells can also upregulate molecules to promote proliferation and survival such as STAT-3 and BCL-2, respectively. Moreover, immune suppressive factors such as IDO, PDL-1 and CD39/CD73 can dampen effector immune responses and further recruit more immunosuppressive cells such as Tregs to the tumour microenvironment. While tumour escape can occur naturally, it has been observed that immunotherapy treatments can also cause a selective pressure leading to tumour outgrowth (relapse).

1.4.2 Colorectal cancer incidence

CRC is the third most common cancer worldwide and second most common cause of cancer related death within the UK. Latest CRUK statistics show that over 41,000 new cases were reported in 2015 (153). While the 5-year survival rate for early-detected CRC is relatively promising (~90%), this dramatically reduces to less than 10% in patients with late stage metastatic disease. Recently a study has estimated that in 2018, across the European Union, CRC will have the second highest mortality rate of all cancers (154). It will account for approximately 180,000 deaths, mostly affecting the older generation (age 60+) (154). Interestingly studies suggest that CRC incidence is strongly related to diet and lifestyle with CRC mortality rates increasing faster than any other cancer type after migration to the Western world (155).

1.4.3 Colorectal cancer aetiology

Associated risk factors for CRC include increased age, obesity, alcohol, smoking, IBD and a poor diet, which includes an excess of red meat (156). Both sporadic and hereditary CRC exist. Hereditary CRC is associated with genetic conditions such as Lynch syndrome and Familial Adenomatous

Polyposis (FAP). However, sporadic CRC is most common, developing often from pre-existing adenomentous polyps through the accumulation of mutations arising in oncogenes and tumour suppressor genes.

1.4.3.1 Hereditary CRC

Heritable factors are associated with CRC development but only 5-10% are attributed to mutations within known CRC susceptibility genes.

1.4.3.1.1 Lynch syndrome

The pathologist Aldred Scott Warthin in the 1800s laid down the foundation for understanding the inherited cancer condition Lynch syndrome, providing the first comprehensive record of familiar clustering of cancer (157). However, it was not formally named until 1984 by Boland and Trancale (158). It is the most common form of hereditary CRC and is genetically heterogeneous. Most patients harbour pathogenic variants in one of four DNA mismatch repair (MMR) genes: MLH1, MSH2, MSH6 or PMS2. Patients can also display germline mutations in the 3' end of EPCAM that can lead to gene silencing of MSH2 (157). As MMR genes are the post-replicative proof reading and editing machinery required to maintain genome integrity, inactivation leads to the accumulation of genetic mutations, driving microsatellite instability (MSI) and an increased risk of developing cancer. However, identification of Lynch syndrome can often be challenging as MMR protein deficiency can also occur within some sporadic forms of CRC. A recent study by Pai *et al*. investigated the expression of MMR proteins in non-neoplastic intestinal mucosa obtained from colorectal surgical resection specimens from patients with Lynch syndrome-associated CRC and from non-Lynch syndrome CRC patients (159). Results showed that MMR protein deficient non-neoplastic colonic crypts could be detected within Lynch patients

but could not be detected in those with sporadic MMR protein deficiency, suggesting a possible additional method for diagnosing Lynch syndrome (159).

1.4.3.1.2 Familial adenomatous polyposis (FAP)

FAP is an autosomal-dominant colorectal cancer syndrome, with patients presenting with hundreds or sometimes thousands of colonic adenomas. Onset is normally seen in early adolescence and carries a nearly 100% risk of developing CRC. If FAP is left untreated the average age for CRC development in 35-40 years, which is significantly younger than sporadic CRC (160). In 1991 Groden *et al*. discovered that FAP develops due to a germline mutation in the adenomatous polyposis coli (APC) gene (161). The APC protein has many functions. It acts as a scaffolding protein, being part of a complex along with GSK3-β that is involved in cell migration and cell adhesion by regulating phosphorylation of the protein β-catenin. β-catenin is an intracellular protein that binds the adhesion molecule E-cadherin, linking it to the cell cytoskeleton. Under normal circumstances phosphorylated β-catenin is targeted for degradation by the proteasome. However, mutations in APC result in an excess of β-catenin within the cell cytoplasm, which binds to the TCF family of transcription factors through the wingless/integration 1 (WNT) signalling pathway (Figure 1.5) (160). This affects the expression of various genes associated with cell proliferation, differentiation, migration and apoptosis. In particular, it has been observed that cyclin D1, c-myc, matrilysin and caspases are altered (160). The cell cycle is influenced as APC prevents progression of cells from the G0/G1 phase to S phase. Furthermore, APC maintains cellular microtubules and preserves chromosomal stability. Consequently, mutations in APC result in uncontrolled cell proliferation as well as chromosomal aneuploidy to drive tumour development (160). There have been over 1000 APC mutations identified, many resulting in the production of a truncated APC protein (162).

Inability of the APC protein to function is seen as an initial step in CRC development and is often seen in sporadic cancer also.

FAP is treated through endoscopy procedures to remove polyps but eventually prophylactic colectomy is required in most cases. However, many studies have observed that NSAID cyclooxygenase (COX) inhibitors can significantly inhibit the development of colorectal polyps within FAP patients (163). It is thought a regime of NSAIDs in conjunction with dietary supplements may be useful for FAP treatment, although further studies are required to confirm this (164).

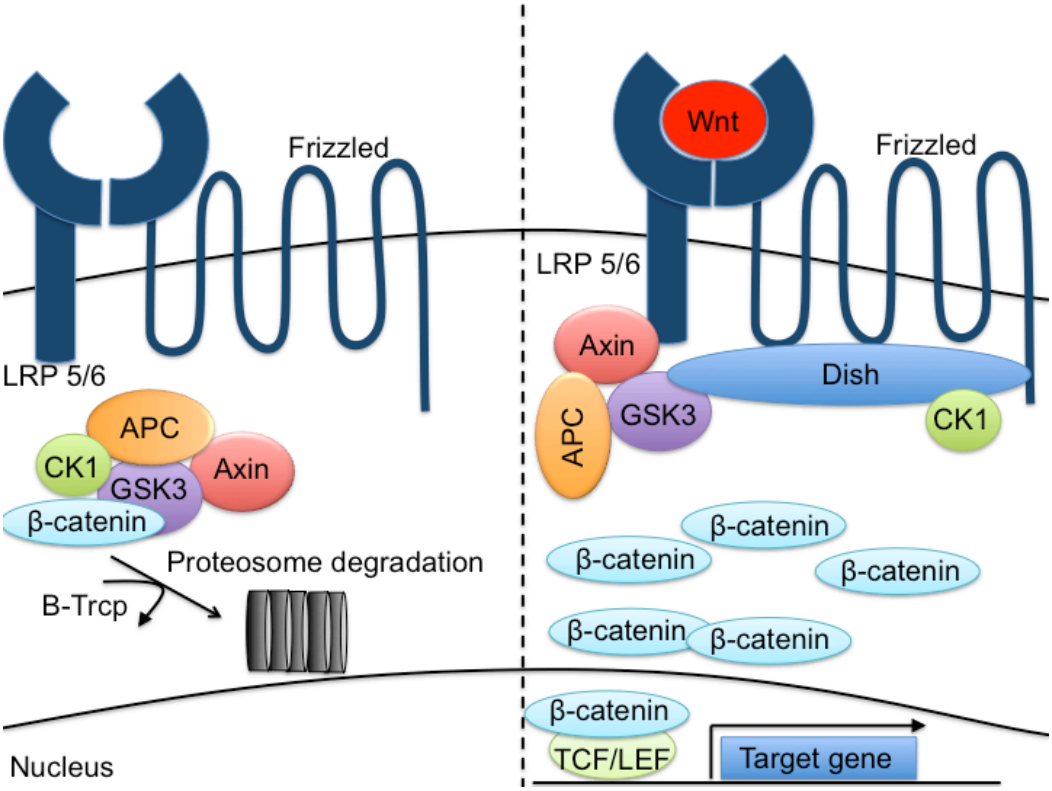

Figure 1.5. Canonical Wnt Signalling.
In the absence of Wnt engagement the protein destruction complex, consisting of APC, causes degradation of β-catenin via the ubiquitination/proteasome pathway. Upon Wnt engagement with Frizzled and the co-receptor LRP 5/6 dual phosphorylation by CK1 and GSK3 occurs. The destruction protein complex is recruited to the plasma membrane along with the protein Dish. Dish inhibits GSK3 activity and induces the stabilisation of β-catenin. β-catenin accumulates, translocating to the nucleus where it can bind with TCF/LEF transcription factors. This complex is then able to bind to the promoter region of genes such as MYC and cyclin D involved in cell proliferation and survival. During APC mutation in cancer the destruction complex is unable to function, resulting in β-catenin translocation and continuous gene transcription. (Figure adapted from Komiya and Habas 2008 (165)

1.4.2 Sporadic CRC

Sporadic CRC is a disease where pathogenesis is influenced by the local colonic environment as well as genetic background. It accounts for two thirds of all CRC seen in clinical practice and particular key mutations other than APC have been associated with sporadic cancer. KRAS is a proto-oncogene that encodes a GTPase, which acts downstream of the epidermal growth factor receptor (EGFR). Mutations in KRAS are evident in approximately 30-40% of CRCs and lead to a continuous active signalling that drives anti-apoptosis, while also promoting cell growth and survival. It has been observed through clinical trials that there is no benefit from neoadjuvant anti-EGFR chemotherapy (Cetuximab) within patients that have KRAS mutations. In contrast, treatment of patients harbouring WT KRAS with Cetuximab in addition to chemotherapy resulted in a significant increase in overall survival and progression free survival (166).

Mutations in the Raf protein BRAF also often occur in CRC (up to 18% of CRCs). BRAF is one of the three RAF proteins found within mammals and activates MEK, which is directly upstream of ERK in the EGFR pathway (167). The most common mutation is $BRAF^{V600E}$ where a single nucleotide change has occurred resulting in constitutive BRAF signalling (168). This again leads to gene activation to drive cells survival, growth and differentiation. Interestingly BRAF mutations are more associated with females, tumours on the right side of the colon and have a distinct pattern of metastasis. Metastatic sites more often develop in the peritoneum and not as often in the lungs (169). A poorer survival prognosis is associated in metastatic CRC patients that have BRAF mutations, with most studies indicating a low 1-year median survival compared to a 2-3 year median survival for patients with WT BRAF (169).

The p53 tumour suppressor gene is the most commonly mutated gene in human cancers and mutated p53 is detected in up to 75% of CRCs. It functions in

response to stress such as DNA damage and actively causes the transcription of a myriad of genes which control cellular process involving cell cycle arrest, apoptosis and senescence (170). p53 upregulates the expression of the pro-apoptotic markers Bcl-2 and FAS as well as cyclin-dependent kinases such as p21, which prevents transition of the cell cycle into S phase from G1 and can promote cells to become senescent. Upregulation of CDC2 by p53 also prevents the cellular process of mitosis (171). Therefore, mutated p53 is seen as a key driver of cancer cell development.

1.4.3 Colorectal cancer development and staging

Several layers, starting with the innermost mucosa then the submucosa, muscularis propria, subserosa and the serosa form the colon (Figure 1.6). Upon surgical resection clinical pathologists will stage the tumour, which can have an impact on further treatments as well as indicating patient prognosis. Two classification systems for staging are currently used. Dukes' staging, from A-D describes increased tumour infiltration into the colonic layers (Figure 1.2). TNM staging is also often used. T evaluates how deeply the tumour has penetrated the bowel lining. N indicates node involvement and M designates the appearance of any metastatic sites (172). The parameters for each stage are described in detail in Chapter 2.

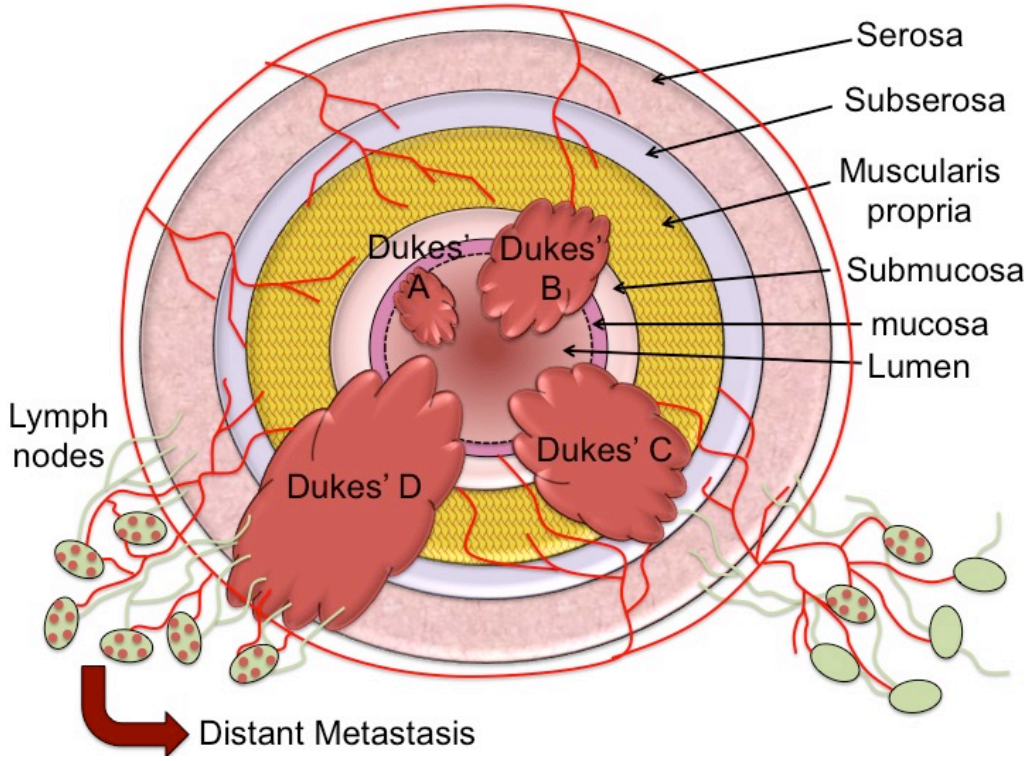

Figure 1.6. Dukes' staging of CRC.
Image delineating the advancement of an adenocarcinoma though the colonic muscle layers in a cross-sectional schematic of the colon. Lymph node involvement and metastatic disease ultimately occurs at late Dukes' C and D staged disease. <MOVED HERE>

1.4.4 Consensus molecular subtypes of CRC

Recently a new classification for CRC tumours has emerged. Guinney and colleagues created a general framework that compared the multiple strategies previously used to define common disease patterns in CRC (173). This enabled the group to elucidate the four consensus molecular subtypes of CRC, based on molecular patterns.

Most tumours that are MSI positive fall into the CMS1 subtype. They are also characterised as having hyper-methylation, hyper-mutation and associated with the presence of $BRAF^{V600E}$ mutations. Furthermore, CMS1 tumours show high infiltration of immune cells such as $CD8^+$ and $CD4^+$ T cells and NK cells (174).

Tumours that show chromosomal instability develop through the traditional tumourigenesis pathway suggested by Fearon and Vogelstein (175), subdivided into three groups: CMS2, CMS3 and CMS4. CMS3 tumours are characterised as a metabolic subtype, being enriched for KRAS mutations and exhibiting metabolic reprogramming with activation of glutaminolysis and lipogenesis (174). CMS2 and CMS4 are both MSS and show low levels of hypermethylation. They can be distinguished as CMS2 tumours have increased upregulation of WNT signalling and expression of downstream targets. In contrast, CMS4 tumours show activation of pathways in relation to epithelial-mesenchymal transition (EMT) such as the TGF-β pathway and overexpression of extracellular remodelling matrix proteins. Furthermore, CMS4 tumours have a pro-angiogenic influence on the microenvironment, predominately promoted by cancer associated fibroblasts (174). Interestingly CMS2 and CMS3 tumours have a low immune and inflammatory signature, showing poor immune cell infiltration and reduced expression of immunoregulatory cytokines. Furthermore, these tumours are most often PD-1 negative, together indicating the CMS2 and CMS3 tumours are less immunogenic (174). There is some crossover between subtypes with not all CRCs falling directly into one of the four subtypes described. It is thought that in this case the tumour may be at an intermediate stage. Nevertheless, it is believed that molecular characterisation of CRC tumours will advance effective drug discovery.

1.4.5 Current treatments

A multidisciplinary team will assess CRC patients to discuss treatment plans including whether the patient should receive neoadjuvant treatment such as chemotherapy or radiotherapy prior to surgical colectomy. Where possible, resection of the affected colon with curative intent is performed. However,

unfortunately 40-50% of patients still relapse and succumb to disease within a 5-year period (176). This highlights the need for better treatments

1.5 Tumour Antigens

1.5.1 Classification of antigens

Tumour antigens can be classified as either tumour specific antigens (TSAs) or tumour associated antigen (TAAs). TSAs are exclusively expressed on tumour cells while TAAs are expressed on both normal and cancerous tissue. A vast number of tumour antigens have been identified for various cancers. Most TSAs arise due to somatic and germline mutations while TAAs are in the form of antigens found on normal cells but overexpressed in cancer or altered during differentiation. One of the most well-known tumour antigens is HER2, an EGFR discovered by Robert Weinberg and colleagues (177). It is a TAA over expressed in breast, gastric, ovarian and CRC as well as others. It signals through several pathways, such as PI3K/Akt and Ras/Erk, associated with cell survival and proliferation. Approximately 25% of breast cancers are HER2 positive and importantly HER2 overexpression is linked with poor survival in breast cancer patients regardless of lymph node involvement. The monoclonal antibody Trastuzumab (brand name Herceptin), which binds to HER2 has been approved as a first line treatment for $HER2^+$ breast cancers since the 1990s with a 50%-80% response rate in patients (178). It is often given in combination with chemotherapy drugs such as docetaxel and paclitaxel. Since 2012 pertuzumab (brand name Perjeta), which also binds HER2 has been approved for use in combination with trastuzumab and docetaxel for treatment of patients with $HER2^+$ metastatic breast cancer (179). Following this, in 2017, the FDA approved the use of pertuzumab in combination with trastuzumab and chemotherapy as adjuvant treatment of patients with $HER2^+$ early breast cancer at high risk of recurrence (180).

Genetic mutations can give rise to tumour antigens described as neo-antigens. Neo-antigens are observed most often in melanoma and lung cancer due to the high rate of exposure to carcinogens such as radiation and tobacco, which leads to DNA damage. In some cases, a high neo-antigen load can be beneficial as some of these antigens can stimulate the anti-tumour immune response. Rizvi and colleagues show that increased mutation and neo-antigen burden in non–small cell lung cancer patients treated with the anti-PD-1 drug pembrolizumab, correlated with better objective response, durable clinical benefit, and progression-free survival (181). However, in some cases the immune system is unable to recognise neo-antigens or in many cases the tumour microenvironment can suppresses anti-tumour responses. Furthermore, developing treatments towards neo-antigens would be patient-specific and a laborious task. This makes it a challenging option as a large-scale cancer treatment strategy.

Other promising targets for cancer therapy are the cancer testis (CT) antigens. In healthy adults, expression of CT antigens are restricted to male germ cells such as spermatocytes. However, ectopic CT expression can be detected within multiple cancers. Melanoma-associated antigen 1 (MAGE-1) was the first CT antigen discovered 20 years ago but other members such as GAGE, SSX and CT45 have been found to be over-expressed in cancerous tissues (182). Male germline cells are unable to express HLA molecules, rendering them incapable of displaying antigens on the cell surface. Studies have shown that CT antigens are expressed within the thymic medulla during T cell development. Nevertheless, cellular and humoral responses to CT antigens have been measured in cancer patients. CT antigens are thought of as neo-antigens when expressed within nascent cells and provide a promising target for therapies.

In our laboratory we focus on two antigens associated with CRC: Carcinoembryonic antigen (CEA) and 5T4.

1.5.2 CEA

Gold and Freedman originally extracted CEA from foetal intestinal tissue and from an adult CRC in 1965 (183). Initially it was believed that CEA was an oncofoetal antigen that was only overexpressed in cancerous tissue. Further studies disproved this, showing that CEA is expressed at low levels within the normal small and large intestine. Anhen and colleagues carried out a comprehensive study investigating the localisation and distribution of CEA. Results showed CEA expression within the small intestine was localised to the luminal surface of epithelial cells and could also be detected within goblet cells. Within the colon CEA was expressed in dense deposits at the apical surface of cells close to the lumen while higher CEA expression was found at the luminal border of cells within the crypt bases (184). The majority of CRCs overexpress CEA, however it can also be detected in lung, breast and ovarian malignancies. Within cancerous tissue CEA expression is approximately 60-fold higher compared to normal tissue (185).

CEA is a highly glycosylated protein belonging to the immunoglobulin supergene family, functioning as a cell adhesion molecule. Some studies have also reported a role for CEA in trapping intestinal bacteria such as *E.coli* (186). CEA is anchored to the plasma membrane of epithelial cells but can also be shed from the cell surface into the circulation. Serum CEA levels are routinely used to monitor CRC patients for tumour recurrence after colectomy (187). In an early study by Wanebo *et al*. a positive correlation between the proportion of patients with high CEA serum levels and tumour stage was also observed (188).

Unfortunately there is no homologue for CEA within rodents; hence the first CEA transgenic mice (CEA-Tg) were established in 1991 to express human CEA in various tissues (189). CEA-Tg mice from the Zimmermann laboratory also importantly showed that the spatiotemporal pattern of CEA was similar to that seen in humans (190). Mice and humans develop tolerance to CEA, however vaccination studies show that this can be broken. This makes CEA an attractive target for immunotherapy. Nonetheless, as CEA is expressed on healthy tissue the safety and long-term implications of targeting CEA are not fully known. In a particular study by Bos and colleagues the safety of CEA-targeted immunotherapy within CEA-Tg mice was evaluated (191). The CEA-specific repertoire was reconstituted through adoptive transfer techniques. WT mice were challenged with the CRC cell line MC38 expressing CEA after inoculation with a CEA peptide loaded vaccine. While WT mice developed a CEA response, only a weak $CD4^+$ T helper response could be detected in CEA-Tg animals. Furthermore transfer of CEA responding cells raised in WT mice failed to prevent tumour growth in CEA-Tg mice, suggesting that the CEA response is governed by peripheral tolerance as well as central tolerance (191). Nevertheless, irradiation of CEA-Tg recipients prior to adoptive transfer of WT CEA specific cells resulted in 35% of tumours being rejected, indicating that suppressive mechanisms to restrain CEA specific cells were in place. Using CD25 specific antibodies in combination with irradiation and CEA specific adoptive transfer the group showed that the majority of tumours could be cleared (191). However, it was observed that under the treatment regimes used in this study, mice developed colitis, showing symptoms of weight loss as well as colon shortening and thickening. Only CEA-Tg mice showed symptoms of experimental colitis, demonstrating the pathology was due to reactivity to normal intestinal CEA expression. In support of this, the colon showed increased

enteropathy compared to the small intestine where CEA expression is lower (191). Furthermore, transfer of Thy 1.1 donor CEA-specific cells into Th1.2 recipients demonstrated CEA-specific cells were involved in generating colitis as donor cells were shown to infiltrate the intestinal epithelium. The authors do state that in this particular CEA-Tg mouse strain the expression of CEA is 10-fold higher to that seen in humans and therefore may provide a worst-case scenario. Nevertheless, this study was one of the first to highlight severe colitis as a possible side effect of CEA targeted immunotherapy (191).

Following this, a human study by the Rosenberg laboratory investigated the use of autologous T cells engineered to express a murine TCR against human CEA to treat three metastatic CRC patients (192). Transfer of engineered T cells resulted in lower CEA serum levels in all patients and one patient did show an objective response with tumour regression. However, as a side effect all three patients developed severe colitis and the authors discussed that this may pose a significant limitation of any treatment that uses CEA as a target (192).

1.5.2.1 Blood anti-CEA responses

The use of TAAs as immunotherapy targets relies on a natural existing pool of T cells able to recognise antigen epitopes. In 2000, a study by Nagorsen *et al*. measured blood derived responses to three tumour antigens and assessed whether reactive T cells could be detected in CRC patients (193). ELISpot technology evaluated the reactivity of PBMC from HLA-A2 positive patients to HLA-A2 restricted peptides from Ep-cam-1, HER-2 and CEA, using IFN-γ secretion to characterise a response. Spontaneous responses to all three antigens were observed in a proportion of metastatic CRC patients. In particular a significant response to CEA could be detected in 6/22 patients (193). This study was one of the first to identify IFN-γ specific CEA responses from the blood of CRC patients.

In our own laboratory, blood responses to CEA are also measured. In a study published in 2015 we reported that CRC patients harbouring blood-derived CEA specific IFN-γ responses prior to surgical colectomy had a poorer survival prognosis compared to non-responding patients (194). Intriguingly this finding was regardless of tumour stage. In contrast responses to the TAA 5T4 did not correlate with tumour recurrence. Furthermore, 5T4 responses provided a protective response as CEA-only responding patients had a worse prognosis than CEA/5T4 dual responding patients (194).

1.5.3 5T4

5T4 trophoblast glycoprotein was discovered during studies attempting to find surface molecules shared between a foetus and a tumour to promote survival in the mother and host, respectively. Hole and colleagues were able to show using monoclonal antibodies that 5T4 was 72 kD in size (195). While not expressed in most tissue, 5T4 was present within developing embryos on the syncytiotrophoblast, some extravillous cytotrophoblast and the amniotic epithelium (195). 5T4 upregulation occurs in many different cancers including CRC. Expression on tumours cells is associated with the process of epithelial-mesenchymal transition (EMT) by impacting on the actin cytoskeleton and promoting epithelial cell motility (196). Furthermore, 5T4 is capable of modulating chemokine signalling, involved in the functional expression of CXCR4 on the tumour cell surface. CXCR4 and CXCL12 have been linked to promoting tumour spread in many cancers, attracting metastatic cells to distant organs such as the liver and lungs (197). Interestingly in the absence of 5T4, CCR7 upregulation can be seen. This leads to stimulation of signalling pathways involving the EGFR signalling pathway resulting in proliferation and anti-apoptotic gene activation. It is thought that 5T4 potentiates the spread of

tumours while in its absence, CCR7 signalling promotes cell growth and survival at the primary site (197).

5T4 has been evaluated as a potential therapeutic target for many years now. Originally 5T4 KO mice were used to evaluate how endogenous 5T4 influenced the immune system. Castro and colleagues showed that vaccination of 5T4 KO mice with an adenovirus encoding mouse 5T4 generates strong $CD8^+$ and $CD4^+$ IFN-γ responses which provide significant protection when challenged with 5T4 expressing melanoma. In contrast, WT mice only developed low level $CD8^+$ IFN-γ production and were unable to control tumour growth (198). The group examined whether host Tregs could be supressing 5T4-specific responses by treating WT mice with a monoclonal antibody specific for folate receptor 4. Treatment halved Treg frequency and in combination with an MVA-5T4 vaccination regime 5T4-sepecific IFN-γ responses increased and a modest reduction in tumour growth was observed within WT mice, indicating that local suppressive mechanisms could be contributing to low anti-5T4 T cell responses (198).

Immunisation has been investigated with other viral vectors such as modified vaccinia Ankara (MVA) also. In a study by Mulryan *et al*. WT mice were challenged with autologous CT26 tumour cells expressing human 5T4, given MVA-5T4 either intravenous or intramuscular injection and followed up for 60 days (199). Results showed a decrease in the number of tumour nodules developing within the lungs of vaccinated animals compared to control groups, which was accompanied by a significant increase in overall survival (198).

The aforementioned studies as well as others supported the clinical development of an MVA-5T4 vaccine termed Trovax. Initial clinical trials were promising for Trovax, indicating that it was well tolerated and was capable of promoting 5T4 cellular and humoral responses in prostate, colorectal and renal cancer. However, in a renal cancer phase III trial recruiting over 700 patients

Trovax was unable to meet its primary endpoint. No significant difference was observed between Trovax and placebo treated groups. It was however elucidated that some patient subgroups (high 5T4 antibody responders) may benefit from MVA-5T4 (200).

Our own laboratory investigated the use of Trovax in a clinical trial aimed at disease-stable, metastatic CRC patients called “Trovax and cyclophosphamide treatment in colorectal cancer (TaCTiCC) (201). Results from the trial demonstrated that MVA-5T4 safely induced T cell and serological responses and significantly prolonged progression free survival (PFS). In one arm of the trial patients received Trovax in combination with low dose cyclophosphamide to reduce Treg numbers, in an attempt to remove possible suppressive mechanisms and boost 5T4-specific responses. However, while it was observed that cyclophosphamide did deplete Treg numbers, which was accompanied by an increase in prolonged PFS, combination treatment of Trovax and cyclophosphamide did not increase any immune response over Trovax alone (201). Interestingly cyclophosphamide treatment alone elicited a striking boost in anti-tumour immunity resulting in increased patient survival (202).

1.6 T cell subsets in cancer

Interactions between malignant cells and the immune system are complex, and as described above key for tumour development. Accordingly, Hanahan and Weinberg pronounced that the ability to avoid the immune system is a “hallmark of cancer” (203). Various immune subsets are known to infiltrate tumours, some associated with driving tumour control and others facilitating tumour progression. Over all, many studies have shown that a high tumoural infiltrate of lymphocytes is associated with better patient survival. For example, meta-analyses of breast cancer patients highlighted that in triple negative breast

cancer patients (TNBC) and Her-2$^+$ patients, the presence of TILS is associated with improved prognosis. Mao and colleagues were able to show that CD8 expressing lymphocytes were associated with better DFS while FoxP3$^+$ cells correlated with poorer DFS (204). This finding was also seen in ovarian cancer with Hwang *et al*. carrying out meta-analysis of 10 studies and observing that both CD3$^+$ and CD8$^+$ cells confer an OS advantage to patients (205). In general a "pro-inflammatory" tumour microenvironment is associated with better clinical outcome.

1.7 T cell subsets in CRC

1.7.1 Th1 and cytotoxic T cells

The immune infiltrate into CRCs also associates with survival prognosis. Meta-analysis by Mei and colleagues of 9 CRC trials investigating the impact of inflammation found that the pooled HR ratio confirmed a high tumour infiltrating lymphocyte (TIL) density provided an OS benefit for patients (206). The group of Ĵerôme Galon has investigated TIL infiltration within CRC further. In particular, in 2005, immune infiltration analysis of 959 resected CRC samples revealed that the absence of metastasis correlated with the presence of effector memory T cells (207). Early metastatic disease can be defined by the presence of vascular emboli, lymphatic invasion, and perineural invasion (VELIPI) and carries a prognostic significance. After adjustment for TNM stage, VELIPI negative tumours were found to associate with better patient survival. Accordingly, VELIPI negative tumours also correlated with a strong immune cell infiltrate. Higher levels of CD8, granzyme B and granulysin were detected as well as a significant increase in Th1 markers such as T-bet, IRF-1 and IFN-γ compared to resected VELIPI positive tumours. Furthermore, flow cytometry using 410 combinations of surface marks showed that CD3$^+$ T cells were the most

prevalent immune cells infiltrating CRC tumours. This was accompanied by increases in $CD4^+$ and $CD8^+$ T cells in VELIPI negative tumours. Effector memory $CD45RO^+$, $CR7^-$ $CD28^-$ $CD27^-$ T cells were also highly abundant. It was observed that the number of memory T cells was associated with lymph node (LN) involvement, with immunohistochemical analysis showing high CD45RO infiltration in VELIPI negative tumours and low numbers of CD45RO cells in VELIPI positive tumours. It was observed that CD45RO status was an independent prognostic factor for overall survival. Accordingly, 5-year survival was found to be 46.3% for high-density CD45RO tumours and 23.7% for CD45RO low-density tumours (207).

Following this study the same group went on to demonstrate that the type, density and location of the immune cell infiltrate can influence clinical outcome regardless of CRC tumour stage; indicating that immunological data could possibly be a better prognostic tool than current histopathological methods (208). When evaluating the expression of genes related to immunity, a cluster of patients emerged with a clear Th1 phenotype. Within this cluster the expression levels of genes including T-bet, IRF-1, IFN-γ, CD3-z, CD8, granulysin, and granzyme B inversely correlated with tumor recurrence (208). Furthermore, *in situ* immune responses were analysed in the center of the tumour (CT) and at the invasive margin (IM). Results from three separate cohorts of CRC patients show that high $CD3^+$ infiltration at either the CT or IM correlated with better DFS. Moreover, combined analysis of CT and IM regions increased the accuracy of DFS and OS prediction compared to single region analysis. Strikingly this correlation between high-density immune infiltration and increased survival remained regardless of the extent of tumour invasion and lymph node involvement. Furthermore, in corroboration with the previous findings, low levels of CD45RO T cells in both CT and IM regions results in an extremely poor prognosis, similar to that seen in patients harboring metastatic disease (208).

1.7.2 Th17

A study by Tosilini and colleagues investigated T helper subpopulations (Th1, Th2, Th17 and Treg) in CRC tumours using gene expression analysis (209). Gene clusters associated with each subpopulation were identified and interestingly it was observed that patients with high expression of the Th17 cluster had a very bad prognosis. In contrast Th1 cluster expression was associated with a good outcome as expected. Further analysis of the complementary effects of Th1 and Th17 immune reactions revealed that patients with a $Th1^{lo}/Th17^{lo}$ phenotype still had a better 5-year survival than patients with $Th1^{lo}/TH17^{hi}$ tumours (209). This indicates that Th17 cells are associated with tumour recurrence. In support of this, Th17 cells within the blood of CRC patients are increased compared to healthy donors and increase further with disease stage (210) As mentioned previously Th17 cells are often involved in driving inflammation in conditions such as IBD. This in turn increases the risk of developing CRC. Mouse studies have investigated the role of IL-17A in the promotion of CRC. In particular, Chae *et al*. observed that in $APC^{min/+}$ mice, which spontaneously develop CRC, develop fewer tumours when IL-17A is ablated (211). This was accompanied by a reduction in proinflammatory cytokines and preservation of intestinal architecture, suggesting that IL-17A helps to drive spontaneous tumourigenesis via inflammatory processes (211). In support of this finding Hyan and colleagues observed a role for IL-17A in a model of colitis-associated cancer (CAC). CAC develops from IBD where chronic inflammation can create damage to induce mutations within tumour-related genes. It was observed that after treatment of IL-17A KO and WT mice with azoxymethane (AOM) and DSS to induce tumour formation. Tumour incidence was lower within KO animals (212). Furthermore, where tumours did develop, they were fewer in number and smaller in size within IL-17A KO mice.

Ki67 staining revealed reduced proliferation of intestinal cells and tumour cells within IL-17 KO mice. This was accompanied by down regulation of cell cycle associated proteins cyclin D and cyclin E, as well as lower levels of β-catenin. Analysis of transcription factor expression also showed a reduction in STAT-3, which is a known tumour promoter. Together this data highlighted the close relationship between IL-17A, inflammation and CRC progression (212). Comparable results were also demonstrated in a mouse model of sporadic cancer. Grivennikov and colleagues used CPC-APC mice that develop tumours within the distal colon due to lack of the APC gene (213). The group show that as within humans, IL-23 and IL-17A is increased within CPC-APC tumours. Removal of IL-23, the promoter of Th17 cells, diminished tumour frequency as well as reducing levels of STAT-3 expression and cell proliferation rates. Flow cytometry analysis revealed that IL-23 production in the tumour is linked to $CD11b^+$ and $F4/80^+$ cells such as tumour associated macrophages (TAM). As discussed earlier, IL-23 can be secreted in response to recognition of the microbiota via PRRs. This study suggested that intestinal epithelial barrier deterioration could allow for the translocation of bacterial product to drive IL-23 expression from myeloid cells in CPC-APC mice. Small sections of colon were clamped and then injected with 4kDa FITC dextran or LPS and the amount detected within the circulation after 1 hour was measured. Results indicate that increased 4kDa FITC and LPS passage occurred in CPC-APC mice compared to WT animals, indicating barrier dysfunction. In support of this, the expression of some TJ molecules was also reduced (213). These finding suggest that microbial products could promote a detrimental Th17 cell response that can encourage tumour progression.

1.7.3 Tregs

The influence of Treg cells in CRC development has been somewhat controversial. Certain studies indicate a high $FoxP3^+$ cell tumour infiltration is associated with better survival while others show the opposite. Ling and colleagues observed that CRC patients have a higher frequency of $FoxP3^+$ cells within peripheral blood compared to healthy donors (8% vs 2.2% respectively) (214). Furthermore, Treg tumour infiltration was significantly increased in relation to healthy background colonic tissue (214). Our laboratory supports these findings. In a detailed study investigating anti-tumour immune responses before and after surgery, it was observed that Tregs did impact on CEA and 5T4 $CD4^+$ T cell responses (215). In particular, after surgery an increased number of patients were able to respond to 5T4. Moreover, the magnitude of response was also increased. While analysing tumour recurrence it was observed that patients relapsing 12 months post-surgery were those found to have pre-operative responses that were Treg suppressed (215). In a follow up study, it was shown that 5T4 responses gradually declined with advanced disease while Treg numbers increased (216). This data implied that a high density of Tregs could detrimentally mask anti-tumour responses. The clinical trial TaCTiCC provided further evidence, showing that reduction of Treg cells with low dose cyclophosphamide resulted in improved IFN-γ responses, correlating with a significant delay in tumour progression (202).

On the other hand, Salama and colleagues have reported that tumour infiltration with $FoxP3^+$ cells resulted in significantly better survival in a study involving 967 CRC patients (217). Frey *et al*. reported a similar result while investigating the prognostic significance of tumour Treg infiltration in MMR-proficient and deficient CRCs (218). The group showed that in two groups of MMR-proficient patients, a

high density of Tregs was associated with earlier pT stage and lymph node negative tumours. In MMR-deficient cases, high density FoxP3 was again more commonly found in tumours with no LN involvement and in those without vascular invasion (218). Upon analysis of 5-year survival, after adjustment for other well established prognostic factors it was observed that high Treg density correlated with better survival in MMR-proficient tumours (218).

A review by Ladoire and colleagues discussed how CRC is a unique type of cancer, in that it develops in close proximity to the intestinal microbiota. Unsurprisingly, studies have shown that a large number of bacterial species are enriched within colorectal tumours. As mentioned previously, it is known that intestinal bacteria can stimulate the production of proinflammatory cytokines, which can lead to pro-angiogenic and tumour enhancing effects through activation of transcription factors such as NFκβ and STAT-3 (219). It has been suggested that T cells infiltrating CRC tumours may in fact be targeting microbial invasion instead of having direct anti-tumour effects. In an early mouse study by Erdman *et al*. it was observed that reducing bacterial inflammation could inhibit colon carcinogenesis (220). Rag-deficient mice orally inoculated with the enteric mouse pathogen *Helicobacter hepaticus* were found to develop intestinal inflammation with adenocarcinoma with muscle invasion within sixty days. In contrast WT animals did not develop an inflammatory or carcinogenic phenotype. Furthermore, the transfer of Tregs into Rag-deficient mice prior to inoculation prevented cancer development. This indicates that Treg control of bacterial induced inflammation can be beneficial in preventing CRC (220). In a more recent study evaluating Treg infiltration it was shown that both $FoxP3^{hi}$ and $FoxP3^{lo}$ Treg populations infiltrate CRC tumours (221). In particular, the abundance of $FoxP3^{lo}$ Tregs was associated with a better survival outcome than those patients with predominantly $FoxP3^{hi}$ infiltration. The authors suggest that

FoxP3^{hi} cells could be preventing anti-tumour responses while FoxP3^{lo} cells could have a role in suppressing inflammation derived from microbial infiltration (221). In support of this it was observed that high FoxP3^{lo} T cell density was associated with the presence of the microbe *Fusobacterium nucleatum*, a gram-negative anaerobe identified as having links with poor survival in CRC patients (222).

1.8 Aims and Hypotheses

Within this study two hypotheses were tested in an attempt to determine why CRC cancer patients with blood derived CEA specific responses have a poor survival outcome compared to non-responding patients (194):

1. IL-17A and/or IL-17A/IFN-γ CEA-specific T cells exist within CRC patients and are involved in the poor survival prognosis associated with preoperative CEA-specific T cell responses.

The following aims were used to test this hypothesis:

- Evaluate the frequency of peripheral blood IFN-γ, IL-17A, and IL-17A/IFN-γ CEA-specific and 5T4-specific responses in a cohort of preoperative CRC patients.
- Determine the frequency and phenotype of T cells within the healthy bowel, tumour and peripheral blood of CEA-responding and non-responding CRC patients.

2. Patients harbouring CEA-specific IFN-γ responses have increased intestinal permeability leading to tumour progression through tumour associated inflammation.

The following aims were used to test this hypothesis:

- Construct and optimise an Ussing chamber system to evaluate intestinal permeability.
- Evaluate the intestinal permeability of colonic biopsies in a cohort of patients undergoing colonoscopy.
- Measure peripheral blood CEA and 5T4 specific T cell responses and analyse with permeability observations.

Chapter 2. Materials and Methods

2.1 Materials

All chemicals were purchased from Sigma Aldrich (unless stated otherwise). Phosphate buffered saline (PBS) pH7.2 was purchased from Gibco, Paisley, UK. Barnstead ultra filtered DNA & RNA free diH_20 (ThermoFisher, UK) was used to prepare all buffers and reagents.

2.1.1 Patient recruitment

Blood and colonic samples were obtained from patients undergoing investigative colonoscopy procedures or colorectal surgery at The University Hospital of Wales. All subjects gave informed consent to take part in this ethically approved study (consent form can be seen in the Appendix). The Wales Research Ethics Committee granted ethical approval (reference number:15/WA/0291). Patient characteristics are summarised in Table 2.1 and Table 2.2 for surgical CRC patients and endoscopy patients respectively.

2.1.2 Histopathological tumour grading

Colorectal tumours used were analysed for overall size, invasive status and lymph node involvement, confirmed by consultant pathologists at the University Hospital of Wales. Each specimen was then graded. Dukes' classification and TNM staging parameters are shown in Table 2.3 and 2.4 respectively.

2.1.3 Healthy donors and age matched controls

Peripheral blood was taken from members of the laboratory and age-matched healthy controls with no history or clinical evidence of malignancy. All donors were consented before obtaining samples.

Table 2.1. Surgical CRC patient characteristics where cultured CEA and 5T4 responses have been analysed (note that 1 patient had two tumours).

	All Patients	Male	Female
Number (%)	40	22 (55)	18 (45)
Age (Range)	67 (42-87)	65 (42-87)	70 (52-87)
Tumour Location (%)	Caecum	5 (12.5)	3 (7.5)
	Ascending	0 (0)	3 (7.5)
	Hepatic Flexure	1 (2.5)	2 (5)
	Transverse	2 (5)	2 (5)
	Sigmoid	9 (22.5)	2 (5)
	Rectum	5 (12.5)	6 (15)
TNM Staging (%)	T1	4 (10)	1 (2.5)
	T2	1 (2.5)	1 (2.5)
	T3	12 (30)	12 (30)
	T4	6 (15)	4 (10)
Lymph Node Spread (%)	N0	11 (27.5)	12 (30)
	N1	7 (17.5)	6 (15)
	N2	4 (10)	1 (2.5)
Dukes' Stage (%)	A	4 (10)	2 (5)
	B	7 (17.5)	10 (25)
	C1	10 (25)	5 (12.5)
	C2	1 (2.5)	0 (0)
	D	1 (2.5)	1 (2.5)

Table 2.2. Endoscopy patient characteristics where cultured CEA and 5T4 responses or intestinal permeability was analysed.

	All patients	Male	Female
Number (%)	26	13 (50)	13 (50)
Age (range)	(29-73)	(29-70)	(52-73)
Adenoma patient number (%)	9	3 (33.3%)	6 (66.6%)
Age (Range)	(52-68)	64 (61-67)	62.5 (52-68)
Location of adenoma	Caecum	1	2
	Transverse	0	1
	Sigmoid	1	2
	Rectum	0	2
	Unidentified	1	0
CRC Patient number	1	1	0
Age	60	-	-
Tumour Location	Rectum	1	0

Table 2.3. Dukes' staging parameters

Grade	Parameters
Dukes' A	Invasion but not through the bowel wall.
Dukes' B	Invasion through the bowel wall; no lymph node involvement.
Dukes' C1	Extending into muscularis propria; local lymph nodes involved.
Dukes' C2	Penetrating muscularis propria; local and apical lymph nodes involved
Dukes' D	One or more metastatic sites

Table 2.4. TNM staging parameters

Grade	Parameters
T1	Tumour no more than 2 cm across (invades submucosa)
T2	Tumour more than 2 cm but no more than 5cm across (invades muscularis propria)
T3	Tumour greater that 5 cm across (invades serosa)
T4	Tumour has grown into adjacent tissues
N0	No spread to regional lymph nodes
N1	1-3 regional lymph nodes involved
N2	4 or more regional lymph nodes involved
M0	No metastasis
M1	Distant metastasis

2.1.4 Media

R+ media

RPMI-1640 media supplemented with 2 mM L-glutamine, 1 mM sodium pyruvate, 50 µg/ml penicillin and streptomycin (Gibco, Paisley, UK) was used for PBMC wash steps.

R5 media

RPMI-1640 media supplemented with 2 mM L-glutamine, 1 mM sodium pyruvate, 50 µg/ml penicillin, streptomycin (Gibco, Paisley, UK) and 5% human AB serum (Welsh Blood Service, Pontyclun, UK) was used for PBMC culture.

R5 IL-2 media

RPMI-1640 media supplemented with 2 mM L-glutamine, 1 mM sodium pyruvate, 50 µg/ml penicillin, streptomycin (Gibco, Paisley, UK), 5% human AB serum (Welsh Blood Service, Pontyclun, UK), 40IU IL-2 was used for PBMC feeds.

CTL test plus serum free media

CTL Test Plus supplemented with 2 mM L-glutamine, 1 mM sodium pyruvate, 50 µg/ml penicillin, streptomycin (Immunospot, Bonn, Germany) was used for PBMC culture in Chapter 5 only.

CTL test plus serum free IL-2 media

CTL Test Plus supplemented with 2 mM L-glutamine, 1 mM sodium pyruvate, 50 µg/ml penicillin, streptomycin and 40IU IL-2 (Immunospot, Bonn, Germany) was used for PBMC feeds in Chapter 5 only.

TIL extraction media

RPMI-1640 supplemented with 2 mM L-glutamine, 1 mM sodium pyruvate, 50 µg/ml penicillin, streptomycin (Gibco, Paisley, UK), and gentamicin (Life Technologies, UK) and 2 µg/ml of Fungizone (Amphotericin B, Life Technologies, UK).

TIL/CIL resting media

RPMI-1640 supplemented with 2 mM L-glutamine, 1 mM sodium pyruvate, 50µg/ml of penicillin and streptomycin (Gibco, Paisley, UK), 10 µg/ml gentamicin (Life Technologies), 1 µg/ml of Fungizone (Amphotericin B, Life Technologies, UK) and 10% human AB serum (Welsh Blood Service, Pontyclun, UK).

2.1.5 Peripheral blood mononuclear cell (PBMC) extraction and primary cell culture reagents:

Lymphoprep

20 ml lymphoprep (Axis-Shield, Dundee, Scotland, UK) was used to separate whole blood.

Novocyte flow cytometer

Used for absolute PBMC cell counts (ACEA Bioscience, Inc, San Diego, USA)

Culture plate

96 well U-bottom plates (Nunc, ThermoFisher Scientific, UK) were used for all PBMC cultures.

Cell kine

Sourced from Helvetica Healthcare, UK.

Antigens/Mitogens

Tuberculin purified protein derivative (PPD; Statens Serum Institute, Denmark), Hemagglutinin (HA; kindly provided by Sir John Skehel, NIMR) and phytohemagglutinin (PHA; Sigma-Aldrich) were used as control antigens/mitogens. All were used at a concentration of 4 µg/ml.

CEA and 5T4 antigens

The CEA protein sequence AAA51967.1 was used to provide seventy 20 amino acid long peptides, each overlapping by 10 residues and covering the entire protein. Synthesized by GLBiochem (Shanghai, Shanghai, China) and with purity greater than 90%, these peptides were used to create two CEA "super pools" suspended in 20% dimethyl sulfoxide (DMSO). CEA peptide pool 1 (PP1) covered peptides 1 to 35 and CEA peptide pool 2 (PP2) covered peptides 36 to 70 (Table 2.5). Forty-one peptides overlapping by 10 amino acids were also synthesized to cover the entire human 5T4 protein (GL Biochem, Shanghai, China). Two 5T4 "super pools" were created with PP1 covering peptides 1 to 20 and PP2 covering peptides 21 to 41 (Table 2.6). All "super pools" were used at a final well concentration of 1.45 µg/ml/peptide

Table 2.5. CEA 20mer peptide sequences

No	Sequence	No	Sequence
P1	MESPSAPPHRWCIPWQRLLL	**P36**	NTTYLWWVNNQSLPVSPRLQ
P2	WCIPWQRLLLTASLLTFWNP	**P37**	QSLPVSPRLQLSNDNRTLTL
P3	ASLLTFWNPPTTAKLTIES	**P38**	LSNDNRTLTLLSVTRNDVGP
P4	PTTAKLTIESTPFNVAEGKE	**P39**	LSVTRNDVGPYECGIQNELS
P5	TPFNVAEGKEVLLLVHNLPQ	**P40**	YECGIQNELSVDHSDPVILN
P6	VLLLVHNLPQHLFGYSWYKG	**P41**	VDHSDPVILNVLYGPDDPTI
P7	HLFGYSWYKGERVDGNRQII	**P42**	VLYGPDDPTISPSYTYYRPG
P8	ERVDGNRQIIGYVIGTQQAT	**P43**	SPSYTYYRPGVNLSLSCHAA
P9	GYVIGTQQATPGPAYSGREI	**P44**	VNLSLSCHAASNPPAQYSWL
P10	PGPAYSGREIIYPNASLLIQ	**P45**	SNPPAQYSWLLIDGNIQQHTQ
P11	IYPNASLLIQNIIQNDDTGFY	**P46**	IDGNIQQHTQELFISNITEK
P12	NIIQNDTGFYYTHVIKSDLV	**P47**	ELFISNITEKNSGLYTCQAN
P13	TLHVIKSDLVNEEATGQFRV	**P48**	NSGLYTCQANNSASGHSRTT
P14	NEEATGQFRVYPELPKPSIS	**P49**	NSASGHSRTTVKTITVSAEL
P15	YPELPKPSISSNNSKPVEDK	**P50**	VKTITVSAELPKPSISSNNS
P16	SNNSKPVEDKDAVAFTCEPE	**P51**	PKPSISSNNSKPVEDKDAVA
P17	DAVAFTCEPETQDATYLWWV	**P52**	KPVEDKDAVAFTCEPEAQNT
P18	TQDATYLWWVNNQSLPVSPR	**P53**	FTCEPEAQNTTYLWWVNGQS
P19	NNQSLPVSPRLQLSNGNRTL	**P54**	TYLWWVNGQSLPVSPRLQLS
P20	LQLSNGNRTLTLFNVTRNDT	**P55**	LPVSPRLQLSNGNRTLTLFN
P21	TLFNVTRNDTASYKCETQNP	**P56**	NGNRTLTLFNVTRNDARAYV
P22	ASYKCETQNPVSARRSDSVI	**P57**	VTRNDARAYVCGIQNSVSAN
P23	VSARRSDSVILNVLYGPDAP	**P58**	CGIQNSVSANRSDPVTLDVL
P24	LNVLYGPDAPTISPLNTSYR	**P59**	RSDPVTLDVLYGPDTPIISP
P25	TISPLNTSYRSGENLNLSCH	**P60**	YGPDTPIISPPDSSYLSGAN
P26	SGENLNLSCHAASNPPAQYS	**P61**	PDSSYLSGANLNLSCHSASN
P27	AASNPPAQYSWFVNGTFQQS	**P62**	LNLSCHSASNPSPQYSWRIN
P28	WFVNGTFQQSTQELFIPNIT	**P63**	PSPQYSWRINGIPQQHTQVL
P29	TQELFIPNITVNNSGSYTCQ	**P64**	GIPQQHTQVLFIAKITPNNN
P30	VNNSGSYTCQAHNSDTGLNR	**P65**	FIAKITPNNNGTYACFVSNL
P31	AHNSDTGLNRTTVTTITVYA	**P66**	GTYACFVSNLATGRNNSIVK
P32	TTVTTITVYAEPPKPFITSN	**P67**	ATGRNNSIVKSITVSASGTS
P33	EPPKPFITSNNSNPVEDEDA	**P68**	SITVSASGTSPGLSAGATVG
P34	NSNPVEDEDAVALTCEPEIQ	**P69**	PGLSAGATVGIMIGVLVGVA
P35	VALTCEPEIQNTTYLWWVNN	**P70**	IMIGVLVGVALI

Table 2.6. 5T4 20mer peptide sequences

No	Sequence	No	Sequence
P1	MPGGCSRGPAAGDGRLRLAR	**P22**	GLRRLELASNHFLYLPRDVL
P2	AGDGRLRLARLALVLLGWVS	**P23**	HFLYLPRDVLAQLPSLRHLD
P3	LALVLLGWVSSSSPTSSASS	**P24**	AQLPSLRHLDLSNNSLVSLT
P4	SSSPTSSASSFSSSAPFLAS	**P25**	LSNNSLVSLTYVSFRNLTHL
P5	FSSSAPFLASAVSAQPPLPD	**P26**	YVSFRNLTHLESLHLEDNAL
P6	AVSAQPPLPDQCPALCECSE	**P27**	ESLHLEDNALKVLHNGTLAE
P7	QCPALCECSEAARTVKCVNR	**P28**	KVLHNGTLAELQGLPHIRVF
P8	AARTVKCVNRNLTEVPTDLP	**P29**	LQGLPHIRVFLDNNPWVCD
P9	NLTEVPTDLPAYVRNLFLTG	**P30**	LDNNPWVCDCHMADMVT
P10	AYVRNLFLTGNQLAVLPAGA	**P31**	HMADMVTWLKETEVVQGKDR
P11	NQLAVLPAGAFARRPPLAEL	**P32**	ETEVVQGKDRLTCAYPEKMR
P12	FARRPPLAELAALNLSGSRL	**P33**	LTCAYPEKMRNRVLLELNSA
P13	AALNLSGSRLDEVRAGAFEH	**P34**	NRVLLELNSADLDCDPILPP
P14	DEVRAGAFEHLPSLRQLDLS	**P35**	DLDCDPILPPSLQTSYVFLG
P15	LPSLRQLDLSHNPLADLSPF	**P36**	SLQTSYVFLGIVLALIGAIF
P16	HNPLADLSPFAFSGSNASVS	**P37**	IVLALIGAIFLLVLYLNRKG
P17	AFSGSNASVSAPSPLVELIL	**P38**	LLVLYLNRKGIKKWMHNIRD
P18	APSPLVELILNHIVPPEDER	**P39**	IKKWMHNIRDACRDHMEGYH
P19	NHIVPPEDERQNRSFEGMVV	**P40**	DACRDHMEGYHYRYEINADPR
P20	QNRSFEGMVVAALLAGRALQ	**P41**	YRYEINADPRLTNLSSNSDV
P21	AALLAGRALQGLRRLELASN		

2.1.6 FluoroSpot assay reagents

FluoroSpot kit

Human IFN-γ/IL-17 was sourced from MabTech, West Sussex, UK.

FluoroSpot plates

PVDF membrane plates (IPFL; Millipore).

Plate reader

Automated CTL-ImmunoSpot Reader (CTL, Bonn, Germany) equipped with filters for FITC (excitation 490 nm/emission 510 nm) and Cy3 (excitation 550 nm/emission 570 nm). Double secreting cells were visualised and enumerated by a computerized overlay.

2.1.7 Flow cytometry reagents

All antibodies used for flow cytometry are shown in Table 2.7 (human) and Table 2.8 (mouse).

Phorbol myristate acetate (PMA)/Ionomycin

Stimulation of PBMC was carried out using PMA and ionomycin (Sigma Aldrich, UK) at final concentrations of 50 ng/ml and 500 ng/ml respectively for five hours in combination with Brefeldin A (Sigma Aldrich, UK) at 2 μg/ml to prevent cytokine release.

FACS buffer

PBS (Gibco, Paisley, UK) containing 2% foetal calf serum (FCS) and 5mM EDTA.

FACS fix/permeabilisation buffer

Fixation/permeabilisation solution was sourced from eBioscience, UK.

FACS permeabilisation buffer

x10 permeabilization buffer (eBioscience, UK) was diluted 1:10 before use.

FACS fix

FACS buffer containing 2% paraformaldehyde (Sigma-Aldrich,UK).

Flow cytometer

Acquisition was carried out on the 8-colour BD FACSCanto II.

Table 2.7. Details of flow cytometry human antibodies.

Marker	Conjugate	Company	Clone	Final Concentration
CD3	PerCPCy5.5	Biolegend	UCHTI	5 µg/ml
CD4	BV421	Biolegend	OKT4	5 µg/ml
CCR6	PeCy7	BD	11A9	1:20
IFN-γ	APC eFluor780	eBioscience	4S.B3	1 µg/ml
IL-17A	APC	eBioscience	64DEC17	1.7 µg/ml
IL-10	PE	Biolegend	JES319F1	1.7 µg/ml
FoxP3	FITC	eBioscience	PCH101	6.6 µg/ml

Table 2.8. Details of flow cytometry mouse antibodies

Marker	Conjugate	Company	Clone	Final Concentration
CD4	FITC	Biolegend	GK1.5	0.25 µg/ml
CD8	BV421	Biolegend	53-6.7	0.5 µg/ml
FoxP3	APC	Invitrogen	FJK-16s	1 µg/ml
CD16/CD32	-	ebioscience	93	5 µg/ml

2.1.8 Animal model reagents

Male and female C57BL/6 FoxP3^{DTR} (109) and Balb/C DREG mice (223) (bread in house) were housed in filter top cages in the specific pathogen free (SPF) Joint Biological Service Unit (Cardiff University). The age and sex of mice are stated throughout this thesis. All experiments were performed in the home cage. Mice were maintained at a constant temperature, with 12-hour light/dark cycle and had access to standard mouse chow and water ad *libitium*. All experiments performed were ethically approved in accordance with the Animal Scientific Procedures Act 1986, in compliance with UK Home Office regulations (project license 30/3428) and were carried out by individuals holding a UK personal licence.

2.1.8.1 Dextran sodium sulphate (DSS) model

DSS

36,000-50,000 M.Wt DSS colitis grade (MP Biomedicals, UK) was prepared at 3% w/v in drinking water.

Occult blood test kits

Kindly provided by Lee Parry (Biosciences, Cardiff University) and sourced from Beckman Coulter, UK Ltd.

2.1.8.2 T-regulatory cell depletion mouse model

Diphtheria toxin

300µl intraperitoneal injection of diphtheria toxin in PBS (Native Antigen, UK) was given to animals giving a final concentration of 15 µg/kg.

Red blood cell lysis buffer

Diluted 1:10 with sterile water before use and sourced from Biolegend, UK.

2.1.9 Ussing chamber system materials and reagents

Equipment components

The Navicyte Ussing Chamber system and Ag/AgCl electrodes were purchased from Harvard Apparatus, UK and USA. EC825A volt/clamp boxes (Warner Instruments Inc, Connecticut, USA), Power-Lab 8/35 and Lab Chart software (AD Instruments, Oxford, UK) were used for data acquisition. Electrical cables were sourced from Maplin Electronics, Cardiff, UK. The aluminium electrical manifold was kindly built by Mr Richard Charlton and Mr Liam Atkinson (Newcastle, UK).

Gas cylinder

During Ussing Chamber experiments a gas supply of 95% oxygen and 5% Carbon dioxide (BOC, UK) was used.

Krebs buffers

All Krebs buffers were pH 7.2. Buffer compositions are shown in Table 2.9.

KCl saturated with Ag

Sourced from Sigma Aldrich, UK.

Permeability probes

Lucifer yellow CH Di-lithium salt and 4kDa Fluorescein isothiocyanate-dextran (Sigma Aldrich, UK) were diluted in Krebs buffer. Concentrations used are described throughout.

Reader

Clariostar plate reader (BMG, Labtech, Ortenberg, Germany) was used to measure fluorescence within Ussing samples.

Forskolin

Forskolin (Sigma Aldrich, UK) stock was made to 10 mM and diluted to give a working concentration of 333μM (15μl into 450μl Krebs buffer). 30μl of the working solution was added to give a final chamber concentration of 6.6μM.

Bleach

Household bleach (Tesco, Cardiff, UK) was used to chloride Ag/AgCl electrodes.

Cleaner

RBS 25 solution was sourced from Sigma Aldrich, UK to clean Ussing chambers.

Sylguard plates

Sylguard plates were made from a Dow Corning sylguard silicone and elastomer kit (Ellsworth Adhesives, East Kilbride, Scotland) by mixing the parts 10:1 respectively, pouring into a petri dish and leaving to dry at room temperature for 48 hours.

Biopsy forceps

EndowJaw oval fenestrated alligator non-spiked swing-jaw disposable biopsy forceps with a working length of 2300mm and minimal channel size of 2.8mm were used to obtain human colonic specimens (Olympus Medical Systems Corporation, Southend-on-Sea, UK).

Table 2.9. Details of Krebs buffers and concentrations.

Buffer	Concentration
Krebs Stock	136 mM NaCl, 1.5 mM $CaCl_2$*$2H_2O$, 4.3 mM KCl, 1.6 mM KH_2PO_4 , 27 mM $NaHCO_3$, 1.4 mM $MgSO_4$*$7H_2$
Glutamate Stock	114 mM Glutamate
Sodium Pyruvate Stock	115 mM Sodium Pyruvate
Glucose Stock	200 mM Glucose
Mannitol Stock	200 mM Mannitol
Transport Krebs	115.6mM NaCl, 1.3mM $CaCl_2$*$2H_2O$, 3.7mM KCl, 1.4mM KH_2PO_4, 23 mM $NaHCO_3$, 1.2 mM $MgSO_4$*$7H_2$
Glucose Krebs	5.8 mM Sodium Pyruvate, 5.7 mM Glutamate, 10 mM Glucose
Mannitol Krebs	5.8 mM Sodium Pyruvate, 5.7 mM Glutamate, 10 mM Mannitol

2.1.10 Histology reagents

Throughout this thesis, alcohol for histology was prepared using industrial methylated spirit (Fisher Scientific, UK).

10% Neutral buffered formalin saline (NBFS)

10% NBFS solution was sourced from Sigma Aldrich, UK.

Agar embedding

2% agar (Fisher, UK) was used to embed small colonic tissue samples

Paraffin embedding

A Shandon Tissue processor from ThermoFisher Scientific, UK was used to process samples for paraffin wax embedding. Processed samples were embedded into wax blocks using a Shandon Histocentre. The cycles used for samples are summarised in Table 2.10.

Cold block

Paraffin blocks were kept on a Leica, Histocore Arcadia C cold block before cutting to allow for easier sectioning.

Sectioning

Mx35 Premier^{+} blades (Thermo Scientific, UK) were used for sectioning colonic tissue on a microtome (Microm HM325, Thermo Scientific, UK). 5µm thick sections were placed on superfrost glass slides (Thermo Fisher Scientific, UK).

Haematoxylin

Haematoxylin stain was sourced from Sigma Aldrich, UK.

Eosin

Eosin-Y stain was sourced from Sigma Aldrich, UK.

DPX mounting medium

Sourced from Raymond A. Lamb waxes and general laboratory suppliers, UK.

Ammonia water solution

A working solution of 2% Ammonium hydroxide (Fisher Scientific, UK) was made by mixing with distilled water.

1% Acid alcohol solution

1ml of hydrochloric acid (Fisher Scientific, UK) was mixed with 100ml 70% ethanol (Fisher Scientific, UK).

CEA immunohistochemistry

The Link 48 autostainer (Agilent Technologies LDA UK Limited, Stockport, UK) was used to stain CRC samples using and flex mouse monoclonal anti-CEA

antibody (Agilent Technologies LDA UK Limited, Stockport, UK) and envision flex high pH kit (Agilent Technologies LDA UK Limited, Stockport, UK).

Histological analysis

Slides were imaged using the digital Axio Scan.z1 slide scanner or Apotome microscope, both from Zeiss, Germany.

Table 2.10. Shandon tissue processor cycles for colonic tissue samples

Reagent	Cycle Time (h)
70% Methanol (v/v)	1:00
90% Methanol	2:00
100% Methanol	2:00
100% Methanol	2:00
100% Methanol	2:00
100% Methanol	2:00
Xylene	2:00
Xylene	2:00
Xylene	2:00
Wax	2:00
Wax	2:00
Wax	2:00
Wax	2:00

2.2 Methods

2.2.1 Peripheral blood mononuclear ell (PBMC) extraction:

Peripheral blood was taken and PBMC were isolated by slowly layering whole blood over lymphoprep. Samples were centrifuged for 20 min, 2000 RPM. Based on size and density, PBMC form a layer (Figure 2.1). The PBMC layer was removed using a pasteur pipette and washed twice with R+ media. Cells were then enumerated using a haemocytometer under a light microscope by mixing cells 1:1 with Trypan blue. In later experiments an absolute PBMC count was determined using the Novocyte flow cytometer.

2.2.2 Primary cell cultures

Cultures of freshly isolated PBMC were set up to detect low frequency tumour-antigen specific responses. PBMC were seeded in a 96 well plate in R5 or CTL Test Plus Serum Free Media (Figure 2.2). On day 0 HA and PPD were added at a final concentration of 4 µg/ml and all peptide pools were added at a final concentration of 1.45 µg/ml/peptide. On day 3 PBMCs were fed with 10µl Cell Kine media and with 100µl fresh IL-2 media on days 6 and 9, resulting in a final concentration of 20 IU/ml IL-2/well. The culture plate was kept in sterile conditions at all times at 37°C for 14-15 days before re-stimulation. The wells on the edge of the plate were filled with PBS to prevent moisture loss from experimental wells

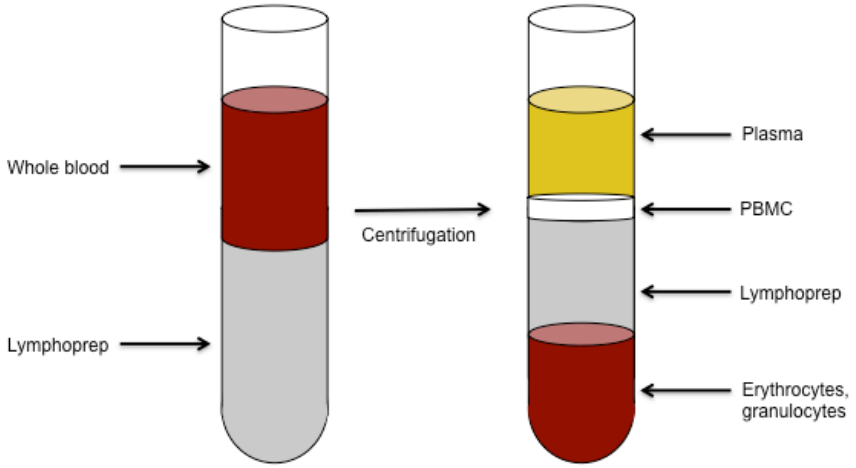

Figure 2 1. Isolation of PBMC from whole blood.
20ml of peripheral blood was layered on top of 20ml lymphoprep. After centrifugation a distinct band of PBMC is formed between the lymphoprep and plasma, as shown above.

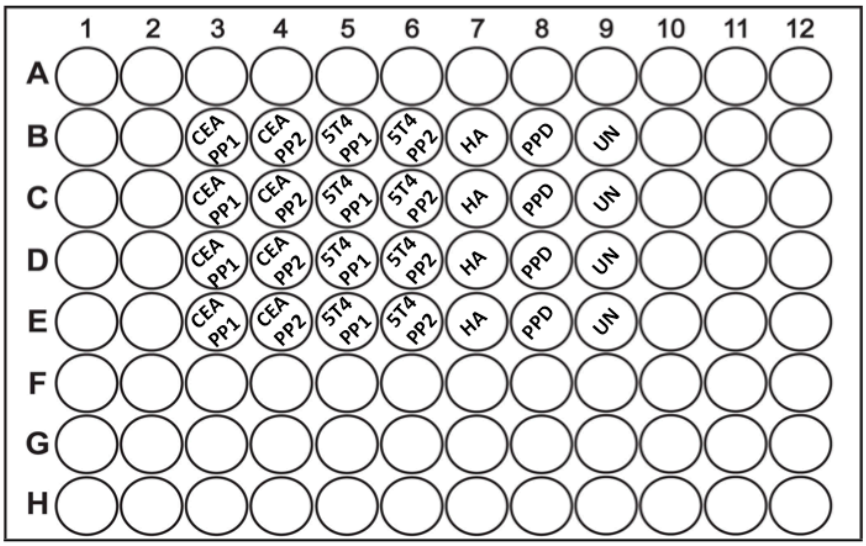

Figure 2.2. PBMC plate layout.
$0.5x10^6$ purified PBMC/well were seeded into a 96 well plate. Four replicate cell lines per condition were set up and PBMC stimulated with CEA, 5T4, control peptides or left un-stimulated.

2.2.3 FluoroSpot assay

A schematic of the FluoroSpot principle is shown in Figure 2.3. Membranes of a 96-well low fluorescent PVDF plate were activated for 1 minute with 35% ethanol then washed five times with PBS. Membranes were coated with 80µl of an anti-IFN-γ (1-D1K) and anti-IL-17A (MT44.6) mix, each at a final concentration of 15 µg/ml. Plates were incubated at 4°C overnight then washed with PBS five times and blocked with 100µl culture media for at least 30 minutes. After 14-15 days PBMC cultured in quadruplicate as shown in Figure 2.2 were removed from the incubator and two identical lines were pooled together, before being washed three times with PBS (e.g. lines in row B were pooled with lines in row C and lines in row D were pooled with lines in row E. PBMC were re-suspended in 200µl culture media. 100µl was added into each FluoroSpot well to provide $5x10^6$ PBMC/well. Peptide pools were added to one half of each culture condition for direct comparison of IFN-γ and IL-17 responses versus background. Plates were incubated at 37°C, 5% CO_2 for approximately 42 hours. PBMC were discarded and plates washed five times with PBS. Primary detection antibodies were prepared by mixing anti-IFN-γ (7-B6-1-FS-FITC, 1:200) and anti-IL17A (MT504-Biotin, 2 µg/mL) diluted in PBS containing 0.1% bovine serum albumin (BSA), before adding 80µl to each well. The plate was incubated for two hours at room temperature then washed five times with PBS. Anti-FITC-490 and anti-SA-550 (1:200) were diluted in PBS containing 0.1% BSA and 80µl of the mix added to each well. The plate was incubated for one hour in the dark at room temperature then washed five times with PBS. 50µl/well of fluorescence enhancer was added for 15 minutes. Fluorescence enhancer was removed by firmly tapping the plate onto paper towels and then the plate was left to dry for 48 hours in the dark at room temperature before spot analysis. Cytokine producing PBMC were enumerated at the single cell level by

counting the number of spots/well using an automated plate reader. Positive IFN-γ, IL-17A and IFN-γ/IL17A responses were identified by a minimum of 50, 25 and 10 spot-forming cells (SFC) per $5x10^5$ cultured cells, respectively, and a minimum 50% increase above background. In Chapter 5 only, $1.25x10^5$ cells were plated into the FluoroSpot plate after culture.

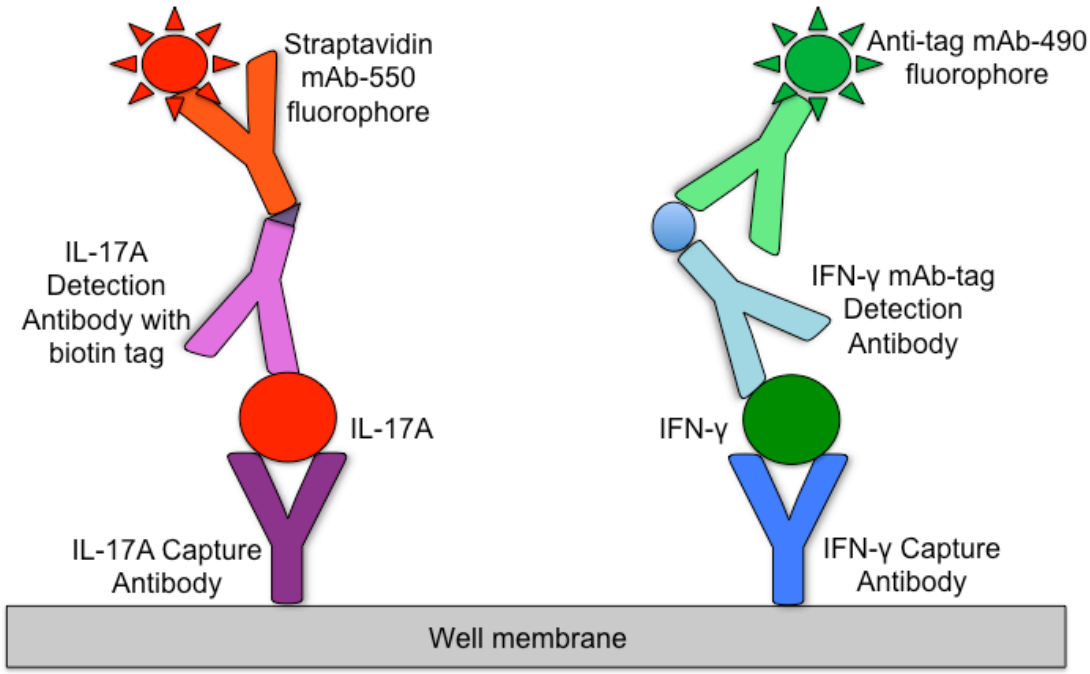

Figure 2.3. FluoroSpot assay principle.
Well membranes are coated with capture antibodies to bind IFN-γ and IL-17A released from activated cells. Once cells are washed away, tagged detection antibodies bind to a different epitope of each analyte. Antibodies conjugated to fluorophores with non-overlapping emission wavelengths bind to each detection antibody. Upon UV stimulation the fluorophores excite, allowing IFN-γ and IL-17A to be visualised simultaneously.

2.2.4 Collecting patient samples

Samples of tumour and healthy bowel were obtained from theatre and dissected by a pathologist. Tissues were then transferred to the laboratory in warm TIL extraction media.

2.2.5 Preparation of single cell suspensions from human tissues

Tumour and colon samples were minced into a fine pulp on a petri dish using a blade and then filtered through a 70μm cell strainer to isolate infiltrating cells. Cells were centrifuged twice in TIL extraction media at 2000 RPM for 10 minutes at room temperature. Supernatants were removed carefully using a stripette to prevent loosening of the cell pellet. Mechanical dissociation was used to obtain a single cell suspension. After washing, cells were left overnight to rest in the incubator suspended in TIL/CIL resting media.

2.2.6 Preparation of murine splenocytes

Single cell suspensions of spleens were prepared by filtering mashed tissue through a 70μm cell strainer with R+ media. 5ml red blood cell lysis buffer was added for 5 minutes to lyse red blood cells.

2.2.7 Animal models

2.2.7.1 DSS mouse model

FoxP3^{DTR} mice were given 50ml of 3% DSS in drinking water to induce intestinal inflammation. Mice were housed individually and a record of water consumption and weight as well as a stool sample was obtained daily. Fresh DSS water was supplied every three days. Animals were harvested when blood was observed within the stool and/or within the cage, this was typically from day 7 to day 9.

2.2.7.2 Occult blood testing

Murine stool samples were smeared onto filter paper treated with guaiac resin (≥0.05 mg). Hydrogen peroxide developer solution was then applied. In the presence of blood, the haem component of haemoglobin catalyses a reaction where hydrogen peroxide oxidises the guaiac resin, producing a blue-coloured quinone compound.

2.2.7.3 FoxP3^{DTR} mouse model

FoxP3^{DTR} mice were injected Intraperitoneally with 300µl of diphtheria toxin (15 µg/kg) three times a week (Monday, Wednesday and Friday) for up to 15 days. Mice were harvested with the onset of autoimmune symptoms (e.g. piloerection, scaly skin).

2.2.8 Flow cytometry

2.2.8.1 Antibody staining

0.2-1x10^6 PBMC, colon infiltrating lymphocytes and TILs were seeded in 96-well plates and washed twice with 200µl sterile PBS. 3µl of aqua amine-reactive viability dye was added directly to the cell pellet to stain dead cells. Cells were incubated in the dark at room temperature for 15 minutes. Cold FACS buffer was used to wash cells three times. After the final wash, 30µl of FACS buffer was added to each well and anti-human surface antibodies added (Table 2.7). Cells were incubated in the dark 4°C for 15-20 minutes and then washed twice with 150µl FACS buffer. Cells were then incubated with 200µl of fixation/permeabilisation solution overnight. Cells were washed with 1x permeabilisation buffer and incubated with 30µl of 1x permeabilisation buffer containing 2% rat serum to block FC receptors for 15 minutes at 4°C. Without washing, anti-human antibodies used to stain intracellular markers/cytokines were added (Table 2.7) and incubated in the dark at 4°C for 30 minutes. Cells were next washed once with 1x permeabilisation buffer and fixed in FACS fix prior to acquisition.

2.2.8.2 Murine antibody staining

The same protocol as above was used. However anti-mouse antibodies detailed in Table 2.8 were used for staining and CD16/CD32 was used to block Fc receptors.

2.2.8.3 Activation for intracellular cytokines

Cells were stimulated with PMA/ionomycin for five hours in combination with Brefeldin A before performing intracellular cytokine staining with the antibodies shown in Table 2.7.

2.2.8.4 Flow cytometry analysis

FlowJo V10.1 was used to analyse flow cytometry data.

2.2.9 Ussing chamber experiments

2.2.9.1 Buffers

Krebs stock buffer and transport buffer were stored at 4°C for a maximum of 3 weeks. Glutamate, sodium pyruvate, mannitol and glucose stock buffers were stored at 4°C for a maximum of 1 week. Glucose and mannitol Krebs buffers were freshly made on the day of Ussing experiments.

2.2.9.2 Glass barrel micro-reference electrode

Electrodes arrived in a “ready to use” state, previously being coated with AgCl. To ensure continued efficiency, electrodes were cleaned with dH_2O after each experiment. The ceramic tip of the electrode was kept in 3M KCl or deionised water in between uses and never allowed to dry out. After experiments, old AgCl coating was removed from electrodes by gently rubbing with steel wool. Electrodes were cleaned with dH_2O and immersed in household bleach for 24-48 hours before the beginning of experiments to ensure efficient chloriding of the silver wire was achieved and washed with deionised water before being assembled.

2.2.9.3 Electrode assembly

Top and bottom sections of the electrode cap are matched sets. The glass barrel was removed and filled with 3M KCl electrolyte solution, saturated with Ag

using a polyethylene filling tube. When assembling voltage detecting electrodes a red O-ring was stretched over the bottom of the glass barrel prior to filling. Electrodes were inserted into glass barrels and the cap ends attached as shown in Figure 2.4A. Voltage detecting electrodes were secured in place on the chambers using a screw while current passing electrodes were placed into grooves located within each chamber half (Figure 2.4B).

2.2.9.4 Chamber set-up

Prior to experiments, chambers were assembled in the absence of tissue and filled with 3ml transport Krebs buffer. The four Ag/AgCl electrodes were inserted into each chamber and connected to an EC825A voltage/Clamp unit to monitor voltage (mV) and to pass current (μA). Offset electrode potential was nullified after a minimum 30-40 minute equilibration period and initial resistance caused by buffer and the presence of a blue x-ray film piece (used to reduce aperture size) was calculated as explained in Chapter 4. Cumulative blue film and fluid resistance values were subtracted from tissue resistance values during analysis.

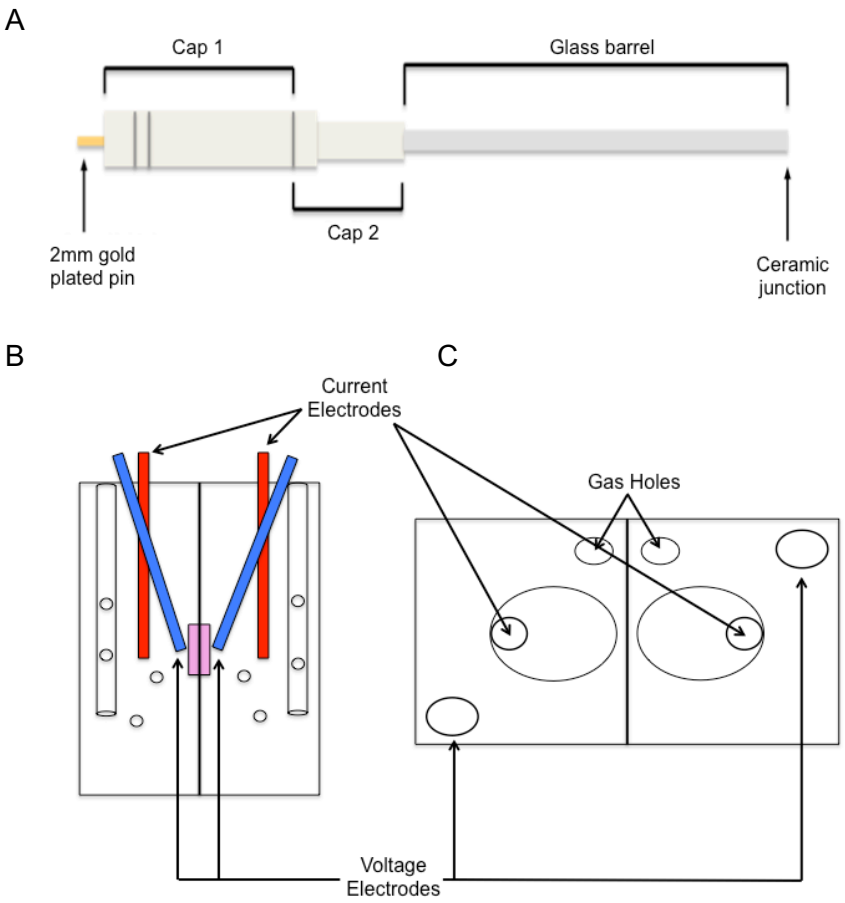

Figure 2.4. Ussing Chamber Electrodes and Chambers.
(A) Assembled electrode diagram. (B) Single chamber set up. Placements of voltage and current electrodes are shown along with the positioning of tissue (depicted as a pink box) and gas ports. (C) Birds eye view of chamber set up. Voltage electrodes are positioned at a 45° angle to be closest to the tissue while current electrodes are situated within small grooves found inside each half of the chamber.

2.2.9.5 Mouse tissue preparation

Prior to tissue collection transport Krebs, glucose Krebs and mannitol Krebs were bubbled with 95% O_2, 5% CO_2 for no less than 30 minutes and pH set to 7.3. Mice were culled by increased exposure to CO_2 and death confirmed by cervical dislocation before being dissected along the ventral midline to expose the abdomen. The gastrointestinal tract from the stomach to the rectum was carefully removed and the colonic region separated by dissecting directly below the cecum. Colonic samples were immediately flushed with 20ml ice-cold

transport Krebs buffer to remove waste products. Under 5x magnification colon samples were pinned down on to cold sylguard plates and opened longitudinally using micro-dissecting scissors. A piece of blue x-ray film punctured with a hole (aperture of 7.1 mm^2) was placed directly onto the mucosal surface and the chosen section dissected from the remainder of the colon. Using the blue X-ray film, sections were mounted mucosal side up onto six pins located on the inner surface of the Ussing chamber. A second piece of blue x-ray film, corresponding in size to the first, is placed on top to "sandwich" the tissue in place, preventing leakage. Once mounted the chamber halves are closed and secured in place with metal circlips. Transport buffer is added to each side of the chamber and chambers transported to the laboratory on ice for electrode addition. All samples were transported to the lab within 30 minutes.

2.2.9.6 Human biopsy preparation

Prior to tissue collection transport Krebs, glucose Krebs and mannitol Krebs were bubbled with 95%O_2, 5% CO_2 for no less than 30 minutes and pH set to 7.3. Qualified clinicians carrying out endoscopy procedures obtained biopsy samples using non-spiked forceps to avoid tissue damage. Up to six biopsy samples per patient were obtained and placed immediately in ice-cold transport Krebs buffer for transport to the laboratory. Under 5X magnification mucosal and serosal surfaces were identified and samples mounted mucosal side up into Ussing chambers. Biopsies were sandwiched between two pieces of blue x-ray film possessing identical holes giving an exposed tissue area of 0.79 mm^2.

2.2.9.7 Equilibration of tissue

Once tissue was mounted, residual transport buffer was removed using an electric vacuum pump. Serosal compartments were filled with 1.5ml 10 mM cold glucose Krebs buffer to provide the tissue with an energy source and mucosal compartments filled with 1.5ml cold 10 mM mannitol Krebs buffer to maintain

osmotic balance without effecting glucose mediated Na^+ transport. Buffers were added at a quick but steady pace to avoid dislodging the tissue. Electrodes were inserted at this time to monitor and achieve steady state potential difference (PD) values. Chambers were kept at 37°C using a circulating water bath and continuously oxygenated with 95% O_2, 5%CO_2 to aid tissue viability and provide buffer circulation. Buffers were renewed after 20 minutes and 30 minutes to remove auto-fluorescent molecules before measurements began.

2.2.9.8 Electrical measurements

The spontaneous tissue potential difference (PD) was measured continuously throughout experiments via the two voltage detecting Ag/AgCl electrodes. Experiments were performed in open circuit conditions where every five minutes short current pulses of 1.5, -1.5, 3 and -3μA with duration of 235ms were sent across the tissue via two Ag/AgCl current passing electrodes. Current stimulation was generated from an EC825A voltage/clamp unit via the PowerLab A/D D/A board controlled by a protocol developed in-house using LabChart software. The response of the tissue to current was measured at every stimulation event and the mean voltage response of four recordings was calculated. Resistance of the tissue at each five-minute recording was calculated using a linear least-squares fit model based on Ohm's Law which describes the relationship between voltage (V) current (I) and Resistance (R) as R=V/I. From the slope of the line resistance was calculated and PD was equal to the intersection of the Y-axis as shown in Figure 2.5. Short circuit current (Isc) can be calculated by PD/R. Note that electrical resistance takes into account both trancellular and paracellular passage (Figure 2.6).

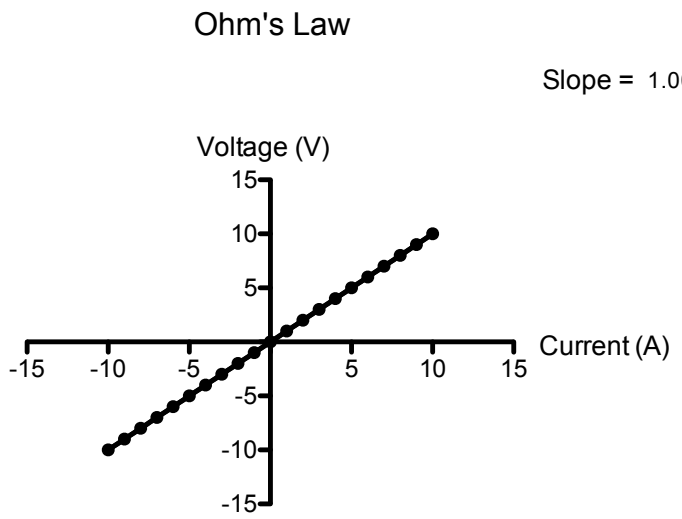

Figure 2.5. The principle of Ohm's law.
Ohm's law states that the flow of electric current is proportional to voltage and inversely proportional to resistance. Epithelial resistance can be calculated as the slope of the line.

2.2.9.9 Permeability Probe Studies

4kDa FITC-dextran and Lucifer yellow (457 daltons) were used as probes for measuring paracellular transport. Once tissue had equilibrated for 30 min and had a steady PD value, mannitol-Krebs buffer from the mucosal chamber was replaced with 150µl 4kDa FITC-dextran or Lucifer yellow to give a final chamber concentration of 500 µg/ml and 250 µg/ml respectively. At 60 and/or 120 minutes paired mucosal and serosal samples (150µl) were taken and fluorescence analysed on a plate reader. Concentrations of 4kDa FITC-dextran and Lucifer yellow were determined based on a standard curve generated from known concentrations to identify paracellular passage (Figure 2.6).

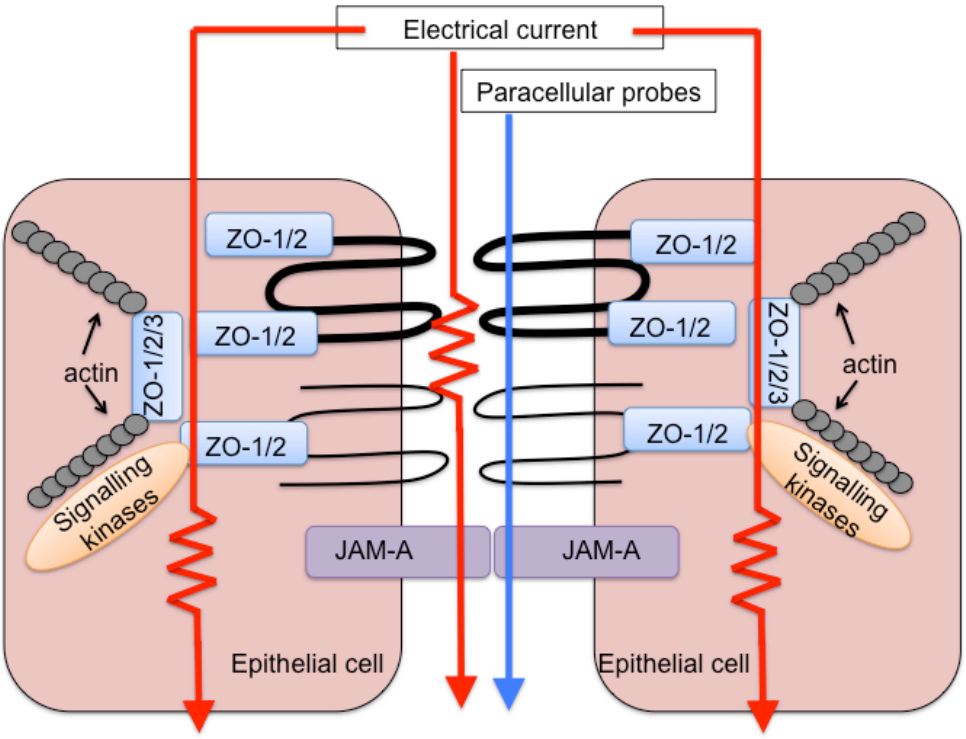

Figure 2.6. Electrical current and paracellular probe passage involved in Ussing experiments.
Current pulses are able to travel across the epithelial barrier through paracellular and transcellular routes. Epithelial cells act as both a conductor and a resistor to the current. TJ structures also give resistance to electrical current as well as to paracellular probe passage.

2.2.10 Immunohistochemistry

2.2.10.1 Tissue preparation

The full mouse colon was opened longitudinally and flattened out, mucosal side facing up. The tissue was wrapped around a large pair of forceps to create a "gut roll". This was pinned in place with a 23G needle and fixed in 10% NBFS buffer. Harvested spleen samples were also fixed using 10% NBFS. For samples ran in Ussing Chambers, 10% NBFS was added directly to chambers upon completion of Ussing experiments. Tissue was removed 2 days later and placed in universals containing 10% NBFS. A day later the 10% NBFS was replaced with 70% ethanol. Small sections of mouse tissue and human biopsies were agar embedded to ensure correct orientation of the tissue for sectioning (Figure 2.7). Samples were processed using a Shandon tissue processor, going

through automatic serial cycles of methanol to dehydrate the tissue in order to remove water from the specimen and allow the infiltration of wax. Cycles of xylene were used to clear the sample of methanol, as both methanol and water are immiscible in wax. Samples were then embedded into paraffin blocks. 5µm sections were cut using a microtome and placed onto glass slides for staining.

2.2.10.2 Haematoxylin and eosin Staining

Tissues were rehydrated by emersion in 100% xylene, 100% ethanol, 90% ethanol and deionized water. Slides were then stained with Harris haematoxylin to observe the cell nucleus and counterstained with eosin to observe cellular cytoplasm. Both stains together provided a view of the colonic structure. Tissues were then dehydrated through a series of ethanol and xylene steps before finally DPX and a coverslip was placed on top to protect tissue staining. Details of staining steps and timings are detailed in Table 2.11.

2.2.10.3 CEA staining

The University Hospital of Wales pathology department kindly stained tumour sections from CRC patients. Tissue was stained using a programmed protocol on the Link 48 autostainer. Antigen retrieval was carried out using a high pH buffer solution for 40 min, followed by a 20 min cool down period. Sections were then stained with the flex mouse monoclonal anti-CEA antibody followed by the envision flex high pH kit, which contains a peroxidase block, HRP, DAB chromagen and buffer, wash buffer and haematoxylin. Slides were imaged using the digital Axio Scan.z1 slide scanner.

2.2.11 Statistical analysis

Prism 5 (GraphPad) was used for all parametric and non-parametric statistical analyses. Normal distribution was tested using the D'Agostino and Pearson omnibus normality test. A P-value ≤ 0.05 was considered statistically significant.

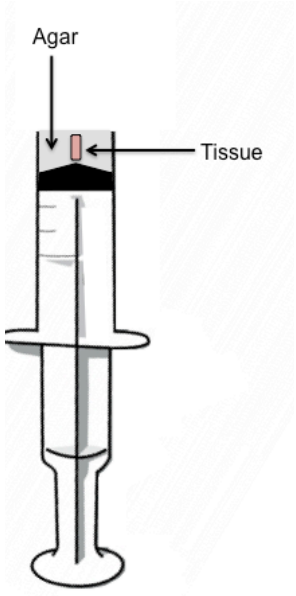

Figure 2.7. Agar embedding of small colonic samples. The tip of a 5ml syringe was removed and filled with approximately 1ml warm 2% agar. Human biopsy samples and small murine colonic samples were inserted upright and kept in place until the agar solidified. This kept small sections in the correct orientation for sectioning to visualise colonic crypts.

Table 2.11. Haematoxylin and eosin staining protocol

Step	
1.	Deparaffinise sections with three changes of xylene (2-3 minutes each)
2.	Re-hydrate in two changes of absolute alcohol (3 minutes each)
3.	90% alcohol and then 70% alcohol (2 minutes each)
4.	Wash briefly in distilled water
5.	Stain with Harris haematoxylin for 8 minutes
6.	Wash in running tap water for 5 minutes
7.	Differentiate in 1% acid alcohol for 30 seconds
8.	Wash in running tap water for 1 minute
9.	Blue slides in 0.2% ammonia water for 1 minute
10.	Wash under running tap water for 5 minutes
11	Rinse in 95% alcohol, 10 dips
12.	Dehydrate through 95% alcohol (15 dips), 2 changes of absolute alcohol (2-3
13.	Clear in three changes of xylene (5 minutes each)
14.	Mount with DPX

Chapter 3. T cell Responses to Carcinoembryonic antigen (CEA) in pre-operative CRC Patients.

3.1 Introduction

The immune system plays an important role in the control of CRC. In particular, IFN-γ producing $CD4^+$ T-lymphocytes, which recognise tumour antigens, are critically involved in anti-tumour immunity. Studies report that an influx of Th1 cells into CRC tumours is linked with favourable patient outcome (208, 224). Our own laboratory has identified peripheral blood-derived IFN-γ responses to the TAA 5T4. In pre-operative CRC patients, 5T4 IFN-γ specific responses correlate positively with patient survival (194, 201, 215). Conversely, we have discovered that a specific IFN-γ response towards the TAA CEA correlates with poor patient survival (194) (Figure 3.1A). This unexpected association is present regardless of tumour stage (Figure 3.1B) (194). Furthermore, individuals with both 5T4 and CEA specific responses had better survival than those responding to CEA alone, confirming a response to 5T4 is advantageous (194). Both TAAs are highly up-regulated in CRC, 5T4 being an oncofelatal antigen not widely expressed in healthy adult tissue. It can be detected in certain tissues with low expression such as the glomeruli in the kidney, villi of the small intestine and bladder epithelium (195). However, CEA is an auto antigen expressed in normal intestinal epithelium, falling into the “over expressed in cancer” category of tumour antigens (225). CEA is up-regulated in other adenocarcinomas such as breast and lung, making it an attractive target for immunotherapy (226, 227). However, the data from our laboratory clearly show there is a clinical significance of mounting a tumour-selective versus an auto-antigen-specific T cell response. This opens up a debate about the potential risks therapies aiming to target CEA may have. Furthermore, this observation raises the question of:

why do CEA specific T cell responses correlate with a detrimental outcome in the first place?

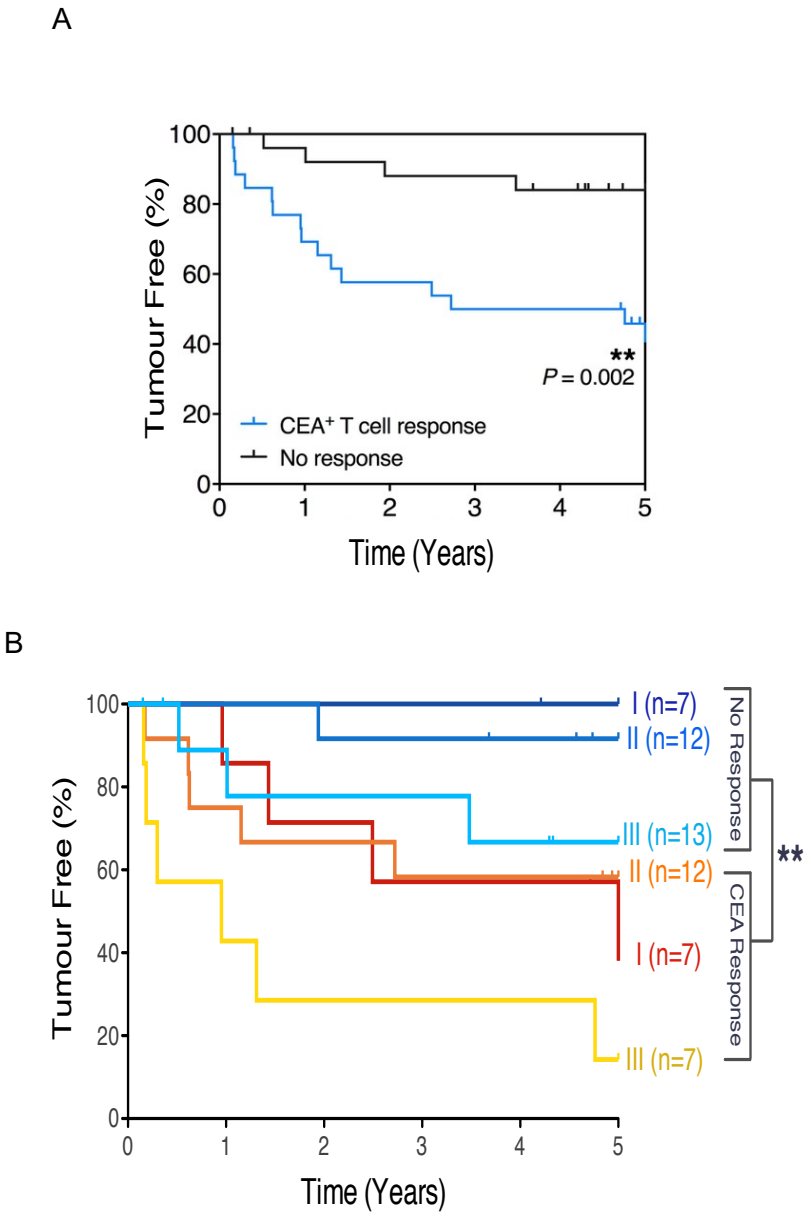

Figure 3.1. CRC cancer patients secreting IFN-γ in response to CEA are at a greater risk of tumour recurrence.
PBMC were taken prior to patients undergoing colectomy for CRC and IFN-γ CEA-specific T cell responses measured by ELISpot. (A) The presence of a CEA response correlated with tumour recurrence over a 5 year time period before and (B) after stratifying patients by tumour stage. This data was generated by Dr Gareth Betts and analysed by Dr Martin Scurr (194).

Th17 cells were first described in mice in 2005 and are characterised by IL-17A production (228). High numbers reside within the colon. They are induced by the presence of intestinal microbes, capable of adhering to intestinal epithelial cells, such as SFB (229). While important for defence against fungal and bacterial pathogens, studies suggest Th17 cells are involved in tumour development, particularly in the progression of CRC (230). Increased Th17 infiltration is seen within stage II and further advanced CRC tumours (210) (231). Tosilini and colleagues have carried out gene expression analysis in three separate cohorts of CRC patients. Results from this have clearly shown that a high intra-tumoral infiltration of Th17 cells, in combination with low levels of Th1 cells, is associated with shorter disease-free survival (209). The presence of Th17 cells in other intestinal diseases such as CD and UC has also been documented. IBD patients show elevated IL-17A levels within mucosal tissue and sera compared to healthy controls. This also increases with disease severity (80). IBD and inflammation has long been linked to CRC development, with an increase in CRC incidence occurring within IBD patients (232, 233). Inflammatory mediators such as IL-6 and TNF-α are known to have pro-tumourigenic properties, due to their ability to activate oncogene associated transcription factors (234). Also implicated in promoting tumour progression is IL-17A, capable of activating the transcription factor STAT-3. This activation can lead to increased tumour cell survival, proliferation and invasion, as well as promoting immune-suppression (235, 236). Moreover, persistent STAT-3 activation can provide a proliferative advantage to myeloid cells within the tumour microenvironment to promote pro-oncogenic inflammation (237) (238). Another key feature of tumour development is the formation of new blood vessels. Liu and colleagues show that IL-17A can play a role in shaping the tumour vasculature, promoting angiogenesis via VEGF and PGE2 production (239), again aiding in tumour development. Based

on this collective knowledge of Th17 cells, I aimed to generate a data set investigating CEA specific IL-17A producing cells.

I hypothesised that CEA specific IL-17A and/or IFN-γ/IL-17A dual producing cells could be responsible for overcoming beneficial IFN-γ responses within CRC patients, ultimately leading to tumour recurrence. This Chapter focuses on i) evaluating IFN-γ and IL-17A secretion in response to CEA and 5T4 in a cohort of CRC patients, and ii) phenotyping $CD4^+$ T cells subsets isolated from primary tumours of CEA responding and non-responding patients.

3.2. Results

3.2.1 CEA and 5T4 specific IFN-γ and IL-17A responses measured by the FluoroSpot assay

The FluoroSpot technique is built on the widely used ELISpot assay, employed to measure the frequency of cytokine-secreting cells. However, unlike ELISpot, FluoroSpot allows for the detection of up to three cytokines in the same assay and from the same single cell. PBMC from patients or healthy donors were cultured for two-weeks with CEA or 5T4 peptide pools to expand antigen specific cells. The recall response to antigens was then measured using the FluoroSpot technology (full method described in Chapter 2). In doing so, it was possible to determine whether cells specific for CEA produced IFN-γ and/or IL-17A. Responses to 5T4 were also measured to determine if they were similar or different to those produced against CEA. Figures 3.2 and 3.3 show representative examples of patients who responded to CEA and 5T4 peptide pools respectively. Green spots indicate IFN-γ secretion and red spots show IL-17A. A computerised overly is used to visualise IFN-γ/IL-17A dual producing

cells, shown in yellow. Responses to control antigens haemagglutinin (HA) and purified protein derivative (PPD) were also measured (Figure 3.4).

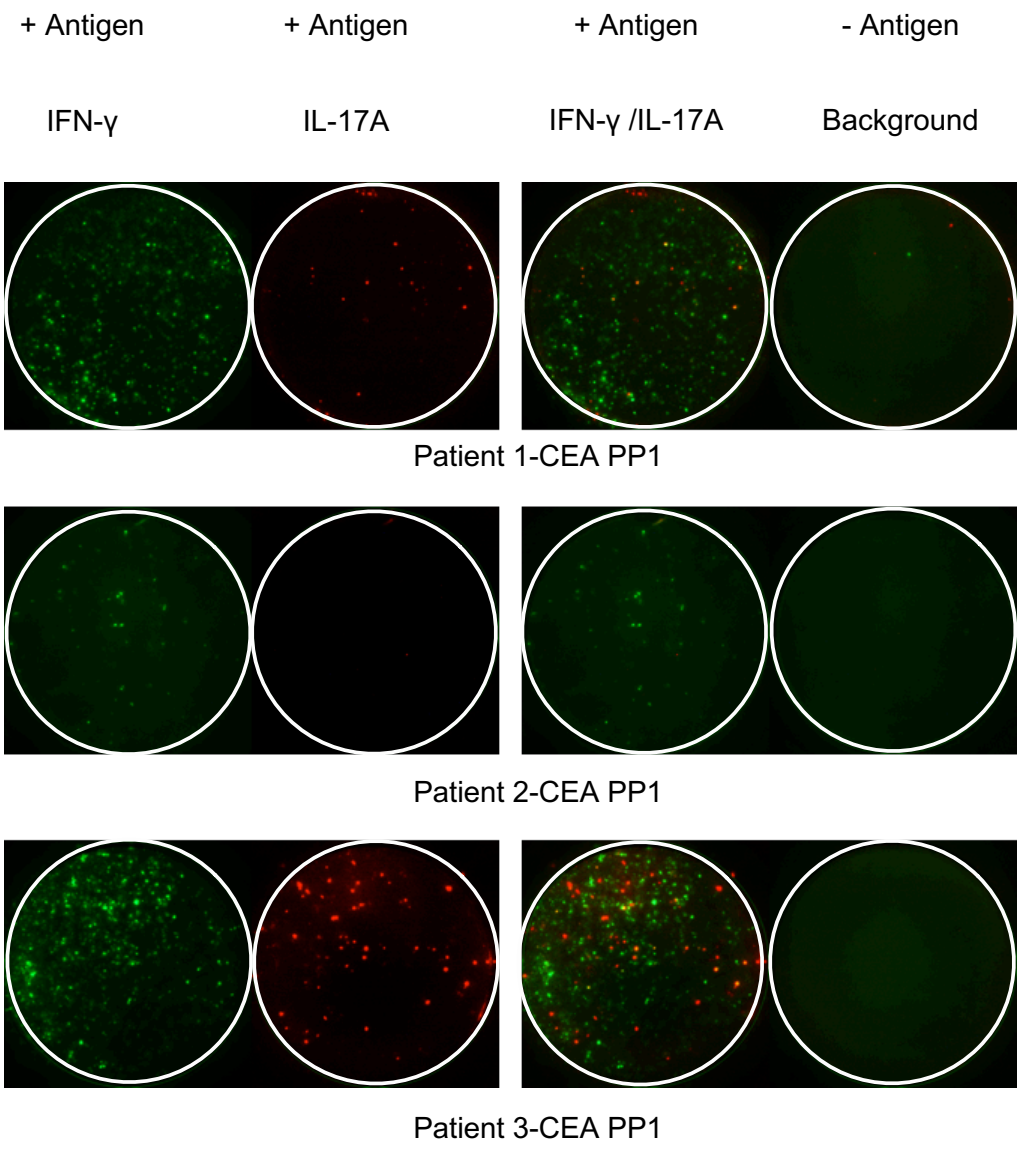

Figure 3.2. Examples of IFN-γ, IL-17A and IFN-γ/IL-17A dual secretion after stimulation with CEA peptide pools.
$5x10^5$ PBMC were stimulated with CEA PP1, incubated for 2 weeks and re-stimulated (+ antigen) or not (- antigen) with CEA PP1 again, before detection of cytokine release. Green spots represent IFN-γ release and red spots IL-17A. Yellow spots indicate IFN-γ/IL-17A dual secretion.

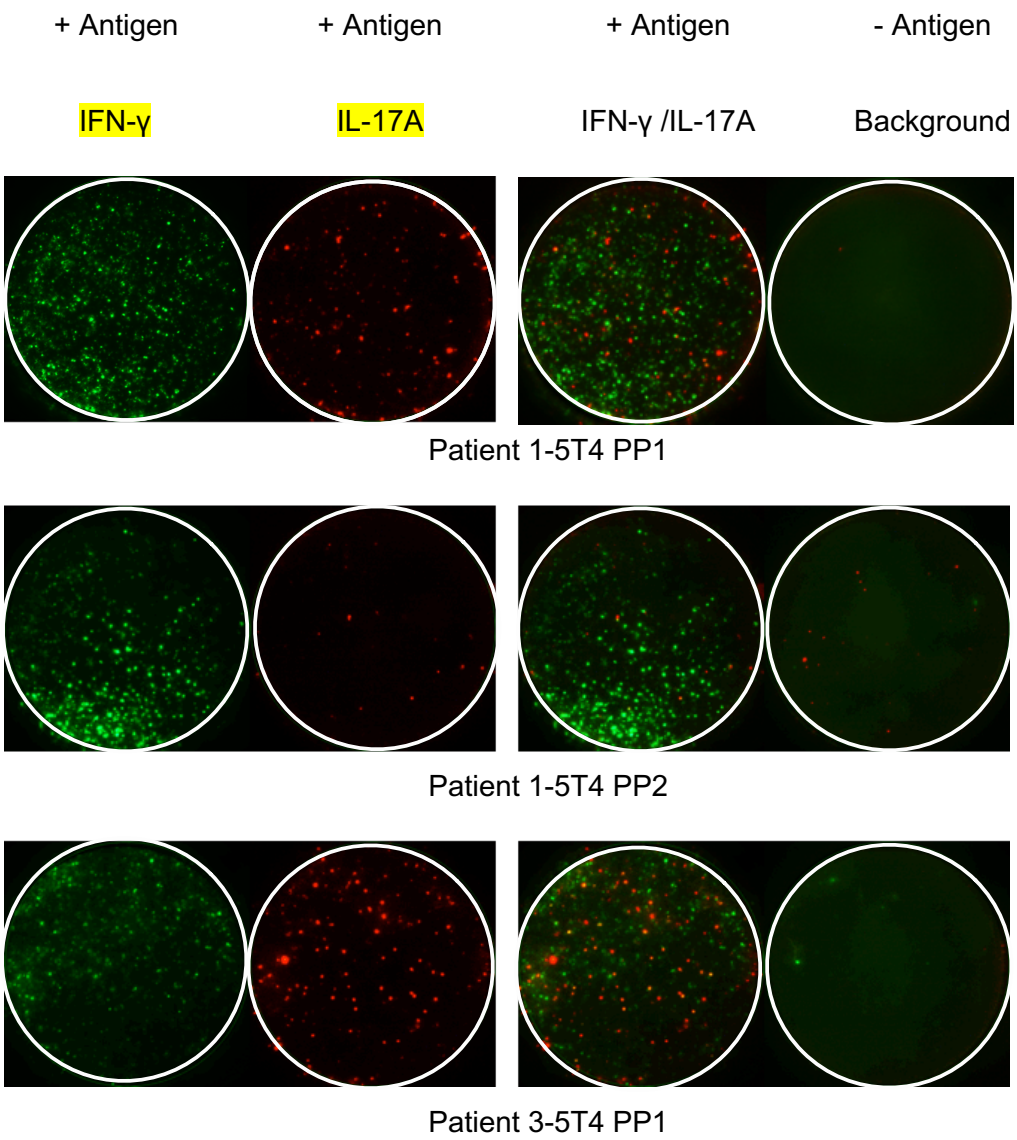

Figure 3.3. Examples of IFN-γ, IL-17A and dual IFN-γ/IL-17A secretion after stimulation with 5T4 peptide pools.
$5x10^5$ PBMC were stimulated with the indicated 5T4 peptide pools, incubated for 2 weeks and re-stimulated (+ antigen) or not (- antigen) with the same antigen, before detection of cytokine release. Green spots represent IFN-γ release and red spots IL-17A. Yellow spots indicate IFN-γ/IL-17A dual secretion.

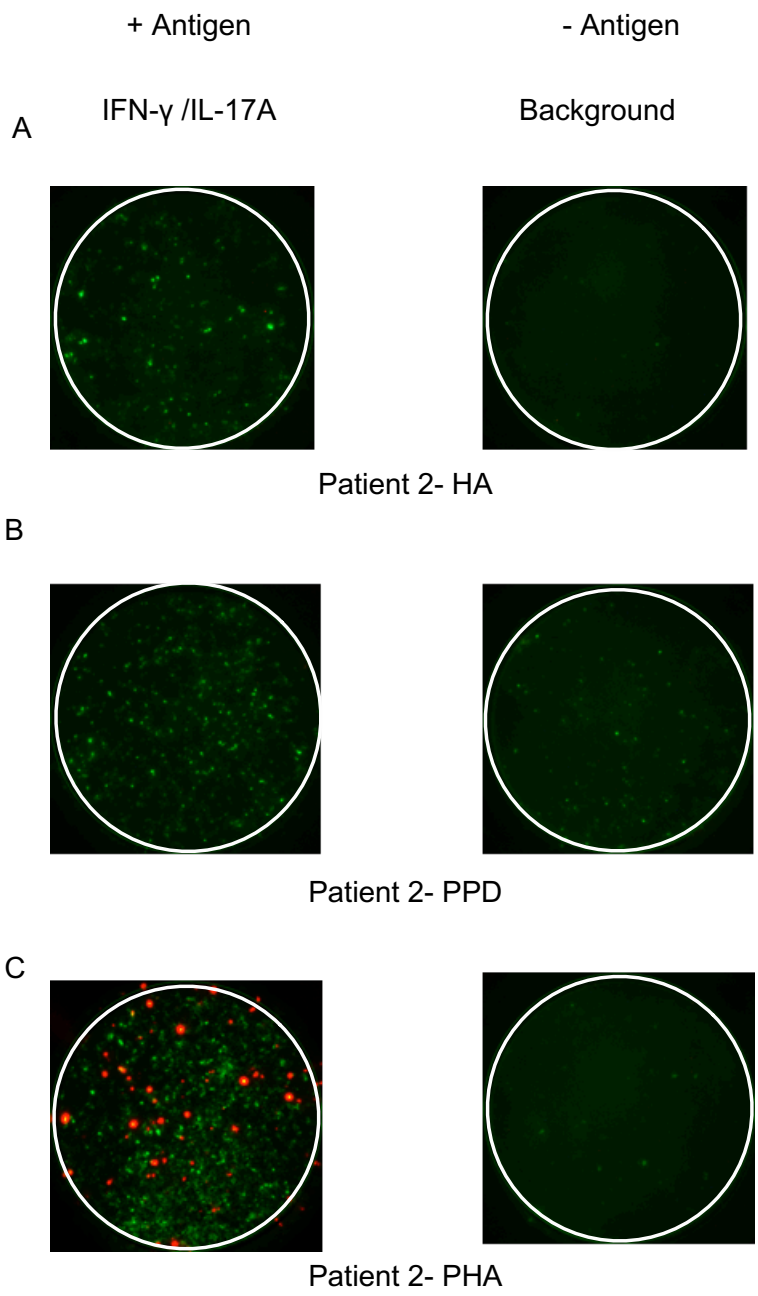

Figure 3.4. Examples of IFN-γ, IL-17A and dual IFN-γ/IL-17A secretion after stimulation with control antigens HA, PPD and PHA.
$5x10^5$ PBMC were stimulated with (A) HA, (B) PPD or (C) PHA, incubated for 2 weeks and re-stimulated (+ antigen) or not (- antigen) with the same antigen, before detection of cytokine release. Green spots represent IFN-γ release and red spots IL-17A. Yellow spots indicate IFN-γ/IL-17A dual secretion.

3.2.2 CEA and 5T4 specific IFN-γ and IL17A responses in pre-op CRC patients and healthy donors

A cohort of patients (n=40) was used to investigate whether CEA-specific IL-17A producing cells could be responsible for the poor survival outcome seen within CEA responding patients. Complementary to previous studies in our laboratory it was observed that healthy donors and CRC patients produced CEA-specific and 5T4-specific responses (Figure 3.5). In this new cohort of patients there was no difference observed between percentages of healthy donors producing IFN-γ in response to CEA or to 5T4 (Figure 3.6A and Figure 3.7A respectively). Conversely, a higher percentage of healthy donors produced an IL-17A CEA response compared to an IL-17A 5T4 response (Figure 3.6B and Figure 3.7B, respectively). This indicates that under non-pathological conditions CEA is a potent promoter of IL-17A. There was however, no increase in the percentage of CRC patients secreting CEA-specific IL-17A in comparison to the healthy donors (Figure 3.6B). Furthermore, CRC patients also secreted IL-17A in response to 5T4 as well as CEA (Figure 3.7B). This data suggests that CEA responding patients are not more likely to generate IL-17A producing cells than healthy donors or patients responding to 5T4.

CEA-specific IFN-γ responses were seen within a similar percentage of CRC patients across disease stage (~60%) (Figure 3.6A). The magnitude of the IFN-γ response (calculated from the combined response to PP1 and PP2) towards CEA and 5T4 are shown Figure 3.8A and 3.8B respectively. Interestingly, the magnitude of response is lower in Dukes C patients compared to healthy controls (Figure 8C and Figure 8D.) This supports previous findings in our laboratory, showing that 5T4 IFN-γ responses decline in advanced CRC (216). Such results indicate that while CRC patients maintain an IFN-γ response to CEA, the total magnitude of that response is reduced in CRC. At present it is

unclear why Dukes B patients do not show a reduced magnitude of response compared to HD. There was no association observed between CEA-specific IL-17A response magnitude and disease stage (Figure 3.8E). Moreover, CEA responses were not increased compared to 5T4-specific IL-17A secretion.

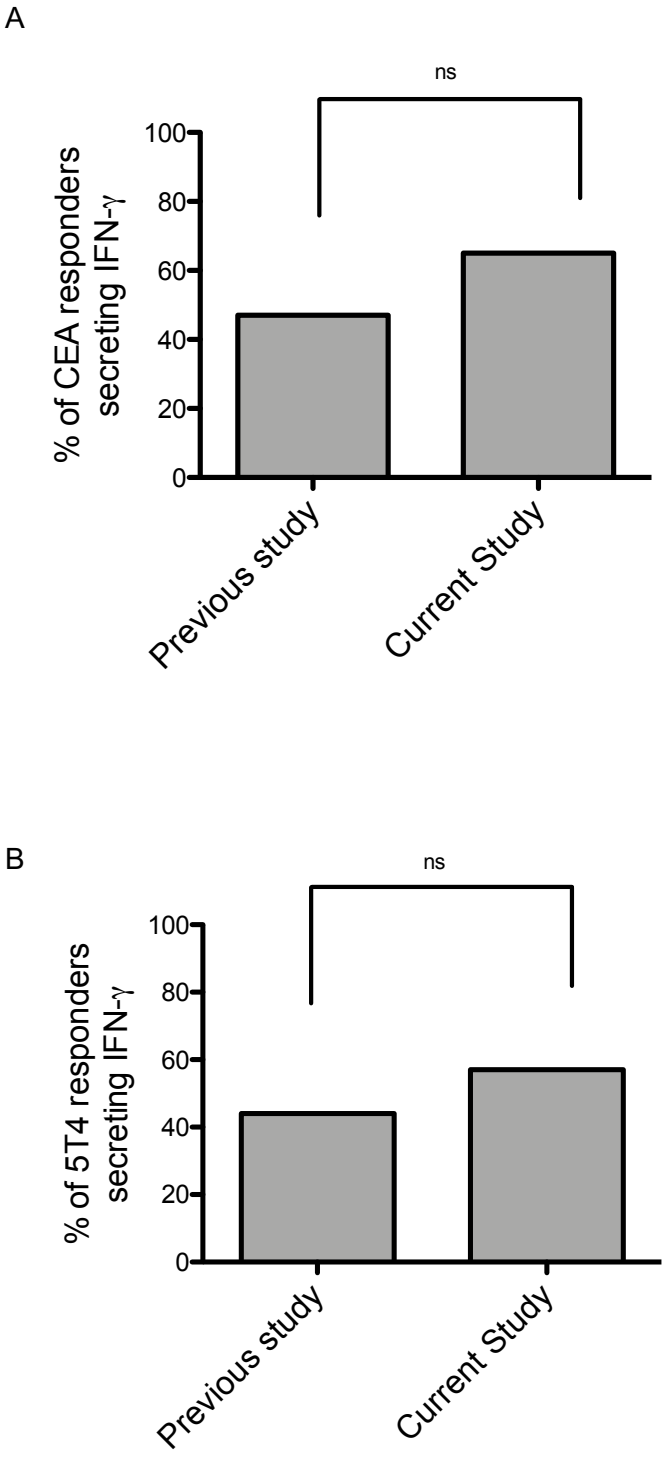

Figure 3.5. Percentage of CRC patients with a CEA and 5T4 response is similar to that seen within our previous study (Scurr et al 2015).
(A) Percentage of IFN-γ CEA specific and (B) IFN-γ 5T4 specific responders. n= 55 patients in previous study vs n= 40 in current study. Fishers exact test was used for comparison.

A

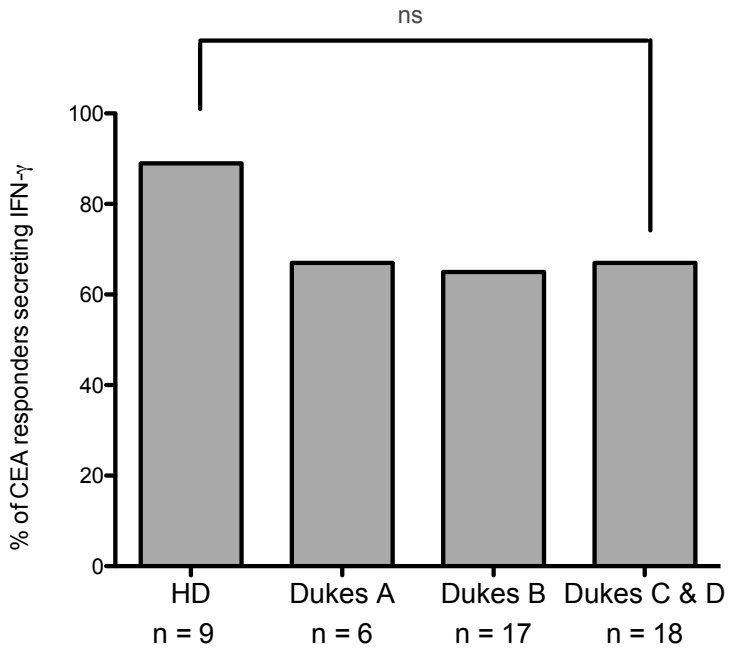

B

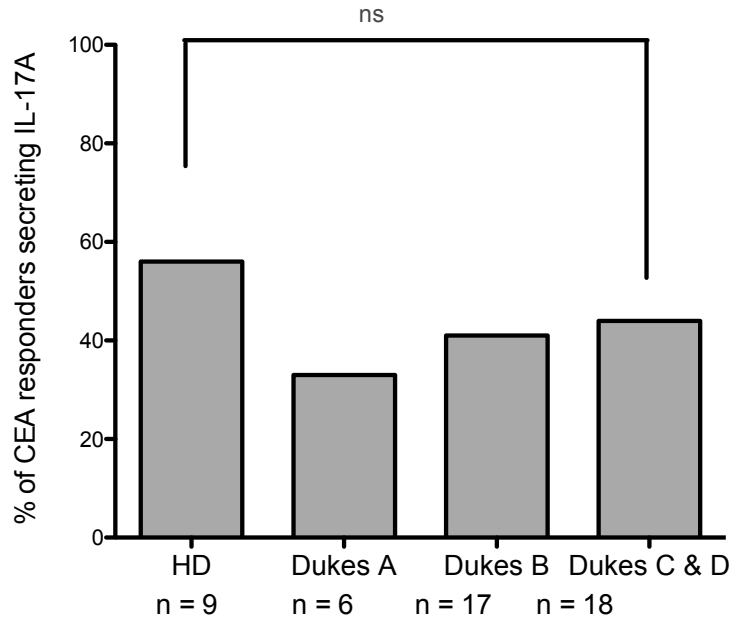

Figure 3.6. CEA responses are present within healthy donors and CRC patients. Percentage of individuals secreting (A) IFN-γ or (B) IL-17A in response to CEA. CRC patients were grouped based on Dukes stage. Fishers exact test was used for comparisons.

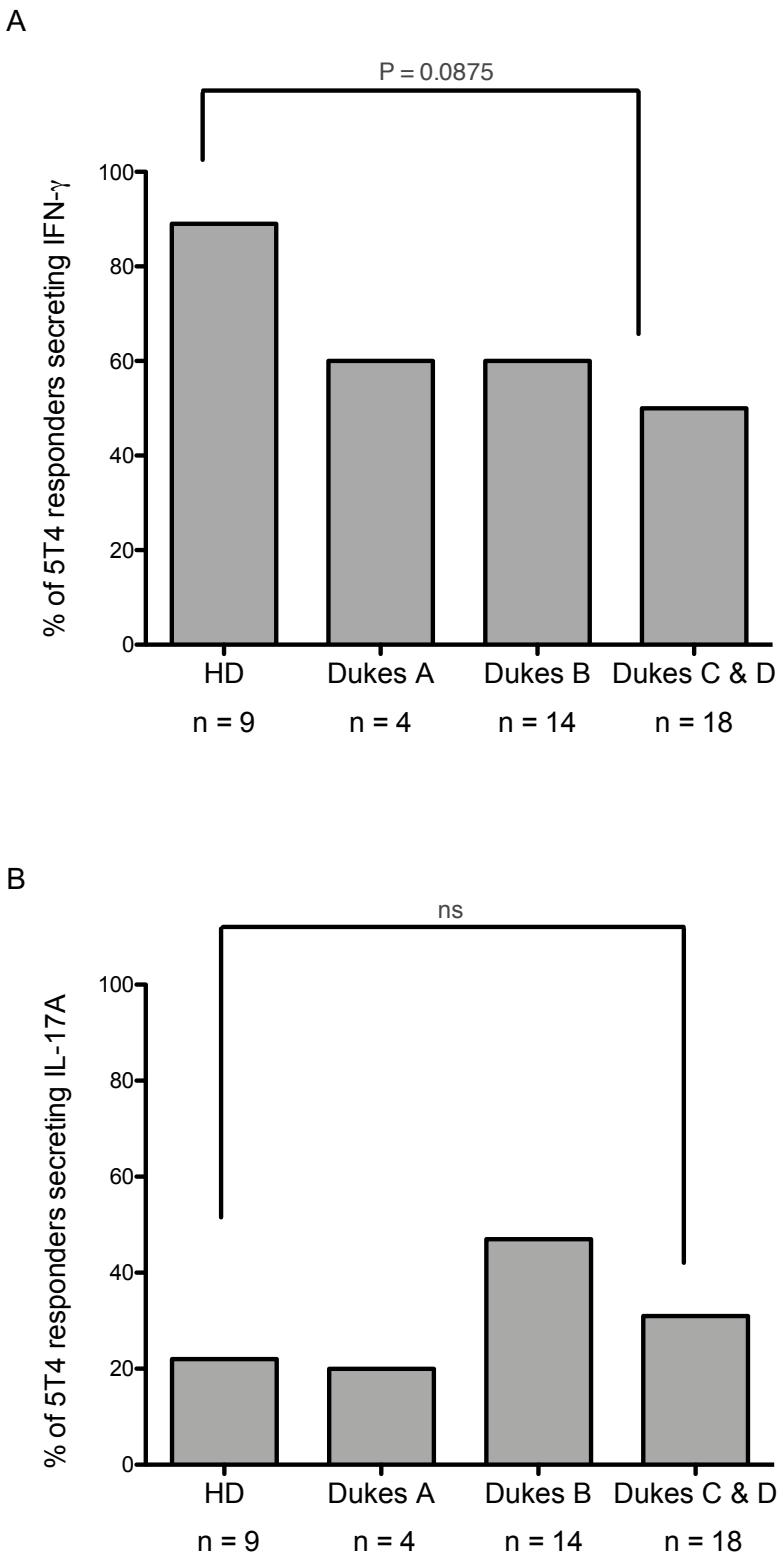

Figure 3.7 The percentage of IFN-γ secreting 5T4 responding patients declines with advanced disease.
The percentage of patients responding to 5T4, secreting either (A) IFN-γ or (B) IL-17A. CRC patients were grouped based on Dukes stage. Fishers exact test was used for comparisons.

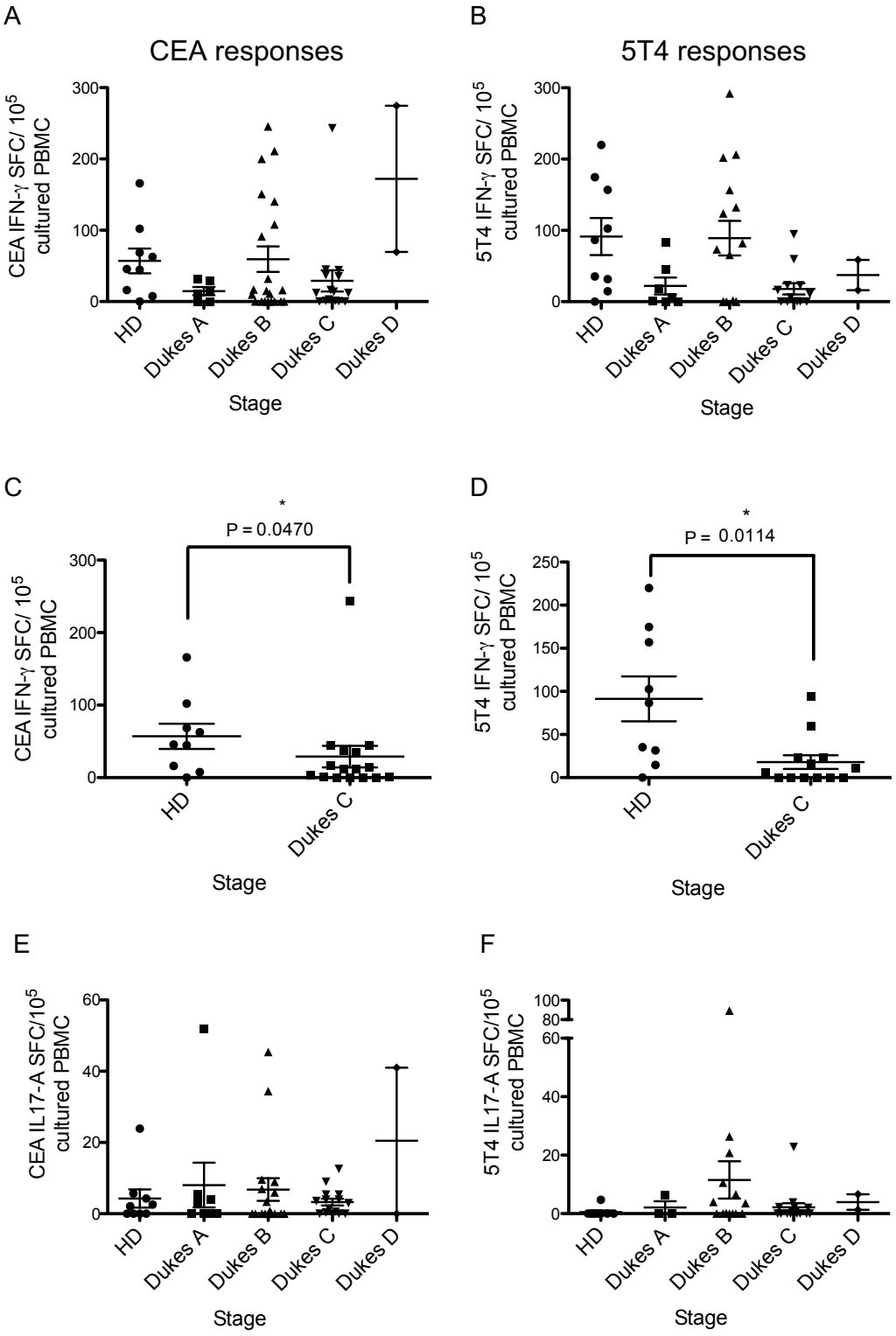

Figure 3.8. Magnitude of IFN-γ but not IL-17A CEA and 5T4 responses decline in CRC patients.

(A) Total magnitude of IFN-γ responses to CEA and (B) 5T4. Patients grouped based on Dukes stage. (C) CEA and (D) 5T4 IFN-γ response magnitude of HD and Dukes C patients. (E) and (F) show total magnitude of IL-17A responses towards CEA and 5T4 respectively. Error bars show mean +/- SEM. Mann Whitney tests were used to test for statistical differences between groups.

Overall it was found that cells producing IFN-γ in response to CEA and 5T4 were more frequent than IL-17A or IFN-γ/IL-17A dual producing cells (Figure 3.9). Furthermore, the magnitude of IFN-γ responses was always higher compared to IL-17A (Figure 3.10). This was also true for HD (Figure 3.11). This suggests that greater IL-17A responses are not outweighing beneficial IFN-γ responses to drive tumour recurrence in CEA responding patients. In fact, IL-17A was only secreted in response to CEA when IFN-γ was also made. PBMC from twenty-six patients produced IFN-γ with seventeen also secreting IL-17A in response to CEA. No solitary IL-17A response was detected in CRC patients or in HD (Figure 3.9A and C). In response to 5T4, only one patient secreted IL-17A alone (Figure 3.9B). The total magnitude of IFN-γ and IL-17A secretion between CEA and 5T4 antigens (Figure 3.12A and 3.12B, respectively) was also the same. This indicates that neither antigen is superior at activating an immune response. Taken together these data demonstrate that CEA and 5T4 are similar in their ability to stimulate IL-17A production, which is low in magnitude and secreted in conjunction with IFN-γ.

Previous studies indicate that low affinity CEA-specific T cells are present within the normal T cell repertoire (240, 241). These data highlight that CEA and 5T4 specific cells are capable of secreting both IFN-γ and IL-17A. However, collectively these data also suggest that IL-17A secreted by CEA-specific cells in the blood does not reflect the increase in tumour occurrence in patients identified previously as IFN-γ CEA-responders from blood samples.

3.2.3 CEA-specific responses, CEA tumour cell expression and CEA serum levels

CEA is an adhesion molecule, implicated as a marker of tumour progression as it is shed from the tumour surface (187). Accordingly, in CRC, high levels of serum derived CEA is linked to advanced disease (242). Studies performed in mice also showed that systemic CEA protein results in increased liver metastases (187). We aimed to investigate whether CEA-specific PBMC responses were a result of high soluble CEA within serum, possibly indicating micro-metastasis not detectable at the time of diagnosis. Serum CEA was measured before primary tumour surgical resection and at least six months after surgery to address whether this had any correlation with IFN-γ or IL-17A CEA-specific responses. However, no association between high levels of serum CEA and generation of CEA-specific responses either before (Figure 3.13A), or after surgical resection (Figure 3.13B) were found.

Also investigated was tumour cell CEA expression itself to determine if this correlated with the presence of CEA-specific T cells in the blood. Seven tumours were selected at random, with six showing positive staining for CEA (Figure 3.14A). However, only two patients with CEA^+ tumours mounted a CEA-specific T cell response (Figure 3.14B). This indicates that the presence of CEA alone either soluble in serum or expressed on the tumour surface does not dictate development of a measurable antigen-specific T cell response.

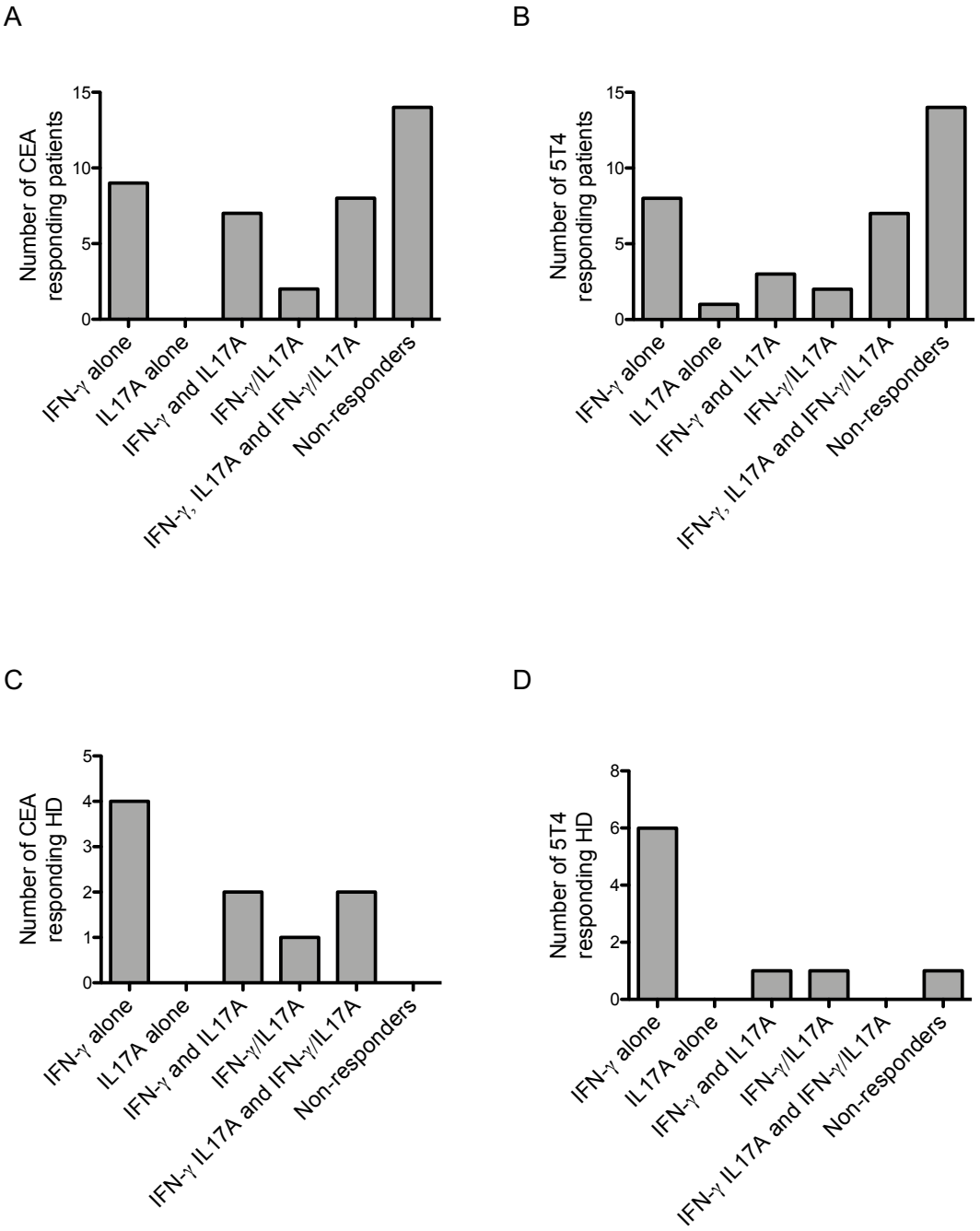

Figure 3.9. An IL-17A CEA or 5T4 specific response occurs alongside an IFN-γ response.

(A) The number of patients secreting IFN-γ alone, IL-17A alone or combinational responses towards CEA and (B) 5T4. (C) The number of HD secreting IFN-γ alone, IL-17A alone or combinational responses towards CEA and (D) 5T4. IFN-γ and IL-17A indicates two separate cell populations secreting each cytokine concurrently. IFN-γ/IL-17A indicates secretion is from the same population.

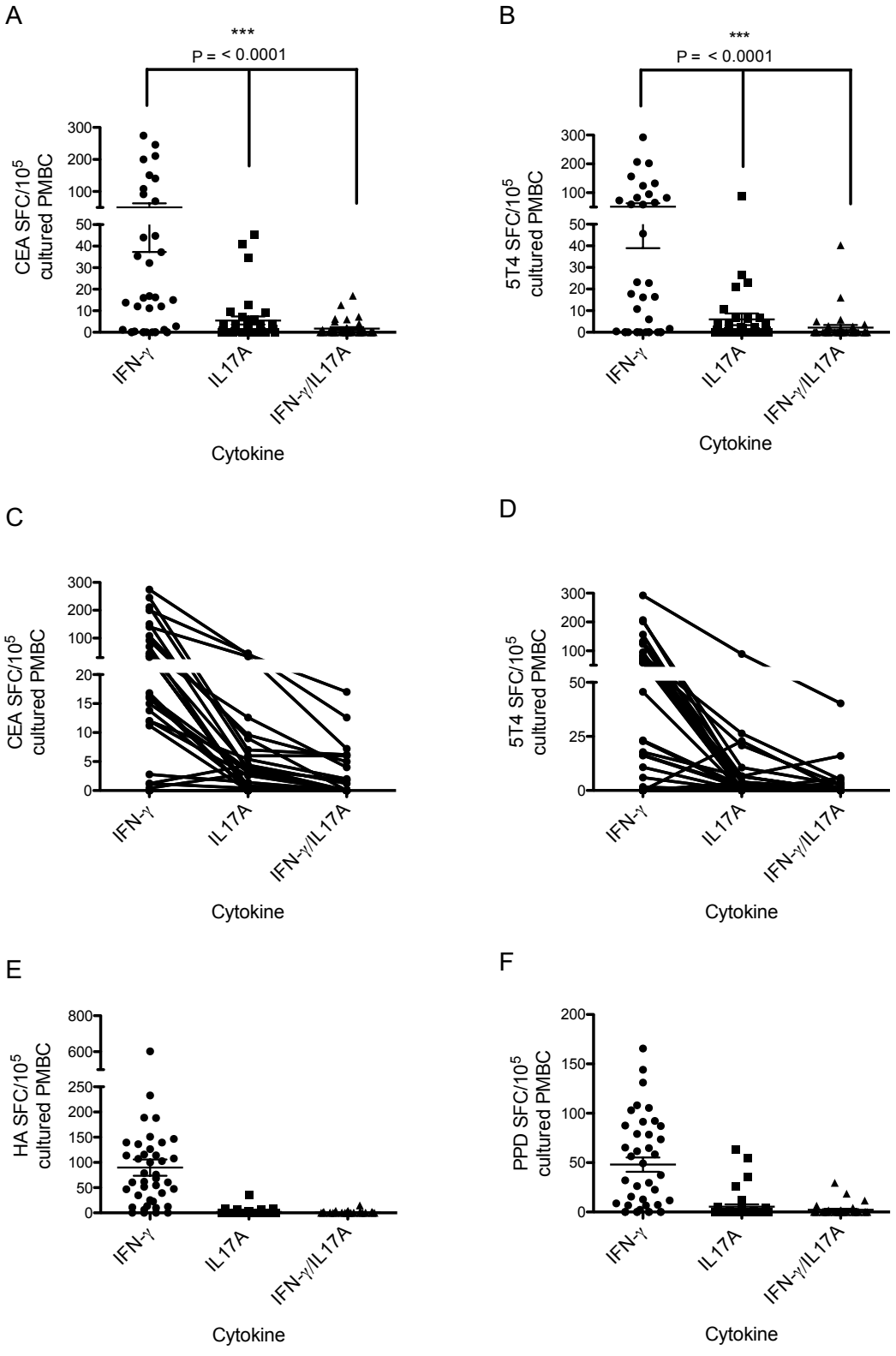

Figure 3.10. CEA specific and 5T4 specific IFN-γ responses are higher in magnitude than IL-17A in CRC patients.
(A) Total magnitude of responses to CEA and (B) 5T4, calculated by combining responses specific for peptide pools 1 and 2. Error bars indicate mean +/- SEM. Kruskal-Wallis test was used for comparisons. (C) CEA specific and (D) 5T4 specific IFN-γ, IL-17A and IFN-γ/IL-17A responses for individual patients. One line represents one patient. (E) Responses specific to control antigens HA and (F) PPD.

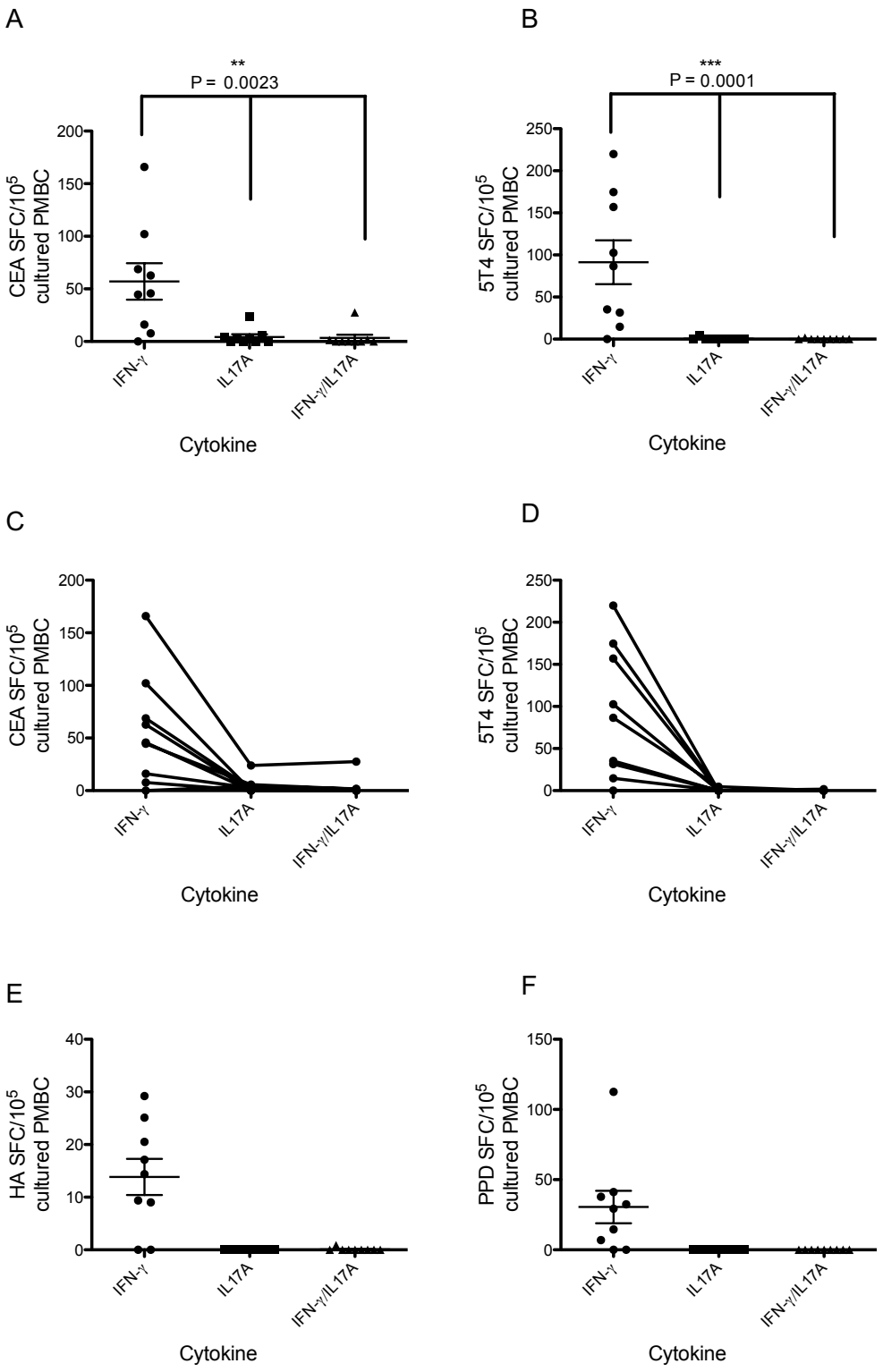

Figure 3.11. CEA specific and 5T4 specific IFN-γ responses are higher in magnitude than IL-17A in HD.
(A) Total magnitude of responses to CEA and (B) 5T4, calculated by combining responses specific for peptide pools 1 and 2. Error bars indicate mean +/- SEM. Kruskal-Wallis test was used for comparisons. (C) CEA specific and (D) 5T4 specific IFN-γ, IL-17A and IFN-γ/IL-17A responses for individual HDs. One line represents one patient. (E) Responses specific to control antigens HA and (F) PPD.

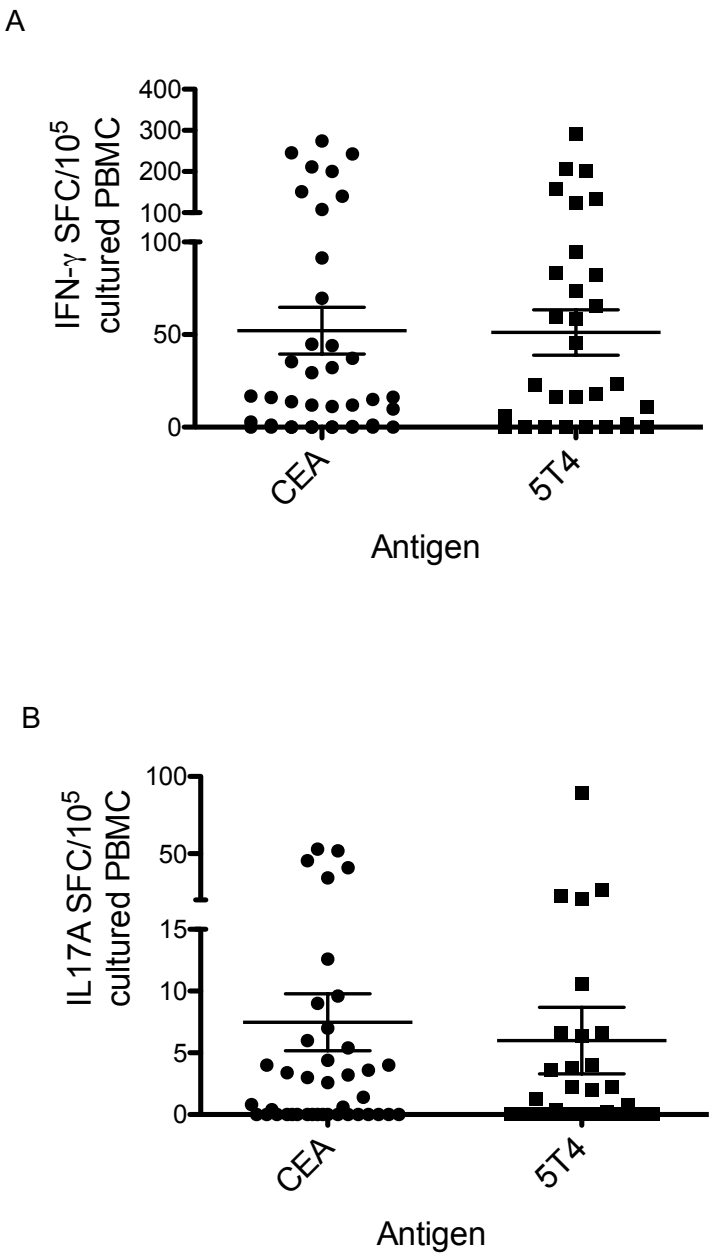

Figure 3.12. There is no difference in magnitude of response towards CEA and 5T4.
(A) IFN-γ response towards CEA and 5T4, calculated by combining peptide pools 1 and 2. (B) IL-17A response to CEA and 5T4. Error bars indicate mean +/- SEM.

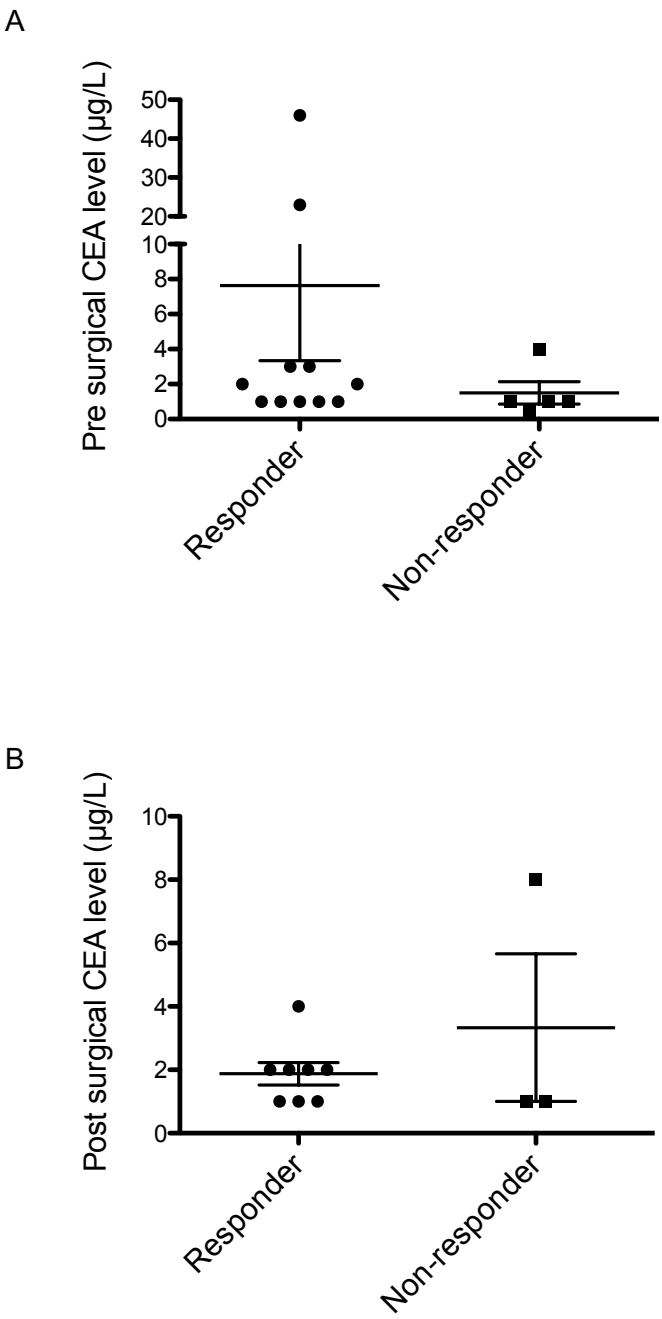

Figure 3.13. Serum CEA levels do not correlate with a CEA specific PBMC response.
(A) Serum CEA level before and (B) after surgical colectomy. Post surgical samples were obtained a minimum of 6 months after the procedure. Responder indicates the presence of an IFN-γ, IL-17A or dual response. Error bars indicate mean +/- SEM.

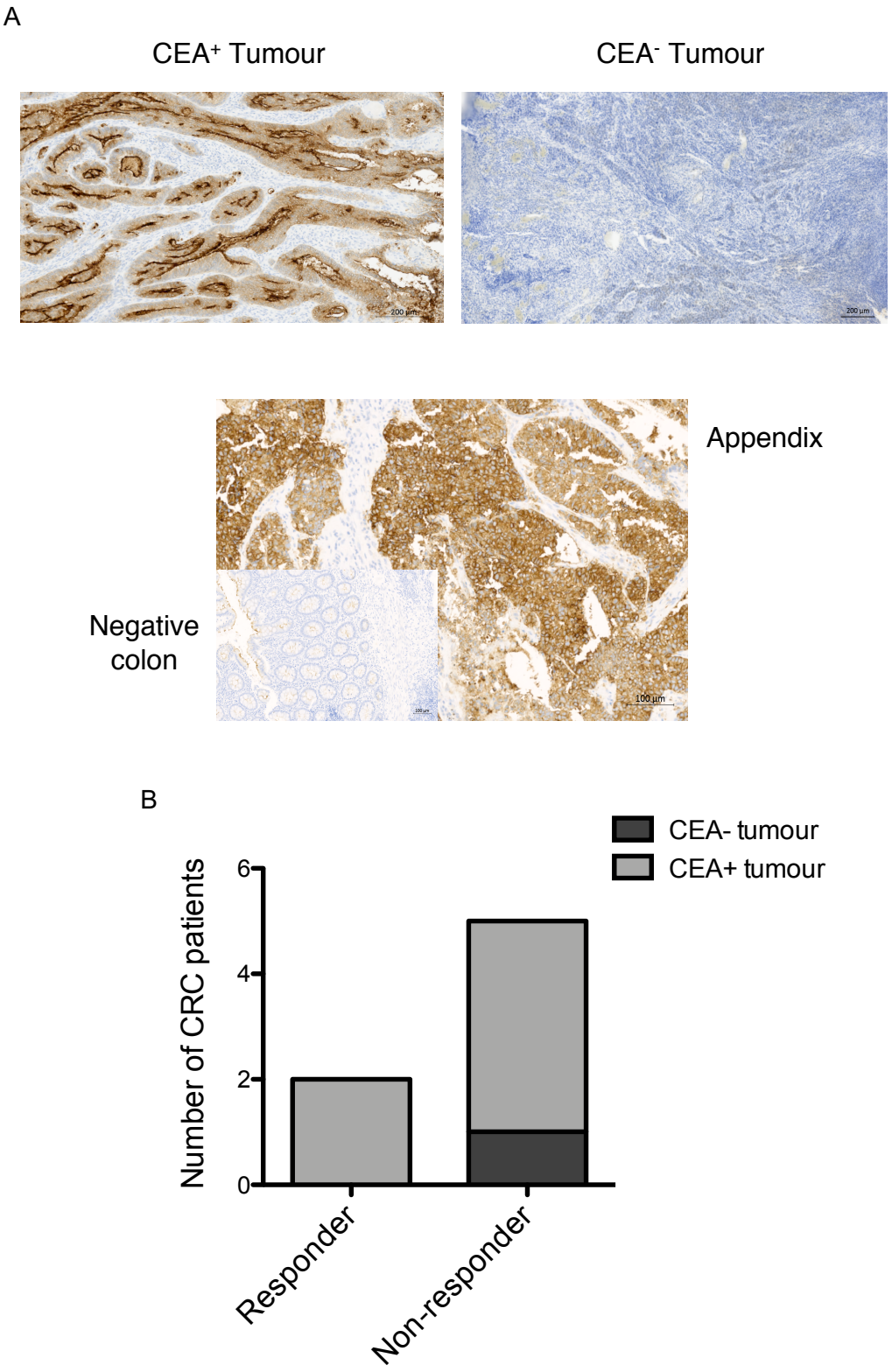

Figure 3.14. CEA expression can be detected on tumours but does not correlate with the presence of a PBMC response.
(A) Immunohistochemistry staining of CRC tissue. Brown stain shows CEA expression. Nuclear stain is blue. Tissues from the appendix and from a known negative colon sample were used as controls. (B) The number of responding or non-responding CRC patients with CEA^+ or CEA^- tumours.

3.2.4 The presence of CEA specific responses in blood correlates with lower percentages of T-lymphocyte subsets

Infiltration of $CD3^+$ T-lymphocytes into tumours has been shown to correlate with better patient survival in many cancers, including breast, ovarian, prostate and colorectal. However, the combination of T cell subsets present is also important. As mentioned previously, Tosilini *et al* showed that within CRC tumours high infiltration of Th17 cells, in combination with low Th1 cells has a negative impact on patient survival (209). However, only expression of genes associated with T cell subsets was assessed and not cytokine secreting cells. In this current study $CD3^+CD4^+$ cells from PBMC, healthy colon and TILs were phenotyped from CEA responding and non-responding patients to investigate infiltrating T cell subsets. This made it possible to determine if presence of an IFN-γ and/or IL-17A CEA-specific response measured in blood reflects a difference in the tumour immune cell profile.

Using PMA/ionomycin stimulation and the staining panel shown in Table 2.7 in Chapter 2, the frequency and phenotype of $CD4^+$ T-helper subsets was identified. Representative gating strategies for PBMC, healthy colon and TILs are shown in Figure 3.15 and Figure 3.16. Analysis showed that CRC patients with a CEA response (IFN-γ or IL17A) had significantly lower frequencies of $CD4^+$ IFN-γ^+, $FoxP3^+$ and $CCR6^+$ TILs compared to CEA non-responders (Figure 3.17C, F and I respectively). Representative FACS plots of reduced marker expression are shown in Figure 3.18A, B and C. A reduced frequency in the Th17 cell associated chemokine receptor CCR6 was also found within the healthy colon and PBMC fractions of CEA responding patients (Figure 3.17G and 3.17H). Interestingly no reduction in IFN-γ^+, $FoxP3^+$ or $CCR6^+$ T cell subset frequency was found between 5T4 responders and non-responders (Figure 3.19). There was also no difference in frequencies of $IL17A^+$ $CD4^+$ or IL10 $^+$

$CD4^+$ T cells in any compartment between CEA or 5T4 responders and non-responders (Figure 3.20A-L).

This data shows there is no increase in IL-17A-producing cells (Th17 cells) within CEA responding patients compared to non-responders. Therefore, an increase in Th17 cells is unlikely to be the cause of poor patient survival within CEA responding patients. The data also shows that a CEA-specific response is linked with low immune cell infiltrated tumours. This suggests that tumours from CEA responsive patients may be poorly immunogenic and/or more aggressive than tumours from CEA non-responsive patients.

PMA/Ionomycin stimulated PBMC gating strategy

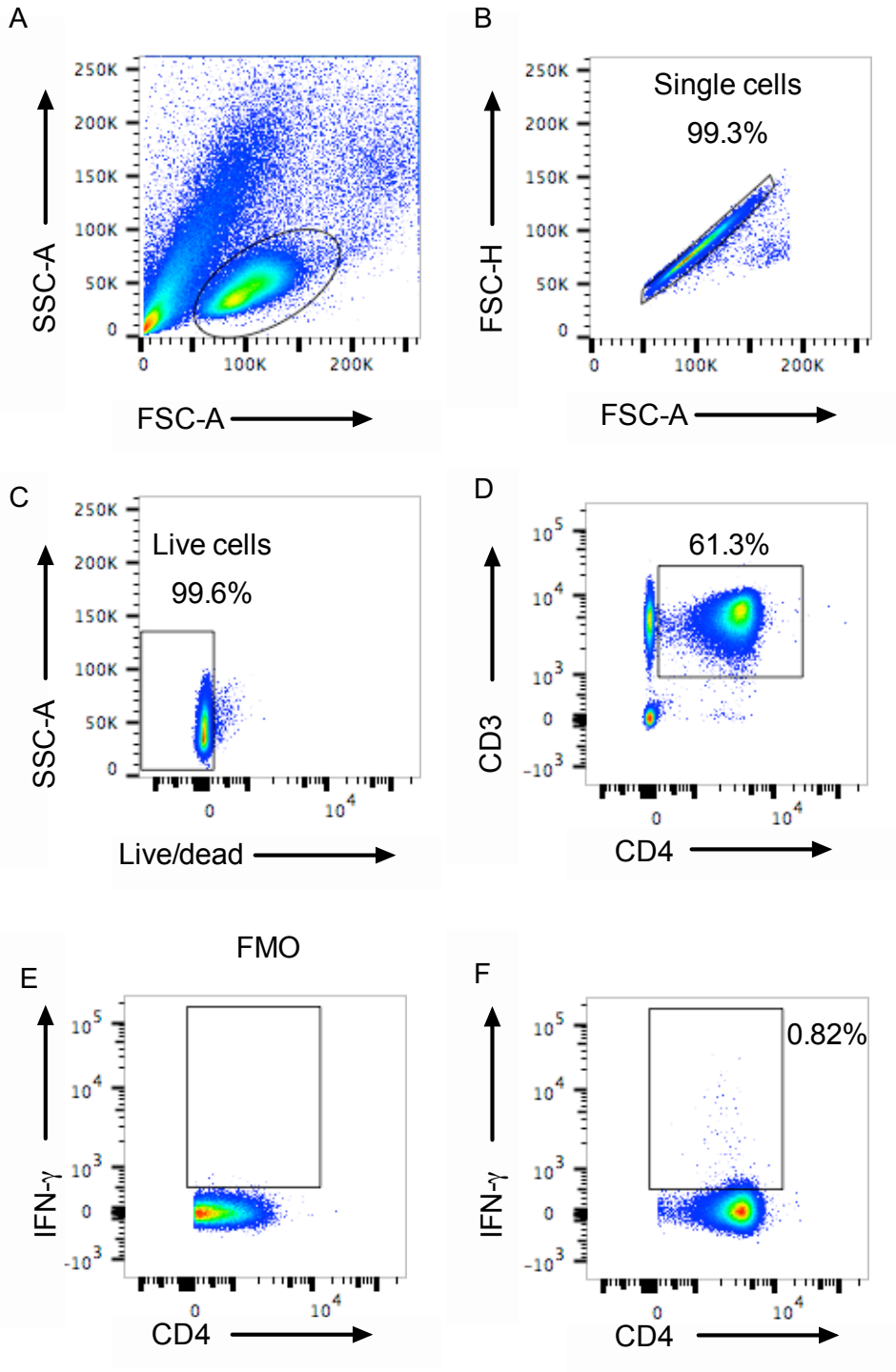

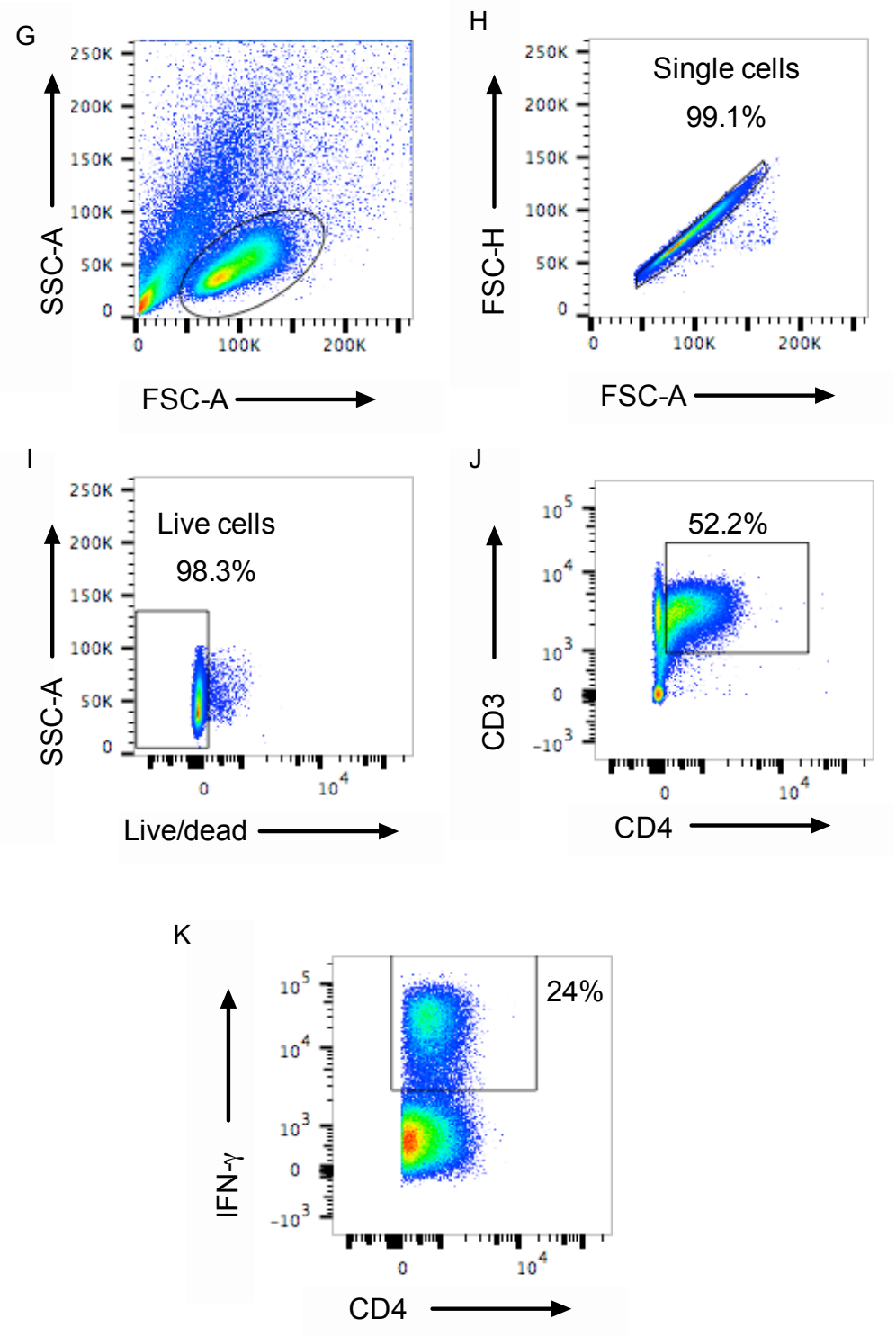

Figure 3.15. Representative gating strategy used to analyse CD3⁺ CD4⁺ PBMCs. Patient PBMCs were isolated and stained using the panel shown in Table 2.7 in Chapter 2. (A) Lymphocytes were gated based on granularity and size using side scatter (SSC) and forward scatter (FSC). (B) Gating on FSC area and height identified single cells. (C) Live cells were selected by the ability to exclude Aqua live/dead dye. (D) $CD3^+$ $CD4^+$ cells were then selected prior to cytokine expression analysis. (E) Fluorescence minus one (FMOs) was used to set gates showing cytokine secretion. (F) Representative gating of IFN-γ secretion by unstimulated PBMC. (G-K) Shows the same gating strategy for PMA/Ionomycin with Brefeldin-A stimulated cells.

Colon

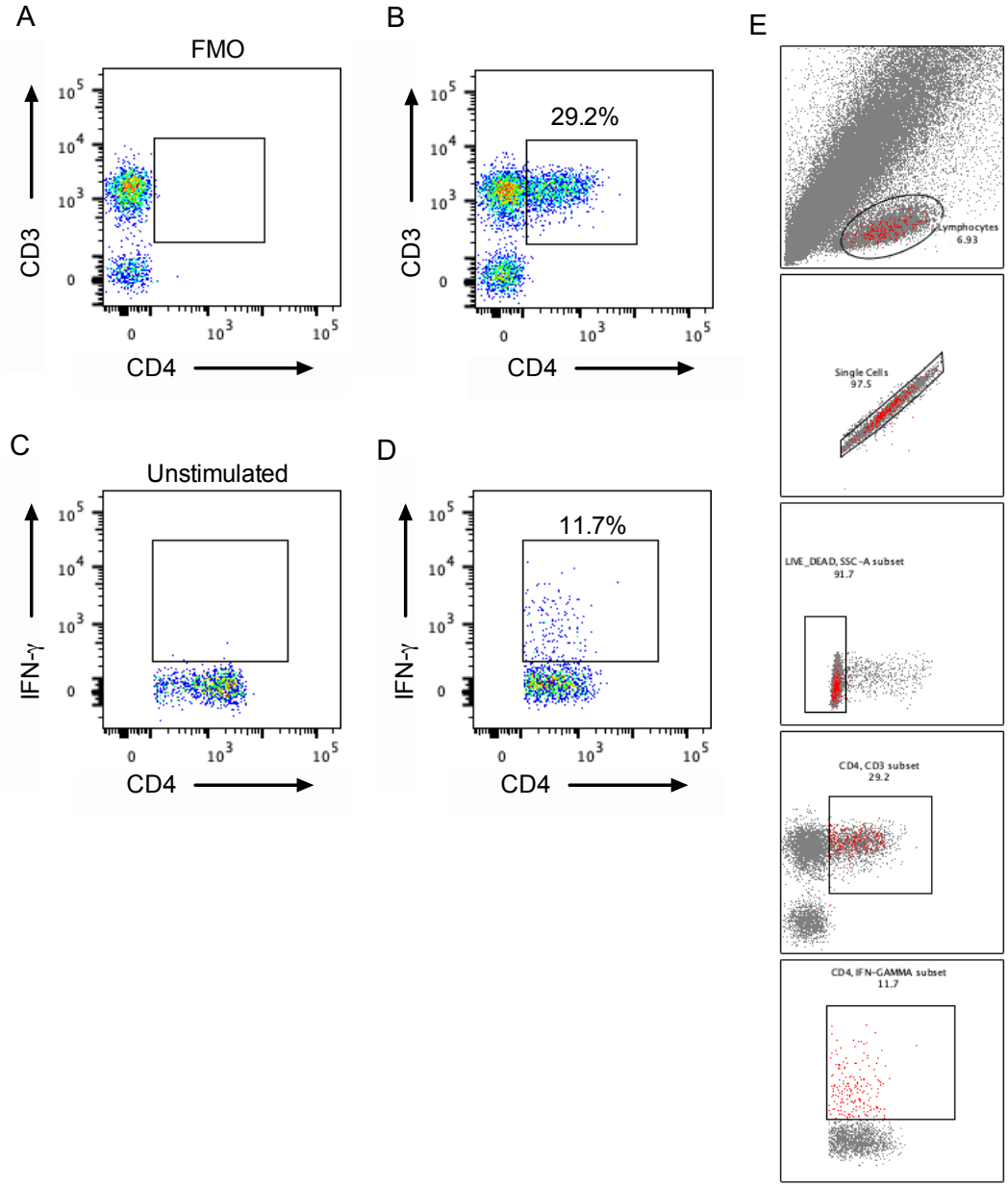
A
FMO
CD3
CD4
B
29.2%
CD3
CD4
C
Unstimulated
IFN-γ
CD4
D
11.7%
IFN-γ
CD4
E
Lymphocytes
6.93
Single Cells
97.5
LIVE_DEAD, SSC-A subset
91.7
CD4, CD3 subset
29.2
CD4, IFN-GAMMA subset
11.7

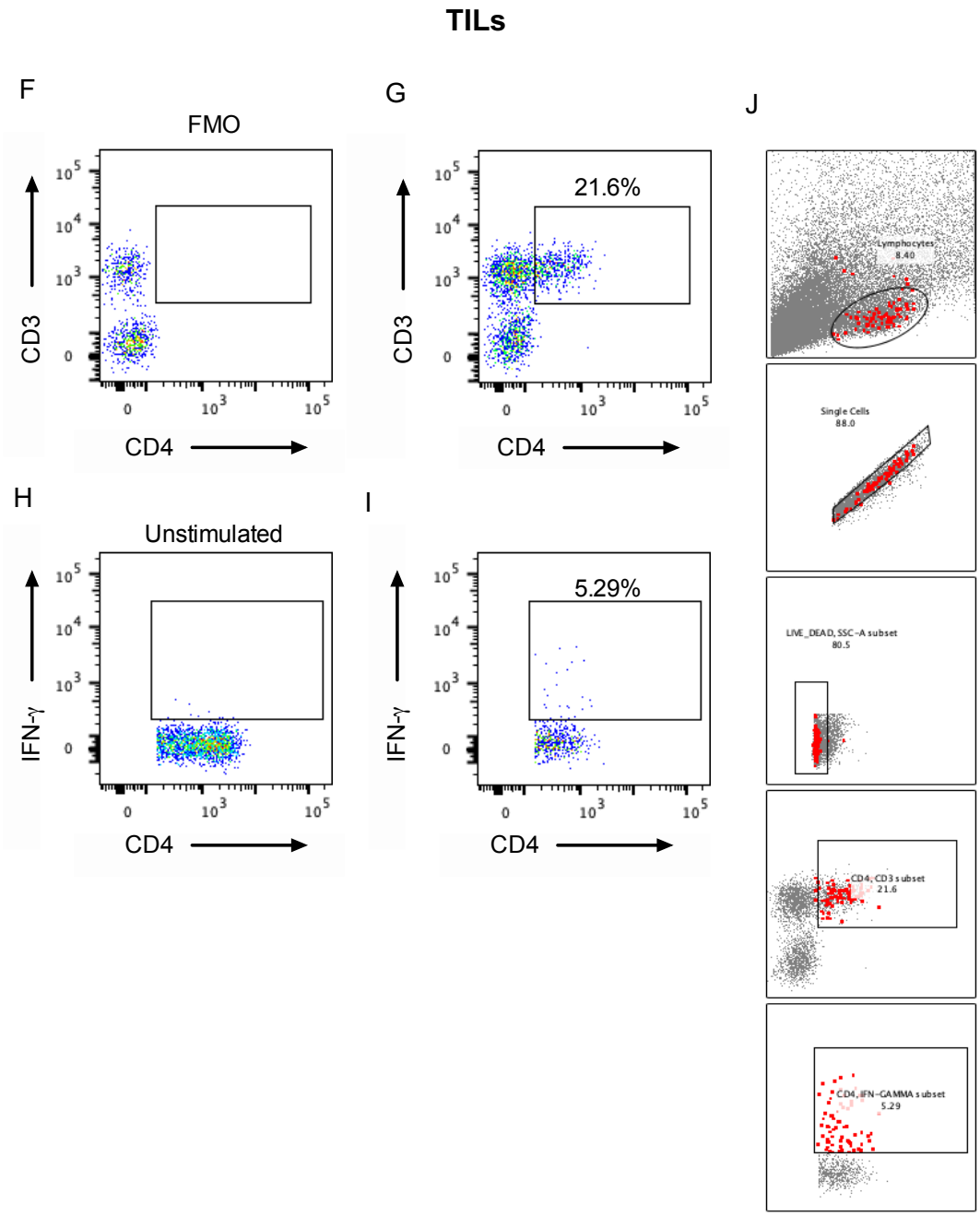

Figure 3.16. Representative gating strategy used to analyse CD3⁺ CD4⁺ colon cells and TILs.
Healthy colon infiltrating lymphocytes and TILs were isolated and stained using the panel shown in Table 2.7 in Chapter 2. The gating strategy was the same as shown in Figure 3.14. FMOs were used in the majority of cases when enough cells were available. Where cell numbers were too low, gates were applied based on comparison with un-stimulated cells. (A-D) Representative plots of IFN-γ release from un-stimulated and stimulated CD3⁺ CD4⁺ cells from healthy colon. (E) Backgating of CD4⁺ IFN-γ⁺ colon cells. (F-I) Representative plots of IFN-γ release from un-stimulated and stimulated CD3⁺ CD4⁺ cells from TILs. (J) Backgating of CD4⁺ IFN-γ⁺ TILs.

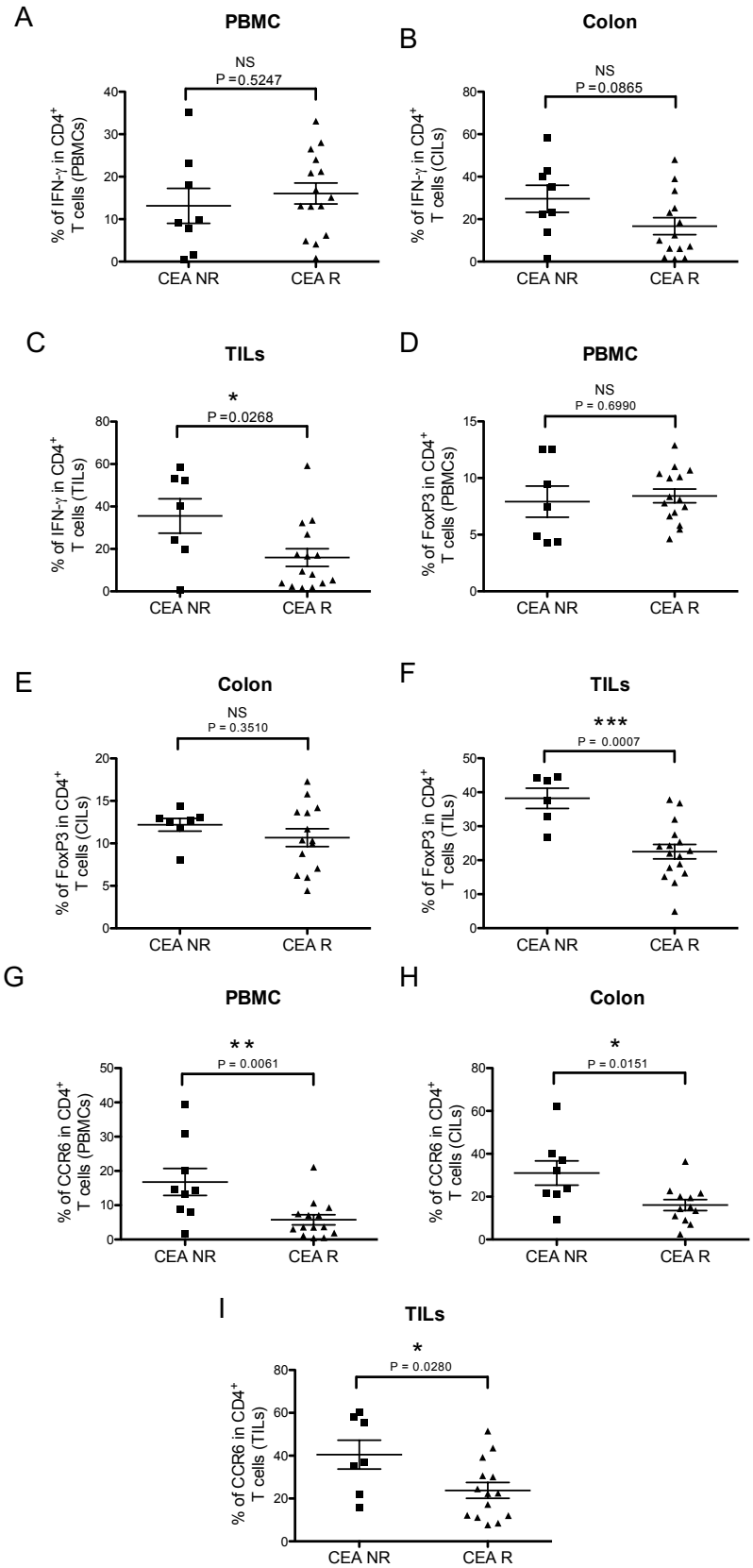

Figure 3.17. CEA responding patients have lower percentages of CCR6$^+$, FoxP3$^+$ and IFN-γ$^+$ T lymphocytes.

(A-C) Percentage of IFN-γ secreting, (D-F) FoxP3$^+$ and (G-I) CCR6$^+$ CD3$^+$ CD4$^+$ cells from PBMC, healthy colon or TILs, isolated from CEA responders and non-responders after stimulation with PMA/Ionomycin. Error bars indicate mean +/- SEM. Unpaired two-tailed students T-test used to test for significant differences.

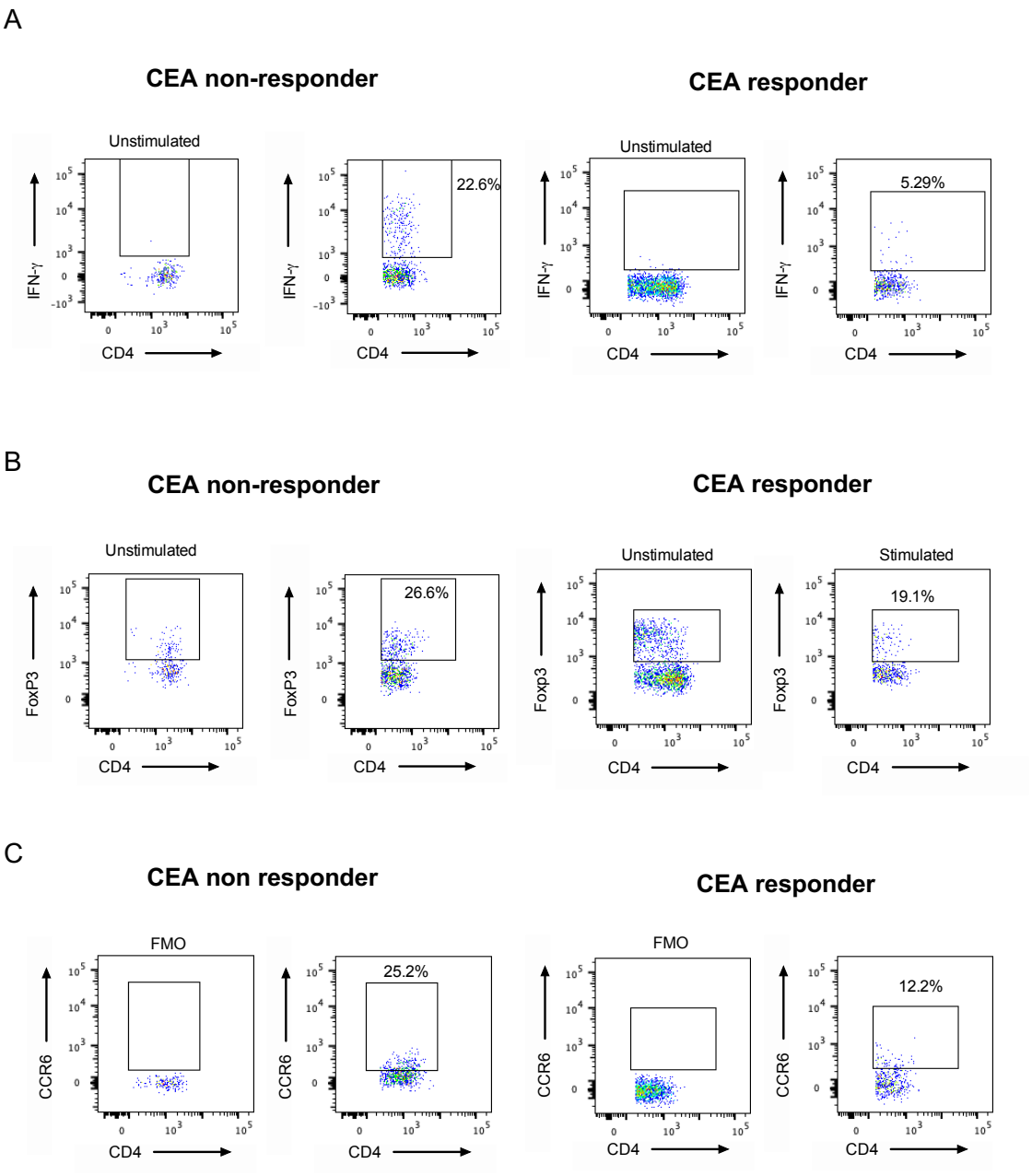

Figure 3.18. Representative FACS plots showing reduced expression of IFN-γ, FoxP3 and CCR6 in CEA responding patients. TILs were gated as described in Figure 15. CEA non-responder and responder (A) IFN-γ secretion, (B) FoxP3 and (C) CCR6 expression. Un-stimulated cells were used to apply gates where cell number was too low for FMO).

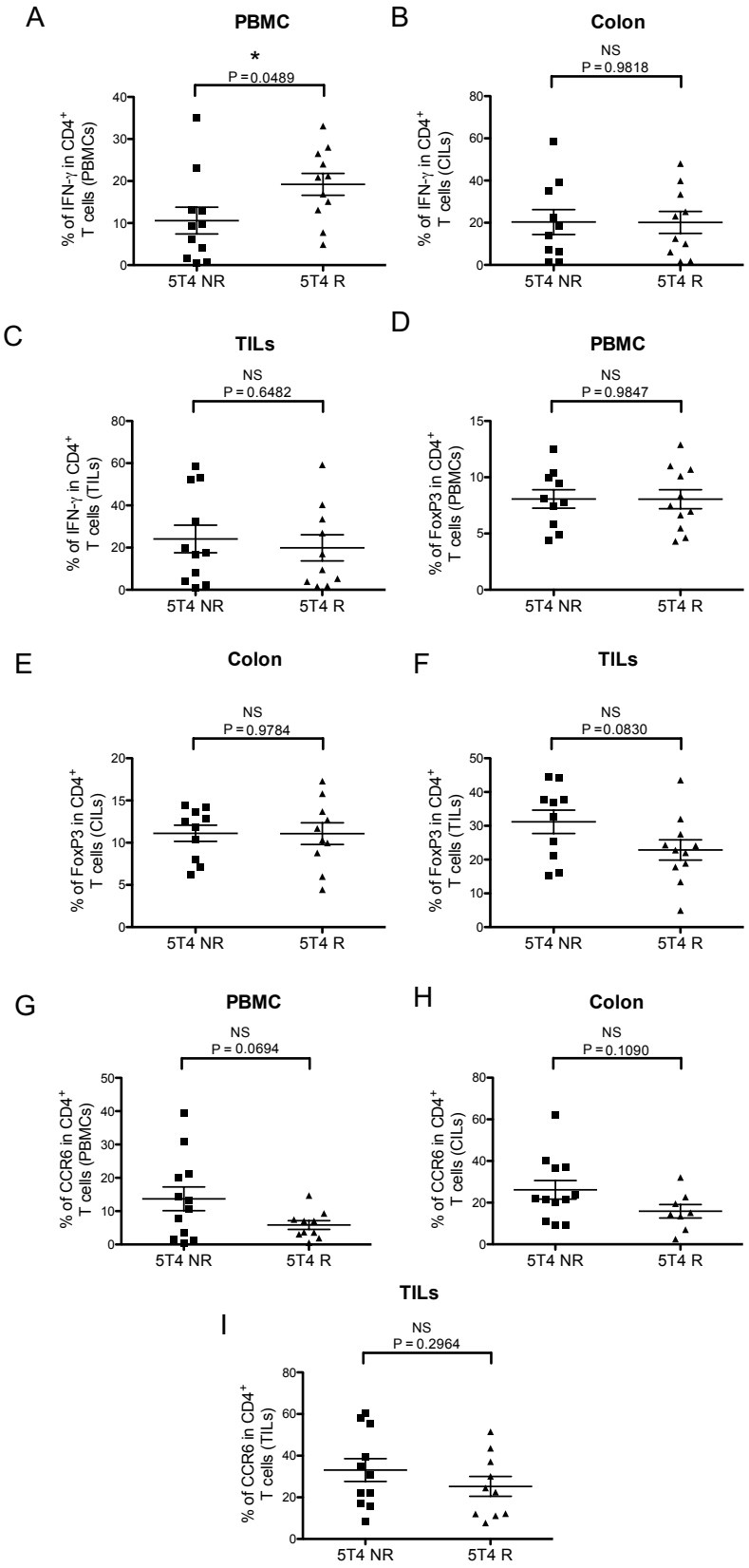

Figure 3.19. No difference was found between CD3⁺CD4⁺ cells from 5T4 responders and non-responders.
(A-C) Percentage of IFN-γ secreting, (D-F) FoxP3+ and (G-I) CCR6+ CD3⁺ CD4⁺ cells from PBMC, healthy colon or TILs, isolated from 5T4 responders and non-responders. Error bars indicate mean +/- SEM. Unpaired two-tailed students T-test used to test for significant difference.

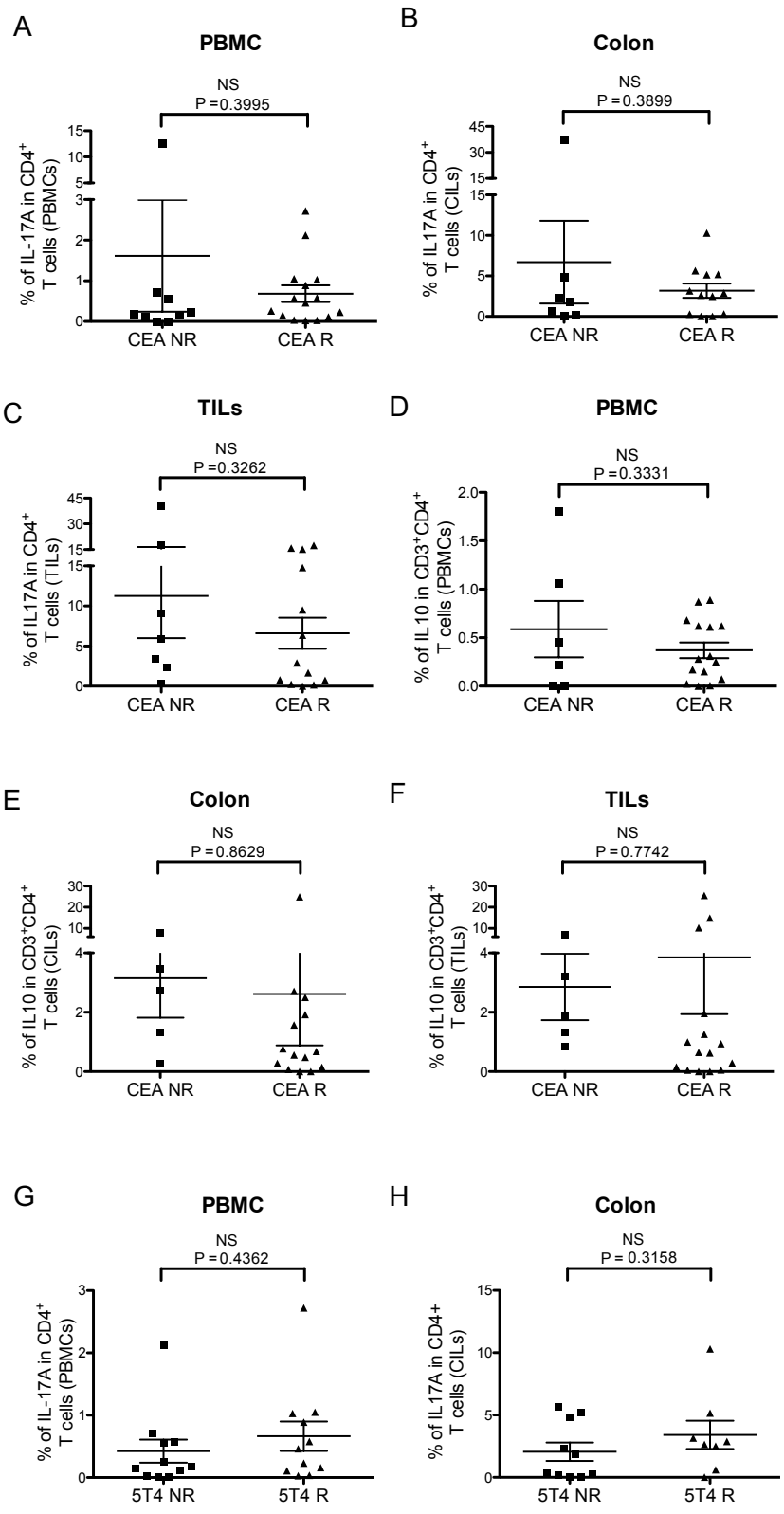
A
PBMC
NS
P = 0.3995
% of IL-17A in CD4+ T cells (PBMCs)
CEA NR
CEA R
B
Colon
NS
P = 0.3899
% of IL17A in CD4+ T cells (CILs)
CEA NR
CEA R
C
TILs
NS
P = 0.3262
% of IL17A in CD4+ T cells (TILs)
CEA NR
CEA R
D
PBMC
NS
P = 0.3331
% of IL10 in CD3+CD4+ T cells (PBMCs)
CEA NR
CEA R
E
Colon
NS
P = 0.8629
% of IL10 in CD3+CD4+ T cells (CILs)
CEA NR
CEA R
F
TILs
NS
P = 0.7742
% of IL10 in CD3+CD4+ T cells (TILs)
CEA NR
CEA R
G
PBMC
NS
P = 0.4362
% of IL-17A in CD4+ T cells (PBMCs)
5T4 NR
5T4 R
H
Colon
NS
P = 0.3158
% of IL17A in CD4+ T cells (CILs)
5T4 NR
5T4 R

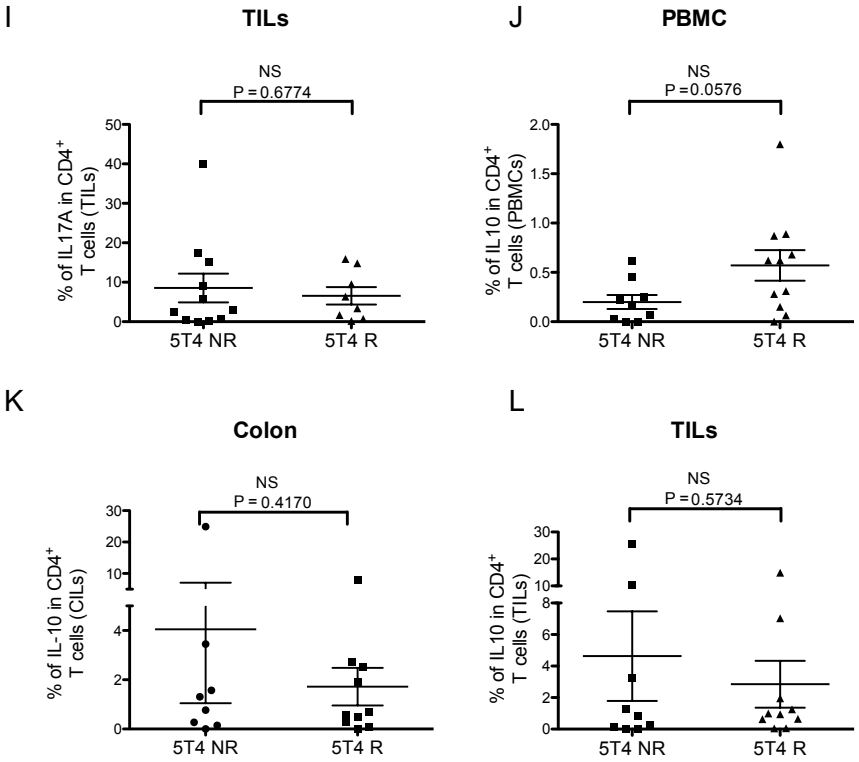

Figure 3.20. IL-17A and IL-10 secretion showed no difference between CEA or 5T4 responders or non-responders.
(A-C) Percentage of IL-17A$^+$ CD3$^+$, CD4$^+$ and (D-F) IL10$^+$ CD3$^+$, CD4$^+$ PBMC, colon cells and TILs from CEA non-responders and responders. (G-I) Percentage of IL-17A$^+$ CD3$^+$, CD4$^+$ and (J-L) IL10$^+$ CD3$^+$, CD4$^+$ PBMC, colon cells and TILs from 5T4 non-responders and responders. Error bars indicate mean +/- SEM. Unpaired two-tailed students T-test used to test for significant differences.

3.3 Discussion

CEA is over-expressed in many adenocarcinomas, widely investigated as a potential therapeutic marker since its discovery in 1965 (183). Mice do not express the CEA protein. Therefore CEA transgenic (Tg) mice, displaying similar CEA expression patterns to that found within humans, were generated for use in animal studies (189). Vaccination work in Tg mice has demonstrated that tolerance can be broken to produce protective immune responses against CEA-tumour expressing cells (240). Human studies have also demonstrated an ability to stimulate CEA-specific T cell responses, after immunisation with CEA-loaded vaccines (243). However, what is not clear from these studies is the association between CEA-specific responses and long-term survival of patients. Studies from our laboratory have shown that CEA-specific T cell responses actually correlate with tumour recurrence in CRC patients.

This Chapter focused on whether IL-17A played a role in promoting the poor survival prognosis seen within CEA responding patients (194). Using FluoroSpot technology we have established for the first time that IL-17A CEA-specific responses can be detected. However, the percentage of IL-17A responding patients did not increase compared to healthy donors. Furthermore, the magnitude of IL-17A responses did not increase compared to IFN-γ secretion. Nor did IL-17A CEA responses differ from 5T4 responses. Collectively these data demonstrate that CEA-specific IL-17A is not the main factor in peripheral blood influencing poor outcome within CEA responding patients. Other explanations therefore must account for the increased tumour recurrence observed.

This study indicates that tumours from IFN-γ/IL-17A CEA-specific responsive patients may be less immunogenic. Significant decreases in IFN-γ^+, FoxP3$^+$ and CCR6$^+$ T cell populations were detected, compared to tumours from non-responsive patients. Low immunogenicity of tumours is often attributed to selective pressures elicited by immune responses within the host themselves and has been shown to be a major factor in the failure of the immune system to cause tumour regression (244). Recently, increased knowledge of genomic and transcriptomic patterns has resulted in a consensus molecular classification system (CMS) to characterise CRC tumours. Based on biological and gene-expression most tumours can be classified into four subtypes (CMS1- CMS4) (174). We suggest that tumours from CEA responsive patients are microsatellite stable, expressing low levels of neopeptides available to stimulate immune responses. Concurrent with this we suggest the tumours are of a chromosomal instable subtype, CMS2 or CMS3, which lack TILs and immunoregulatory cytokines. CMS2 and CMS3 tumours are also typically PDL-1 negative, suggesting they are poorly immunogenic (174, 245). A study by Spragner and colleagues however has pointed out that in melanoma tumours the density of antigen does not dictate the presence of a tumour response and that batf-3 linage dendritic cells, which were not investigated in this study, are key to generating T cell responses (246). With this in mind, it would be advantageous to investigate the molecular signature of tumours from CEA-specific responsive patients.

A key fact about CRC, which one must take into account, is that tumours develop in close proximity to intestinal micro-biota. The field of host–microbe mutualism and its relationship with intestinal disease is becoming of great interest. Recent studies indicate that the micro-biota is dysregulated in CRC patients compared to healthy controls (247). This is also the case in IBD

patients (248, 249) Furthermore the presence or absence of bacterial strains have correlated with differences in response to immunotherapy. In particular Daillere et al (2016) have shown that bacterial species *Enterococcus hirae* and *Barnesiella intestinihominis* can alter the immune landscape of the tumour microenvironment to reduce regulatory T cells and stimulate cognate antitumor cytotoxic T lymphocyte responses (250). As a result, this correlated with better efficacy during treatment with the anti-cancer immunomodulatory agent cyclophosphamide.

On the other hand, it is possible that micro-biota can stimulate immune responses, driving intestinal inflammation, which could aid tumour development. There is strong evidence that aspirin and other nonsteroidal anti-inflammatory drugs help to prevent the growth of polyps and cancer in the colon, findings which support a role for inflammation in disease pathogenesis (251). A study by Grivennikov et al has shown that IL-23 and IL-17A levels are increased in a CRC mouse model and within patients. IL-23 is secreted in response to stimulation of toll-like receptors (TLRs) on myeloid cells, activated by bacterial products derived from the microbiota. IL-23 is then capable of acting on downstream cells, including lymphocytes, contributing to an inflammatory signature comprising of IL-17, IL-6, and IL-22. Such cytokines and other inflammatory molecules (TNF-α) have been shown to promote activation of pro-oncogenic genes, capable of stimulating tumour cell survival and proliferation (234). Associated with intestinal inflammation is loss of epithelial barrier function, shown by reduced tight junctional protein and surface mucin expression (252). Disruption of the epithelial barrier can lead to further translocation of microbes and microbial products from the intestinal lumen. This can result in further IL-23 secretion and downstream effects, resulting in a continuous cycle of inflammation (213) (253). Loss of the tight junctional protein claudin-3,

responsible for maintaining barrier function in the colon has been shown to induce IL-6 and STAT-3 signalling. The authors of this study observed increased STAT-3 activation was associated with CRC malignancy in mice and also correlated with CRC progression in humans (254). Together this data implies there is an important role for intestinal barrier function in CRC development.

CEA is a glycoprotein, expressed on the normal intestinal epithelium at low levels as well being up-regulated in adenocarcinomas. It is possible that a dysfunctional epithelial barrier may allow cross reactivity of CEA-specific T cells to luminal microbial products; generating local inflammation. In turn, inflammation and CEA-specific T cells could drive further barrier deterioration and provide a pro-tumorigenic niche for tumour cells to survive and proliferate. As CEA specific IL-17A secreting cells were found not to be the cause of poor survival within CEA responding patients, we next hypothesised that CEA responsive patients had increased intestinal mucosal permeability. In support of this hypothesis, IL-17A has been shown in some studies to actually promote mucosal barrier function and in its absence there is an increase in epithelial injury and compromised barrier function (255, 256). It is possible the reduction in Th17 cells seen within CEA responding patients (lower $CCR6^+$ T cell infiltration) could have a role in tumourigenesis though lack of epithelial barrier maintenance. Investigations into epithelial barrier function are discussed in Chapter 4 and Chapter 5.

3.4 Conclusion

In this chapter it has been shown that CEA and 5T4 TAAs are capable of stimulating IFN-γ and IL-17A responses from PBMC obtained from CRC patients. However, it has been concluded that blood CEA-specific IL-17A

secreting cells are not responsible for the increased tumour recurrence seen within CEA responding patients, identified in the laboratory's previous study. However, a response to CEA could be used as a biomarker for monitoring disease as CEA responders may have less immunogenic tumours, indicating tumour recurrence would be more likely.

An investigation into epithelial barrier function playing a role in the correlation seen within CEA-specific responses and tumour recurrence is discussed in the remainder of this thesis.

Chapter 4. Optimisation of the Ussing Chamber system

4.1 Introduction

The Ussing Chamber system was originally developed by Danish biologist Hans Ussing in the 1950's to understand the phenomenon of active Na^+ transport (257). At the heart of the system lies the chambers, with a perfusion system, electrodes, an amplifier and a data acquisition system performing supporting roles (Figure 4.1).

The chambers support epithelial tissue or cell monolayers in such a way that each side of the membrane is isolated and faces a separate chamber-half. The chambers are then filled with a physiologically relevant solution, such as Krebs buffer. This configuration allows for adjustments to either side of the tissue membrane with complete control. The initial work performed by Hans Ussing led to the two-membrane hypothesis for epithelial transport, where the apical membrane is permeable to Na^+ and the basolateral permeable to K^+ (258). This paradigm served as the foundation for our present models of transepithelial transport. In later years it was discovered that primary active transport via the Na^+/K^+ ATPase pump is capable of transporting Na^+ ions out of the cell in exchange for K^+. It is this mechanism which provides absorption of Na^+, establishing an electrochemical gradient for secondary active transport of other ions and water absorption (259). Together these studies unravelled a fundamental physiological cellular process.

Ussing chambers have also been utilised in the investigation of diseases, including cystic fibrosis. The CFTR receptor, found on the apical membrane, is defective within patients. As seen by Ussing measurements this leads to increased Cl^- secretion and Na^+ absorption within epithelial cells, located in the

intestine and airways (260, 261). This abnormal ion movement causes an inability to effectively absorb nutrients from the gut. Moreover, it results in a reduction of airway surface liquid and excess mucus production. This affects sterility of the airways, leading to susceptibility to infection and the development of inflammation (262).

While Ussing can be used to monitor ionic movements, the system is also able to evaluate permeability of tissues via electrical and fluorescent probe flux measurements. Various methods to measure permeability exist, with tracer molecules including Cr-EDTA (263), polyethylene glycols (PEGs) (264, 265) and fluorescently labelled dextran (256, 266) often used to monitor passage across epithelial tissue. In more recent studies, 4kDa FITC-dextran is frequently used *in vivo,* where animals are orally administered dextran and levels in blood plasma are measured four hours later (267). However, the passage of tracer molecules *in vivo* fails to provide information on precise locations of increased permeability. Other factors including gastrointestinal motility, surface area and mucosal blood flow differences may also lead to inaccuracy of measurements. The e*x-vivo* Ussing system aims to remove some of these limitations, by investigating permeability of isolated tissue sections under consistent environmental conditions and with the same exposed surface area. The epithelial barrier is semi-permeable, with charge and size selectivity limiting the passage of liquids, ions and larger solutes. By using both tracer molecule and electrical measurements, explained within this chapter, Ussing takes into account both ionic and paracellular permeability, often referred to as the pore and leak pathways (268). This gives a robust insight into the overall permeability of tissue specimens. Increased 4kDa FITC-dextran passage can be seen across the gut during colonic enteropathy. Studies show that inflammatory molecules TNF-α and IFN-γ have key roles in modifying tight junctional (TJ) protein complexes,

found between epithelial cells, through myosin light chain kinase expression (269). Down regulation of TJ "sealing" proteins such as claudins 3, 5, 8 and JAM-A, as well as up-regulation of the pore forming claudin-2 are associated with increased permeability (27, 270-274). Furthermore over expression of the tight junctional protein occludin was found to prevent increased permeability within Madin-Darby canine kidney (MDCK) cell monolayers (10). There was no increased permeability seen within occludin$^{-/-}$ mice (275), however it may be important for cell adhesion (276). Human studies of intestinal tissue from IBD patients also show TJ differences between inflamed tissues compared to healthy samples, as reviewed by Landy and colleagues (277). Complementary to these findings, Ussing chamber analysis has demonstrated that IBD patients have increased intestinal permeability, shown both by electrical and probe flux measurements (278, 279). It is clear from these studies that distribution and composition of TJ proteins impacts intestinal barrier function, which can be measured using the Ussing chamber system.

Current data from our laboratory indicates that CRC patients responding to the tumour-associated antigen CEA have a poorer survival prognosis than non-responding patients (194). The majority of CRCs overexpress the CEA protein but it can also be detected at low levels on the surface of healthy intestinal mucosa (280). Soler and colleagues have previously shown that the permeability of colonic tissue in CRC is increased compared to healthy specimens (281). Furthermore, mouse models have suggested barrier defects could aid in tumour progression through generation of an inflammatory environment (213, 253). Based on this information and as mentioned in Chapter 3, I hypothesised that CEA responding patients have reduced intestinal barrier function. This could allow cross reactivity of CEA-specific T cells to luminal microbial products, possibly creating an inflammatory environment. In turn,

inflammation could drive further barrier deterioration and provide a pro-tumorigenic niche for tumour cells to thrive. This could explain why a CEA-specific T cell response is associated with tumour recurrence. To address measuring intestinal permeability I aimed to successfully construct an Ussing chamber system within our laboratory. This chapter describes the design of our Ussing system, optimisation of the method and validation of the technique in two mouse models of intestinal inflammation.

4.2: Results

4.2.1 Ussing System Design

I first set out to assemble an Ussing chamber system selecting each element individually for the purpose of this study, thereby creating a system unique to our laboratory.

The Navicyte Ussing design was used. It accommodates six individual Ussing chambers, providing analysis of six tissue samples simultaneously (Figure 4.2A). The chambers themselves are a modified version designed by Grass and Sweetana in 1988 (282) (Figure 4.2B and 4.2C). The chambers consist of two halves with the intestinal tissue specimen mounted as a semi-permeable membrane in-between (Figure 4.2D).

During electrical evaluation of intestinal integrity, the three main building blocks of electricity are required: voltage, current and resistance. Each Ussing chamber is therefore equipped with four Ag/AgCl electrodes to obtain electrical readings (Figure 4.2B and Figure 4.2C). The Ag/AgCl electrode is stable at various temperatures and pH levels. Also the use of glass barrels with a ceramic junction at the end of the electrode renders the use of agar bridges obsolete. Electrodes are connected to an EC825A voltage/clamp box to monitor both voltage and current (Figure 4.2E).

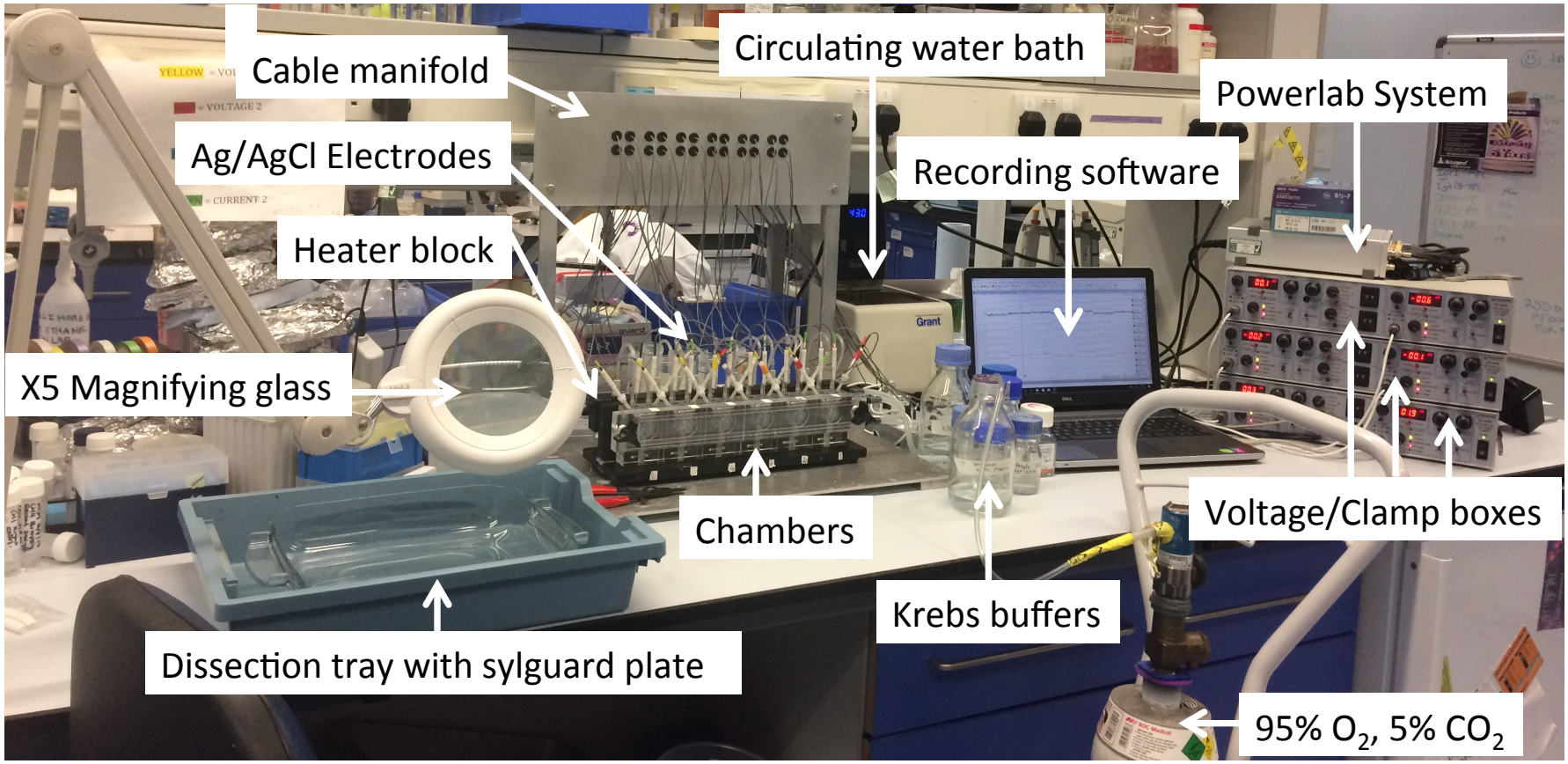

Figure 4.1. The Ussing chamber system.
Image of laboratory bench showing Ussing chambers and all other supporting equipment required for permeability experiments.

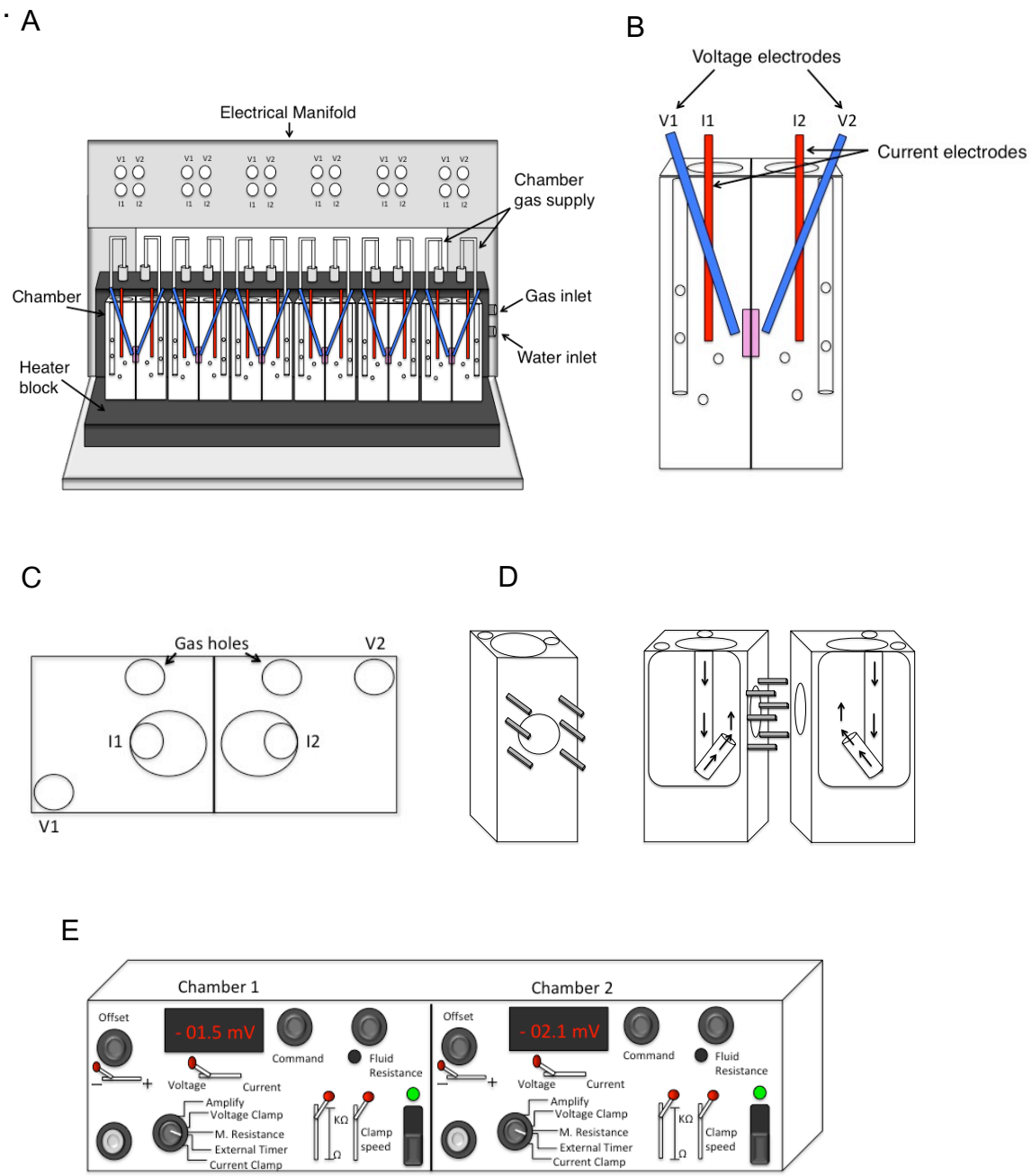

Figure 4.2. Design of the Ussing chamber system.
(A) Navicyte Ussing system unit supporting six chambers with custom made electrical manifold. (B) Individual Ussing chamber with voltage and current Ag/AgCl electrodes. (C) Birds-eye view of individual Ussing chamber showing electrode and gas inserts. (D) Chamber halves showing metal pins used to secure tissue. Gas flow direction to stir buffer is depicted by arrows. (E) Amplifying EC825A voltage clamp box containing a volt and amp meter to record voltage and current respectively. External timer is selected to connect to computer software.

4.2.2 Electrical Resistance Measurements and Optimisation of Software

Columnar epithelial cells that line the intestine are polarised structures, with cations and anions being transported across apical and basal membranes at different rates (32, 283). The separation of charged ions across the phospholipid bi-layer creates a membrane potential at each side of the epithelium. This polarisation is a fundamental property of epithelial cells and is essential for the absorption of electrolytes, water and salt. By inserting the Ag/AgCl electrodes at the apical and basal membranes each potential can be detected and the overall spontaneous tissue voltage across the epithelium determined. This value is termed the potential difference (PD), measured in volts and is displayed on the EC825A volt/clamp box. The PD is an indicator of tissue viability and essential for all Ussing chamber experiments (284).

Electrical resistance of tissue is often used as a measurement of gut integrity, with low electrical resistance indicating tissue is leaky. An open circuit current clamping technique was used for all experiments. PD was continuously measured and small square current pulses of 1.5, -1.5, 3 and -3 μA were delivered across the specimen. Injections of external current pulses charge the apical and serosal membranes towards depolarisation and hyperpolarisation resulting in a change of tissue PD. Voltage electrodes sense this change in PD and it can be visualised using computer software. An overview of the electrical circuit can be seen in Figure 4.3.

Initially murine colonic samples were clamped at particular current amplitudes manually and the effect on tissue voltage was measured using the EC825A volt/clamp box. This provided expected values that could be used validate the values obtained using our new computer-controlled stimulation. As shown previously by Asa Keita and colleagues, current stimulation pulses with the magnitudes chosen were sufficient to detect a voltage response from small

tissue samples (285). However, the number of current pulses to be delivered across the tissue was tested (Figure 4.4A, B and C). As pulses resulted in almost identical tissue response peaks, a repeat of four current pulses at each magnitude was selected. This allowed for a mean voltage response to be calculated and reduced tissue exposure to unnecessary current pulses. The stimulation protocol was created and delivered across the tissue at five-minute intervals during a total of 90-minute experimental periods (Figure 4.4D). Stimulation traces were assessed before every experiment as damage to electrodes, air bubbles, or blockages can result in excess noise within the system leading to abnormal stimulation peaks (Figure 4.4E).

Electrical resistance measurements are based on Ohm's law (Figure 4.5A). Using a linear least squares fit analysis, the paired relationship between voltage and current was used to calculate electrical resistance of colonic tissue, measured in Ω/cm^2 at the time of current stimulation (Figure 4.5B).

4.2.3 Temperature

The six Ussing chambers sit within a black heating unit that is connected via tubing to a circulating water bath, maintained at 45°C. Due to heat loss through the system this higher temperature is required to ensure chambers are kept at a constant 37°C.

4.2.4 Optimising Ag/AgCl electrodes

Ag/AgCl electrodes function as a redox electrode with an equilibrium existing between the silver (Ag) metal and its low soluble salt and the anion of that salt (AgCl). The electrode maintenance protocol had to be optimised for this study as the purchased pre-chlorided electrodes began to show drifting potential difference values over time in the absence of tissue. This made it impossible to

“zero” offset potential prior to the start of experiments. Various methods for re-chloriding, including electroplating, were investigated. The best method to achieve stable electrodes was removing the old AgCl coating using steel wool, wiping the silver wire with deionised water and 70% ethanol to remove oils and immersing in sodium hyperchlorite (NaClO). By exposing the Ag wire to OCl^-, spontaneous oxidation occurs creating a coat of AgCl on the metal surface.

Electrode glass barrels were filled with an electrolyte solution of 3M KCl, saturated with Ag. However, efficient electrolyte solution filing technique is imperative as small air bubbles located within the glass barrel leads to electrical noise within the system (Figure 4.4E). To achieve good filling technique, electrolyte solution was dispensed into a small bottle containing a holder for a thin plastic tube. The tube is inserted to the end of the glass barrel where the ceramic junction is located. Using constant pressure so electrolyte solution flows continually the barrel is filled as the tube is slowly withdrawn. By tapping lightly against the ceramic junction during this process air bubbles are dislodged. KCl salt, formed when exposed to air can be deposited at the opening of the glass barrel. It must be carefully removed and not descend to the ceramic junction as this can cause blockages, leading to interference or obstruction of electrical readings.

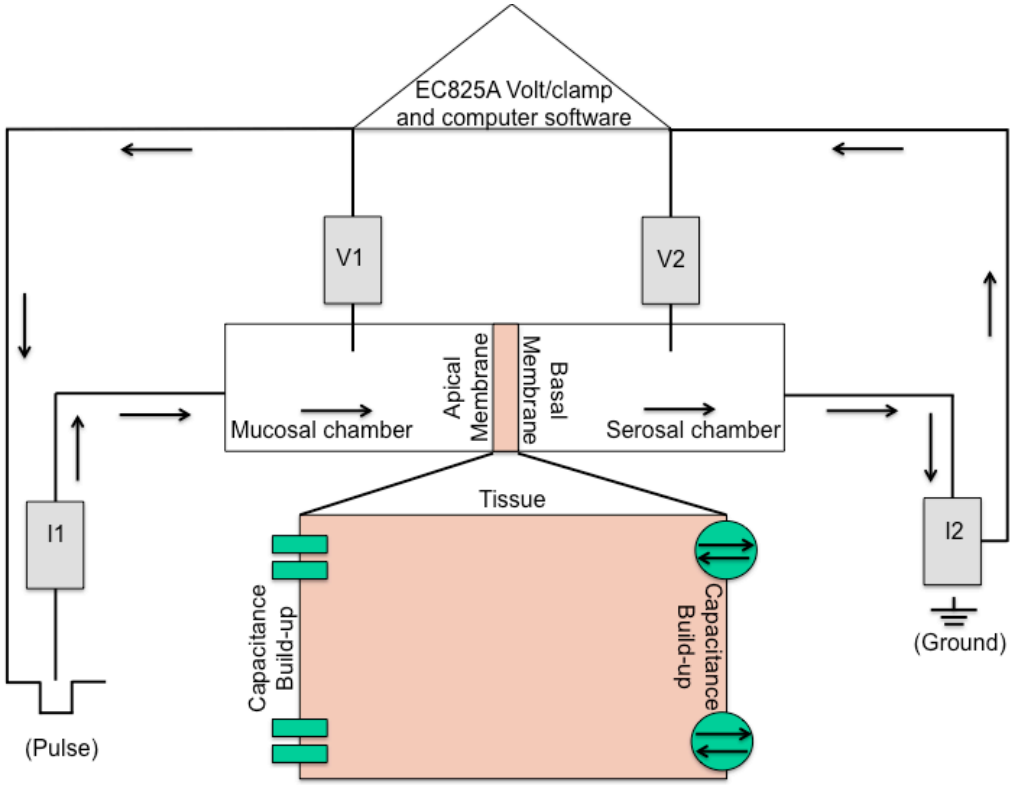

Figure 4.3. Schematic of the electrical circuit used in the Ussing chamber system.
Computer controlled current pulses are sent from the EC825A volt/clamp box amplifier via current electrode I1 through the mucosal chamber-half (indicated by arrows), across tissue apical and basal membranes and through the serosal chamber-half. Current electrode I2 connecting back to the EC825A volt/clamp box completes the circuit. Voltage electrodes V1 and V2, connected to the EC825A amplifier box and computer software continuously monitor voltage at the apical and basal tissue membranes.

A

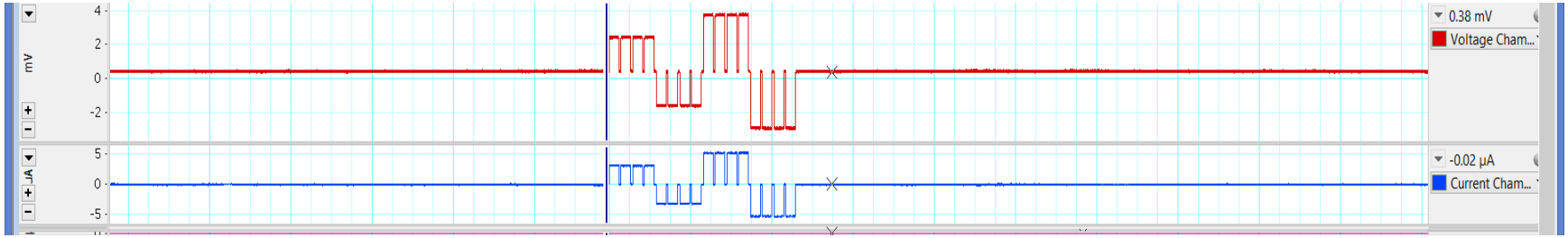
mV
4
2
0
-2
μA
5
0
-5
0.38 mV
Voltage Cham...
-0.02 μA
Current Cham...

B

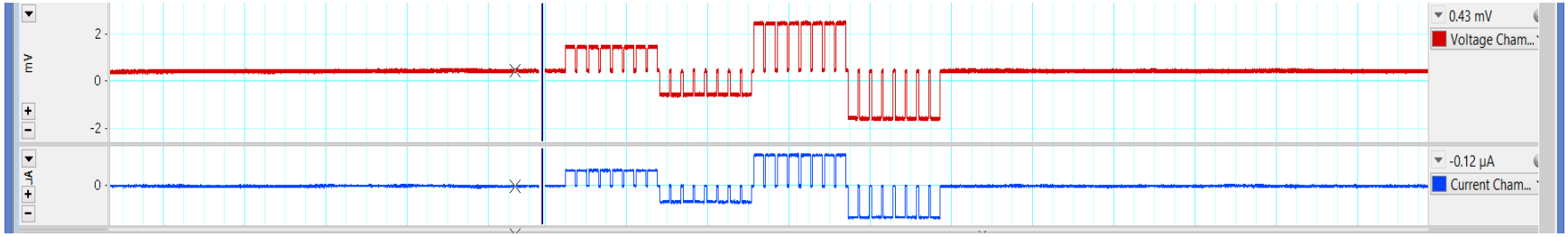
mV
2
0
-2
μA
0
0.43 mV
Voltage Cham...
-0.12 μA
Current Cham...

C

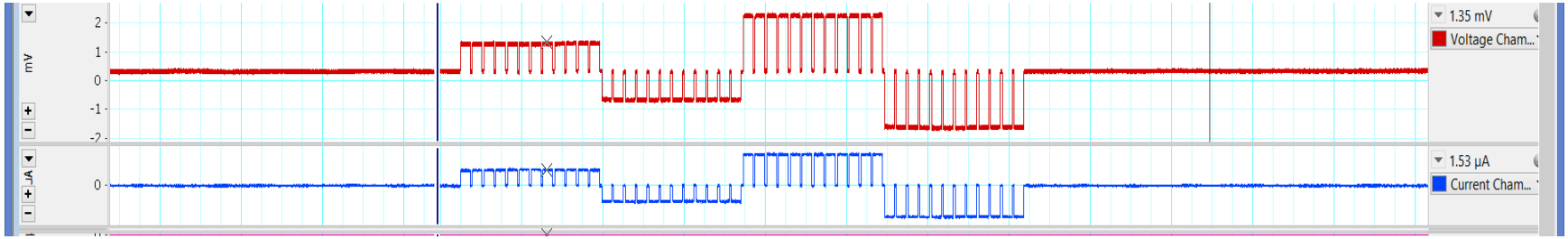
mV
2
1
0
-1
-2
μA
0
1.35 mV
Voltage Cham...
1.53 μA
Current Cham...

D

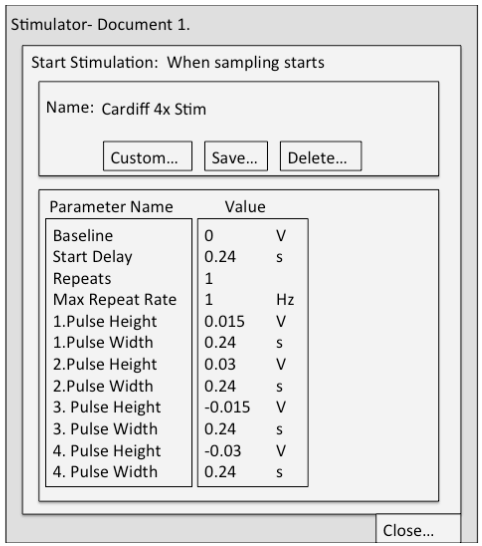

E

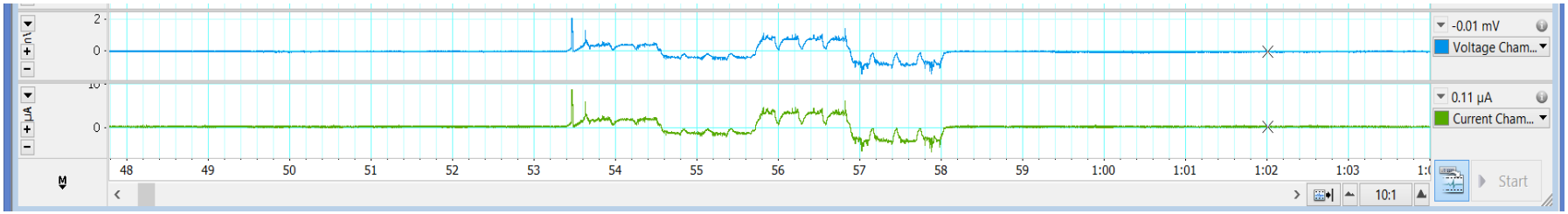

Figure 4.4 A stimulation protocol of four pulses was adequate to determine tissue resistance.
Current pulse traces using four (A), eight (B) or twelve (C) current stimulations. (D) Chosen current pulse stimulation event protocol. (E) Current pulse trace showing air bubbles within electrodes causing electrical noise.

4.3.5 Optimisation of Chambers for small tissue samples

Chambers had to be optimised to accommodate small mouse tissues, as the standard chamber aperture size is 9mm diameter. To do so, X-ray film was cut into square pieces, large enough to cover all six chamber pins. In the centre of each, a 3mm hole was punched to reduce the tissue area exposed (Figure 4.5C). The x-ray film was made so that each square had a matching counterpart. Initial experiments showed this was necessary as samples had to be mounted in-between two x-ray film squares, securing tissue in place to prevent leakage.

4.3.6 Optimisation of dissection technique and handling of tissue

Tissue viability is key to obtaining accurate measurements and can be determined by the steady state PD value (284). This value generally is negative due to the active transport of ions at the apical and serosal membranes (284) (286). Preliminary experiments using untreated FoxP3^{DTR} mice resulted in positive PD values (Figure 4.6A). Multiple investigations were made to ascertain why (Table 4.1). Ultimately it was found that the mucosal surface of the colonic tissue was more delicate and prone to damage. I therefore optimised my dissection technique and tissue handling when mounting samples into chambers. An overview is shown in Figure 4.6B and 4.6C and a detailed description in Chapter 2. Improved handling resulted in tissue displaying a negative PD (Figure 4.6D). Furthermore, responses to the chloride secretion enhancer Forskolin (287), as seen by a drop in PD (Figure 4.6D) and low 4kDa FITC passage (Figure 4.6E) were seen. Only samples showing a PD value of 0.5 mV or less at the beginning of experiments and a response to Forskolin were included within analyses.

A

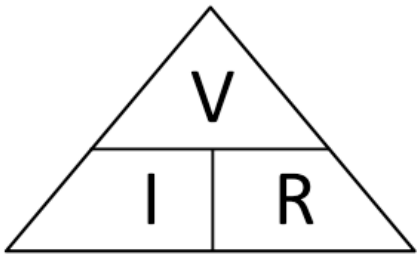

B

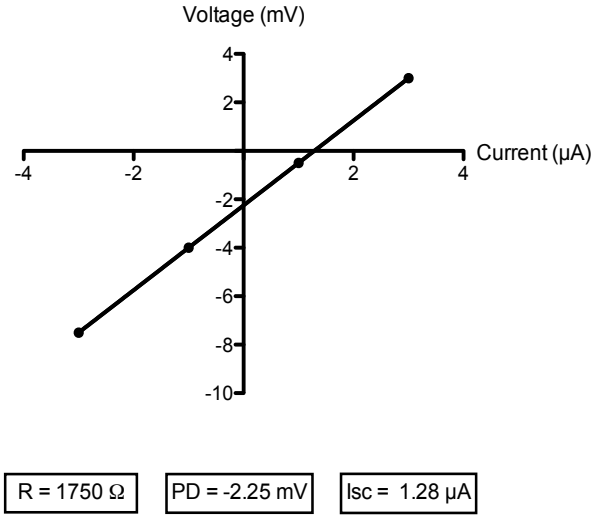

C

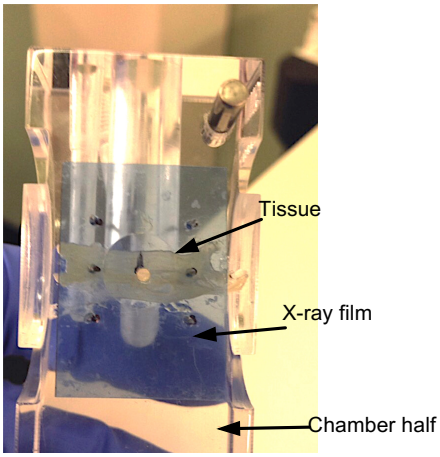

Figure 4.5. Calculation of electrical resistance.
Linear least fit squares analysis based on Ohm's law (A) used to plot current stimulation against tissue voltage (B). Linear regression is equal to resistance. The y-intercept equals the PD value of tissue and Isc can be calculated by PD/R. (C) X-ray films with a hole size of 3mm were placed over chamber pins to reduce exposed tissue area.

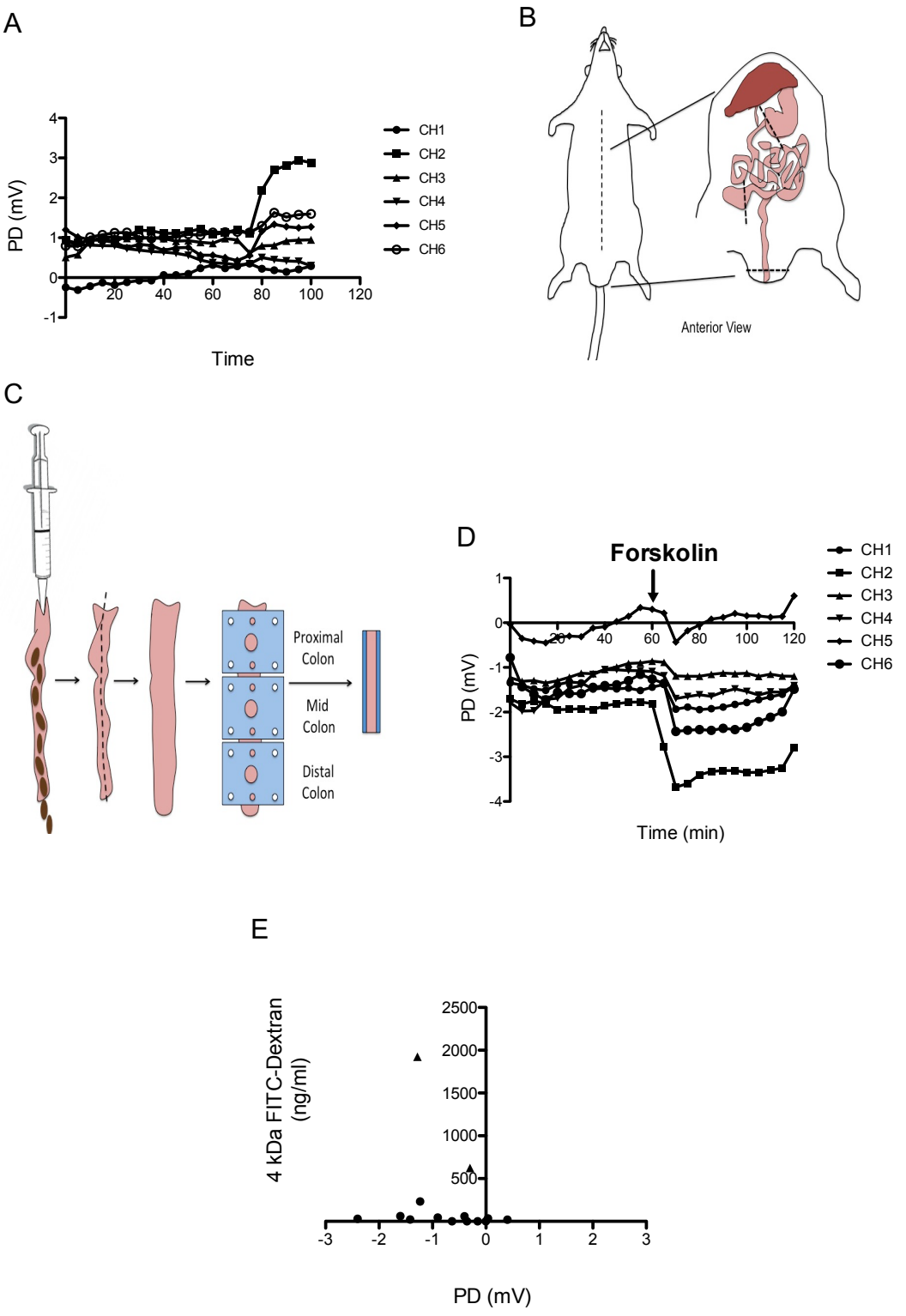

Figure 4.6. Optimised dissection and mounting technique gives rise to negative PD values, indicative of healthy tissue.

(A) Positive PD values of tissue before dissection optimisation. (B) The colon is dissected as indicated by dashed lines and (C) flushed out before being opened longitudinally with micro dissection scissors. X-ray film is used to select colonic regions. (D) Negative PD values after optimisation showing tissue responds to Forskolin at 60 minutes. (E) Tissue with a negative PD value shows little or no 4kDa FITC-dextran passage. Black triangles indicate tissue not responsive to Forskolin.

Table 4.1. Alterations to Ussing experiments investigated to obtain reliable electrical readings.

	Variable investigated
1.	Fresh buffers immediately before experiment
2.	Chloriding of electrodes in bleach
3.	Glass barrel ceramic tips cleaned with hot water
4.	Tissue orientation altered
5.	Method of culling (CO_2 Vs cervical dislocation)
6.	Buffer pH
7.	Dissection technique to avoid touching the mucosal surface

4.3.7 Regional variation in electrical resistance

To assess baseline permeability distal, mid and proximal sections of colon were harvested from untreated FoxP3^{DTR} mice. Results show the proximal region of the colon has the highest electrical resistance and the mid section the lowest (mean=41.12Ω/cm^2 and 26.34 Ω/cm^2 respectively) (Figure 4.7A). This difference was stable throughout experiments (Figure 4.7B and 4.7C). Although not significant, this trend was also detected in Balb/C DEREG mice (Figure 4.7D). These data validate use of the Ussing system to measure electrical resistance of mouse tissue and demonstrate the natural variability in permeability along the colon. Variations are suggested by embryological origins of hind vs midgut (288), different patterns of disease distribution seen in IBD, variability in drug absorption and expression patterns of TJ proteins (23, 289, 290). This was taken into consideration for future Ussing experiments. Distinct regional variations of colonic permeability have not been well defined previously.

4.3.8 Optimisation of FITC-dextran and Lucifer yellow

As mentioned previously the diffusion of fluorescent probes across tissue is often used as a measurement of intestinal permeability. 4kDa FITC-dextran and Lucifer yellow (457 daltons) were titrated to ascertain optimal mucosal chamber starting concentrations. Initial experiments showed that in healthy mice 4kDa FITC-dextran, at 0.5 mg/ml, was only detectable after 120 minutes (Figure 4.8A). High concentrations of either 0.5 mg/ml or 1 mg/ml 4kDa FITC-dextran were used to saturate the mucosal chamber in future experiments. Lucifer yellow passage could be detected in all tissue samples, showing its usefulness as a positive control (Figure 4.8B) with 250 µg/ml and 125 µg/ml starting concentrations showing the most passage to the serosal chamber (Figure 4.8B). However, since the 125 µg/ml starting concentration was detected using the mid section of the colon, previously shown to be most leaky (Figure 4.7A), a starting

concentration of 250 µg/ml lucifer yellow was chosen to ensure good passage through all tissue regions.

4.3.9 Gas supply

A constant supply of carbogen (95% oxygen, 5% CO_2) must be supplied to each Ussing chamber in order to maintain tissue viability. Loss of oxygen leads to quicker deterioration of tissue resistance (Figure 4.9A and 4.9B). Consistent with this was increased passage of Lucifer yellow in both proximal and distal colonic regions investigated (Figure 4.9C).

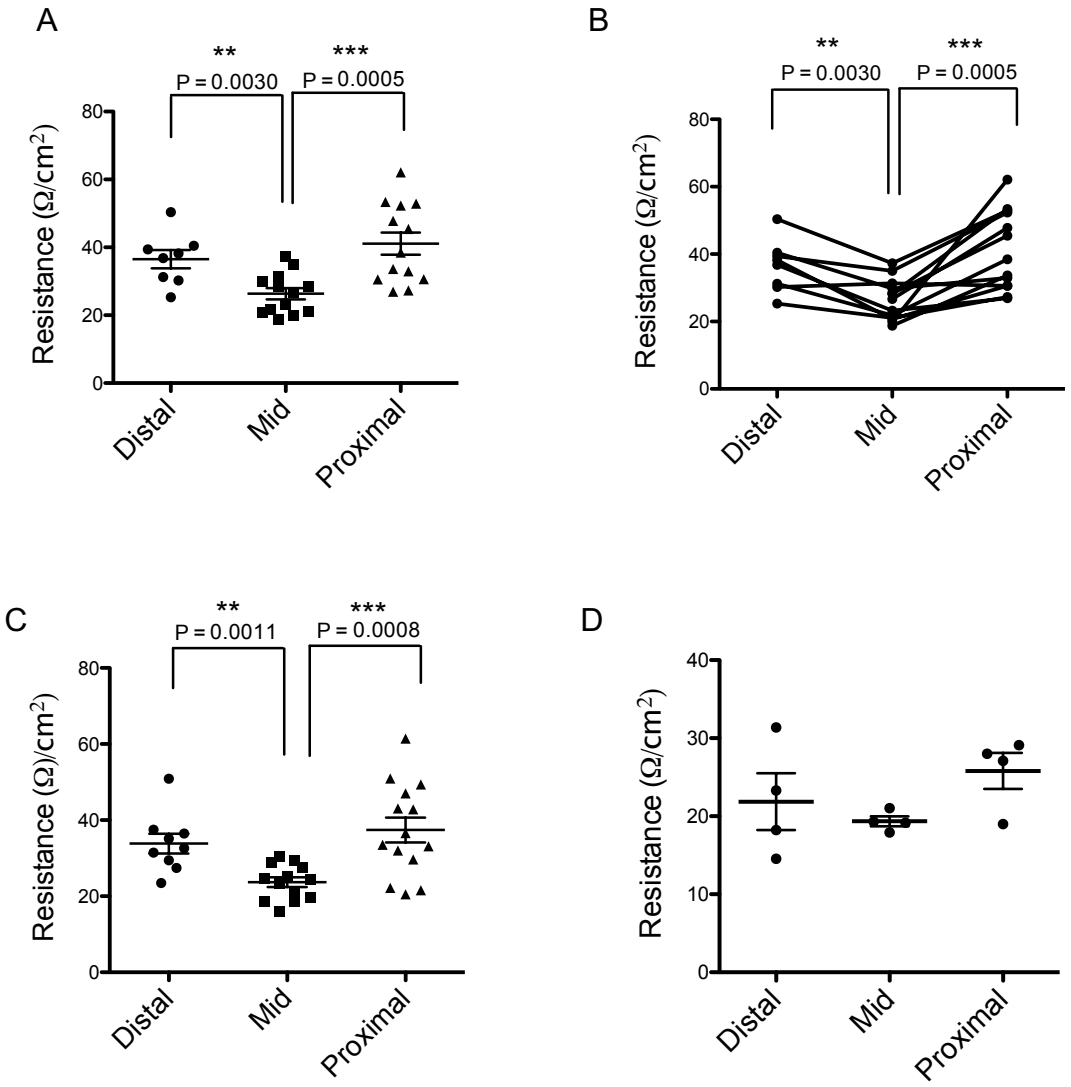

Figure 4.7 Baseline electrical resistance identifies regions permeability differences.

(A) Electrical resistance of matched distal, mid and proximal colonic regions from untreated FoxP3^{DTR} mice. Electrical resistance at (B) twenty minutes and (C) sixty minutes during experiments. (D) Electrical resistance of distal, mid and proximal colonic sections from untreated DEREG mice. Unpaired students T test used to test for significant differences. Error bars show +/- SEM.

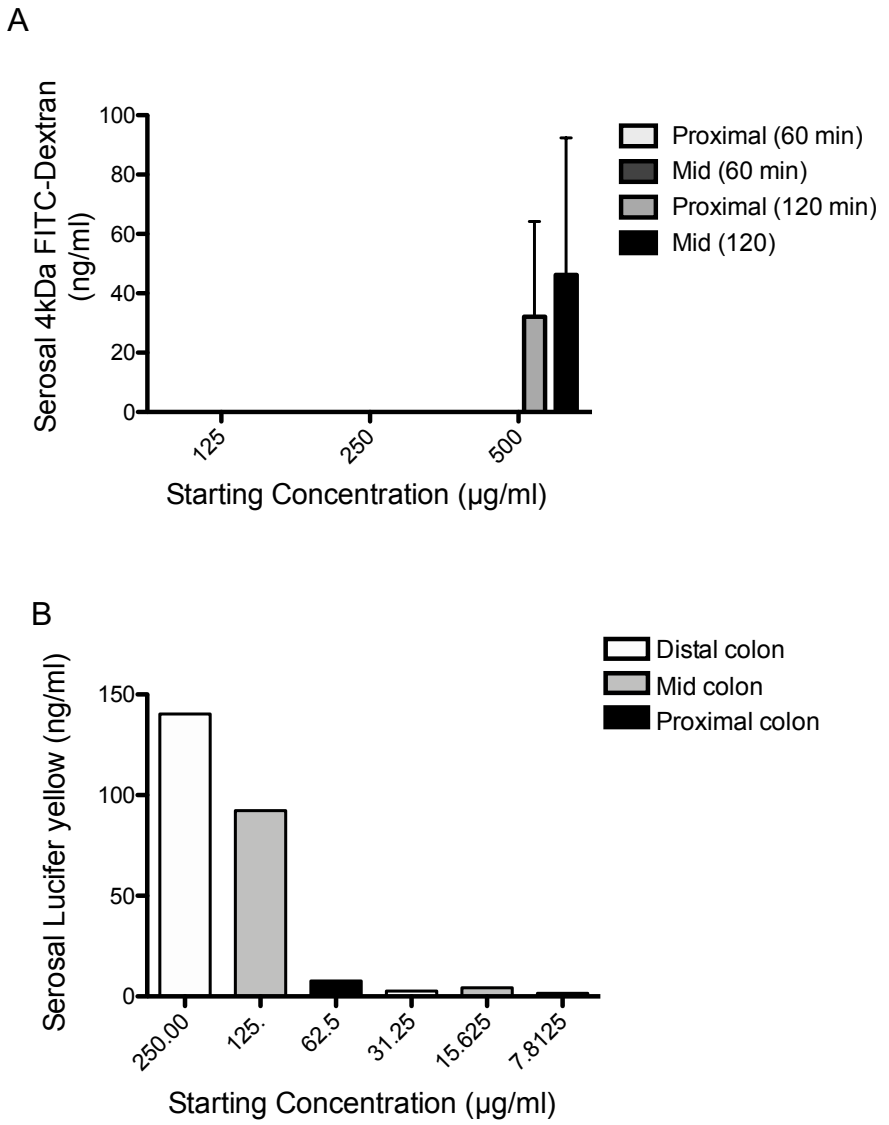

Figure 4.8. Lucifer yellow passage across colonic epithelium is higher than 4kDa FITC-dextran passage.

(A) Serosal 4kDa FITC-Dextran concentration with various starting mucosal concentrations after 1 hour using mid and proximal colonic regions. (B) Lucifer yellow serosal chamber concentration after 1 hour with various starting concentrations. 62.5 µg/ml and 7.8 µg/ml, 125 µg/ml and 15.6 µg/ml, 250 µg/ml and 31.25 µg/ml starting concentrations were used for proximal, mid and distal colon sections respectively. Error bars show SEM.

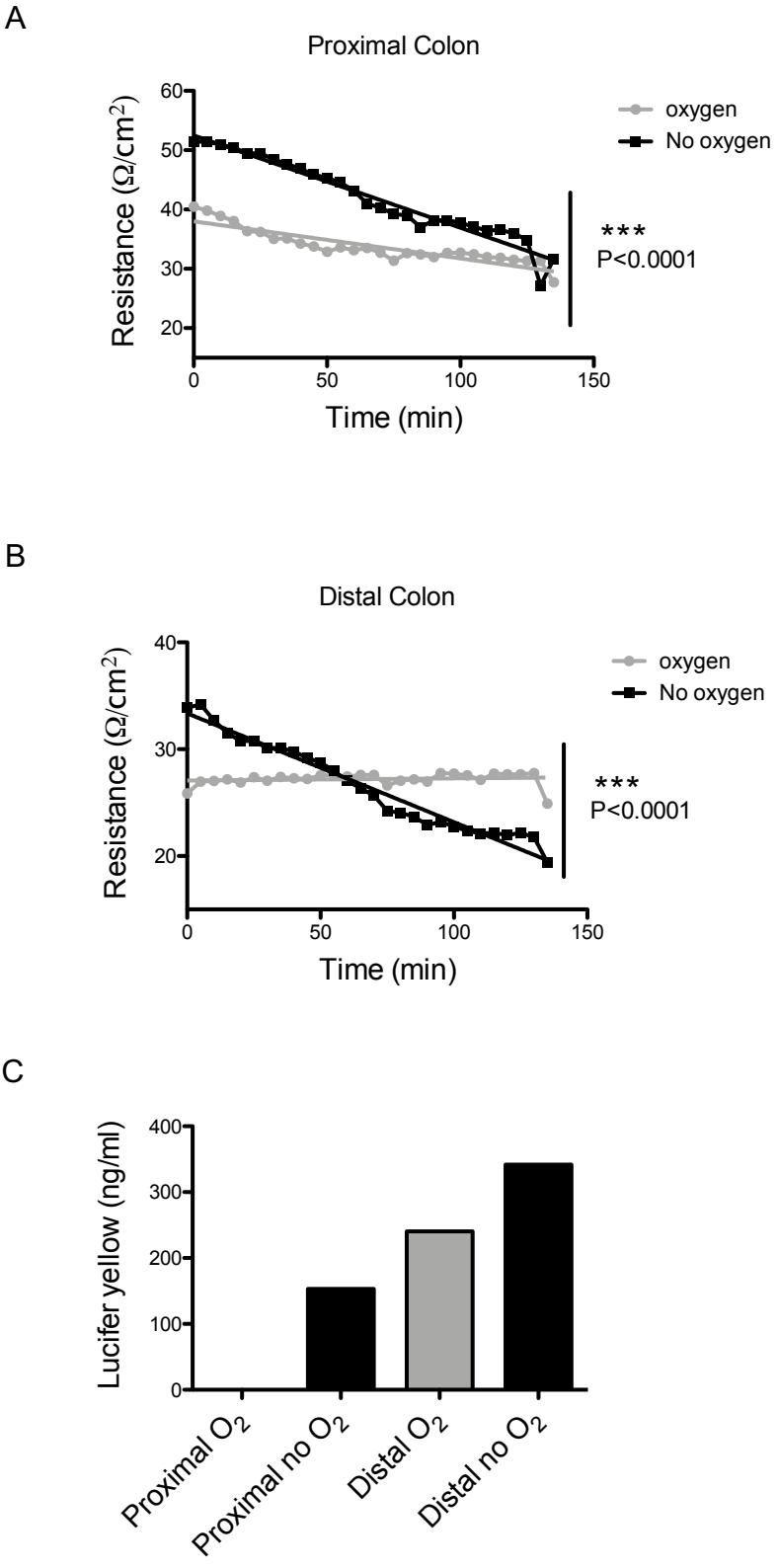

Figure 4.9. Loss of oxygen reduces electrical resistance and increases paracellular permeability.

Electrical resistance of (A) proximal and (B) distal colonic regions with or without an oxygen supply. (C) Lucifer yellow serosal chamber-half concentration after one hour. Linear regression comparison of electrical resistance slopes tested for significant differences.

4.3.10 Dextran sodium sulphate (DSS) mouse model

DSS is an irritant, widely used to induce intestinal inflammation as a model of IBD (291, 292). It has been shown that under inflammatory conditions colonic permeability is increased, due to inflammatory molecules altering TJ proteins (269). Therefore the DSS model was used as a positive control to evaluate if the Ussing system was capable of detecting increased permeability in inflamed tissue. Using the 3% DSS treatment schedule described in Chapter 2, a reduction in mouse weight was seen within nine days (Figure 4.10A). Upon harvest, treated mice were also found to have a shortened colon length (Figure 4.10B) and positive occult blood test results compared to untreated animals (Figure 4.10C). Furthermore histological analysis revealed gross abnormalities of the intestinal architecture along with increased cellular infiltration, indicative of inflammation (Figure 4.10D). Ussing analysis showed a decrease in electrical resistance (Figure 4.10E) and an increase of 4kDa FITC-dextran flux (Figure 4.10F) across the proximal region of the intestinal epithelium. Together this data shows that our Ussing system was capable of identifying alterations in gut integrity under inflammatory conditions.

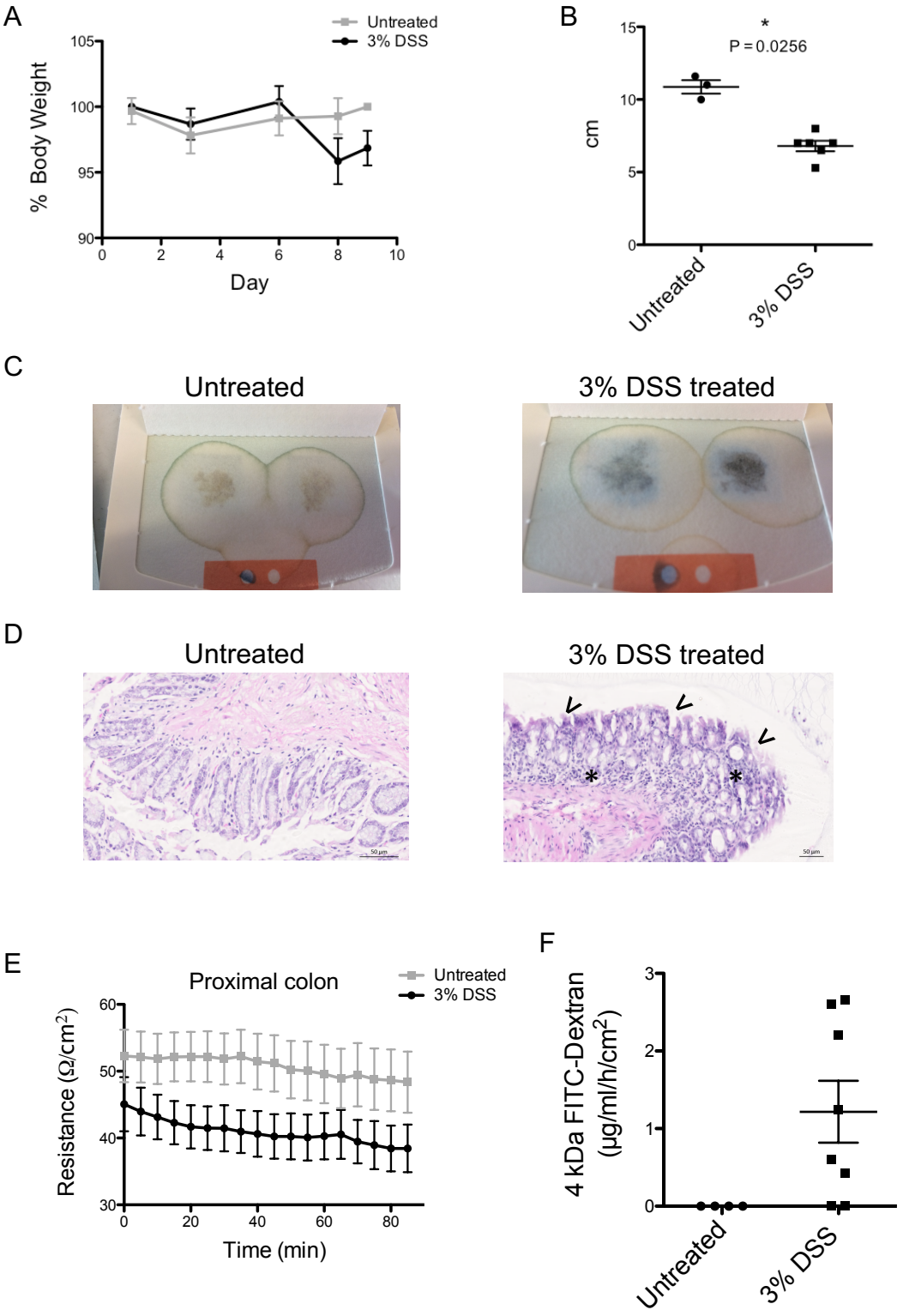

Figure 4.10. 3% Dextran Sodium Sulphate causes intestinal inflammation and increase intestinal permeability.

(A) Body weight and (B) colon length of 3% DSS treated and untreated 10 week old female Fop3$^{DTR/DTR}$ mice. (C) Hemoccult blood testing of stool samples. (D) Haematoxylin & eosin staining of colonic gut rolls. Asterisks and arrows indicate increased immune cell infiltration and disrupted crypt structure respectively. (E) Electrical resistance of proximal colon and (F) 4kDa FITC-dextran passage. Mucosal starting concentration was 0.5 mg/ml. n=4 treated vs 8 untreated. Error bars show SEM. Mann Whitney test used to test for significant differences.

4.3.11 Depletion of T-regulatory cells leads to increase intestinal permeability

Depletion of Tregs causes the development of autoimmune symptoms, including colitis, which as shown by Mottet and colleagues can be rescued in adoptive transfer models (293). Using FoxP3^{DTR} mice described by *Kim et al*. (109), treatment with diphtheria toxin (DTx) depleted the FoxP3^{+} Treg population (Figure 4.11A). DTx Treated mice did develop autoimmune symptoms such as scaly skin seen around the eyes (Figure 4.12B), listless behaviour, extreme splenomegaly (Figure 4.11C) and began to lose weight after two-weeks of treatment (Figure 4.11D). Colon length was not altered by T-reg depletion (Figure 4.11E). However, histological analysis showed architectural differences between DTx treated and untreated mice, constant with enteropathy (Figure 4.11F).

Over a 90-minute experimental period, electrical resistance of mid and proximal colonic sections from DTx mice was lower and declined more rapidly than colonic sections from untreated animals (Figure 4.12A and 4.12C). Regardless, all samples did respond to Forskolin addition and had a negative PD. Although not significant, paracellular flux of 4kDa FITC-dextran was higher within treated mice (Figure 4.12B and 4.12D). These data suggest that T-regs cells play a role in maintaining gut integrity within the intestine. Furthermore it validated that our Ussing system could detect permeability differences within this mouse model.

A

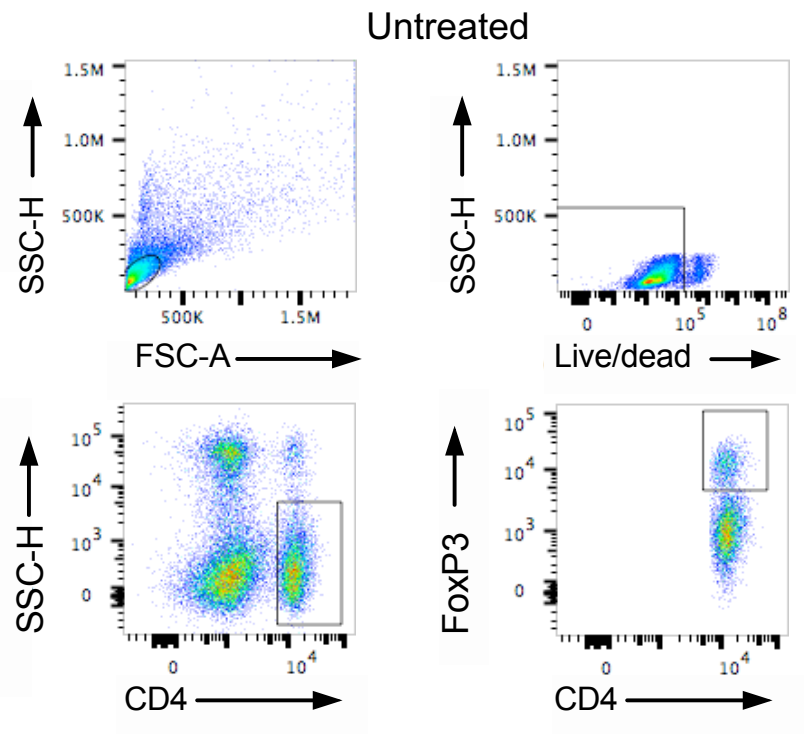
Untreated
SSC-H
FSC-A
1.5M
1.0M
500K
Live/dead
CD4
FoxP3

B

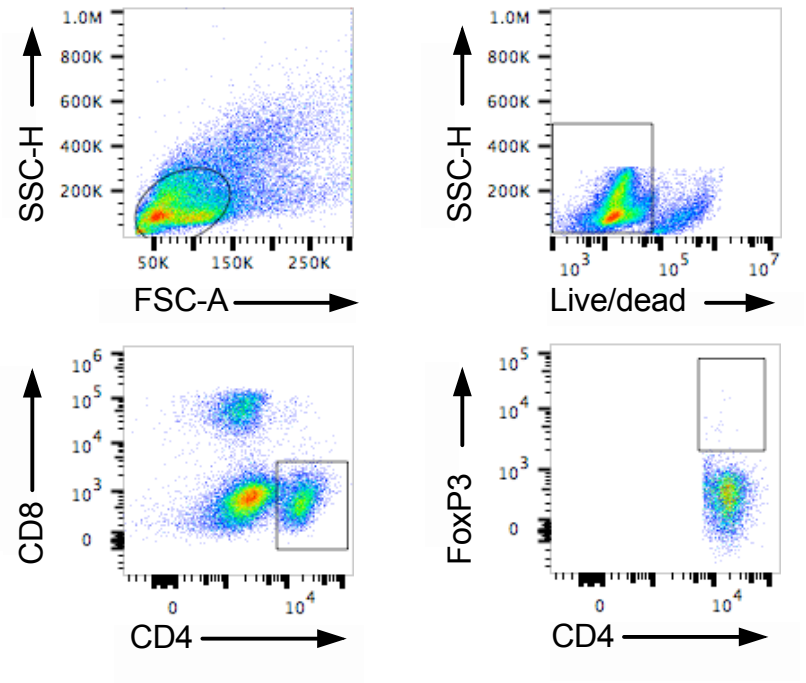
DTx treated
SSC-H
FSC-A
1.0M
800K
600K
400K
200K
Live/dead
CD8
CD4
FoxP3

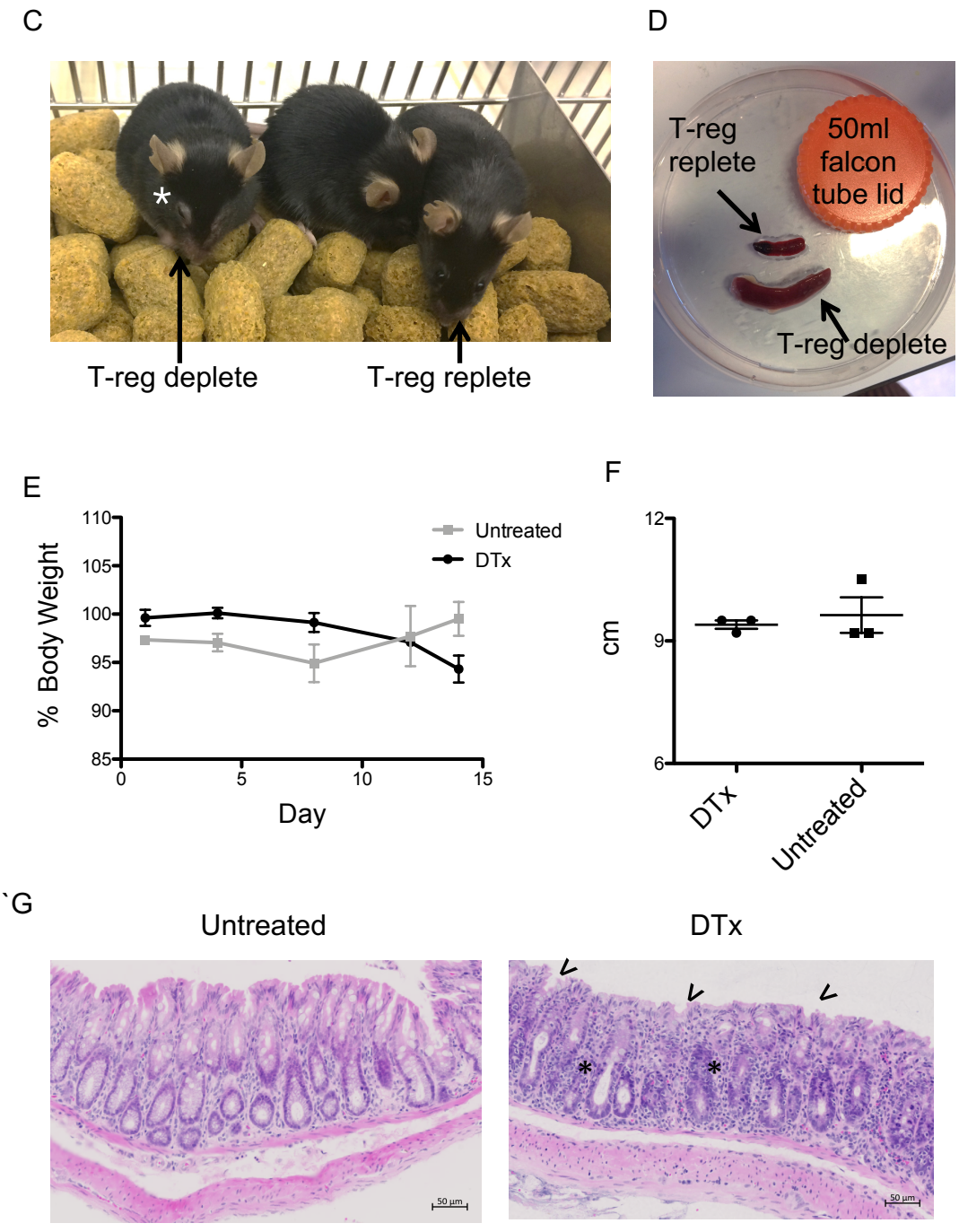

Figure 4.11. Depletion of T-regulatory cells causes autoimmunity.
Splenocytes were harvested from mice and stained with the panel of antibodies show in Table 3.1 in Chapter 2. Lymphocytes were identified by size and granularity using side scatter (SSC) and forward scatter (FSC), respectively. Live cells were selected based on the ability to exclude aqua stain. $CD4^+$ cells were gated and then FoxP3 expression analysed. (A) Gating strategy of splenocytes harvested from untreated and (B) DTx treated mice to identify $CD4^+$ $FoxP3^+$ cells. (C) Image of mice showing autoimmune eye symptom, indicated by asterisk. (D) Image showing splenomegaly in T-reg deplete mice. 50ml falcon tube diameter is 34mm. (E) Percentage body weight of mice. (F) Colon lengths of mice. (G) H&E staining of distal colonic sections from treated and untreated animals. Asterisks and arrows indicate increased immune cell infiltration and disrupted crypt structure respectively n=3 treated vs 3 untreated. Error bars show SEM.

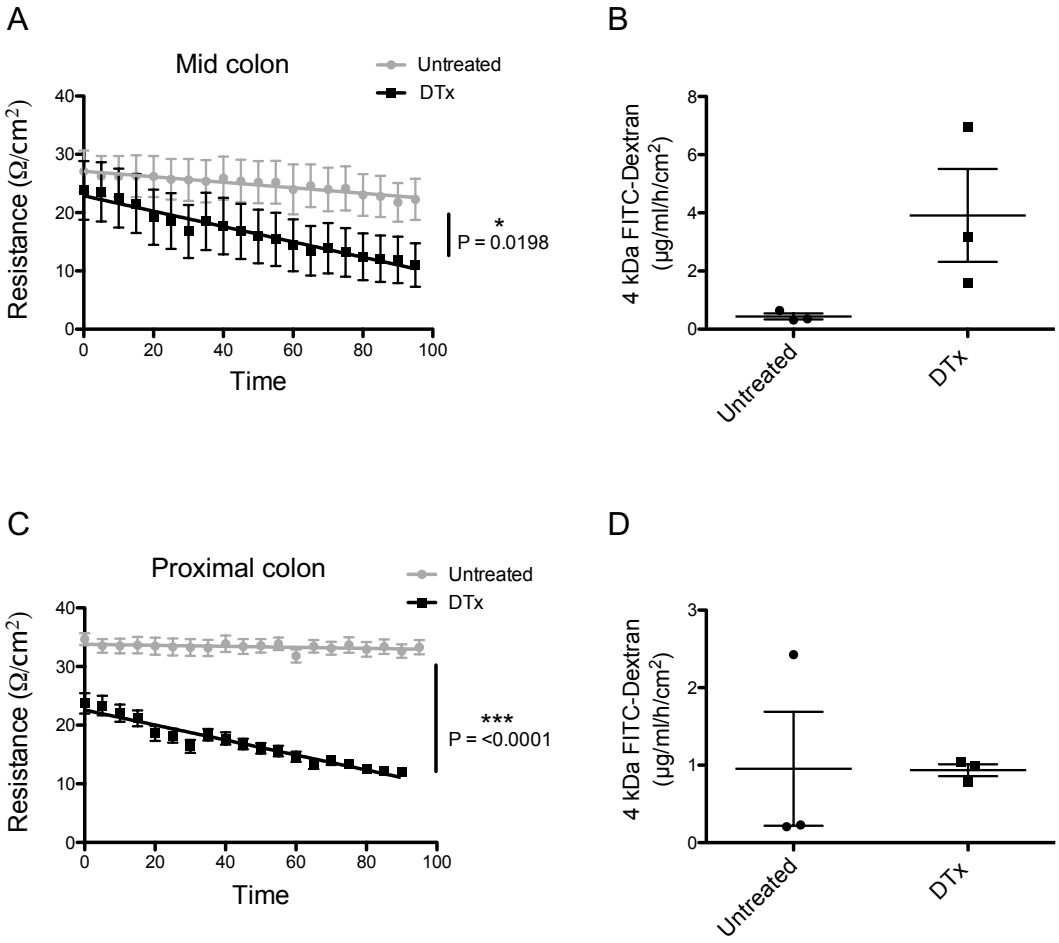

Figure 4.12. T-regulatory cell depleted mice show increased intestinal permeability.

(A) Electrical resistance and (B) 4kDa FITC-dextran passage of mid colonic sections from 14 week old female FoxP3^{DTR} mice. (C) Electrical resistance and (D) 4kDa FITC-dextran passage of proximal colonic sections. Mucosal starting concentration was 1 mg/ml. An ANOVA was used to test for significant differences between linear regression slopes. n=3 treated vs 3 untreated. Error bars show SEM.

4.4 Discussion

It is accepted that intestinal inflammation is a risk factor associated with CRC development. Accordingly the risk of CRC in IBD patients is 1.5-2 times greater than the general population (294). IBD patients also exhibit increased intestinal permeability and it is thought barrier breakdown enhances disease. It was hypothesised that the unfavourable outcome identified in CRC patients responding to the TAA CEA was due to increased intestinal permeability, which in theory could result in a pro-tumorigenic environment (194). This chapter has focused on the design, optimisation and validation of the Ussing chamber system as a tool for measuring gut integrity.

The Navicyte system was chosen over classic Ussing designs as this increased analysis from one tissue sample per experiment to six (286). This increase in sample number was beneficial as a major limitation of Ussing experiments is tissue viability, resulting in samples being disregarded. Wallon and colleagues show that tissue samples displaying a negative PD value have lower rates of paracellular transport as well as stable levels of lactate and ATP (284). By optimising dissection and mounting techniques tissue sample health was greatly improved. I also measured tissue viability using the compound Forskolin. An adenylate cyclase agonist, Forskolin increases cAMP and activation of PKA, leading to CFTR stimulation to promote Cl^- secretion (287, 295). This causes a decline in PD values. As this process requires energy only healthy tissue are able to respond. By measuring both baseline PD and responses to Forskolin we could be confident that only viable tissue samples were included within our analysis.

After electrode optimisation it was possible to re-use Ag/AgCl electrodes to nullify offset potential differences and achieve stability over 90-mintute

experimental periods. The chloriding method used (immersion in household bleach) may however be harsh as the Ag wire often breaks from the electrode cap. An investigation into electroplating electrodes was attempted but unsuccessful. It may therefore be worth exploring electroplating options further in an effort to make the electrodes longer lasting.

Validation of the custom-made Ussing system was achieved using mouse models. DSS treatment, which causes enteropathy, is widely used as animals develop features similar to those seen within IBD patients. We therefore used DSS treatment as a positive control to identify leaky epithelium using our Ussing system. The exact mechanism of DSS action is not fully understood. However, Laroui and colleagues suggest that DSS binds to medium chain fatty acids within the gut, allowing the formation of lipid nanoparticles. Nanoparticles can bind to the membrane of colonocytes and once inside can stimulate inflammatory signalling pathways (296). Multiple repeated cycles of DSS treatment followed by water results in chronic intestinal inflammation (291, 297) but unnecessary for this study since one cycle of 3% DSS treatment induced acute intestinal inflammation. The permeability of the proximal region of the colon was analysed as it had the highest electrical resistance in healthy animals. Furthermore, unlike the mid colonic region, the proximal region could be clearly identified even though colon length was reduced. Both electrical resistance and 4kDa FITC-dextran passage data confirmed that the Ussing system could identify increased permeability within DSS treated mice.

A mouse model of intestinal inflammation driven by Treg depletion was also used to validate the Ussing system. Tregs are a major component of the immune system. They are critical for maintaining immune homeostasis and reducing inflammation (298). Furthermore, they promote tolerance towards

commensal micro-biota and food antigens within the intestine to maintain a healthy intestinal environment (298-300). Transfer of naïve $CD4^+$ T cells into $Rag^{-/-}$ mice results in T cell-driven colitis (301). However, transfer of $CD4^+$ $CD25^+$ Tregs prevent disease development (293). Treg depletion is a valuable model for investigating colonic permeability using the new Ussing system. Upon DTx treatment of $FoxP3^{DTR}$ mice, depletion of the $FoxP3^+$ Treg population was achieved and colonic inflammation developed. I report here for the first-time increased permeability within Treg depleted mice, measured directly using an Ussing chamber system. These data confirm the robustness of the system as a tool for measuring permeability.

4.5 Conclusion

The unforeseen complex assembly of the Ussing chamber system did slow the initial momentum of this project. Nonetheless, I did successfully construct and optimise an Ussing chamber system, which has proved capable of effectively measuring gut integrity. This technique was therefore used to measure intestinal permeability of human tissue, described in Chapter 5.

Chapter 5. Human Permeability Studies

5.1 Introduction

There is a link between inflammation and the development of CRC, highlighted by increased tumour incidence within IBD patients. Furthermore, studies have identified an association with the use of non-steroidal anti-inflammatory drugs (NSAIDs) and a reduced risk of developing CRC. In particular, the Cancer Prevention Programme (CAPP2) investigated the role of aspirin within Lynch syndrome patients, which extended to 43 different centres covering 16 countries (302). Patients were randomly assigned to receive 600mg of aspirin daily or placebo comprising 30g resistant starch for 2-4 years. Results showed that with a group mean follow up of 55.7 months, patients receiving aspirin had up to a 60% risk reduction in developing cancer compared to the placebo group (302). Similar findings have been observed for sporadic CRC as reported in a meta-analysis study by Algra and colleagues (303). Appropriately, inflammation has been recognised as one of the "hallmarks of cancer" (203).

Unlike most cancers, CRC develops next to a wide range of microbial species. Moreover, the microbiota can influence the anti-tumour immune response. This appears to be a complex process, with an on-going debate on the beneficial and detrimental aspects of microbial invasion. Differences in microbial composition have been identified in CRC patients compared to healthy controls. However, as of yet a clear signature that unifies "CRC microbiota" across studies has not been identified. Nevertheless, particular bacterial species have been recognised as having the ability to promote intestinal inflammation that can aid in tumour progression. For example, two back-to-back recently published studies identify *Escherichia coli* and *Bacteroides fragilis* as being pro-carcinogenic through initiation of an inflammatory cascade by targeting colonic epithelial cells (304,

305). Biofilms predominately containing *E.coli* and *B.fragilis* were identified within FAP patients, the genetic condition associated with heredity CRC. Both can also be found in sporadic CRC patients (304). Strong experimental evidence exists to support the carcinogenic potential of *E. coli* and *B..fragilis*. *E.coli* containing the polyketide synthase (pks) genotoxic island encodes genes for the bacterial toxin colibactin. This toxin has been shown *in vitro* and *in vivo* to induce DNA damage in host cells, as well as promoting tumourigenesis in a CRC mouse model (304). Meanwhile, *B.fragilis* toxin (BFT) can act as a metalloproteinase to affect epithelial cell TJ structures (306). This signalling process, which relies on an unidentified epithelial cell receptor, results in cleavage of E-cadherin. This causes impaired barrier integrity and the activation of pathways associated with tumour progression such as Wnt/β-catenin signalling (305, 306). Interestingly, when co-colonised with *E.coli* and *B.fragilis* azoxymethane (AOM) treated mice showed increased tumourigenesis compared to mono-colonised animals, indicating that a synergistic effect is required for tumour development (304). This change in microbial composition also correlated with higher levels of epithelial cell DNA damage within AOM treated mice. Furthermore, bacterial induced IL-17 immune responses were found to play a role in tumour development. While not sufficient alone to drive tumourigenesis, it was observed that AOM treated IL-17 deficient mice co-colonised with *E.coli* and *B.fragilis* did not develop tumours (304). Such findings corroborate with the observations of Grivennikov and colleagues (213). Using $APC^{F/WT}$ mice that develop tumours primarily in the distal colon, marked upregulation of IL-17A and IL-23 was detected. However, ablation of either cytokine diminished tumour growth. Furthermore, short-term treatment with broad-spectrum antibiotics depleted the microbiota, leading to reduced IL-23 and IL-17A, as well as STAT-3 activation in cancer cells (213). Using an *in vivo*

FITC-dextran passage approach, an increase in intestinal permeability was also observed within $APC^{F/WT}$ mice. This was associated with penetration of microbial products such as LPS, shown to associate with tumour associated macrophages (TAMs) located in tumour tissue (213). Based on this evidence it is possible that reduced epithelial barrier function aids tumour development through bacterial induced inflammation.

As mentioned previously our laboratory observed that CRC patients responding to the TAA CEA were found to have a poorer prognosis than non-responding patients (194). Reasons to explain this observation were explored.

CEA is expressed on normal healthy gastrointestinal tissue and it has been shown that cytokines such as IFN-γ and TNF-α can act on barrier function, causing increased permeability in a myosin light chain kinase dependant manner (269). Therefore, activation of IFN-γ producing auto-reactive CEA T cells could potentially play a role in altering gut epithelial barrier function. Based on this and the evidence suggesting that impaired barrier function can assist tumour-associated inflammation, we hypothesised that CEA responding patients have increased colonic mucosal permeability. This could lead to the translocation of microbes or their products into the lamina propria, creating an inflammatory setting capable of aiding tumour progression, and hence earlier tumour relapse compared to non-responding patients.

To address this hypothesis the Ussing chamber was employed to investigate the permeability of human biopsy samples obtained from patients undergoing colonoscopy procedures.

In this chapter I aimed to (i) obtain baseline readings from healthy biopsy samples, (ii) examine any alterations in gut permeability upon adenoma formation and (iii) investigate if CEA blood responses correlated with increased intestinal permeability.

5.2 Results

5.2.1 Human biopsy samples remained viable within Ussing chambers for up to 90 minutes.

To determine the permeability of human colonic tissue, Ussing chambers were modified to support biopsy samples, approximately 1-1.5 mm in diameter. Biopsies were mounted into chambers in between two pieces of x-ray film with a 1 mm hole to reduce the exposed tissue area to 0.79 mm^2 (Figure 5.1A). Unlike mouse tissue, which was full thickness when mounted, biopsy samples consisted of the epithelial and sub-mucosal layers of the colon only. Nevertheless, by applying the same techniques it was observed that biopsy samples could remain viable during 90-minute experimental periods. Overall, 82% of all biopsy samples ran in Ussing chambers were viable and included in analyses. Figure 5.1 shows representative images of a viable biopsy sample, demonstrating consistent electrical resistance (Figure 5.1B) and a PD response to Forskolin at 60 minutes (Figure 5.1C). Furthermore, the Forskolin-induced drop in PD is mirrored by an increase in short circuit current (Isc), indicating increased ion movement as a result of CFTR activation (Figure 5.1D). From use of the animal models described in Chapter 4, it was found that passage of 4kDa FITC dextran across the colon was minimal in healthy mice and on some occasions no passage was detected at all. Due to this, a second paracellular probe called Lucifer yellow was used to investigate paracellular flux across biopsy tissues. Only 457Da in size, Lucifer yellow was able to translocate the tissue barrier, leading to a more sensitive measurement of paracellular passage in healthy samples. Moreover, Lucifer yellow passage correlated with tissue electrical resistance measurements in biopsy samples obtained from both the right (Figure 5.1E) and left side of the colon (Figure 5.1F).

5.2.2 Baseline Ussing measurements show regional variation in colonic biopsies

Tumours can develop within any region of the colon. However, cancers arising in the right side of the colon (caecum/ascending) often have different characteristics than left sided cancers (descending/sigmoid). The clinical relevance of tumour location is still debated however some studies suggest that right and left sided CRCs should be treated as distinct biological entities. In contrast, it has been proposed that tumour location is secondary to other tumour and host factors such as the tumour microenvironment.

In Chapter 4 it was demonstrated that regional variation in intestinal permeability existed within the mouse colon (Figure 4.8). With this in mind, and the suggestion that tumour location associates with particular disease characteristics, patients found to have no macroscopic disease during colonoscopy examination had three biopsies taken from the right and left side of the colon. This was to evaluate baseline permeability within healthy individuals. The average electrical resistance of right and left biopsies was calculated as well as the flux of Lucifer yellow. A difference in intestinal permeability between the left and right colon was observed. Left sided biopsies had lower electrical resistance (Figure 5.2A) and higher Lucifer yellow passage (Figure 5.2B), indicating the left side of the colon is more permeable than the right.

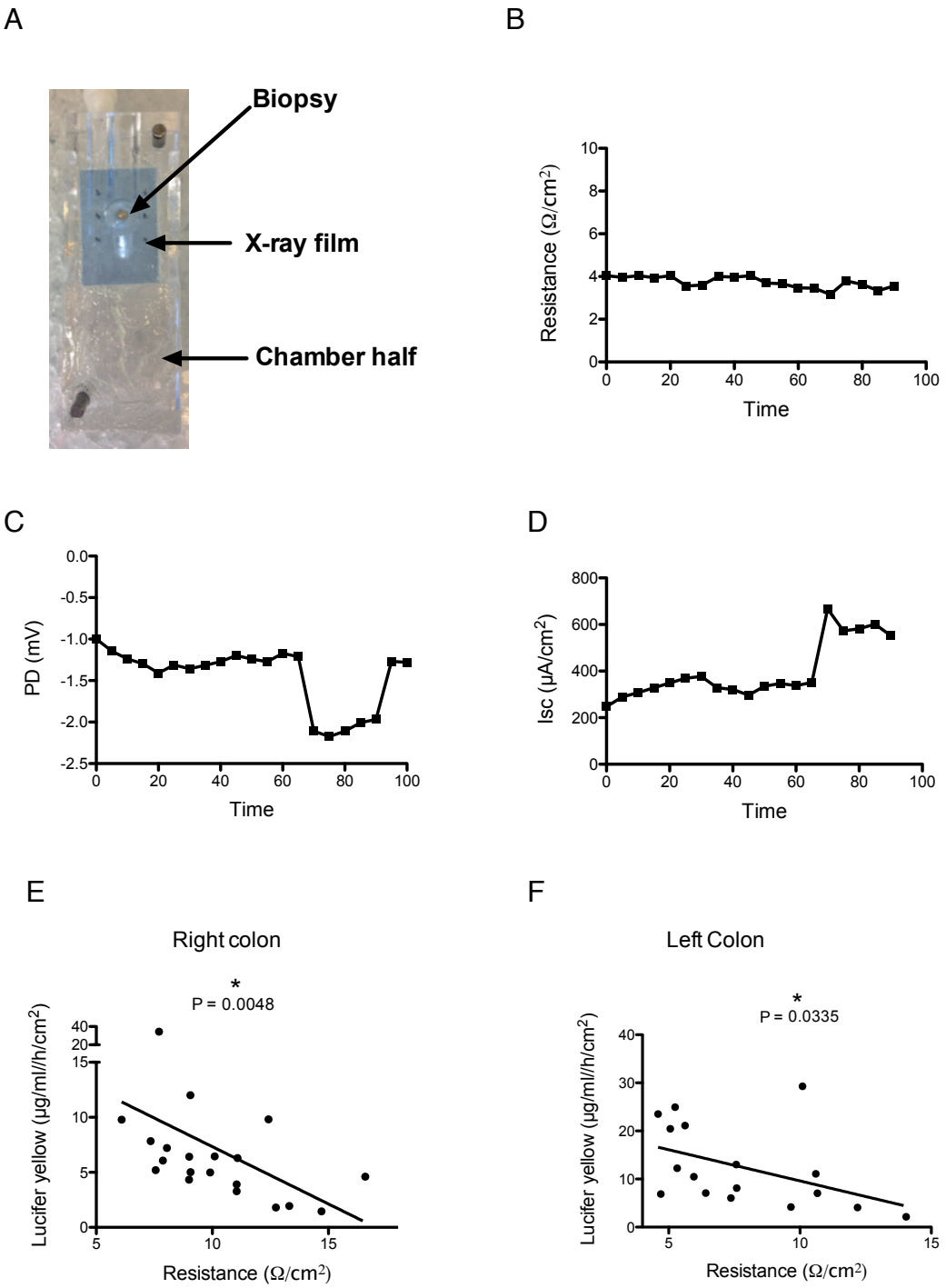

Figure 5.1. Human biopsy samples remained viable within Ussing chambers for up to 90 minutes.
(A) Image of colonic biopsy mounted in Ussing chamber. (B) Resistance, (C) PD and (D) Isc of viable biopsy sample. Flux of the fluorescent probe Lucifer yellow correlates with tissue electrical resistance in both the (E) right and (F) left side of the colon. A Spearmans' test was used to test for a significant correlation.

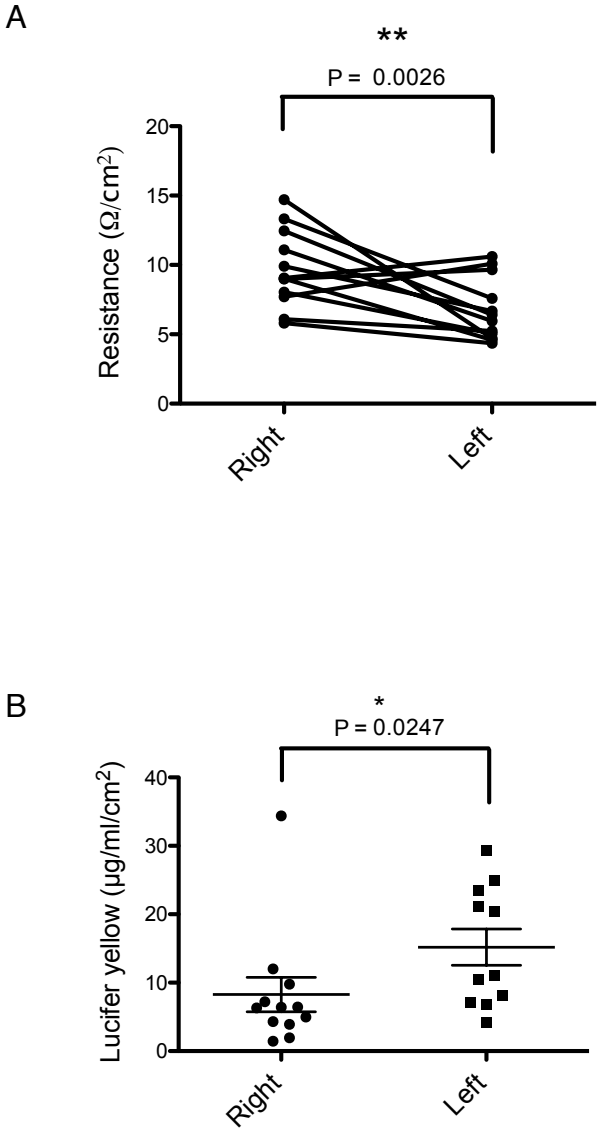

Figure 5.2. Baseline Ussing measurements show regional variation in healthy colonic biopsies.
(A) Baseline electrical resistance at 20 minutes of biopsy samples taken from the right and left colon. A significant difference between groups was tested for using an unpaired two-tailed students T test. (B) Lucifer yellow flux across right and left colonic biopsies at 20 minutes. A Mann Whitney test was used to test for statistically significant differences. Error bars show SEM.

5.2.3 Adenoma lesion biopsies show increased permeability

Adenomatous polyps (adenomas) are benign growths that develop within the intestine but have the potential to become cancerous over an extended period of time. Therefore, if an adenoma is detected it is most often removed by clinicians. Figure 5.3A and 5.3B show colonoscopy images of an adenoma and an adenocarcinoma (CRC tumour) from patients in this study. I sought to evaluate whether adenoma formation was a result of individuals having a permeable gut. I hypothesised that a permeable gut would acquire more genetic mutations as a result of bacterial-driven inflammation, leading to adenoma formation. I also hypothesised that adenoma formation itself would result in a local leaky environment at the lesion site. Upon colonoscopy examination, right and left sided biopsy samples were obtained from adenoma patients, taken from sites greater than 5 cm away from the adenoma itself. Biopsy permeability was then measured using the Ussing system. As a control, “lesion” samples within 1 cm of an adenoma were obtained where possible. Tumour biopsies obtained from a single CRC patient were also included within the lesion sub-group. Results showed that samples obtained greater than 5 cm away from the adenoma site were not more permeable than biopsy samples from healthy patients. Surprisingly it was observed that left sided biopsies from adenoma patients actually had a statistically significant higher electrical resistance (Figure 5.3C) and a lower mean passage of Lucifer yellow (Figure 5.3D) than left sided samples from healthy individuals. In contrast to what was hypothesised, this indicates increased epithelial integrity within left colon background tissue of adenoma patients. Due to this, the regional variation in colonic permeability detected within healthy individuals (Figure 5.2) disappears within adenoma patients (Figure 5.3E).

Biopsy samples obtained from adenoma lesion sites (within 1 cm) had a significantly lower electrical resistance, as did tumour biopsies, compared to

healthy samples which indicates increased permeability (Figure 5.3C). However, while lesion site Lucifer yellow passage was relatively high (mean = 16.83 μg/ml/h/cm^2), similar flux was also observed for some healthy left sided biopsy samples (mean = 15.2 μg/ml/h/cm^2) (Figure 5.3D). To investigate further, histological analysis of biopsy samples post-Ussing was carried out where possible. Background tissue (greater than 5 cm from adenoma) and tissue from a lesion site from the same adenoma patient was compared, with no dramatic histological differences in epithelial architecture observed. Only a small increase in immune cell infiltrate could be seen, along with some possible deterioration of the epithelial layer (Figure 5.3G). However, this was very subtle compared to the inflammation-induced damage observed within the mouse models used in Chapter 4 (Figure 4.11D). Blood derived CEA-specific T cell responses were also measured. Interestingly, adenoma patients had a higher magnitude CEA-specific IFN-γ T cell response compared to healthy controls (Figure 5.3F).

These data show that very mild tissue damage does occur near the site of adenoma development. While mouse and human tissue is not directly comparable, inflamed mouse intestine (shown in Chapter 4) was permeable to 4kD FITC dextran probe. However, lesion human biopsy samples did not show increased flux of the smaller sized Lucifer yellow probe in comparison to healthy biopsies. This suggests that any tissue damage that may have formed near the site of adenoma formation now has normalised compared to the damage caused by DSS treatment or Treg depletion in mice. However, the fall in electrical resistance within lesion samples compared to healthy biopsies suggests that the passage of small molecules/ions is still affected. The increase in epithelial integrity of background tissue from adenoma patients compared to healthy controls also argues against the hypothesis that patients who develop adenomas do so as a result of having a more permeable intestine than healthy individuals.

However a study by Laukoetter and colleagues suggests that epithelial cell proliferation could play a role in decreasing tissue injury (27). The authors show that JAM-A$^{-/-}$ mice have increased susceptibility to DSS treatment compared to untreated JAM-A$^{-/-}$ animals. However, colonic disease was not as severe when compared to DSS treated WT mice. The group were able to demonstrate that JAM-A$^{-/-}$ mice have higher levels of Ki67^{+} epithelial cells compared to WT animals. This high percentage of Ki67^{+} cells remained during DSS treatment of JAM-A$^{-/-}$ mice but a decrease was seen during treatment of WT animals. Such findings suggest that enhanced cell proliferation could result in rapid repair of epithelial defects (27). Its possible that the increased gut integrity of background tissue detected in adenoma patients is a consequence of a feedback mechanism resulting in barrier tightening in response to adenoma formation, potentially through enhanced epithelial cell proliferation.

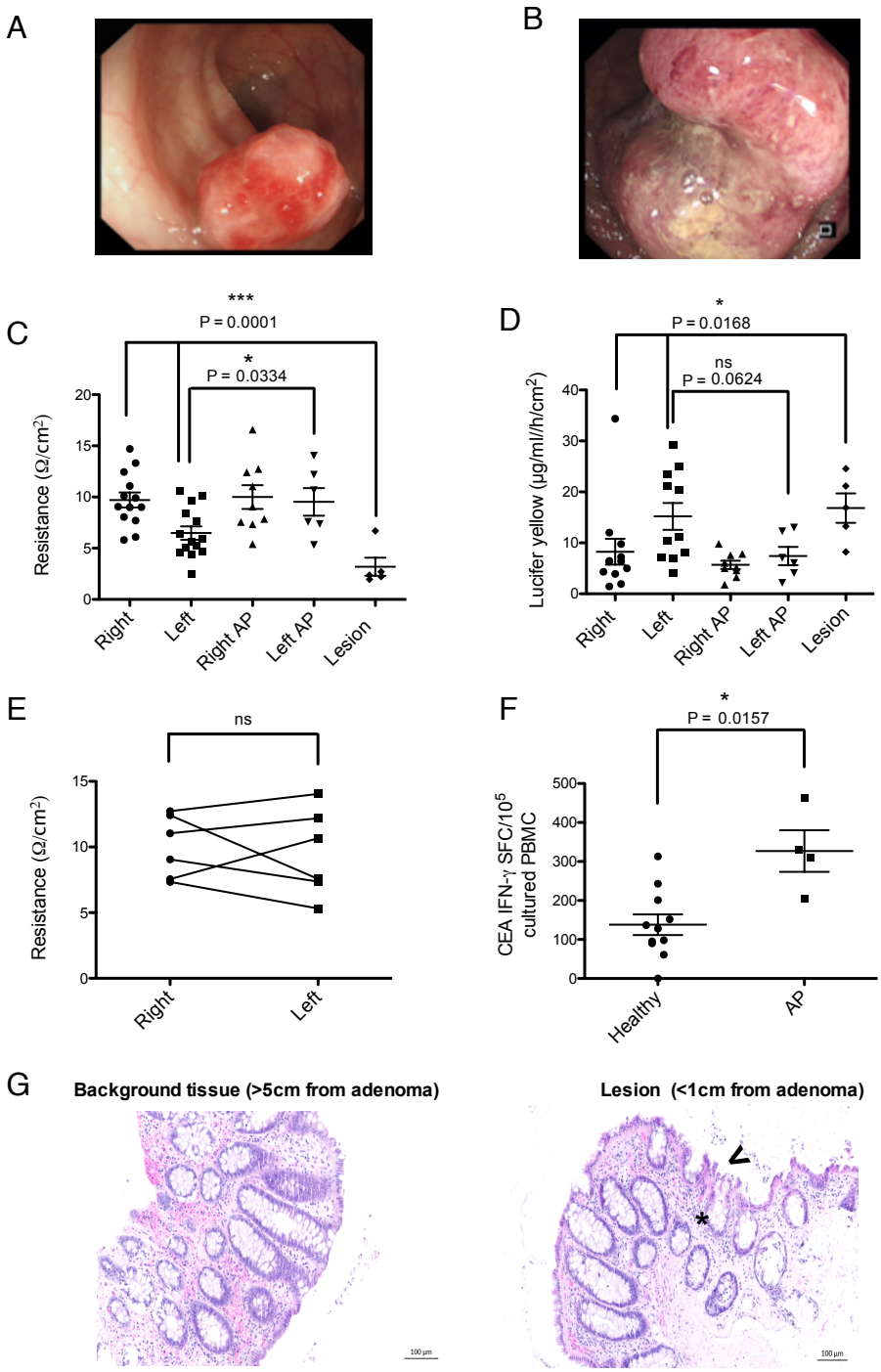

Figure 5.3. Lesion biopsies show increased permeability but tissue obtained >5cm from the adenoma site does not.

(A) Representative image of an adenoma and (B) adenocarcinoma. (C) Electrical resistance and (D) Lucifer yellow flux of biopsy samples from the right and left colon of healthy patients and adenoma patients (AP). Biopsy samples from lesion sites are also shown. A one-way anova was used to test for significant differences between right, left healthy samples and lesion sites. An unpaired students T test was used to test for statistical significance between healthy and AP left biopsies (E) Paired electrical resistance between right and left colonic biopsy samples from adenoma patients. (F) CEA-specific IFN-γ^+ T cell response in healthy and AP patients. Significant differences tested for using A Mann Whitney test. (G) H and E staining of healthy background tissue (>5cm from adenoma) and tissue obtained from a lesion (<1cm of an adenoma). Asterisk and arrow indicate increased immune cell infiltration and epithelial damage, respectively. Error bars show SEM.

5.2.4 CEA responses and permeability

As shown by our laboratory, CEA-specific T cell responses in CRC patients reflected in a poor 5-year outcome for patients (194). To address the hypothesis that patients harbouring CEA-specific IFN-γ T cell responses have increased intestinal permeability biopsy samples were obtained and run on the Ussing system. Peripheral blood was also taken from patients where possible and CEA-specific responses were measured using the FluoroSpot technique (described in Chapter 2). Results showed that all patients in this cohort had an IFN-γ T cell response to CEA. However, there was variation in the magnitude of response that patients produced (Figure 5.4A). Detection of a CEA T cell response in all patients is due to an unavoidable change of culture medium used for FluoroSpot assays compared to that used in Chapter 3. Side by side comparison showed that T cell responses to the same peptide pools were detected when using either media. However, due to better growth factor conditions that support T cell responses, the magnitude of T cell response in some cases was increased by up to 10% when using the new media (see appendix). This resulted in “low and high” responding patients as opposed to responding and non-responding patients as seen in Chapter 3. Patients were split based on the magnitude of CEA response generated. A low T cell response was defined as a FluoroSpot spot forming cell count (SFC) lower than the group median. A high T cell response was defined as a SFC greater than the group median. Low and high T cell response was then correlated with the electrical resistance and Lucifer yellow flux of colonic biopsies. In healthy patients it was found that a higher CEA-specific IFN-γ T cell response significantly correlated with decreased electrical resistance in the right side of the colon (Figure 5.4B). This was mirrored by an increase in Lucifer yellow flux (P=0.0571) (Figure 5.4C). Interestingly, this finding was not observed in the left side of the colon (Figure 5.4D and 5.4E). Also evaluated was the correlation between CEA-specific IL-

17A and IL-17/IFN-γ dual T cell responses and intestinal permeability (Figures 5.5 and 5.6, respectively). No associations in either the right or left side of the colon were observed. As a comparison 5T4-specific responses, which were shown not to be associated with a poor prognosis in CRC were also measured. This made it possible to evaluate if increased permeability was due to T cell responses to a tumour antigen or whether it particularly correlated with CEA-specific T cell IFN-γ responses. Figures 5.7B-5.7E show that no association between high or low magnitude 5T4-specific IFN-γ T cell response and intestinal permeability were observed. This was also true when permeability was correlated with IL-17A (Figure 5.8B-5.8D) and IL-17A/IFN-γ dual 5T4-specific T cell responses (Figure 5.9B-5.9D).

Together these data suggest that CEA-specific IFN-γ T cell responses are specifically linked with decreased epithelial integrity in the right side of the colon.

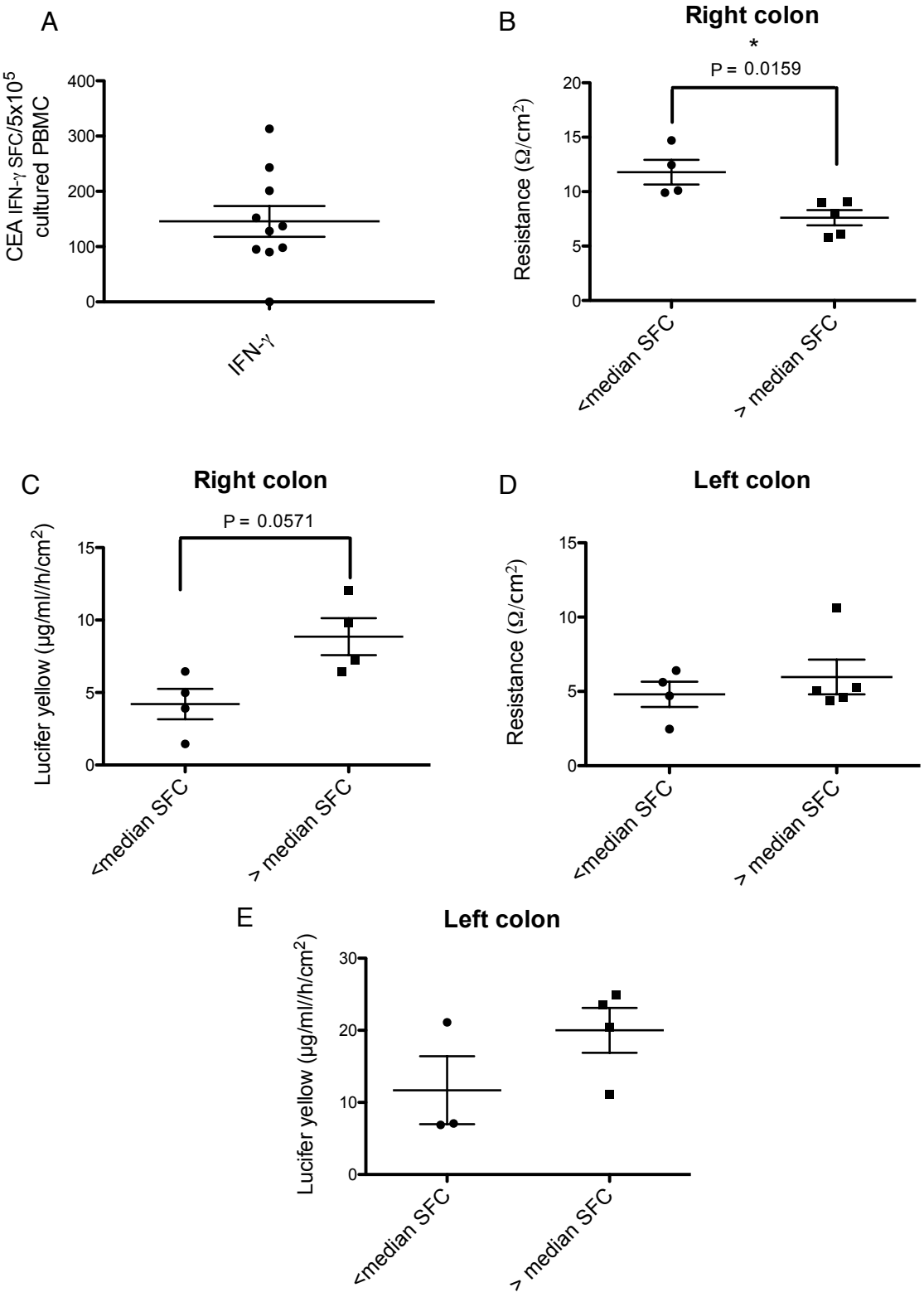

Figure 5.4. Higher magnitude CEA-specific IFN-γ T cell responses correlate with increased intestinal permeability in the right side of the colon but not the left. Electrical resistance and Lucifer yellow passage of colonic biopsies was measured. Patients were then divided based on magnitude of CEA response, defined as having a FluoroSpot IFN-γ SFC higher or lower than the group median. (A) Magnitude of IFN-γ responses from all patients. (B) Right and (D) left colon electrical resistance. (C) Right colon and (E) left colon Lucifer yellow passage. Data shown is at 20 minutes. Mann Whitney test used to test for statistically significant differences. Error bars show SEM.

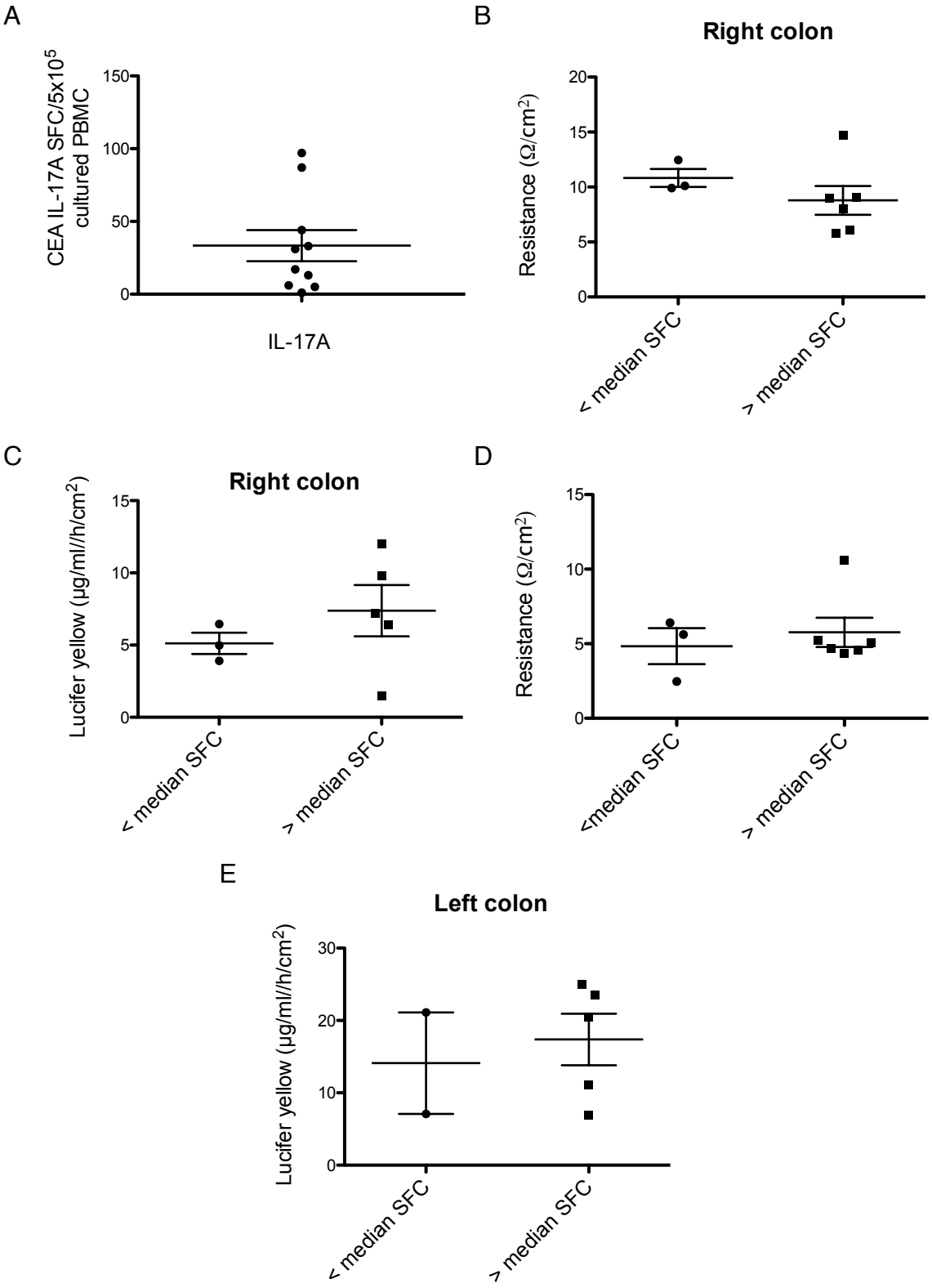

Figure 5.5 CEA-specific IL-17A T cell responses do not correlate with intestinal permeability.

Electrical resistance and Lucifer yellow passage of colonic biopsies was measured. Patients were then divided based on magnitude of CEA response, defined as having a FluoroSpot IL-17A SFC higher or lower than the group median. (A) Magnitude of IL-17A responses from all patients. (B) Right and (D) left colon electrical resistance. (C) Right colon and (E) left colon Lucifer yellow passage. Data shown is at 20 minutes. Error bars show SEM.

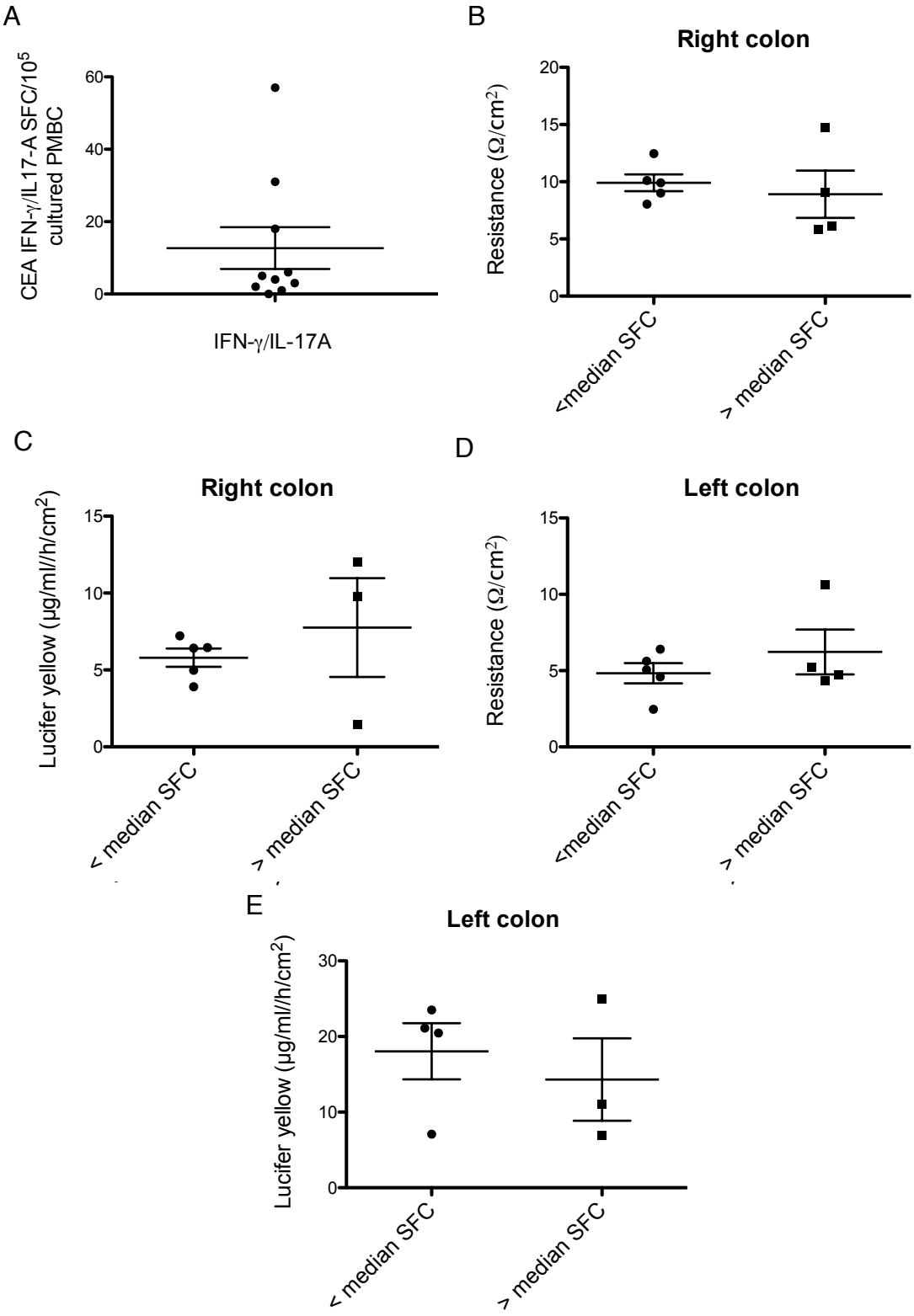

Figure 5.6. CEA-specific IFN-γ/IL-17A dual T cell responses do not correlate with intestinal permeability.

Electrical resistance and Lucifer yellow passage of colonic biopsies was measured. Patients were then divided based on CEA magnitude of response, defined as having a FluoroSpot IFN-γ/IL-17A SFC higher or lower than the group median. (A) Magnitude of IFN-γ/IL-17A responses from all patients. (B) Right and (D) left colon electrical resistance. (C) Right colon and (E) left colon Lucifer yellow passage. Data shown is at 20 minutes. Error bars show SEM.

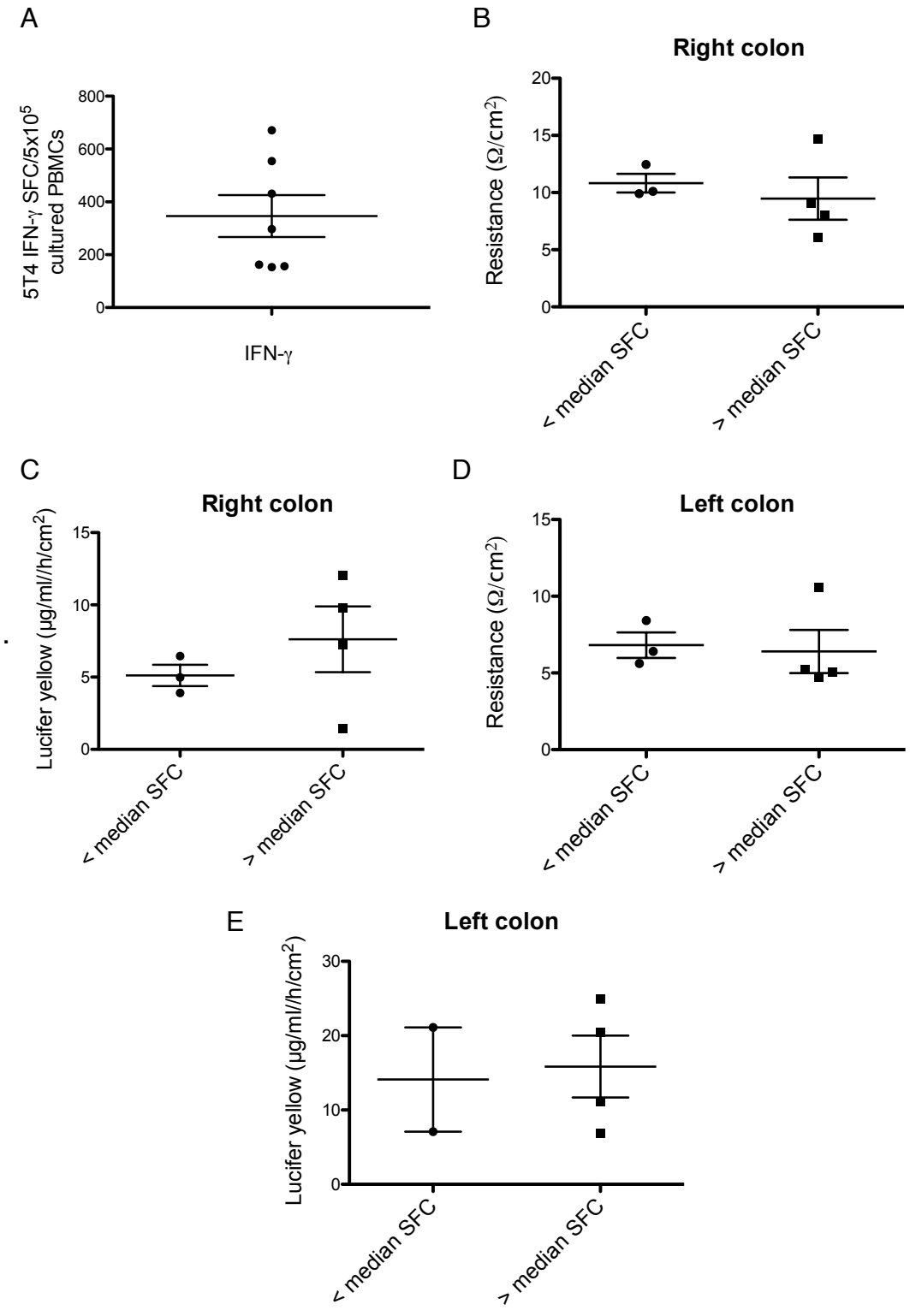

Figure 5.7 5T4-specific IFN-γ T cell responses do not correlate with intestinal permeability.

Electrical resistance and Lucifer yellow passage of colonic biopsies was measured. Patients were then divided based on 5T4 magnitude of response, defined as having a FluoroSpot IFN-γ SFC higher or lower than the group median. (A) Magnitude of IFN-γ responses from all patients. (B) Right and (D) left colon electrical resistance. (C) Right colon and (E) left colon Lucifer yellow passage. Data shown is at 20 minutes. Error bars show SEM.

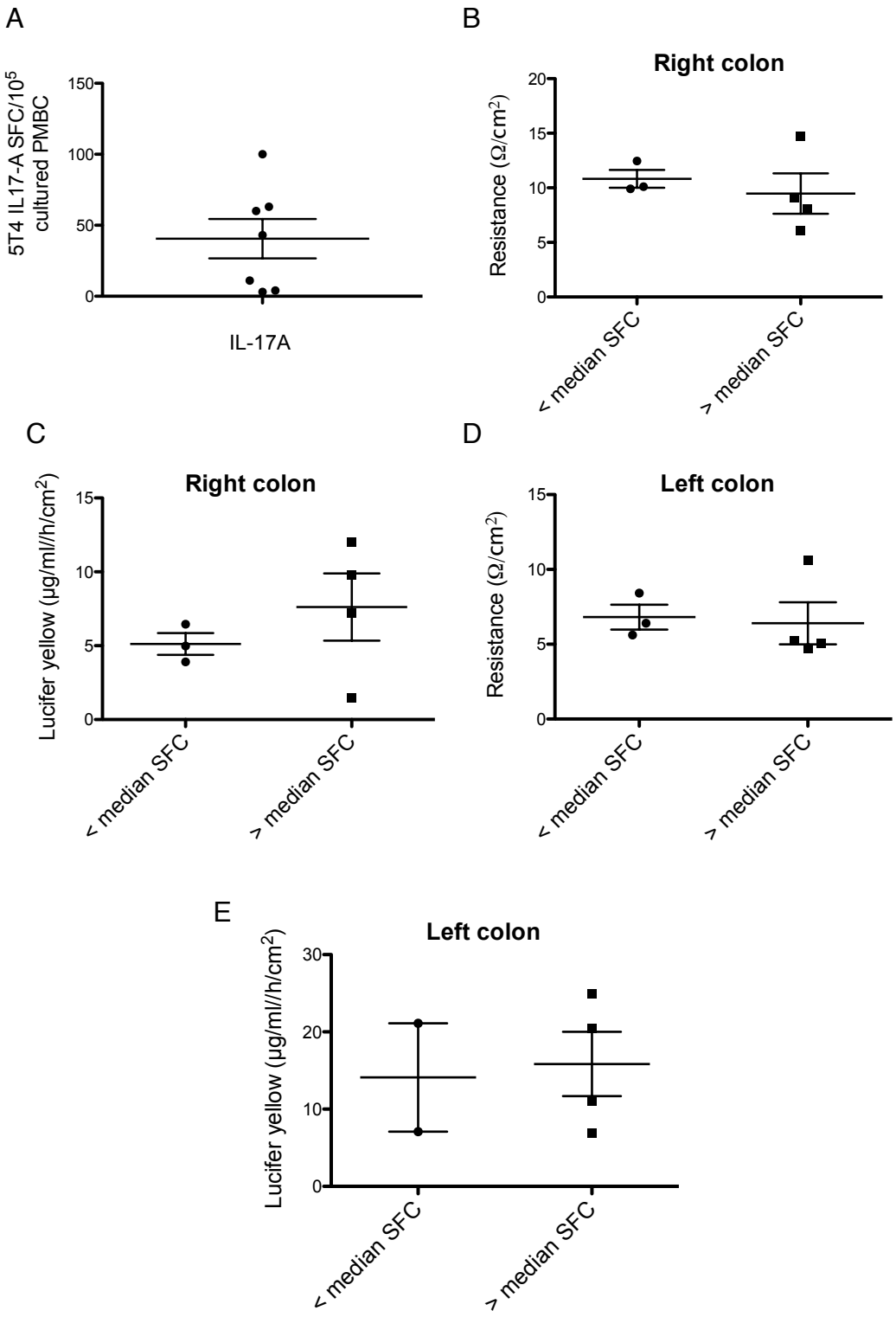

Figure 5.8. 5T4-specific IL-17A T cell responses do not correlate with intestinal permeability.

Electrical resistance and Lucifer yellow passage of colonic biopsies was measured. Patients were then divided based on 5T4 magnitude of response, defined as having a FluoroSpot IL-17A SFC higher or lower than the group median. (A) Magnitude of IL-17A responses from all patients. (B) Right and (D) left colon electrical resistance. (C) Right colon and (E) left colon Lucifer yellow passage. Data shown is at 20 minutes. Error bars show SEM.

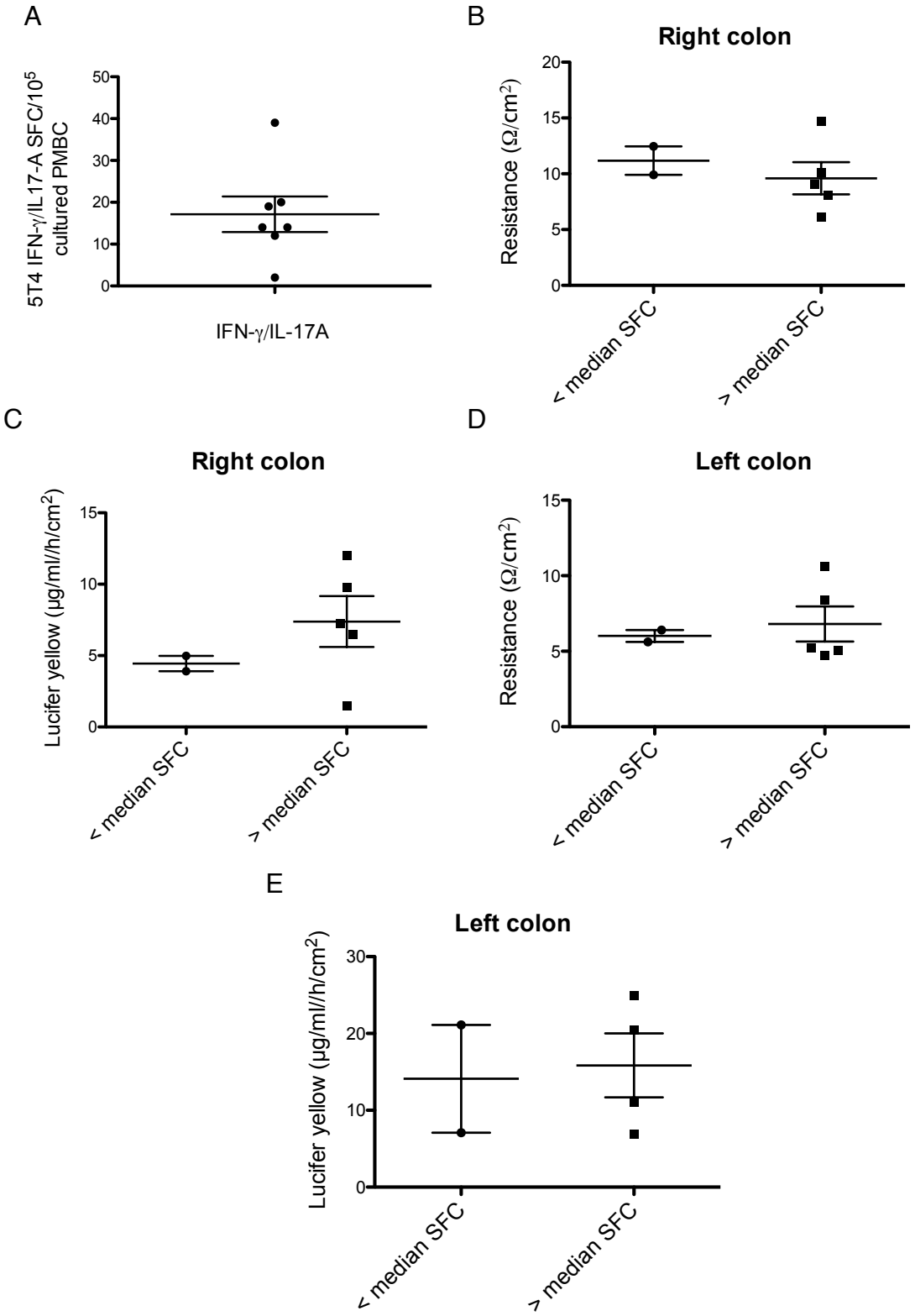

Figure 5.9. 5T4-specific IFN-γ/IL-17A dual T cell responses do not correlate with intestinal permeability.

Electrical resistance and Lucifer yellow passage of colonic biopsies was measured. Patients were then divided based on 5T4 magnitude of response, defined as having a FluoroSpot IFN-γ/IL-17A SFC higher or lower than the group median. (A) Magnitude of IFN-γ/IL-17A responses from all patients. (B) Right and (D) left colon electrical resistance. (C) Right colon and (E) left colon Lucifer yellow passage. Data shown is at 20 minutes. Error bars show SEM.

5.3 Discussion

This chapter focused on whether CEA blood responses correlated with increased intestinal permeability. Firstly, it was established that human colonic biopsy permeability could be measured within the Ussing chamber system. Acquiring biopsy samples was extremely beneficial, as historically surgical samples would have been used. Logistically surgical samples are difficult to work with; as tissue viability is often sub-optimal by the time it reaches the laboratory from theatre. Furthermore, surgical specimens require dissection of the colonic muscle layer prior to mounting. In contrast, biopsy samples can be transported directly to the laboratory and mounted immediately. Moreover, as patients often receive repeat colonoscopies there are opportunities to obtain samples on more than one occasion from the same patient. However, one drawback of biopsy samples is that the small tissue size can sometimes induce edge damage, which may not be present in larger samples. Edge damage can create a shunt pathway, providing a lower resistance pathway for current to travel. This can lead to an underestimation of the true tissue electrical resistance. Nevertheless, biopsy samples do provide a good tissue source for Ussing experiments.

There has been conflicting data regarding the prognostic impact of right versus left sided tumours. Most studies indicate a poorer prognosis for right-sided CRC (307) (308, 309). However, Weiss *et al* found no difference in outcome based on tumour site and Warschkow and colleagues observed a better survival for patients with right-sided tumours (310) (311). What is clear however is that left and right tumours do have characteristic differences. For example right-sided tumours are associated more often with increased age, female gender and are poorly differentiated (307). Furthermore, primary tumour location has been

linked with clinical outcome during treatment. For example, in RAS wild-type CRC, cetuximab treatment was associated with a poorer survival outcome in patients with right-sided tumours than left sided. (312). In this study it was observed that intestinal permeability between the right and left colon of healthy patients also differed. The left side of the colon is more permeable that the right. Interestingly, tumour occurrence is also more common in the left (sigmoid = 23% for males and 20% for females) colonic region that the right (caecum = 12% for males and 17% for females) according to Cancer Research UK statistics (313). When permeability was correlated with CEA T cell response it was observed that magnitude of CEA-specific IFN-γ T cell response only associated with increased intestinal permeability in the right side of the colon, not the left. This data supports our hypothesis that CEA responding patients have increased mucosal permeability compared to non-responding patients. A high magnitude CEA response under normal circumstances appears to be somewhat insignificant, as this association with increased permeability was observed in healthy patients who had no indication of colonic disease. However, in the case where a tumour has developed this natural increase in intestinal permeability within the right colon may contribute to tumour progression through bacterial driven inflammation (Figure 5.10). Our data investigating adenoma patients also supports this idea, as those with a lesion displayed a higher magnitude CEA-specific IFN-γ T cell response than healthy controls, suggesting that damage to the epithelial barrier may enhance CEA responses, perhaps through cross-reactivity to microbes.

Since CEA is highly upregulated in cancer it has been suggested as a target for immunotherapy and for use in vaccination. However, while studies have shown that immune tolerance to CEA can be broken, the long-term effects of this are unknown. Both mouse and human studies have provided evidence that

stimulation of anti-CEA immune responses can reduce tumour size however as a consequence very severe colitis ensues (191, 192). This supports our findings that CEA responses are linked with increased intestinal permeability and therefore may be detrimental in the case of CRC patients. Based on our data, CEA T cell blood responses should be considered a risk factor for poor prognosis in CRC, with data obtained using the Ussing system suggesting that this may be due to intestinal epithelial barrier dysfunction, at least within the right side of the colon.

5.4 Conclusion

The Ussing Chamber system was successfully modified to accommodate small human colonic biopsy samples and intestinal permeability could be evaluated. A blood CEA specific T cell response appears to associate with increased right-sided intestinal permeability.

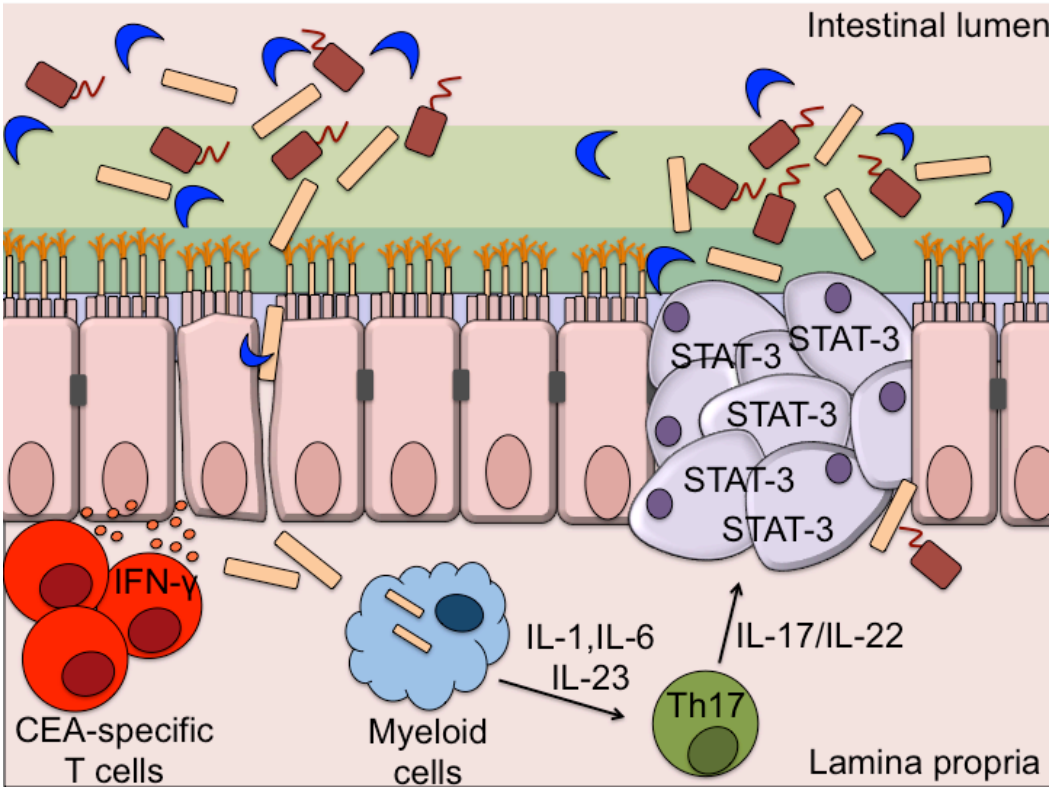

Figure 5.10. Schematic showing the hypothesis that increased intestinal permeability helps drive bacterial induced inflammation, aiding tumour progression in CEA responding patients.
Cancerous cells develop due to genetic mutations within colonic epithelial cells, resulting in disruption of the epithelial barrier locally at the tumour site. This results in translocation of microbes, which are detected by myeloid cells within the lamina propria via TLRs, driving the release of inflammatory products such as IL-1, IL-6 and IL-23 that can activate T helper cells. IL-23 activation of Th17 cells in particular can drive STAT-3 production in tumour cells through the release of IL-17 and IL-22 to aid survival and proliferation. Auto-reactive CEA specific T cells in the lamina propria contribute to the inflammatory setting as IFN-γ released can act directly on TJ proteins in-between epithelial cells, further increasing mucosal permeability and bacterial translocation. Consistent inflammation can drive further CEA T cell activation, increase the chance of developing additional genetic mutations, more epithelial barrier dysfunction and ultimately promote tumour progression. Figure adapted from Gallimore and Godkin, 2013 (253).

Chapter 6. Final Discussion

6.1 Introduction

This thesis has investigated the role of auto-reactive T cells in CRC, a disease where typically treatment consists of a surgical colectomy with curative intent. However, unfortunately up to 50% of patients will relapse within a 5-year period (176). A better understanding of CRC development and progression is key to the generation of superior treatments for patients.

Current dogma suggests that IFN-γ producing T cells are beneficial for CRC patient outcome. However, the clinical consequences of such a response with respect to long-term outcome is not properly understood. In a study carried out by our laboratory blood derived IFN-γ responses to two well-known tumour antigens, 5T4 and CEA, were evaluated in a cohort of CRC patients prior to surgical colectomy (194). As expected, results showed that disease recurrence was most associated with late stage III disease. However, surprisingly the presence of a CEA-specific IFN-γ response identified patients with a statistically significant increased risk of tumour recurrence irrespective of tumour stage. In contrast, a 5T4 response alone did not reflect outcome, but did provide a protective affect within patients also harbouring a CEA response. The major focus of the work within this thesis centred around two hypotheses to determine why IFN-γ responses towards CEA correlate with earlier tumour recurrence.

My first hypothesis stated that IL-17A and/or IL-17A/IFN-γ dual producing CEA-specific T cells existed within CRC patients and contributed to tumour relapse. Results from Chapter 3 showed that CEA-specific IL-17A and IL-17A/IFN-γ T cell responses were present within healthy donors and CRC patients. However,

the magnitude of CEA-specific IL-17A response was constantly lower than CEA-specific IFN-γ responses. Furthermore CEA-specific IL-17A secretion was always accompanied by CEA-specific IFN-γ release. IL-17A/IFN-γ dual responses towards CEA were also rarely detected. Together this indicates that CEA-specific IL-17A is not the main factor influencing patient outcome.

Interestingly it was observed that tumours from CEA responding patients have a lower immune cell infiltrate compared to non-responding patients. High immune cell infiltration, particularly the presence of $CD3^+$ T cells, is associated with better patient survival in CRC (208). Therefore lack of T cell infiltration could allow for earlier relapse in CEA responding patients.

My second hypothesis stated that patients harbouring CEA-specific T cell IFN-γ responses had increased intestinal permeability, which could lead to tumour progression through bacterial driven inflammation. Importantly, data supporting this hypothesis emerged from experiments using the Ussing chamber system, which I recently established within our laboratory. A high magnitude CEA-specific IFN-γ T cell response was associated with increased permeability within the right colon. To better explain this finding further investigations should be carried out. Firstly due to the regional differences in intestinal permeability detected, the distribution of CEA expression throughout the colon should be explored using immunohistochemistry. Thus far the localisation of CEA has been determined in the small intestine and the colon with results showing high luminal expression at both sites (184). However, the pattern of CEA expression along the length of the colon is yet to be defined. In our initial data set showing that an IFN-γ CEA response correlated with earlier relapse, tumour location was shown to not be an associated factor (194). However, in this study increased intestinal permeability is linked with CEA responses in the right colon but not the left. Interestingly baseline permeability Ussing measurements showed that the

left colon is more permeable compared to the right. It may be possible that this increase in baseline permeability makes it more difficult to extrapolate a positive correlation between CEA response and increased permeability in the left colon. If a correlation does exist it may be subtle, making it difficult to observe with Ussing measurements on a low number of patients. Increasing the size of this cohort should confirm if IFN-γ T cell CEA responses only correlate with increased permeability of the right colon or not.

Reduced epithelial integrity is associated with a change in TJ protein composition in-between epithelial cells. Inflammation is linked with the down regulation of "sealing" TJ proteins and increased barrier permeability (19). Through the use of cell lines, mouse models and patient samples, Ahmad *et al* recently investigated the role of the TJ protein claudin-3 in CRC (254). The group were able to show that claudin-3 is the most abundant cell adhesion molecule in the normal colon but there is a significant loss of expression in colonic tumours. It was also observed that claudin-3 deficient mice had dedifferentiated colonic epithelium as well increased mucosal leakage compared to WT animals, indicating a role for claudin-3 in promoting intestinal barrier function. Moreover, claudin-3 deficiency resulted in increased susceptibility to AOM/DSS induced colon carcinogenesis, with 33% of mice developing invasive tumours while WT mice developed none. Loss of claudin-3 was also shown to induce the Wnt/β-catenin signalling pathway to aid in tumour progression (254). CRC patient samples also revealed that claudin-3 expression had a prognostic significance, with greater claudin-3 expression correlating with better patient OS (254). It's clear from such observations that TJ proteins play a major role in gut homeostasis. Within our cohort of endoscopy patients it is unknown if there is a correlation between TJ composition and CEA response. Therefore exploring the expression of TJ proteins at various colonic regions and within CEA high and low responding patients would be extremely advantageous.

6.2 Microbial influence in colorectal cancer

The influence of the microbiota in intestinal disease is a rapidly expanding field. Studies have identified a dramatic alteration in microbial composition between CRC patients and healthy controls (314) (315). It is believed this is in part due to the substantial change in diet, which has occurred over the last few decades in the western world. Dietary behaviour can influence microbial composition, which in turn can affects susceptibility to intestinal disease (316, 317). With the colon exhibiting the highest bacterial density of the GI tract a potential role for the microbiota in CRC progression should therefore be considered. Throughout this thesis it has been suggested that translocation of microbes across the epithelial barrier could aid in tumour development. Some studies support this theory, showing that specific bacterial species are linked with tumourigenesis (222, 304, 305). However, there is now evidence to suggest that bacterial species can impact the effectiveness of cancer therapy also. This makes microbial composition a crucial factor to consider not only for understanding tumour progression but also for developing better treatment strategies for CRC patients.

In particular, the group of Laurence Zitvogel showed that treatment with the drug cyclophosphamide, a prominent alkylating anticancer agent, alters the intestinal microbial composition and promotes the translocation of distinct gram$^+$ bacteria across the gut. This was associated with the generation of better anti-tumour immune responses in a mouse model (318). Moreover, tumour-bearing germ-free and antibiotic treated mice had reduced anti-tumour responses and any beneficial effects of cyclophosphamide were diminished, suggesting that the microbiota are of great importance. In a follow up study it was shown that oral gavage of mice with a particular Gram$^+$ bacterial strain called *Enterococcus hirae* (clone 13144) could restore cyclophosphamide-mediated anti-tumour

effects (250). The group stated that *E.hirae* had translocated across the gut epithelium, identified by cultivation of the mesenteric lymph nodes (mLN) of colonised mice on agar plates, followed by mass spectrometry to identify the presence of bacterial species. While results implied that *E.hirae* had translocated the epithelium, it is not unreasonable to suggest that *E.hirae* detected within the mLN is in fact a result of antigen presenting cells such as DCs sampling the intestinal luminal environment, consuming *E.hirae* and migrating to lymphoid tissue as opposed to direct translocation. In scenarios such as this the Ussing chamber system can be a valuable tool. Preliminary data from our laboratory based on one experiment suggests that *E.hirae* is able to translocate across the intestinal barrier after 20 minutes of being in contact with the intestinal mucosal surface (see appendix). Such findings highlight a useful future use for the Ussing chamber system, potentially investigating the direct impact of particular bacterial species on barrier integrity during disease. Findings from our laboratory also support the observations that cyclophosphamide can promote anti-tumour responses. Data emerged from our clinical trial (TaCTiCC) showing that cyclophosphamide treatment was able to reduce Treg numbers within CRC patients, which led to the expansion of effector T cells producing IFN-γ and granzyme-B. Furthermore, cyclophosphamide-treated patients demonstrating the most enhanced IFN-γ/granzyme-B tumor-specific T-cell responses exhibited a significant delay in tumor progression (202). As mentioned previously CRC patients have a high risk of tumour recurrence, with up to 50% of patients relapsing within 5-years post-surgery. It is possible that alterations in microbial composition and/or intestinal permeability occur after surgical colectomy. Using the Ussing chamber system intestinal permeability before surgery could be measured. Following this, permeability measurements at various time points after surgery (e.g. every year) may make it possible to ascertain whether intestinal permeability changes occur

over time, and whether this increases the risk of tumour recurrence. The impact of therapies such as cyclophosphamide on barrier function within post-operative patients could also be assessed. Further to this, it would be interesting to determine if the effectiveness of cancer therapy is altered as a consequence of having increased baseline intestinal permeability, such as that seen within individuals harbouring a high CEA response.

Not many studies exist where intestinal permeability has been successfully restored. However Yi *et al* recently reported that administration of the antimicrobial peptide (AMP) Cathelicidin-WA (CWA) provides enhanced barrier function in the intestine. Intraperitoneal injection of CWA into piglets experiencing post-weaning diarrhoea resulted in reduced pro-inflammatory cytokines such as IL-6 and IL-8, compared to control animals. Moreover, symptoms of disease were also reduced. Furthermore, it was also shown that CWA treatment was associated with the upregulation of TJ proteins ZO-1 and occludin, known to have a key role in barrier integrity. Moreover, *in vitro* experiments using IPEC-J2 cell monolayers, a porcine epithelial cell line, showed that treatment with CWA ameliorated LPS induced reductions in electrical resistance (319). In a follow-up study it was shown that CWA treatment could also attenuate intestinal colitis driven by enterohemorrhagic *Escherichia coli* (320). Additionally, there were differences in microbial composition between animals treated with CWA versus those treated with the standard antibiotic enrofloxacin. This change was accompanied by restoration of SCFA levels to that observed in control animals. Such observations indicate that CWA treatment exhibits different effects on the bacterial community and can help to restore gut homeostasis. While the area of modulating intestinal barrier function is still in its infancy, studies such as this indicate that barrier function potentially could be promoted during inflammatory disease. Potentially

treatments to enhance intestinal function alongside cancer therapies may be beneficial for patients.

6.3 Concluding remarks

Superior treatments for CRC are required and immune based therapies could potentially be life saving for patients. However, one of the major difficulties is developing agents that are useful for the majority of patients. For this reason the development of treatments that target non-mutated self-antigens is very attractive. On the other-hand the long-term effects of unleashing such immune responses is still largely unknown. As shown in this thesis immune responses to particular targets, such as CEA, may be detrimental. The consequences of immune based therapies must therefore be fully understood to ensure the most effective targets are selected.

APPENDIX

Appendix Figure 1. Magnitude of cytokine responses in FluoroSpot assays when using CTL Test Plus Serum Free media or R5 Media for culture. n=1. Error bars show SEM. Note that HA was not tested in CTL Test Plus Serum Free Media.

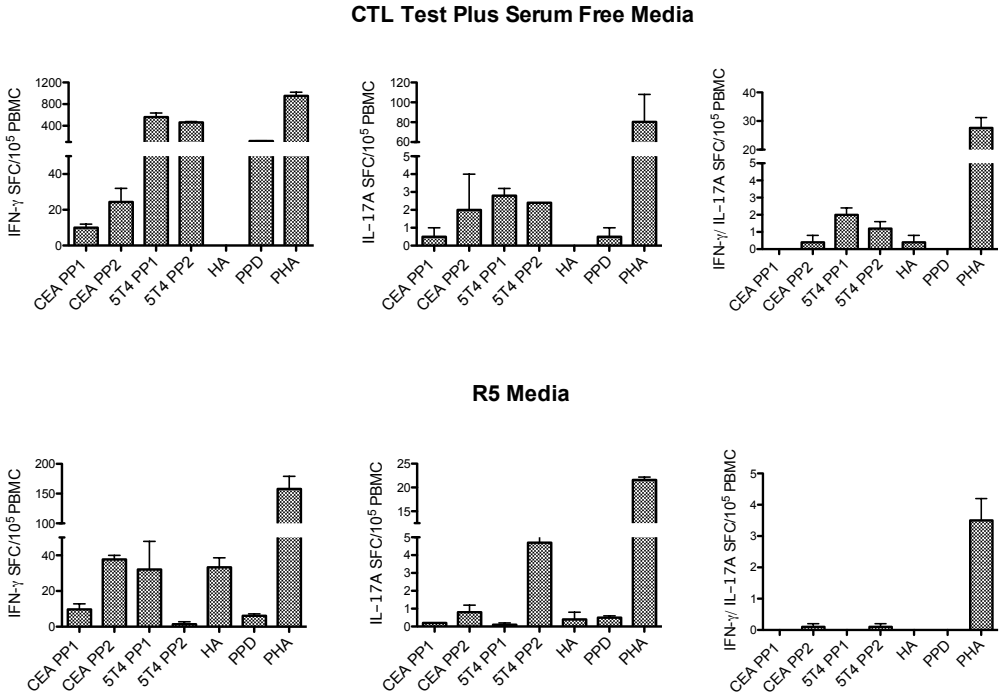

Appendix Figure 2. *E.Hirae* translocation across sigmoid biopsy tissue mounted in Ussing chambers. (A) Staining of *E.hirae* with the fluorescent dye SYBR-Green. 1 billion E.Hirae were added to the mucosal chamber and (B) shows the percentage of *E.Hirae* detected in the serosal chamber at various time points. (C) The number of E.Hirae/µl detected in serosal samples. (D) FACS plots of mucosal and serosal samples at 0, 20, 40, 60, 90 and 960 minutes.

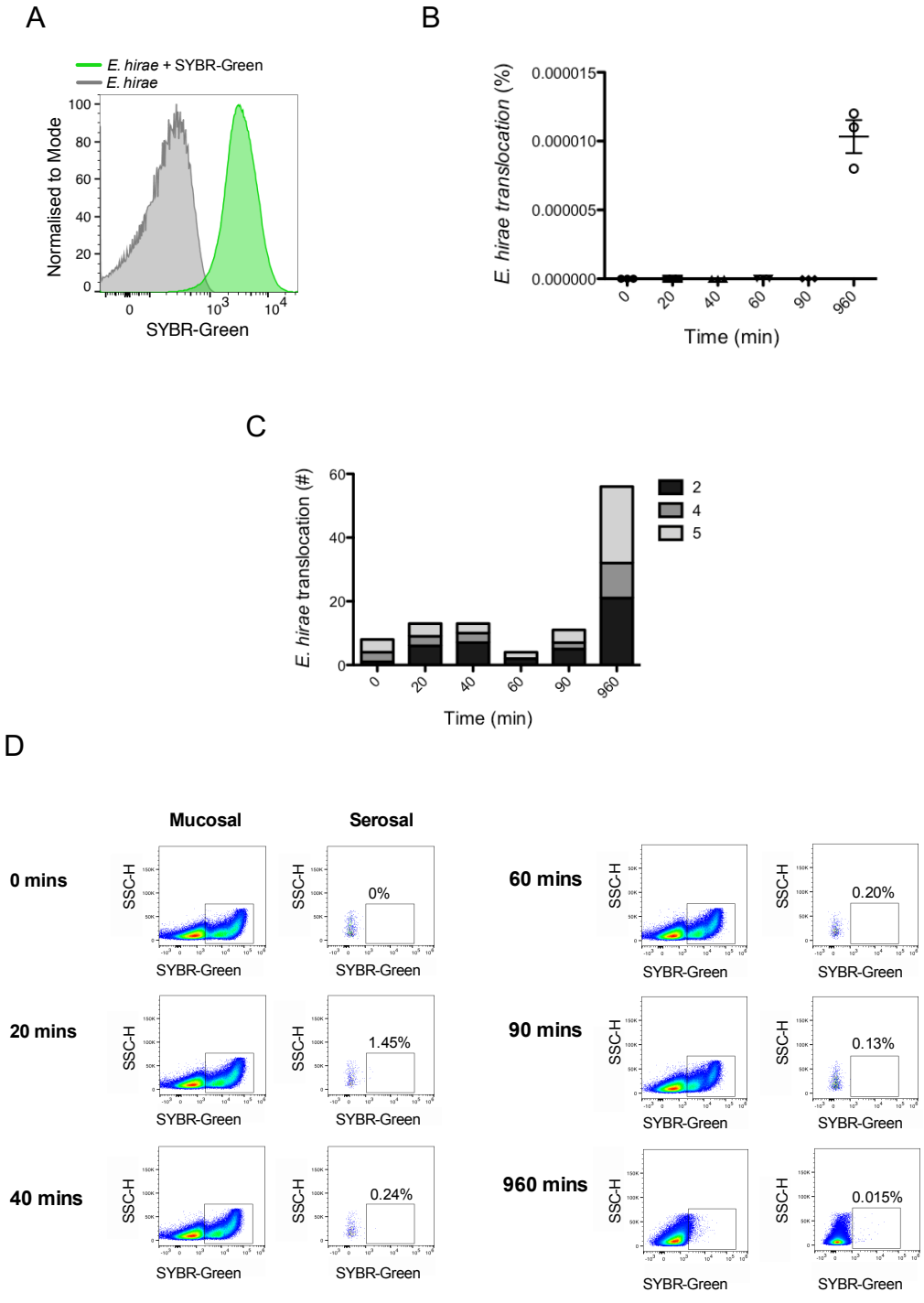

References

1. den Besten G, van Eunen K, Groen AK, Venema K, Reijngoud DJ, Bakker BM. The role of short-chain fatty acids in the interplay between diet, gut microbiota, and host energy metabolism. Journal of lipid research. 2013;54(9):2325-40. doi: 10.1194/jlr.R036012
2. LeBlanc JG, Laino JE, del Valle MJ, Vannini V, van Sinderen D, Taranto MP, et al. B-group vitamin production by lactic acid bacteria--current knowledge and potential applications. Journal of applied microbiology. 2011;111(6):1297-309. doi: 10.1111/j.1365-2672.2011.05157.x
3. Beulens JW, Booth SL, van den Heuvel EG, Stoecklin E, Baka A, Vermeer C. The role of menaquinones (vitamin K(2)) in human health. The British journal of nutrition. 2013;110(8):1357-68. doi: 10.1017/s0007114513001013
4. Wahlstrom A, Sayin SI, Marschall HU, Backhed F. Intestinal Crosstalk between Bile Acids and Microbiota and Its Impact on Host Metabolism. Cell metabolism. 2016;24(1):41-50. doi: 10.1016/j.cmet.2016.05.005
5. Okumura R, Takeda K. Roles of intestinal epithelial cells in the maintenance of gut homeostasis. Experimental & molecular medicine. 2017;49(5):e338. doi: 10.1038/emm.2017.20
6. Farquhar MG, Palade GE. Junctional complexes in various epithelia. The Journal of cell biology. 1963;17:375-412.
7. Stevenson BR, Siliciano JD, Mooseker MS, Goodenough DA. Identification of ZO-1: a high molecular weight polypeptide associated with the tight junction (zonula occludens) in a variety of epithelia. The Journal of cell biology. 1986;103(3):755-66.
8. Gumbiner B, Lowenkopf T, Apatira D. Identification of a 160-kDa polypeptide that binds to the tight junction protein ZO-1. Proc Natl Acad Sci U S A. 1991;88(8):3460-4.
9. Furuse M, Hirase T, Itoh M, Nagafuchi A, Yonemura S, Tsukita S, et al. Occludin: a novel integral membrane protein localizing at tight junctions. The Journal of cell biology. 1993;123(6 Pt 2):1777-88.
10. Balda MS, Whitney JA, Flores C, Gonzalez S, Cereijido M, Matter K. Functional dissociation of paracellular permeability and transepithelial electrical resistance and disruption of the apical-basolateral intramembrane diffusion barrier by expression of a mutant tight junction membrane protein. The Journal of cell biology. 1996;134(4):1031-49.
11. Mineta K, Yamamoto Y, Yamazaki Y, Tanaka H, Tada Y, Saito K, et al. Predicted expansion of the claudin multigene family. FEBS letters. 2011;585(4):606-12. doi: 10.1016/j.febslet.2011.01.028
12. Furuse M, Furuse K, Sasaki H, Tsukita S. Conversion of zonulae occludentes from tight to leaky strand type by introducing claudin-2 into Madin-Darby canine kidney I cells. The Journal of cell biology. 2001;153(2):263-72.
13. Furuse M, Sasaki H, Fujimoto K, Tsukita S. A single gene product, claudin-1 or -2, reconstitutes tight junction strands and recruits occludin in fibroblasts. The Journal of cell biology. 1998;143(2):391-401.
14. Van Itallie C, Rahner C, Anderson JM. Regulated expression of claudin-4 decreases paracellular conductance through a selective decrease in sodium permeability. J Clin Invest. 2001;107(10):1319-27. doi: 10.1172/jci12464
15. Matsuda M, Kubo A, Furuse M, Tsukita S. A peculiar internalization of claudins, tight junction-specific adhesion molecules, during the intercellular movement of epithelial cells. Journal of cell science. 2004;117(Pt 7):1247-57. doi: 10.1242/jcs.00972
16. Capaldo CT, Nusrat A. Claudin switching: Physiological plasticity of the Tight Junction. Seminars in cell & developmental biology. 2015;42:22-9. doi: 10.1016/j.semcdb.2015.04.003
17. Ahmad R, Chaturvedi R, Olivares-Villagomez D, Habib T, Asim M, Shivesh P, et al. Targeted colonic claudin-2 expression renders resistance to epithelial injury, induces immune suppression, and protects from colitis. Mucosal Immunol. 2014;7(6):1340-53. doi: 10.1038/mi.2014.21

18. Lameris AL, Huybers S, Kaukinen K, Makela TH, Bindels RJ, Hoenderop JG, et al. Expression profiling of claudins in the human gastrointestinal tract in health and during inflammatory bowel disease. Scandinavian journal of gastroenterology. 2013;48(1):58-69. doi: 10.3109/00365521.2012.741616
19. Garcia-Hernandez V, Quiros M, Nusrat A. Intestinal epithelial claudins: expression and regulation in homeostasis and inflammation. Annals of the New York Academy of Sciences. 2017;1397(1):66-79. doi: 10.1111/nyas.13360
20. Tanaka H, Takechi M, Kiyonari H, Shioi G, Tamura A, Tsukita S. Intestinal deletion of Claudin-7 enhances paracellular organic solute flux and initiates colonic inflammation in mice. Gut. 2015;64(10):1529-38. doi: 10.1136/gutjnl-2014-308419
21. Marasco WA, Phan SH, Krutzsch H, Showell HJ, Feltner DE, Nairn R, et al. Purification and identification of formyl-methionyl-leucyl-phenylalanine as the major peptide neutrophil chemotactic factor produced by Escherichia coli. J Biol Chem. 1984;259(9):5430-9.
22. Shi B, Song D, Xue H, Li N, Li J. PepT1 mediates colon damage by transporting fMLP in rats with bowel resection. The Journal of surgical research. 2006;136(1):38-44. doi: 10.1016/j.jss.2006.05.025
23. Lu Z, Ding L, Lu Q, Chen YH. Claudins in intestines: Distribution and functional significance in health and diseases. Tissue barriers. 2013;1(3):e24978. doi: 10.4161/tisb.24978
24. Malergue F, Galland F, Martin F, Mansuelle P, Aurrand-Lions M, Naquet P. A novel immunoglobulin superfamily junctional molecule expressed by antigen presenting cells, endothelial cells and platelets. Molecular immunology. 1998;35(17):1111-9.
25. Liu Y, Nusrat A, Schnell FJ, Reaves TA, Walsh S, Pochet M, et al. Human junction adhesion molecule regulates tight junction resealing in epithelia. Journal of cell science. 2000;113 (Pt 13):2363-74.
26. Bazzoni G, Martinez-Estrada OM, Orsenigo F, Cordenonsi M, Citi S, Dejana E. Interaction of junctional adhesion molecule with the tight junction components ZO-1, cingulin, and occludin. J Biol Chem. 2000;275(27):20520-6. doi: 10.1074/jbc.M905251199
27. Laukoetter MG, Nava P, Lee WY, Severson EA, Capaldo CT, Babbin BA, et al. JAM-A regulates permeability and inflammation in the intestine in vivo. J Exp Med. 2007;204(13):3067-76. doi: 10.1084/jem.20071416
28. Vetrano S, Rescigno M, Cera MR, Correale C, Rumio C, Doni A, et al. Unique role of junctional adhesion molecule-a in maintaining mucosal homeostasis in inflammatory bowel disease. Gastroenterology. 2008;135(1):173-84. doi: 10.1053/j.gastro.2008.04.002
29. Kiela PR, Ghishan FK. Physiology of Intestinal Absorption and Secretion. Best practice & research Clinical gastroenterology. 2016;30(2):145-59. doi: 10.1016/j.bpg.2016.02.007
30. Sandle GI. Salt and water absorption in the human colon: a modern appraisal. Gut. 1998;43(2):294-9.
31. Cutting GR. Cystic fibrosis genetics: from molecular understanding to clinical application. Nature reviews Genetics. 2015;16(1):45-56. doi: 10.1038/nrg3849
32. Field M. Intestinal ion transport and the pathophysiology of diarrhea. J Clin Invest. 2003;111(7):931-43. doi: 10.1172/jci18326
33. Song P, Onishi A, Koepsell H, Vallon V. Sodium glucose cotransporter SGLT1 as a therapeutic target in diabetes mellitus. Expert opinion on therapeutic targets. 2016;20(9):1109-25. doi: 10.1517/14728222.2016.1168808
34. Johansson ME, Phillipson M, Petersson J, Velcich A, Holm L, Hansson GC. The inner of the two Muc2 mucin-dependent mucus layers in colon is devoid of bacteria. Proc Natl Acad Sci U S A. 2008;105(39):15064-9. doi: 10.1073/pnas.0803124105
35. Desai MS, Seekatz AM, Koropatkin NM, Kamada N, Hickey CA, Wolter M, et al. A Dietary Fiber-Deprived Gut Microbiota Degrades the Colonic Mucus Barrier and Enhances Pathogen Susceptibility. Cell. 2016;167(5):1339-53.e21. doi: 10.1016/j.cell.2016.10.043
36. Cunliffe RN, Mahida YR. Expression and regulation of antimicrobial peptides in the gastrointestinal tract. Journal of leukocyte biology. 2004;75(1):49-58. doi: 10.1189/jlb.0503249

37. Brogden KA. Antimicrobial peptides: pore formers or metabolic inhibitors in bacteria? Nature reviews Microbiology. 2005;3(3):238-50. doi: 10.1038/nrmicro1098
38. Lamm ME, Phillips-Quagliata JM. Origin and homing of intestinal IgA antibody-secreting cells. J Exp Med. 2002;195(2):F5-8.
39. Gutzeit C, Magri G, Cerutti A. Intestinal IgA production and its role in host-microbe interaction. Immunological reviews. 2014;260(1):76-85. doi: 10.1111/imr.12189
40. Okumura R, Kurakawa T, Nakano T, Kayama H, Kinoshita M, Motooka D, et al. Lypd8 promotes the segregation of flagellated microbiota and colonic epithelia. Nature. 2016;532(7597):117-21. doi: 10.1038/nature17406
41. Garrett WS, Gallini CA, Yatsunenko T, Michaud M, DuBois A, Delaney ML, et al. Enterobacteriaceae act in concert with the gut microbiota to induce spontaneous and maternally transmitted colitis. Cell host & microbe. 2010;8(3):292-300. doi: 10.1016/j.chom.2010.08.004
42. Papamichael K, Konstantopoulos P, Mantzaris GJ. Helicobacter pylori infection and inflammatory bowel disease: is there a link? World journal of gastroenterology. 2014;20(21):6374-85. doi: 10.3748/wjg.v20.i21.6374
43. Mukhopadhya I, Hansen R, El-Omar EM, Hold GL. IBD-what role do Proteobacteria play? Nature reviews Gastroenterology & hepatology. 2012;9(4):219-30. doi: 10.1038/nrgastro.2012.14
44. Miller JF. The discovery of the immunological function of the thymus. Immunology today. 1991;12(1):42-5. doi: 10.1016/0167-5699(91)90111-6
45. Owen JJ, Ritter MA. Tissue interaction in the development of thymus lymphocytes. J Exp Med. 1969;129(2):431-42.
46. Haynes BF, Heinly CS. Early human T cell development: analysis of the human thymus at the time of initial entry of hematopoietic stem cells into the fetal thymic microenvironment. J Exp Med. 1995;181(4):1445-58.
47. Liu C, Ueno T, Kuse S, Saito F, Nitta T, Piali L, et al. The role of CCL21 in recruitment of T-precursor cells to fetal thymi. Blood. 2005;105(1):31-9. doi: 10.1182/blood-2004-04-1369
48. Wurbel MA, Malissen M, Guy-Grand D, Meffre E, Nussenzweig MC, Richelme M, et al. Mice lacking the CCR9 CC-chemokine receptor show a mild impairment of early T- and B-cell development and a reduction in T-cell receptor gammadelta(+) gut intraepithelial lymphocytes. Blood. 2001;98(9):2626-32.
49. Rossi FM, Corbel SY, Merzaban JS, Carlow DA, Gossens K, Duenas J, et al. Recruitment of adult thymic progenitors is regulated by P-selectin and its ligand PSGL-1. Nat Immunol. 2005;6(6):626-34. doi: 10.1038/ni1203
50. Scollay RG, Butcher EC, Weissman IL. Thymus cell migration. Quantitative aspects of cellular traffic from the thymus to the periphery in mice. European journal of immunology. 1980;10(3):210-8. doi: 10.1002/eji.1830100310
51. Egerton M, Scollay R, Shortman K. Kinetics of mature T-cell development in the thymus. Proc Natl Acad Sci U S A. 1990;87(7):2579-82.
52. Fahl SP, Coffey F, Wiest DL. Origins of gammadelta T cell effector subsets: a riddle wrapped in an enigma. J Immunol. 2014;193(9):4289-94. doi: 10.4049/jimmunol.1401813
53. Takada K, Takahama Y. Positive-selection-inducing self-peptides displayed by cortical thymic epithelial cells. Advances in immunology. 2015;125:87-110. doi: 10.1016/bs.ai.2014.09.003
54. Murata S, Sasaki K, Kishimoto T, Niwa S, Hayashi H, Takahama Y, et al. Regulation of CD8+ T cell development by thymus-specific proteasomes. Science. 2007;316(5829):1349-53. doi: 10.1126/science.1141915
55. Anderson MS, Venanzi ES, Klein L, Chen Z, Berzins SP, Turley SJ, et al. Projection of an immunological self shadow within the thymus by the aire protein. Science. 2002;298(5597):1395-401. doi: 10.1126/science.1075958
56. Meyer S, Woodward M, Hertel C, Vlaicu P, Haque Y, Karner J, et al. AIRE-Deficient Patients Harbor Unique High-Affinity Disease-Ameliorating Autoantibodies. Cell. 2016;166(3):582-95. doi: 10.1016/j.cell.2016.06.024
57. Takaba H, Morishita Y, Tomofuji Y, Danks L, Nitta T, Komatsu N, et al. Fezf2 Orchestrates a Thymic Program of Self-Antigen Expression for Immune Tolerance. Cell. 2015;163(4):975-87. doi: 10.1016/j.cell.2015.10.013

58. Takaba H, Takayanagi H. The Mechanisms of T Cell Selection in the Thymus. Trends in immunology. 2017;38(11):805-16. doi: 10.1016/j.it.2017.07.010
59. Matloubian M, Lo CG, Cinamon G, Lesneski MJ, Xu Y, Brinkmann V, et al. Lymphocyte egress from thymus and peripheral lymphoid organs is dependent on S1P receptor 1. Nature. 2004;427(6972):355-60. doi: 10.1038/nature02284
60. Mosmann TR, Cherwinski H, Bond MW, Giedlin MA, Coffman RL. Two types of murine helper T cell clone. I. Definition according to profiles of lymphokine activities and secreted proteins. J Immunol. 1986;136(7):2348-57.
61. Ohshima Y, Yang LP, Avice MN, Kurimoto M, Nakajima T, Sergerie M, et al. Naive human CD4+ T cells are a major source of lymphotoxin alpha. J Immunol. 1999;162(7):3790-4.
62. Stevens TL, Bossie A, Sanders VM, Fernandez-Botran R, Coffman RL, Mosmann TR, et al. Regulation of antibody isotype secretion by subsets of antigen-specific helper T cells. Nature. 1988;334(6179):255-8. doi: 10.1038/334255a0
63. Del Prete GF, De Carli M, Mastromauro C, Biagiotti R, Macchia D, Falagiani P, et al. Purified protein derivative of Mycobacterium tuberculosis and excretory-secretory antigen(s) of Toxocara canis expand in vitro human T cells with stable and opposite (type 1 T helper or type 2 T helper) profile of cytokine production. J Clin Invest. 1991;88(1):346-50. doi: 10.1172/jci115300
64. Rouvier E, Luciani MF, Mattei MG, Denizot F, Golstein P. CTLA-8, cloned from an activated T cell, bearing AU-rich messenger RNA instability sequences, and homologous to a herpesvirus saimiri gene. J Immunol. 1993;150(12):5445-56.
65. Nakae S, Nambu A, Sudo K, Iwakura Y. Suppression of immune induction of collagen-induced arthritis in IL-17-deficient mice. J Immunol. 2003;171(11):6173-7.
66. Park H, Li Z, Yang XO, Chang SH, Nurieva R, Wang YH, et al. A distinct lineage of CD4 T cells regulates tissue inflammation by producing interleukin 17. Nat Immunol. 2005;6(11):1133-41. doi: 10.1038/ni1261
67. Bettelli E, Korn T, Oukka M, Kuchroo VK. Induction and effector functions of T(H)17 cells. Nature. 2008;453(7198):1051-7. doi: 10.1038/nature07036
68. Tesmer LA, Lundy SK, Sarkar S, Fox DA. Th17 cells in human disease. Immunological reviews. 2008;223:87-113. doi: 10.1111/j.1600-065X.2008.00628.x
69. Cua DJ, Sherlock J, Chen Y, Murphy CA, Joyce B, Seymour B, et al. Interleukin-23 rather than interleukin-12 is the critical cytokine for autoimmune inflammation of the brain. Nature. 2003;421(6924):744-8. doi: 10.1038/nature01355
70. Yang L, Anderson DE, Baecher-Allan C, Hastings WD, Bettelli E, Oukka M, et al. IL-21 and TGF-beta are required for differentiation of human T(H)17 cells. Nature. 2008;454(7202):350-2. doi: 10.1038/nature07021
71. Yang XO, Panopoulos AD, Nurieva R, Chang SH, Wang D, Watowich SS, et al. STAT3 regulates cytokine-mediated generation of inflammatory helper T cells. J Biol Chem. 2007;282(13):9358-63. doi: 10.1074/jbc.C600321200
72. Ivanov, II, McKenzie BS, Zhou L, Tadokoro CE, Lepelley A, Lafaille JJ, et al. The orphan nuclear receptor RORgammat directs the differentiation program of proinflammatory IL-17+ T helper cells. Cell. 2006;126(6):1121-33. doi: 10.1016/j.cell.2006.07.035
73. Acosta-Rodriguez EV, Rivino L, Geginat J, Jarrossay D, Gattorno M, Lanzavecchia A, et al. Surface phenotype and antigenic specificity of human interleukin 17-producing T helper memory cells. Nat Immunol. 2007;8(6):639-46. doi: 10.1038/ni1467
74. Eyerich K, Foerster S, Rombold S, Seidl HP, Behrendt H, Hofmann H, et al. Patients with chronic mucocutaneous candidiasis exhibit reduced production of Th17-associated cytokines IL-17 and IL-22. The Journal of investigative dermatology. 2008;128(11):2640-5. doi: 10.1038/jid.2008.139
75. Mogensen TH. STAT3 and the Hyper-IgE syndrome: Clinical presentation, genetic origin, pathogenesis, novel findings and remaining uncertainties. Jak-stat. 2013;2(2):e23435. doi: 10.4161/jkst.23435
76. Zheng Y, Valdez PA, Danilenko DM, Hu Y, Sa SM, Gong Q, et al. Interleukin-22 mediates early host defense against attaching and effacing bacterial pathogens. Nat Med. 2008;14(3):282-9. doi: 10.1038/nm1720

77. Ivanov, II, Atarashi K, Manel N, Brodie EL, Shima T, Karaoz U, et al. Induction of intestinal Th17 cells by segmented filamentous bacteria. Cell. 2009;139(3):485-98. doi: 10.1016/j.cell.2009.09.033
78. Goto Y, Panea C, Nakato G, Cebula A, Lee C, Diez MG, et al. Segmented filamentous bacteria antigens presented by intestinal dendritic cells drive mucosal Th17 cell differentiation. Immunity. 2014;40(4):594-607. doi: 10.1016/j.immuni.2014.03.005
79. Panea C, Farkas AM, Goto Y, Abdollahi-Roodsaz S, Lee C, Koscso B, et al. Intestinal Monocyte-Derived Macrophages Control Commensal-Specific Th17 Responses. Cell reports. 2015;12(8):1314-24. doi: 10.1016/j.celrep.2015.07.040
80. Fujino S, Andoh A, Bamba S, Ogawa A, Hata K, Araki Y, et al. Increased expression of interleukin 17 in inflammatory bowel disease. Gut. 2003;52(1):65-70.
81. Franke A, McGovern DP, Barrett JC, Wang K, Radford-Smith GL, Ahmad T, et al. Genome-wide meta-analysis increases to 71 the number of confirmed Crohn's disease susceptibility loci. Nature genetics. 2010;42(12):1118-25. doi: 10.1038/ng.717
82. Anderson CA, Boucher G, Lees CW, Franke A, D'Amato M, Taylor KD, et al. Meta-analysis identifies 29 additional ulcerative colitis risk loci, increasing the number of confirmed associations to 47. Nature genetics. 2011;43(3):246-52. doi: 10.1038/ng.764
83. Mannon PJ, Fuss IJ, Mayer L, Elson CO, Sandborn WJ, Present D, et al. Anti-interleukin-12 antibody for active Crohn's disease. N Engl J Med. 2004;351(20):2069-79. doi: 10.1056/NEJMoa033402
84. Hue S, Ahern P, Buonocore S, Kullberg MC, Cua DJ, McKenzie BS, et al. Interleukin-23 drives innate and T cell-mediated intestinal inflammation. J Exp Med. 2006;203(11):2473-83. doi: 10.1084/jem.20061099
85. Imamura E, Taguchi K, Sasaki-Iwaoka H, Kubo S, Furukawa S, Morokata T. Anti-IL-23 receptor monoclonal antibody prevents CD4(+) T cell-mediated colitis in association with decreased systemic Th1 and Th17 responses. European journal of pharmacology. 2018;824:163-9. doi: 10.1016/j.ejphar.2018.01.045
86. Tang MS, Bowcutt R, Leung JM, Wolff MJ, Gundra UM, Hudesman D, et al. Integrated Analysis of Biopsies from Inflammatory Bowel Disease Patients Identifies SAA1 as a Link Between Mucosal Microbes with TH17 and TH22 Cells. Inflammatory bowel diseases. 2017;23(9):1544-54. doi: 10.1097/mib.0000000000001208
87. Ogawa A, Andoh A, Araki Y, Bamba T, Fujiyama Y. Neutralization of interleukin-17 aggravates dextran sulfate sodium-induced colitis in mice. Clinical immunology (Orlando, Fla). 2004;110(1):55-62. doi: 10.1016/j.clim.2003.09.013
88. Sugimoto K, Ogawa A, Mizoguchi E, Shimomura Y, Andoh A, Bhan AK, et al. IL-22 ameliorates intestinal inflammation in a mouse model of ulcerative colitis. J Clin Invest. 2008;118(2):534-44. doi: 10.1172/jci33194
89. Kinugasa T, Sakaguchi T, Gu X, Reinecker HC. Claudins regulate the intestinal barrier in response to immune mediators. Gastroenterology. 2000;118(6):1001-11.
90. Hueber W, Sands BE, Lewitzky S, Vandemeulebroecke M, Reinisch W, Higgins PD, et al. Secukinumab, a human anti-IL-17A monoclonal antibody, for moderate to severe Crohn's disease: unexpected results of a randomised, double-blind placebo-controlled trial. Gut. 2012;61(12):1693-700. doi: 10.1136/gutjnl-2011-301668
91. Feagan BG, Sandborn WJ, Gasink C, Jacobstein D, Lang Y, Friedman JR, et al. Ustekinumab as Induction and Maintenance Therapy for Crohn's Disease. N Engl J Med. 2016;375(20):1946-60. doi: 10.1056/NEJMoa1602773
92. Annunziato F, Cosmi L, Santarlasci V, Maggi L, Liotta F, Mazzinghi B, et al. Phenotypic and functional features of human Th17 cells. J Exp Med. 2007;204(8):1849-61. doi: 10.1084/jem.20070663
93. Cosmi L, De Palma R, Santarlasci V, Maggi L, Capone M, Frosali F, et al. Human interleukin 17-producing cells originate from a CD161+CD4+ T cell precursor. J Exp Med. 2008;205(8):1903-16. doi: 10.1084/jem.20080397
94. Harbour SN, Maynard CL, Zindl CL, Schoeb TR, Weaver CT. Th17 cells give rise to Th1 cells that are required for the pathogenesis of colitis. Proc Natl Acad Sci U S A. 2015;112(22):7061-6. doi: 10.1073/pnas.1415675112
95. Zielinski CE, Mele F, Aschenbrenner D, Jarrossay D, Ronchi F, Gattorno M, et al. Pathogen-induced human TH17 cells produce IFN-gamma or IL-10 and are regulated by IL-1beta. Nature. 2012;484(7395):514-8. doi: 10.1038/nature10957
96. Nishizuka Y, Sakakura T. Thymus and reproduction: sex-linked dysgenesia of the gonad after neonatal thymectomy in mice. Science. 1969;166(3906):753-5.

97. Taguchi O, Nishizuka Y, Sakakura T, Kojima A. Autoimmune oophoritis in thymectomized mice: detection of circulating antibodies against oocytes. Clinical and experimental immunology. 1980;40(3):540-53.
98. Sakaguchi S, Sakaguchi N, Asano M, Itoh M, Toda M. Immunologic self-tolerance maintained by activated T cells expressing IL-2 receptor alpha-chains (CD25). Breakdown of a single mechanism of self-tolerance causes various autoimmune diseases. J Immunol. 1995;155(3):1151-64.
99. Asano M, Toda M, Sakaguchi N, Sakaguchi S. Autoimmune disease as a consequence of developmental abnormality of a T cell subpopulation. J Exp Med. 1996;184(2):387-96.
100. Read S, Greenwald R, Izcue A, Robinson N, Mandelbrot D, Francisco L, et al. Blockade of CTLA-4 on CD4+CD25+ regulatory T cells abrogates their function in vivo. J Immunol. 2006;177(7):4376-83.
101. Corthay A. How do regulatory T cells work? Scand J Immunol. 2009;70(4):326-36. doi: 10.1111/j.1365-3083.2009.02308.x
102. Fontenot JD, Gavin MA, Rudensky AY. Foxp3 programs the development and function of CD4+CD25+ regulatory T cells. Nat Immunol. 2003;4(4):330-6. doi: 10.1038/ni904
103. Santegoets SJ, Dijkgraaf EM, Battaglia A, Beckhove P, Britten CM, Gallimore A, et al. Monitoring regulatory T cells in clinical samples: consensus on an essential marker set and gating strategy for regulatory T cell analysis by flow cytometry. Cancer immunology, immunotherapy : CII. 2015;64(10):1271-86. doi: 10.1007/s00262-015-1729-x
104. Liu W, Putnam AL, Xu-Yu Z, Szot GL, Lee MR, Zhu S, et al. CD127 expression inversely correlates with FoxP3 and suppressive function of human CD4+ T reg cells. J Exp Med. 2006;203(7):1701-11. doi: 10.1084/jem.20060772
105. Bennett CL, Christie J, Ramsdell F, Brunkow ME, Ferguson PJ, Whitesell L, et al. The immune dysregulation, polyendocrinopathy, enteropathy, X-linked syndrome (IPEX) is caused by mutations of FOXP3. Nature genetics. 2001;27(1):20-1. doi: 10.1038/83713
106. Godfrey VL, Wilkinson JE, Russell LB. X-linked lymphoreticular disease in the scurfy (sf) mutant mouse. Am J Pathol. 1991;138(6):1379-87.
107. Brunkow ME, Jeffery EW, Hjerrild KA, Paeper B, Clark LB, Yasayko SA, et al. Disruption of a new forkhead/winged-helix protein, scurfin, results in the fatal lymphoproliferative disorder of the scurfy mouse. Nature genetics. 2001;27(1):68-73. doi: 10.1038/83784
108. Fontenot JD, Dooley JL, Farr AG, Rudensky AY. Developmental regulation of Foxp3 expression during ontogeny. J Exp Med. 2005;202(7):901-6. doi: 10.1084/jem.20050784
109. Kim JM, Rasmussen JP, Rudensky AY. Regulatory T cells prevent catastrophic autoimmunity throughout the lifespan of mice. Nat Immunol. 2007;8(2):191-7. doi: 10.1038/ni1428
110. D'Cruz LM, Klein L. Development and function of agonist-induced CD25+Foxp3+ regulatory T cells in the absence of interleukin 2 signaling. Nat Immunol. 2005;6(11):1152-9. doi: 10.1038/ni1264
111. Marie JC, Letterio JJ, Gavin M, Rudensky AY. TGF-beta1 maintains suppressor function and Foxp3 expression in CD4+CD25+ regulatory T cells. J Exp Med. 2005;201(7):1061-7. doi: 10.1084/jem.20042276
112. Jordan MS, Boesteanu A, Reed AJ, Petrone AL, Holenbeck AE, Lerman MA, et al. Thymic selection of CD4+CD25+ regulatory T cells induced by an agonist self-peptide. Nat Immunol. 2001;2(4):301-6. doi: 10.1038/86302
113. Gratz IK, Rosenblum MD, Abbas AK. The life of regulatory T cells. Annals of the New York Academy of Sciences. 2013;1283:8-12. doi: 10.1111/nyas.12011
114. Thornton AM, Korty PE, Tran DQ, Wohlfert EA, Murray PE, Belkaid Y, et al. Expression of Helios, an Ikaros transcription factor family member, differentiates thymic-derived from peripherally induced Foxp3+ T regulatory cells. J Immunol. 2010;184(7):3433-41. doi: 10.4049/jimmunol.0904028
115. Gottschalk RA, Corse E, Allison JP. Expression of Helios in peripherally induced Foxp3+ regulatory T cells. J Immunol. 2012;188(3):976-80. doi: 10.4049/jimmunol.1102964

116. Yadav M, Louvet C, Davini D, Gardner JM, Martinez-Llordella M, Bailey-Bucktrout S, et al. Neuropilin-1 distinguishes natural and inducible regulatory T cells among regulatory T cell subsets in vivo. J Exp Med. 2012;209(10):1713-22, s1-19. doi: 10.1084/jem.20120822
117. Szurek E, Cebula A, Wojciech L, Pietrzak M, Rempala G, Kisielow P, et al. Differences in Expression Level of Helios and Neuropilin-1 Do Not Distinguish Thymus-Derived from Extrathymically-Induced CD4+Foxp3+ Regulatory T Cells. PloS one. 2015;10(10):e0141161. doi: 10.1371/journal.pone.0141161
118. Curotto de Lafaille MA, Kutchukhidze N, Shen S, Ding Y, Yee H, Lafaille JJ. Adaptive Foxp3+ regulatory T cell-dependent and -independent control of allergic inflammation. Immunity. 2008;29(1):114-26. doi: 10.1016/j.immuni.2008.05.010
119. Haribhai D, Williams JB, Jia S, Nickerson D, Schmitt EG, Edwards B, et al. A requisite role for induced regulatory T cells in tolerance based on expanding antigen receptor diversity. Immunity. 2011;35(1):109-22. doi: 10.1016/j.immuni.2011.03.029
120. Atarashi K, Tanoue T, Shima T, Imaoka A, Kuwahara T, Momose Y, et al. Induction of colonic regulatory T cells by indigenous Clostridium species. Science. 2011;331(6015):337-41. doi: 10.1126/science.1198469
121. Kim KS, Hong SW, Han D, Yi J, Jung J, Yang BG, et al. Dietary antigens limit mucosal immunity by inducing regulatory T cells in the small intestine. Science. 2016;351(6275):858-63. doi: 10.1126/science.aac5560
122. Milling S, Yrlid U, Cerovic V, MacPherson G. Subsets of migrating intestinal dendritic cells. Immunological reviews. 2010;234(1):259-67. doi: 10.1111/j.0105-2896.2009.00866.x
123. Rescigno M, Urbano M, Valzasina B, Francolini M, Rotta G, Bonasio R, et al. Dendritic cells express tight junction proteins and penetrate gut epithelial monolayers to sample bacteria. Nat Immunol. 2001;2(4):361-7. doi: 10.1038/86373
124. Tanoue T, Atarashi K, Honda K. Development and maintenance of intestinal regulatory T cells. Nat Rev Immunol. 2016;16(5):295-309. doi: 10.1038/nri.2016.36
125. Mucida D, Park Y, Kim G, Turovskaya O, Scott I, Kronenberg M, et al. Reciprocal TH17 and regulatory T cell differentiation mediated by retinoic acid. Science. 2007;317(5835):256-60. doi: 10.1126/science.1145697
126. Thornton AM, Shevach EM. CD4+CD25+ immunoregulatory T cells suppress polyclonal T cell activation in vitro by inhibiting interleukin 2 production. J Exp Med. 1998;188(2):287-96.
127. Deaglio S, Dwyer KM, Gao W, Friedman D, Usheva A, Erat A, et al. Adenosine generation catalyzed by CD39 and CD73 expressed on regulatory T cells mediates immune suppression. J Exp Med. 2007;204(6):1257-65. doi: 10.1084/jem.20062512
128. Bettini M, Vignali DA. Regulatory T cells and inhibitory cytokines in autoimmunity. Current opinion in immunology. 2009;21(6):612-8. doi: 10.1016/j.coi.2009.09.011
129. Li MO, Wan YY, Sanjabi S, Robertson AK, Flavell RA. Transforming growth factor-beta regulation of immune responses. Annu Rev Immunol. 2006;24:99-146. doi: 10.1146/annurev.immunol.24.021605.090737
130. Marie JC, Liggitt D, Rudensky AY. Cellular mechanisms of fatal early-onset autoimmunity in mice with the T cell-specific targeting of transforming growth factor-beta receptor. Immunity. 2006;25(3):441-54. doi: 10.1016/j.immuni.2006.07.012
131. Nakamura K, Kitani A, Strober W. Cell contact-dependent immunosuppression by CD4(+)CD25(+) regulatory T cells is mediated by cell surface-bound transforming growth factor beta. J Exp Med. 2001;194(5):629-44.
132. Andersson J, Tran DQ, Pesu M, Davidson TS, Ramsey H, O'Shea JJ, et al. CD4+ FoxP3+ regulatory T cells confer infectious tolerance in a TGF-beta-dependent manner. J Exp Med. 2008;205(9):1975-81. doi: 10.1084/jem.20080308
133. Asseman C, Mauze S, Leach MW, Coffman RL, Powrie F. An essential role for interleukin 10 in the function of regulatory T cells that inhibit intestinal inflammation. J Exp Med. 1999;190(7):995-1004.
134. Franke A, Balschun T, Karlsen TH, Sventoraityte J, Nikolaus S, Mayr G, et al. Sequence variants in IL10, ARPC2 and multiple other loci contribute to ulcerative colitis susceptibility. Nature genetics. 2008;40(11):1319-23. doi: 10.1038/ng.221

135. Collison LW, Workman CJ, Kuo TT, Boyd K, Wang Y, Vignali KM, et al. The inhibitory cytokine IL-35 contributes to regulatory T-cell function. Nature. 2007;450(7169):566-9. doi: 10.1038/nature06306
136. Wei X, Zhang J, Gu Q, Huang M, Zhang W, Guo J, et al. Reciprocal Expression of IL-35 and IL-10 Defines Two Distinct Effector Treg Subsets that Are Required for Maintenance of Immune Tolerance. Cell reports. 2017;21(7):1853-69. doi: 10.1016/j.celrep.2017.10.090
137. Gondek DC, Lu LF, Quezada SA, Sakaguchi S, Noelle RJ. Cutting edge: contact-mediated suppression by CD4+CD25+ regulatory cells involves a granzyme B-dependent, perforin-independent mechanism. J Immunol. 2005;174(4):1783-6.
138. Grossman WJ, Verbsky JW, Barchet W, Colonna M, Atkinson JP, Ley TJ. Human T regulatory cells can use the perforin pathway to cause autologous target cell death. Immunity. 2004;21(4):589-601. doi: 10.1016/j.immuni.2004.09.002
139. Cao X, Cai SF, Fehniger TA, Song J, Collins LI, Piwnica-Worms DR, et al. Granzyme B and perforin are important for regulatory T cell-mediated suppression of tumor clearance. Immunity. 2007;27(4):635-46. doi: 10.1016/j.immuni.2007.08.014
140. Janssens W, Carlier V, Wu B, VanderElst L, Jacquemin MG, Saint-Remy JM. CD4+CD25+ T cells lyse antigen-presenting B cells by Fas-Fas ligand interaction in an epitope-specific manner. J Immunol. 2003;171(9):4604-12.
141. Huang CT, Workman CJ, Flies D, Pan X, Marson AL, Zhou G, et al. Role of LAG-3 in regulatory T cells. Immunity. 2004;21(4):503-13. doi: 10.1016/j.immuni.2004.08.010
142. Burnet M. Cancer; a biological approach. I. The processes of control. British medical journal. 1957;1(5022):779-86.
143. Foley EJ. Antigenic properties of methylcholanthrene-induced tumors in mice of the strain of origin. Cancer Res. 1953;13(12):835-7.
144. Shankaran V, Ikeda H, Bruce AT, White JM, Swanson PE, Old LJ, et al. IFNgamma and lymphocytes prevent primary tumour development and shape tumour immunogenicity. Nature. 2001;410(6832):1107-11. doi: 10.1038/35074122
145. Boshoff C, Weiss R. AIDS-related malignancies. Nature reviews Cancer. 2002;2(5):373-82. doi: 10.1038/nrc797
146. Dunn GP, Bruce AT, Ikeda H, Old LJ, Schreiber RD. Cancer immunoediting: from immunosurveillance to tumor escape. Nat Immunol. 2002;3(11):991-8. doi: 10.1038/ni1102-991
147. Dighe AS, Richards E, Old LJ, Schreiber RD. Enhanced in vivo growth and resistance to rejection of tumor cells expressing dominant negative IFN gamma receptors. Immunity. 1994;1(6):447-56.
148. Kaplan DH, Shankaran V, Dighe AS, Stockert E, Aguet M, Old LJ, et al. Demonstration of an interferon gamma-dependent tumor surveillance system in immunocompetent mice. Proc Natl Acad Sci U S A. 1998;95(13):7556-61.
149. Cui Z, Willingham MC, Hicks AM, Alexander-Miller MA, Howard TD, Hawkins GA, et al. Spontaneous regression of advanced cancer: identification of a unique genetically determined, age-dependent trait in mice. Proc Natl Acad Sci U S A. 2003;100(11):6682-7. doi: 10.1073/pnas.1031601100
150. Takeda K, Hayakawa Y, Smyth MJ, Kayagaki N, Yamaguchi N, Kakuta S, et al. Involvement of tumor necrosis factor-related apoptosis-inducing ligand in surveillance of tumor metastasis by liver natural killer cells. Nat Med. 2001;7(1):94-100. doi: 10.1038/83416
151. Koebel CM, Vermi W, Swann JB, Zerafa N, Rodig SJ, Old LJ, et al. Adaptive immunity maintains occult cancer in an equilibrium state. Nature. 2007;450(7171):903-7. doi: 10.1038/nature06309
152. Wu X, Peng M, Huang B, Zhang H, Wang H, Huang B, et al. Immune microenvironment profiles of tumor immune equilibrium and immune escape states of mouse sarcoma. Cancer letters. 2013;340(1):124-33. doi: 10.1016/j.canlet.2013.07.038
153. UK CR. Cancer statistics Report: Bowel Cancer Incedence in the UK in 2014. 2014 [accessed. Available from:
154. Malvezzi M, Carioli G, Bertuccio P, Boffetta P, Levi F, La Vecchia C, et al. European cancer mortality predictions for the year 2018 with focus on colorectal cancer. Annals of oncology : official journal of the European Society for Medical Oncology. 2018;29(4):1016-22. doi: 10.1093/annonc/mdy033

155. Kolonel LN WL. Migrant Studies. In D Schottenfeld, JF Fraumeni (eds) Cancer Epidemiology and Prevention. 3rd Edition ed. New York: Oxford University Press; 2006.
156. Brenner H, Kloor M, Pox CP. Colorectal cancer. Lancet (London, England). 2014;383(9927):1490-502. doi: 10.1016/s0140-6736(13)61649-9
157. Lynch HT, Snyder CL, Shaw TG, Heinen CD, Hitchins MP. Milestones of Lynch syndrome: 1895-2015. Nature reviews Cancer. 2015;15(3):181-94. doi: 10.1038/nrc3878
158. Boland CR, Troncale FJ. Familial colonic cancer without antecedent polyposis. Annals of internal medicine. 1984;100(5):700-1.
159. Pai RK, Dudley B, Karloski E, Brand RE, O'Callaghan N, Rosty C, et al. DNA mismatch repair protein deficient non-neoplastic colonic crypts: a novel indicator of Lynch syndrome. Modern pathology : an official journal of the United States and Canadian Academy of Pathology, Inc. 2018 doi: 10.1038/s41379-018-0079-6
160. Galiatsatos P, Foulkes WD. Familial adenomatous polyposis. The American journal of gastroenterology. 2006;101(2):385-98. doi: 10.1111/j.1572-0241.2006.00375.x
161. Groden J, Thliveris A, Samowitz W, Carlson M, Gelbert L, Albertsen H, et al. Identification and characterization of the familial adenomatous polyposis coli gene. Cell. 1991;66(3):589-600.
162. Leoz ML, Carballal S, Moreira L, Ocana T, Balaguer F. The genetic basis of familial adenomatous polyposis and its implications for clinical practice and risk management. The application of clinical genetics. 2015;8:95-107. doi: 10.2147/tacg.s51484
163. Samadder NJ, Kuwada SK, Boucher KM, Byrne K, Kanth P, Samowitz W, et al. Association of Sulindac and Erlotinib vs Placebo With Colorectal Neoplasia in Familial Adenomatous Polyposis: Secondary Analysis of a Randomized Clinical Trial. JAMA oncology. 2018;4(5):671-7. doi: 10.1001/jamaoncol.2017.5431
164. Lynch PM. Chemoprevention of familial adenomatous polyposis. Familial cancer. 2016;15(3):467-75. doi: 10.1007/s10689-016-9901-9
165. Komiya Y, Habas R. Wnt signal transduction pathways. Organogenesis. 2008;4(2):68-75.
166. Bokemeyer C, Van Cutsem E, Rougier P, Ciardiello F, Heeger S, Schlichting M, et al. Addition of cetuximab to chemotherapy as first-line treatment for KRAS wild-type metastatic colorectal cancer: pooled analysis of the CRYSTAL and OPUS randomised clinical trials. European journal of cancer (Oxford, England : 1990). 2012;48(10):1466-75. doi: 10.1016/j.ejca.2012.02.057
167. Dhillon AS, Hagan S, Rath O, Kolch W. MAP kinase signalling pathways in cancer. Oncogene. 2007;26(22):3279-90. doi: 10.1038/sj.onc.1210421
168. Comprehensive molecular characterization of human colon and rectal cancer. Nature. 2012;487(7407):330-7. doi: 10.1038/nature11252
169. Strickler JH, Wu C, Bekaii-Saab T. Targeting BRAF in metastatic colorectal cancer: Maximizing molecular approaches. Cancer treatment reviews. 2017;60:109-19. doi: 10.1016/j.ctrv.2017.08.006
170. Vousden KH, Lane DP. p53 in health and disease. Nature reviews Molecular cell biology. 2007;8(4):275-83. doi: 10.1038/nrm2147
171. Li XL, Zhou J, Chen ZR, Chng WJ. P53 mutations in colorectal cancer-Molecular pathogenesis and pharmacological reactivation. World journal of gastroenterology. 2015;21(1):84-93. doi: 10.3748/wjg.v21.i1.84
172. Akkoca AN, Yanik S, Ozdemir ZT, Cihan FG, Sayar S, Cincin TG, et al. TNM and Modified Dukes staging along with the demographic characteristics of patients with colorectal carcinoma. International journal of clinical and experimental medicine. 2014;7(9):2828-35.
173. Guinney J, Dienstmann R, Wang X, de Reynies A, Schlicker A, Soneson C, et al. The consensus molecular subtypes of colorectal cancer. Nat Med. 2015;21(11):1350-6. doi: 10.1038/nm.3967
174. Dienstmann R, Vermeulen L, Guinney J, Kopetz S, Tejpar S, Tabernero J. Consensus molecular subtypes and the evolution of precision medicine in colorectal cancer. Nature reviews Cancer. 2017;17(2):79-92. doi: 10.1038/nrc.2016.126
175. Fearon ER, Vogelstein B. A genetic model for colorectal tumorigenesis. Cell. 1990;61(5):759-67.

176. Kanwar SS, Poolla A, Majumdar AP. Regulation of colon cancer recurrence and development of therapeutic strategies. World journal of gastrointestinal pathophysiology. 2012;3(1):1-9. doi: 10.4291/wjgp.v3.i1.1
177. Schechter AL, Stern DF, Vaidyanathan L, Decker SJ, Drebin JA, Greene MI, et al. The neu oncogene: an erb-B-related gene encoding a 185,000-Mr tumour antigen. Nature. 1984;312(5994):513-6.
178. Baselga J, Albanell J. Mechanism of action of anti-HER2 monoclonal antibodies. Annals of oncology : official journal of the European Society for Medical Oncology. 2001;12 Suppl 1:S35-41.
179. Baselga J, Cortes J, Kim SB, Im SA, Hegg R, Im YH, et al. Pertuzumab plus trastuzumab plus docetaxel for metastatic breast cancer. N Engl J Med. 2012;366(2):109-19. doi: 10.1056/NEJMoa1113216
180. von Minckwitz G, Procter M, de Azambuja E, Zardavas D, Benyunes M, Viale G, et al. Adjuvant Pertuzumab and Trastuzumab in Early HER2-Positive Breast Cancer. N Engl J Med. 2017;377(2):122-31. doi: 10.1056/NEJMoa1703643
181. Rizvi NA, Hellmann MD, Snyder A, Kvistborg P, Makarov V, Havel JJ, et al. Cancer immunology. Mutational landscape determines sensitivity to PD-1 blockade in non-small cell lung cancer. Science. 2015;348(6230):124-8. doi: 10.1126/science.aaa1348
182. Gjerstorff MF, Andersen MH, Ditzel HJ. Oncogenic cancer/testis antigens: prime candidates for immunotherapy. Oncotarget. 2015;6(18):15772-87. doi: 10.18632/oncotarget.4694
183. Gold P, Freedman SO. Specific carcinoembryonic antigens of the human digestive system. J Exp Med. 1965;122(3):467-81.
184. Ahnen DJ, Nakane PK, Brown WR. Ultrastructural localization of carcinoembryonic antigen in normal intestine and colon cancer: abnormal distribution of CEA on the surfaces of colon cancer cells. Cancer. 1982;49(10):2077-90.
185. Duffy MJ. Carcinoembryonic antigen as a marker for colorectal cancer: is it clinically useful? Clinical chemistry. 2001;47(4):624-30.
186. Korotkova N, Cota E, Lebedin Y, Monpouet S, Guignot J, Servin AL, et al. A subfamily of Dr adhesins of Escherichia coli bind independently to decay-accelerating factor and the N-domain of carcinoembryonic antigen. J Biol Chem. 2006;281(39):29120-30. doi: 10.1074/jbc.M605681200
187. Hostetter RB, Augustus LB, Mankarious R, Chi KF, Fan D, Toth C, et al. Carcinoembryonic antigen as a selective enhancer of colorectal cancer metastasis. Journal of the National Cancer Institute. 1990;82(5):380-5.
188. Wanebo HJ, Rao B, Pinsky CM, Hoffman RG, Stearns M, Schwartz MK, et al. Preoperative carcinoembryonic antigen level as a prognostic indicator in colorectal cancer. N Engl J Med. 1978;299(9):448-51. doi: 10.1056/nejm197808312990904
189. Hasegawa T, Isobe K, Tsuchiya Y, Oikawa S, Nakazato H, Ikezawa H, et al. Establishment and characterisation of human carcinoembryonic antigen transgenic mice. Br J Cancer. 1991;64(4):710-4.
190. Eades-Perner AM, van der Putten H, Hirth A, Thompson J, Neumaier M, von Kleist S, et al. Mice transgenic for the human carcinoembryonic antigen gene maintain its spatiotemporal expression pattern. Cancer Res. 1994;54(15):4169-76.
191. Bos R, van Duikeren S, Morreau H, Franken K, Schumacher TN, Haanen JB, et al. Balancing between antitumor efficacy and autoimmune pathology in T-cell-mediated targeting of carcinoembryonic antigen. Cancer Res. 2008;68(20):8446-55. doi: 10.1158/0008-5472.can-08-1864
192. Parkhurst MR, Yang JC, Langan RC, Dudley ME, Nathan DA, Feldman SA, et al. T cells targeting carcinoembryonic antigen can mediate regression of metastatic colorectal cancer but induce severe transient colitis. Mol Ther. 2011;19(3):620-6. doi: 10.1038/mt.2010.272
193. Nagorsen D, Keilholz U, Rivoltini L, Schmittel A, Letsch A, Asemissen AM, et al. Natural T-cell response against MHC class I epitopes of epithelial cell adhesion molecule, her-2/neu, and carcinoembryonic antigen in patients with colorectal cancer. Cancer Res. 2000;60(17):4850-4.
194. Scurr MJ, Brown CM, Costa Bento DF, Betts GJ, Rees BI, Hills RK, et al. Assessing the prognostic value of preoperative carcinoembryonic antigen-specific T-cell

responses in colorectal cancer. Journal of the National Cancer Institute. 2015;107(4) doi: 10.1093/jnci/djv001
195. Hole N, Stern PL. A 72 kD trophoblast glycoprotein defined by a monoclonal antibody. Br J Cancer. 1988;57(3):239-46.
196. Awan A, Lucic MR, Shaw DM, Sheppard F, Westwater C, Lyons SA, et al. 5T4 interacts with TIP-2/GIPC, a PDZ protein, with implications for metastasis. Biochemical and biophysical research communications. 2002;290(3):1030-6. doi: 10.1006/bbrc.2001.6288
197. McGinn OJ, Marinov G, Sawan S, Stern PL. CXCL12 receptor preference, signal transduction, biological response and the expression of 5T4 oncofoetal glycoprotein. Journal of cell science. 2012;125(Pt 22):5467-78. doi: 10.1242/jcs.109488
198. Castro FV, Al-Muftah M, Mulryan K, Jiang HR, Drijfhout JW, Ali S, et al. Regulation of autologous immunity to the mouse 5T4 oncofoetal antigen: implications for immunotherapy. Cancer immunology, immunotherapy : CII. 2012;61(7):1005-18. doi: 10.1007/s00262-011-1167-3
199. Mulryan K, Ryan MG, Myers KA, Shaw D, Wang W, Kingsman SM, et al. Attenuated recombinant vaccinia virus expressing oncofetal antigen (tumor-associated antigen) 5T4 induces active therapy of established tumors. Molecular cancer therapeutics. 2002;1(12):1129-37.
200. Amato RJ, Hawkins RE, Kaufman HL, Thompson JA, Tomczak P, Szczylik C, et al. Vaccination of metastatic renal cancer patients with MVA-5T4: a randomized, double-blind, placebo-controlled phase III study. Clin Cancer Res. 2010;16(22):5539-47. doi: 10.1158/1078-0432.ccr-10-2082
201. Scurr M, Pembroke T, Bloom A, Roberts D, Thomson A, Smart K, et al. Effect of Modified Vaccinia Ankara-5T4 and Low-Dose Cyclophosphamide on Antitumor Immunity in Metastatic Colorectal Cancer: A Randomized Clinical Trial. JAMA oncology. 2017;3(10):e172579. doi: 10.1001/jamaoncol.2017.2579
202. Scurr M, Pembroke T, Bloom A, Roberts D, Thomson A, Smart K, et al. Low-Dose Cyclophosphamide Induces Antitumor T-Cell Responses, which Associate with Survival in Metastatic Colorectal Cancer. Clin Cancer Res. 2017;23(22):6771-80. doi: 10.1158/1078-0432.ccr-17-0895
203. Hanahan D, Weinberg RA. Hallmarks of cancer: the next generation. Cell. 2011;144(5):646-74. doi: 10.1016/j.cell.2011.02.013
204. Mao Y, Qu Q, Chen X, Huang O, Wu J, Shen K. The Prognostic Value of Tumor-Infiltrating Lymphocytes in Breast Cancer: A Systematic Review and Meta-Analysis. PloS one. 2016;11(4):e0152500. doi: 10.1371/journal.pone.0152500
205. Hwang WT, Adams SF, Tahirovic E, Hagemann IS, Coukos G. Prognostic significance of tumor-infiltrating T cells in ovarian cancer: a meta-analysis. Gynecologic oncology. 2012;124(2):192-8. doi: 10.1016/j.ygyno.2011.09.039
206. Mei Z, Liu Y, Liu C, Cui A, Liang Z, Wang G, et al. Tumour-infiltrating inflammation and prognosis in colorectal cancer: systematic review and meta-analysis. Br J Cancer. 2014;110(6):1595-605. doi: 10.1038/bjc.2014.46
207. Pages F, Berger A, Camus M, Sanchez-Cabo F, Costes A, Molidor R, et al. Effector memory T cells, early metastasis, and survival in colorectal cancer. N Engl J Med. 2005;353(25):2654-66. doi: 10.1056/NEJMoa051424
208. Galon J, Costes A, Sanchez-Cabo F, Kirilovsky A, Mlecnik B, Lagorce-Pages C, et al. Type, density, and location of immune cells within human colorectal tumors predict clinical outcome. Science. United States; 2006. p. 1960-4.
209. Tosolini M, Kirilovsky A, Mlecnik B, Fredriksen T, Mauger S, Bindea G, et al. Clinical impact of different classes of infiltrating T cytotoxic and helper cells (Th1, th2, treg, th17) in patients with colorectal cancer. Cancer Res. 2011;71(4):1263-71. doi: 10.1158/0008-5472.can-10-2907
210. Wang J, Xu K, Wu J, Luo C, Li Y, Wu X, et al. The changes of Th17 cells and the related cytokines in the progression of human colorectal cancers. BMC cancer. 2012;12:418. doi: 10.1186/1471-2407-12-418
211. Chae WJ, Gibson TF, Zelterman D, Hao L, Henegariu O, Bothwell AL. Ablation of IL-17A abrogates progression of spontaneous intestinal tumorigenesis. Proc Natl Acad Sci U S A. 2010;107(12):5540-4. doi: 10.1073/pnas.0912675107

212. Hyun YS, Han DS, Lee AR, Eun CS, Youn J, Kim HY. Role of IL-17A in the development of colitis-associated cancer. Carcinogenesis. 2012;33(4):931-6. doi: 10.1093/carcin/bgs106
213. Grivennikov SI, Wang K, Mucida D, Stewart CA, Schnabl B, Jauch D, et al. Adenoma-linked barrier defects and microbial products drive IL-23/IL-17-mediated tumour growth. Nature. 2012;491(7423):254-8. doi: 10.1038/nature11465
214. Ling KL, Pratap SE, Bates GJ, Singh B, Mortensen NJ, George BD, et al. Increased frequency of regulatory T cells in peripheral blood and tumour infiltrating lymphocytes in colorectal cancer patients. Cancer immunity. 2007;7:7.
215. Betts G, Jones E, Junaid S, El-Shanawany T, Scurr M, Mizen P, et al. Suppression of tumour-specific CD4(+) T cells by regulatory T cells is associated with progression of human colorectal cancer. Gut. 2012;61(8):1163-71. doi: 10.1136/gutjnl-2011-300970
216. Scurr M, Bloom A, Pembroke T, Srinivasan R, Brown C, Smart K, et al. Escalating regulation of 5T4-specific IFN-gamma(+) CD4(+) T cells distinguishes colorectal cancer patients from healthy controls and provides a target for in vivo therapy. Cancer immunology research. 2013;1(6) doi: 10.1158/2326-6066.cir-13-0035
217. Salama P, Phillips M, Grieu F, Morris M, Zeps N, Joseph D, et al. Tumor-infiltrating FOXP3+ T regulatory cells show strong prognostic significance in colorectal cancer. J Clin Oncol. 2009;27(2):186-92. doi: 10.1200/jco.2008.18.7229
218. Frey DM, Droeser RA, Viehl CT, Zlobec I, Lugli A, Zingg U, et al. High frequency of tumor-infiltrating FOXP3(+) regulatory T cells predicts improved survival in mismatch repair-proficient colorectal cancer patients. Int J Cancer. 2010;126(11):2635-43. doi: 10.1002/ijc.24989
219. Ladoire S, Martin F, Ghiringhelli F. Prognostic role of FOXP3+ regulatory T cells infiltrating human carcinomas: the paradox of colorectal cancer. Cancer immunology, immunotherapy : CII. 2011;60(7):909-18. doi: 10.1007/s00262-011-1046-y
220. Erdman SE, Poutahidis T, Tomczak M, Rogers AB, Cormier K, Plank B, et al. CD4+ CD25+ regulatory T lymphocytes inhibit microbially induced colon cancer in Rag2-deficient mice. Am J Pathol. 2003;162(2):691-702. doi: 10.1016/s0002-9440(10)63863-1
221. Saito T, Nishikawa H, Wada H, Nagano Y, Sugiyama D, Atarashi K, et al. Two FOXP3(+)CD4(+) T cell subpopulations distinctly control the prognosis of colorectal cancers. Nat Med. 2016;22(6):679-84. doi: 10.1038/nm.4086
222. Shang F-M, Liu H-L. Fusobacterium nucleatum and colorectal cancer: A review. World Journal of Gastrointestinal Oncology. 2018;10(3):71-81. doi: 10.4251/wjgo.v10.i3.71
223. Lahl K, Loddenkemper C, Drouin C, Freyer J, Arnason J, Eberl G, et al. Selective depletion of Foxp3+ regulatory T cells induces a scurfy-like disease. J Exp Med. 2007;204(1):57-63. doi: 10.1084/jem.20061852
224. Nizri E, Greenman-Maaravi N, Bar-David S, Ben-Yehuda A, Weiner G, Lahat G, et al. Analysis of histological and immunological parameters of metastatic lymph nodes from colon cancer patients reveals that T-helper 1 type immune response is associated with improved overall survival. Medicine. 2016;95(45):e5340. doi: 10.1097/md.0000000000005340
225. Davidson BR, Sams VR, Styles J, Dean C, Boulos PB. Comparative study of carcinoembryonic antigen and epithelial membrane antigen expression in normal colon, adenomas and adenocarcinomas of the colon and rectum. Gut. 1989;30(9):1260-5.
226. Wang J, Ma Y, Zhu ZH, Situ DR, Hu Y, Rong TH. Expression and prognostic relevance of tumor carcinoembryonic antigen in stage IB non-small cell lung cancer. Journal of thoracic disease. 2012;4(5):490-6. doi: 10.3978/j.issn.2072-1439.2012.09.01
227. Shao Y, Sun X, He Y, Liu C, Liu H. Elevated Levels of Serum Tumor Markers CEA and CA15-3 Are Prognostic Parameters for Different Molecular Subtypes of Breast Cancer. PloS one. 2015;10(7):e0133830. doi: 10.1371/journal.pone.0133830
228. Harrington LE, Hatton RD, Mangan PR, Turner H, Murphy TL, Murphy KM, et al. Interleukin 17-producing CD4+ effector T cells develop via a lineage distinct from the T helper type 1 and 2 lineages. Nat Immunol. 2005;6(11):1123-32. doi: 10.1038/ni1254
229. Atarashi K, Tanoue T, Ando M, Kamada N, Nagano Y, Narushima S, et al. Th17 Cell Induction by Adhesion of Microbes to Intestinal Epithelial Cells. Cell. 2015;163(2):367-80. doi: 10.1016/j.cell.2015.08.058

230. Li X, Wang Y, Han C, Li P, Zhang H. Colorectal cancer progression is associated with accumulation of Th17 lymphocytes in tumor tissues and increased serum levels of interleukin-6. The Tohoku journal of experimental medicine. 2014;233(3):175-82.
231. Tseng JY, Yang CY, Liang SC, Liu RS, Yang SH, Lin JK, et al. Interleukin-17A modulates circulating tumor cells in tumor draining vein of colorectal cancers and affects metastases. Clin Cancer Res. 2014;20(11):2885-97. doi: 10.1158/1078-0432.ccr-13-2162
232. Munkholm P. Review article: the incidence and prevalence of colorectal cancer in inflammatory bowel disease. Alimentary pharmacology & therapeutics. 2003;18 Suppl 2:1-5.
233. Rutter M, Saunders B, Wilkinson K, Rumbles S, Schofield G, Kamm M, et al. Severity of inflammation is a risk factor for colorectal neoplasia in ulcerative colitis. Gastroenterology. 2004;126(2):451-9.
234. Grivennikov SI, Karin M. Inflammatory cytokines in cancer: tumour necrosis factor and interleukin 6 take the stage. Annals of the rheumatic diseases. 2011;70 Suppl 1:i104-8. doi: 10.1136/ard.2010.140145
235. Yu H, Lee H, Herrmann A, Buettner R, Jove R. Revisiting STAT3 signalling in cancer: new and unexpected biological functions. Nature reviews Cancer. 2014;14(11):736-46. doi: 10.1038/nrc3818
236. Wang L, Yi T, Kortylewski M, Pardoll DM, Zeng D, Yu H. IL-17 can promote tumor growth through an IL-6-Stat3 signaling pathway. J Exp Med. 2009;206(7):1457-64. doi: 10.1084/jem.20090207
237. Deng J, Liu Y, Lee H, Herrmann A, Zhang W, Zhang C, et al. S1PR1-STAT3 signaling is crucial for myeloid cell colonization at future metastatic sites. Cancer Cell. 2012;21(5):642-54. doi: 10.1016/j.ccr.2012.03.039
238. Yu H, Liu Y, McFarland BC, Deshane JS, Hurst DR, Ponnazhagan S, et al. SOCS3 Deficiency in Myeloid Cells Promotes Tumor Development: Involvement of STAT3 Activation and Myeloid-Derived Suppressor Cells. Cancer immunology research. 2015;3(7):727-40. doi: 10.1158/2326-6066.cir-15-0004
239. Liu J, Duan Y, Cheng X, Chen X, Xie W, Long H, et al. IL-17 is associated with poor prognosis and promotes angiogenesis via stimulating VEGF production of cancer cells in colorectal carcinoma. Biochemical and biophysical research communications. 2011;407(2):348-54. doi: 10.1016/j.bbrc.2011.03.021
240. Hance KW, Zeytin HE, Greiner JW. Mouse models expressing human carcinoembryonic antigen (CEA) as a transgene: evaluation of CEA-based cancer vaccines. Mutation research. 2005;576(1-2):132-54. doi: 10.1016/j.mrfmmm.2004.10.014
241. Bos R, van Duikeren S, van Hall T, Kaaijk P, Taubert R, Kyewski B, et al. Expression of a natural tumor antigen by thymic epithelial cells impairs the tumor-protective CD4+ T-cell repertoire. Cancer Res. 2005;65(14):6443-9. doi: 10.1158/0008-5472.can-05-0666
242. Tampellini M, Ottone A, Alabiso I, Baratelli C, Forti L, Berruti A, et al. The prognostic role of baseline CEA and CA 19-9 values and their time-dependent variations in advanced colorectal cancer patients submitted to first-line therapy. Tumour biology : the journal of the International Society for Oncodevelopmental Biology and Medicine. 2015;36(3):1519-27. doi: 10.1007/s13277-014-2693-3
243. Liu KJ, Wang CC, Chen LT, Cheng AL, Lin DT, Wu YC, et al. Generation of carcinoembryonic antigen (CEA)-specific T-cell responses in HLA-A*0201 and HLA-A*2402 late-stage colorectal cancer patients after vaccination with dendritic cells loaded with CEA peptides. Clin Cancer Res. 2004;10(8):2645-51.
244. Blankenstein T, Coulie PG, Gilboa E, Jaffee EM. The determinants of tumour immunogenicity. Nature reviews Cancer. 2012;12(4):307-13. doi: 10.1038/nrc3246
245. Linnekamp JF, Hooff SRV, Prasetyanti PR, Kandimalla R, Buikhuisen JY, Fessler E, et al. Consensus molecular subtypes of colorectal cancer are recapitulated in in vitro and in vivo models. Cell death and differentiation. 2018 doi: 10.1038/s41418-017-0011-5
246. Spranger S, Luke JJ, Bao R, Zha Y, Hernandez KM, Li Y, et al. Density of immunogenic antigens does not explain the presence or absence of the T-cell-inflamed

tumor microenvironment in melanoma. Proc Natl Acad Sci U S A. 2016;113(48):E7759-e68. doi: 10.1073/pnas.1609376113
247. Hibberd AA, Lyra A, Ouwehand AC, Rolny P, Lindegren H, Cedgard L, et al. Intestinal microbiota is altered in patients with colon cancer and modified by probiotic intervention. BMJ open gastroenterology. 2017;4(1):e000145. doi: 10.1136/bmjgast-2017-000145
248. Ott SJ, Musfeldt M, Wenderoth DF, Hampe J, Brant O, Folsch UR, et al. Reduction in diversity of the colonic mucosa associated bacterial microflora in patients with active inflammatory bowel disease. Gut. 2004;53(5):685-93.
249. Manichanh C, Rigottier-Gois L, Bonnaud E, Gloux K, Pelletier E, Frangeul L, et al. Reduced diversity of faecal microbiota in Crohn's disease revealed by a metagenomic approach. Gut. 2006;55(2):205-11. doi: 10.1136/gut.2005.073817
250. Daillere R, Vetizou M, Waldschmitt N, Yamazaki T, Isnard C, Poirier-Colame V, et al. Enterococcus hirae and Barnesiella intestinihominis Facilitate Cyclophosphamide-Induced Therapeutic Immunomodulatory Effects. Immunity. 2016;45(4):931-43. doi: 10.1016/j.immuni.2016.09.009
251. Burn J, Sheth H. The role of aspirin in preventing colorectal cancer. British medical bulletin. 2016;119(1):17-24. doi: 10.1093/bmb/ldw028
252. Cornick S, Tawiah A, Chadee K. Roles and regulation of the mucus barrier in the gut. Tissue barriers. 2015;3(1-2):e982426. doi: 10.4161/21688370.2014.982426
253. Gallimore AM, Godkin A. Epithelial barriers, microbiota, and colorectal cancer. N Engl J Med. 2013;368(3):282-4. doi: 10.1056/NEJMcibr1212341
254. Ahmad R, Kumar B, Chen Z, Chen X, Muller D, Lele SM, et al. Loss of claudin-3 expression induces IL6/gp130/Stat3 signaling to promote colon cancer malignancy by hyperactivating Wnt/beta-catenin signaling. Oncogene. 2017 doi: 10.1038/onc.2017.259
255. Maxwell JR, Zhang Y, Brown WA, Smith CL, Byrne FR, Fiorino M, et al. Differential Roles for Interleukin-23 and Interleukin-17 in Intestinal Immunoregulation. Immunity. 2015;43(4):739-50. doi: 10.1016/j.immuni.2015.08.019
256. Lee JS, Tato CM, Joyce-Shaikh B, Gulen MF, Cayatte C, Chen Y, et al. Interleukin-23-Independent IL-17 Production Regulates Intestinal Epithelial Permeability. Immunity. 2015;43(4):727-38. doi: 10.1016/j.immuni.2015.09.003
257. Ussing HH, Zerahn K. Active transport of sodium as the source of electric current in the short-circuited isolated frog skin. Acta physiologica Scandinavica. 1951;23(2-3):110-27. doi: 10.1111/j.1748-1716.1951.tb00800.x
258. Koefoed-Johnsen V, Ussing HH. The nature of the frog skin potential. Acta physiologica Scandinavica. 1958;42(3-4):298-308. doi: 10.1111/j.1748-1716.1958.tb01563.x
259. Skou JC. Nobel Lecture. The identification of the sodium pump. Bioscience reports. 1998;18(4):155-69.
260. Hobbs CA, Da Tan C, Tarran R. Does epithelial sodium channel hyperactivity contribute to cystic fibrosis lung disease? The Journal of physiology. 2013;591(18):4377-87. doi: 10.1113/jphysiol.2012.240861
261. Itani OA, Chen JH, Karp PH, Ernst S, Keshavjee S, Parekh K, et al. Human cystic fibrosis airway epithelia have reduced Cl- conductance but not increased Na+ conductance. Proc Natl Acad Sci U S A. 2011;108(25):10260-5. doi: 10.1073/pnas.1106695108
262. Sabharwal S. Gastrointestinal Manifestations of Cystic Fibrosis. Gastroenterology & hepatology. 2016;12(1):43-7.
263. Keita AV, Salim SY, Jiang T, Yang PC, Franzen L, Soderkvist P, et al. Increased uptake of non-pathogenic E. coli via the follicle-associated epithelium in longstanding ileal Crohn's disease. The Journal of pathology. 2008;215(2):135-44. doi: 10.1002/path.2337
264. Ma TY, Hollander D, Krugliak P, Katz K. PEG 400, a hydrophilic molecular probe for measuring intestinal permeability. Gastroenterology. 1990;98(1):39-46.
265. Eaton KK, Howard M, Howard JM. Gut permeability measured by polyethylene glycol absorption in abnormal gut fermentation as compared with food intolerance. Journal of the Royal Society of Medicine. 1995;88(2):63-6.
266. Han F, Zhang H, Xia X, Xiong H, Song D, Zong X, et al. Porcine beta-defensin 2 attenuates inflammation and mucosal lesions in dextran sodium sulfate-induced colitis. J Immunol. 2015;194(4):1882-93. doi: 10.4049/jimmunol.1402300

267. Volynets V, Reichold A, Bardos G, Rings A, Bleich A, Bischoff SC. Assessment of the Intestinal Barrier with Five Different Permeability Tests in Healthy C57BL/6J and BALB/cJ Mice. Digestive diseases and sciences. 2016;61(3):737-46. doi: 10.1007/s10620-015-3935-y
268. Shen L, Weber CR, Raleigh DR, Yu D, Turner JR. Tight junction pore and leak pathways: a dynamic duo. Annual review of physiology. 2011;73:283-309. doi: 10.1146/annurev-physiol-012110-142150
269. Wang F, Graham WV, Wang Y, Witkowski ED, Schwarz BT, Turner JR. Interferon-gamma and tumor necrosis factor-alpha synergize to induce intestinal epithelial barrier dysfunction by up-regulating myosin light chain kinase expression. Am J Pathol. 2005;166(2):409-19.
270. Angelow S, Kim KJ, Yu AS. Claudin-8 modulates paracellular permeability to acidic and basic ions in MDCK II cells. The Journal of physiology. 2006;571(Pt 1):15-26. doi: 10.1113/jphysiol.2005.099135
271. Amasheh S, Schmidt T, Mahn M, Florian P, Mankertz J, Tavalali S, et al. Contribution of claudin-5 to barrier properties in tight junctions of epithelial cells. Cell and tissue research. 2005;321(1):89-96.
272. Milatz S, Krug SM, Rosenthal R, Gunzel D, Muller D, Schulzke JD, et al. Claudin-3 acts as a sealing component of the tight junction for ions of either charge and uncharged solutes. Biochimica et biophysica acta. 2010;1798(11):2048-57. doi: 10.1016/j.bbamem.2010.07.014
273. Rosenthal R, Milatz S, Krug SM, Oelrich B, Schulzke JD, Amasheh S, et al. Claudin-2, a component of the tight junction, forms a paracellular water channel. Journal of cell science. 2010;123(Pt 11):1913-21. doi: 10.1242/jcs.060665
274. Amasheh S, Meiri N, Gitter AH, Schoneberg T, Mankertz J, Schulzke JD, et al. Claudin-2 expression induces cation-selective channels in tight junctions of epithelial cells. Journal of cell science. 2002;115(Pt 24):4969-76.
275. Schulzke JD, Gitter AH, Mankertz J, Spiegel S, Seidler U, Amasheh S, et al. Epithelial transport and barrier function in occludin-deficient mice. Biochimica et biophysica acta. 2005;1669(1):34-42. doi: 10.1016/j.bbamem.2005.01.008
276. Furuse M, Fujimoto K, Sato N, Hirase T, Tsukita S, Tsukita S. Overexpression of occludin, a tight junction-associated integral membrane protein, induces the formation of intracellular multilamellar bodies bearing tight junction-like structures. Journal of cell science. 1996;109 (Pt 2):429-35.
277. Landy J, Ronde E, English N, Clark SK, Hart AL, Knight SC, et al. Tight junctions in inflammatory bowel diseases and inflammatory bowel disease associated colorectal cancer. World journal of gastroenterology. 2016;22(11):3117-26. doi: 10.3748/wjg.v22.i11.3117
278. Soderholm JD, Peterson KH, Olaison G, Franzen LE, Westrom B, Magnusson KE, et al. Epithelial permeability to proteins in the noninflamed ileum of Crohn's disease? Gastroenterology. 1999;117(1):65-72.
279. Soderholm JD, Streutker C, Yang PC, Paterson C, Singh PK, McKay DM, et al. Increased epithelial uptake of protein antigens in the ileum of Crohn's disease mediated by tumour necrosis factor alpha. Gut. 2004;53(12):1817-24. doi: 10.1136/gut.2004.041426
280. Nap M, Mollgard K, Burtin P, Fleuren GJ. Immunohistochemistry of carcino-embryonic antigen in the embryo, fetus and adult. Tumour biology : the journal of the International Society for Oncodevelopmental Biology and Medicine. 1988;9(2-3):145-53.
281. Soler AP, Miller RD, Laughlin KV, Carp NZ, Klurfeld DM, Mullin JM. Increased tight junctional permeability is associated with the development of colon cancer. Carcinogenesis. 1999;20(8):1425-31.
282. Grass GM, Sweetana SA. In vitro measurement of gastrointestinal tissue permeability using a new diffusion cell. Pharmaceutical research. 1988;5(6):372-6.
283. Eisenhut M. Changes in ion transport in inflammatory disease. Journal of inflammation (London, England). 2006;3:5. doi: 10.1186/1476-9255-3-5
284. Wallon C, Braaf Y, Wolving M, Olaison G, Soderholm JD. Endoscopic biopsies in Ussing chambers evaluated for studies of macromolecular permeability in the human colon. Scandinavian journal of gastroenterology. 2005;40(5):586-95. doi: 10.1080/00365520510012235

285. Keita AV, Gullberg E, Ericson AC, Salim SY, Wallon C, Kald A, et al. Characterization of antigen and bacterial transport in the follicle-associated epithelium of human ileum. Lab Invest. 2006;86(5):504-16. doi: 10.1038/labinvest.3700397
286. Clarke LL. A guide to Ussing chamber studies of mouse intestine. American journal of physiology Gastrointestinal and liver physiology. 2009;296(6):G1151-66. doi: 10.1152/ajpgi.90649.2008
287. Weiner SA, Caputo C, Bruscia E, Ferreira EC, Price JE, Krause DS, et al. Rectal potential difference and the functional expression of CFTR in the gastrointestinal epithelia in cystic fibrosis mouse models. Pediatric research. 2008;63(1):73-8. doi: 10.1203/PDR.0b013e31815b4bc6
288. Wang F, Bai L, Liu TS, Yu YY, He MM, Liu KY, et al. Right-sided colon cancer and left-sided colorectal cancers respond differently to cetuximab. Chinese journal of cancer. 2015;34(9):384-93. doi: 10.1186/s40880-015-0022-x
289. Langholz E. Current trends in inflammatory bowel disease: the natural history. Therapeutic advances in gastroenterology. 2010;3(2):77-86. doi: 10.1177/1756283x10361304
290. Sjoberg A, Lutz M, Tannergren C, Wingolf C, Borde A, Ungell AL. Comprehensive study on regional human intestinal permeability and prediction of fraction absorbed of drugs using the Ussing chamber technique. European journal of pharmaceutical sciences : official journal of the European Federation for Pharmaceutical Sciences. 2013;48(1-2):166-80. doi: 10.1016/j.ejps.2012.10.007
291. Chassaing B, Aitken JD, Malleshappa M, Vijay-Kumar M. Dextran sulfate sodium (DSS)-induced colitis in mice. Current protocols in immunology. 2014;104:Unit 15.25. doi: 10.1002/0471142735.im1525s104
292. Okayasu I, Hatakeyama S, Yamada M, Ohkusa T, Inagaki Y, Nakaya R. A novel method in the induction of reliable experimental acute and chronic ulcerative colitis in mice. Gastroenterology. 1990;98(3):694-702.
293. Mottet C, Uhlig HH, Powrie F. Cutting edge: cure of colitis by CD4+CD25+ regulatory T cells. J Immunol. 2003;170(8):3939-43.
294. Lin YC, Lin YC, Chen CJ. Cancers Complicating Inflammatory Bowel Disease. N Engl J Med. 2015;373(2):194-5. doi: 10.1056/NEJMc1505689
295. Insel PA, Ostrom RS. Forskolin as a tool for examining adenylyl cyclase expression, regulation, and G protein signaling. Cellular and molecular neurobiology. 2003;23(3):305-14.
296. Laroui H, Ingersoll SA, Liu HC, Baker MT, Ayyadurai S, Charania MA, et al. Dextran sodium sulfate (DSS) induces colitis in mice by forming nano-lipocomplexes with medium-chain-length fatty acids in the colon. PloS one. 2012;7(3):e32084. doi: 10.1371/journal.pone.0032084
297. Dieleman LA, Palmen MJ, Akol H, Bloemena E, Pena AS, Meuwissen SG, et al. Chronic experimental colitis induced by dextran sulphate sodium (DSS) is characterized by Th1 and Th2 cytokines. Clinical and experimental immunology. 1998;114(3):385-91.
298. Barnes MJ, Powrie F. Regulatory T cells reinforce intestinal homeostasis. Immunity. 2009;31(3):401-11. doi: 10.1016/j.immuni.2009.08.011
299. Hadis U, Wahl B, Schulz O, Hardtke-Wolenski M, Schippers A, Wagner N, et al. Intestinal tolerance requires gut homing and expansion of FoxP3+ regulatory T cells in the lamina propria. Immunity. 2011;34(2):237-46. doi: 10.1016/j.immuni.2011.01.016
300. Chistiakov DA, Bobryshev YV, Kozarov E, Sobenin IA, Orekhov AN. Intestinal mucosal tolerance and impact of gut microbiota to mucosal tolerance. Frontiers in microbiology. 2014;5:781. doi: 10.3389/fmicb.2014.00781
301. Izcue A, Coombes JL, Powrie F. Regulatory lymphocytes and intestinal inflammation. Annu Rev Immunol. 2009;27:313-38. doi: 10.1146/annurev.immunol.021908.132657
302. Burn J, Gerdes AM, Macrae F, Mecklin JP, Moeslein G, Olschwang S, et al. Long-term effect of aspirin on cancer risk in carriers of hereditary colorectal cancer: an analysis from the CAPP2 randomised controlled trial. Lancet (London, England). 2011;378(9809):2081-7. doi: 10.1016/s0140-6736(11)61049-0
303. Algra AM, Rothwell PM. Effects of regular aspirin on long-term cancer incidence and metastasis: a systematic comparison of evidence from observational studies versus randomised trials. The Lancet Oncology. 2012;13(5):518-27. doi: 10.1016/s1470-2045(12)70112-2

304. Dejea CM, Fathi P, Craig JM, Boleij A, Taddese R, Geis AL, et al. Patients with familial adenomatous polyposis harbor colonic biofilms containing tumorigenic bacteria. Science. 2018;359(6375):592-7. doi: 10.1126/science.aah3648
305. Chung L, Thiele Orberg E, Geis AL, Chan JL, Fu K, DeStefano Shields CE, et al. Bacteroides fragilis Toxin Coordinates a Pro-carcinogenic Inflammatory Cascade via Targeting of Colonic Epithelial Cells. Cell host & microbe. 2018;23(2):203-14.e5. doi: 10.1016/j.chom.2018.01.007
306. Wu S, Rhee KJ, Zhang M, Franco A, Sears CL. Bacteroides fragilis toxin stimulates intestinal epithelial cell shedding and gamma-secretase-dependent E-cadherin cleavage. Journal of cell science. 2007;120(Pt 11):1944-52. doi: 10.1242/jcs.03455
307. Benedix F, Kube R, Meyer F, Schmidt U, Gastinger I, Lippert H. Comparison of 17,641 patients with right- and left-sided colon cancer: differences in epidemiology, perioperative course, histology, and survival. Diseases of the colon and rectum. 2010;53(1):57-64. doi: 10.1007/DCR.0b013e3181c703a4
308. Suttie SA, Shaikh I, Mullen R, Amin AI, Daniel T, Yalamarthi S. Outcome of right- and left-sided colonic and rectal cancer following surgical resection. Colorectal disease : the official journal of the Association of Coloproctology of Great Britain and Ireland. 2011;13(8):884-9. doi: 10.1111/j.1463-1318.2010.02356.x
309. Derwinger K, Gustavsson B. Variations in demography and prognosis by colon cancer location. Anticancer research. 2011;31(6):2347-50.
310. Weiss JM, Pfau PR, O'Connor ES, King J, LoConte N, Kennedy G, et al. Mortality by stage for right- versus left-sided colon cancer: analysis of surveillance, epidemiology, and end results--Medicare data. J Clin Oncol. 2011;29(33):4401-9. doi: 10.1200/jco.2011.36.4414
311. Warschkow R, Sulz MC, Marti L, Tarantino I, Schmied BM, Cerny T, et al. Better survival in right-sided versus left-sided stage I - III colon cancer patients. BMC cancer. 2016;16:554. doi: 10.1186/s12885-016-2412-0
312. Kim D, Kim SY, Lee JS, Hong YS, Kim JE, Kim KP, et al. Primary tumor location predicts poor clinical outcome with cetuximab in RAS wild-type metastatic colorectal cancer. BMC gastroenterology. 2017;17(1):121. doi: 10.1186/s12876-017-0694-6
313. Cancer-Research-UK. Bowel Cancer (C18-C20): 2010-2012. Distribution of Cases Diagnosed By Anatomical Site, UK. Cancer Reearch UK; 2015 [accessed. Available from: https://www.cancerresearchuk.org/sites/default/files/cstream-node/inc_anatomicalsite_bowel.pdf
314. Feng Q, Liang S, Jia H, Stadlmayr A, Tang L, Lan Z, et al. Gut microbiome development along the colorectal adenoma-carcinoma sequence. Nature communications. 2015;6:6528. doi: 10.1038/ncomms7528
315. Liang Q, Chiu J, Chen Y, Huang Y, Higashimori A, Fang J, et al. Fecal Bacteria Act as Novel Biomarkers for Noninvasive Diagnosis of Colorectal Cancer. Clin Cancer Res. 2017;23(8):2061-70. doi: 10.1158/1078-0432.ccr-16-1599
316. Song M, Garrett WS, Chan AT. Nutrients, foods, and colorectal cancer prevention. Gastroenterology. 2015;148(6):1244-60.e16. doi: 10.1053/j.gastro.2014.12.035
317. Shanahan F, van Sinderen D, O'Toole PW, Stanton C. Feeding the microbiota: transducer of nutrient signals for the host. Gut. 2017;66(9):1709-17. doi: 10.1136/gutjnl-2017-313872
318. Viaud S, Saccheri F, Mignot G, Yamazaki T, Daillere R, Hannani D, et al. The intestinal microbiota modulates the anticancer immune effects of cyclophosphamide. Science. 2013;342(6161):971-6. doi: 10.1126/science.1240537
319. Yi H, Zhang L, Gan Z, Xiong H, Yu C, Du H, et al. High therapeutic efficacy of Cathelicidin-WA against postweaning diarrhea via inhibiting inflammation and enhancing epithelial barrier in the intestine. Scientific reports. 2016;6:25679. doi: 10.1038/srep25679
320. Yi H, Hu W, Chen S, Lu Z, Wang Y. Cathelicidin-WA Improves Intestinal Epithelial Barrier Function and Enhances Host Defense against Enterohemorrhagic Escherichia coli O157:H7 Infection. J Immunol. 2017;198(4):1696-705. doi: 10.4049/jimmunol.1601221

Participant Information Sheet (09/09/2015 version 1.3)

PART 1

1. Study title

The role of leukocytes in the colon and blood

2. Invitation paragraph

We would like to invite you to take part in a research study. Before you decide you need to understand why the research is being done and what it would involve for you. Please take time to read the following information carefully. Talk to others about the study if you wish. Take time to decide whether or not you wish to take part. The person running this study is Professor Andrew Godkin who looks after patients with diseases of the colon in Cardiff and Vale University Health Board and undertakes research with scientific colleagues from Cardiff University.

3. What is the purpose of the study?

The purpose of the study is to study the role of white blood cells (leucocytes) and the way they work in differing diseases of the colon and in people without disease of the colon.

We request samples from four different groups, one of which you fall into:

Group 1 – Samples of blood from healthy people without diseases of the colon

Group 2 – Samples of blood and normal colon from patients undergoing surgery of the colon

Group 3 – Samples of blood, normal colon and tumour from patients undergoing surgery for cancer of the colon

Group 4 – Samples of blood and bowel from patients undergoing gastointestinal endoscopy for clinical reasons

4. Why have I been invited?

You have been invited to take part as a member of Group *[insert group]*……..

5. Do I have to take part?

It is up to you to decide. We will describe the study and go through this information sheet, which we will then give to you. We will then ask you to sign a consent form to show you have agreed to take part. You are free to withdraw at any time, without giving a reason. This will not affect the standard of care you receive.

6. What will happen to me if I take part?

For all Groups – You will be told by the surgeon or physician who is looking after your clinical care about the study and asked if you are interested in taking part. If you are interested and agree to take part in the study, samples will be taken by staff involved in your clinical care and will be passed to the research team at Cardiff University. When the research group get your sample, it will have no details that can identify you with it, only a code number. The master copy with your identification details will stay with the chief investigator in a locked office, and will not be disclosed to the researchers. Where useful to understand the pathology, clinical outcomes may be recorded. We will allocate a code number to each person so that the clinicians can provide this additional information (e.g. on the outcome of your surgery if you are having an operation) at a later date. The data on each subject will be retained for 10 years.

Group 1 - If you agree to participate, we will take a sample of your blood (3-5 teaspoonfuls) and use it to identify white blood cells and to perform studies in the laboratory on how they work.

Group 2 - If you agree to participate, we will take a sample from the normal part of your colon or bowel when it is removed during surgery and look at how the wall of the bowel works. This material would normally be disposed of after surgery. We would also like to take a sample of your blood (3-5 teaspoonfuls), both the bowel and the blood sample will be used to look at how the white cells work.

Group 3 - If you agree to participate, we will take a sample from part of the tumour in your colon and the normal part of colon when it is removed during surgery. This material would normally be disposed of after surgery. We would also take a sample of your blood (3-5 teaspoonfuls), both the normal bowel/tumour and the blood sample will be used to look at how the white cells work.

Group 4 - If you agree to take part, we will take two or three additional biopsies when you undergo your routine clinical endoscopy. We would also like to take a sample of your blood (3-5 teaspoonfuls), both the bowel and the blood sample will be used to look at how the white cells work.

It is possible you may be approached for an additional blood sample after 4-8 weeks; you would be asked for repeat consent.

7. What are the possible disadvantages and risks of taking part?

For Groups 1-3 there are no disadvantages or risks in taking part (other than a small bruise from the blood test)

For Group 4 there is a risk in having additional biopsy samples taken for research. In the course of over 25 years of performing endoscopies, in over 10 000 patients, and taking 1000s of biopsies, the chief investigator is yet to witness a significant problem. Guidelines from the British Society of Gastroenterology in 2006 stated that an endoscopic biopsy is rarely complicated by significant bleeding. In theory, bleeding may occur.

8. What are the possible benefits of taking part?

Taking part in this study will not help you but the information we get from this study will help to improve our understanding of the role of white blood cells in the body, and how they react to different diseases.

Part 2

1. Will my taking part in the study be kept confidential?

Yes. We will follow ethical and legal practice and all information about you will be handled in confidence. The data that is sent outside the clinical team will be anonymised so that the research team will not have access to your information

2. What will happen to my samples?

The samples are transferred to the laboratory where they are prepared for experiments. These include looking at how white blood cells and other cells, and compounds such as proteins function in different tissues.

3. What will happen if I don't want to carry on with the study?

You can decide to withdraw from the study at any point. If you want to withdraw you can contact the research team and make that request. If any samplesare stored they can destroyed at your request. If the results from experiments with your sample have been included in an analysis, it will not be possible to withdraw it retrospectively.

4. What if there is a problem?

If you have any concerns about the conduct of this study, you should ask to speak to the Chief Investigator who will do his best to answer your questions (029 20687129). If you remain unhappy and wish to raise a formal concern then you should contact Cardiff University Research and Innovation Service via the governance officer (029 20879131).

If you have a concern about the clinical care you have received, you can do this through the Cardiff and Vale Concerns Team (029 21847391).

5. Future research

With your consent, we might store the sample/s you have given us for use in future research, we do not yet know what the research might involve but it may include collaborators abroad or working for a commercial company. The stored samples may include serum and cells including the genetic material in the cell i.e. DNA. This will be done in accordance with the Human Tissue Act which lays down requirements for the storage and use of all samples. No identifiable personal information will be stored with the sample. If you wish, you can agree for the sample to be used for the current project but not for future research. If so, you should not sign this part of the consent form.

6. Will any genetic tests be done?

No familial genetic testing will be done on these samples during the current study, but genetic material may be stored for future analysis.

7. What will happen to the results of the research study?

It is intended to submit the results of this study for publication in medical journals and to present the results at national and international meetings. You will not be identified in any report/publication.

8. Who is organising and funding the research?

This study is being funded by charitable trusts and scientific grant giving bodies. The funding will pay for the salaries of some of the participating researchers, for purchasing the reagents

required for carrying out these studies, and for disseminating the new knowledge gained by these studies.

9. Who has reviewed the study?

All research in the NHS is looked at by an independent group of people, called a Research Ethics Committee to protect your safety, rights, wellbeing and dignity. This study has been reviewed and given favourable opinion by the Research Ethics Committee.

Contact details of the Researcher for further information:

Professor Andrew Godkin

Henry Wellcome Building,

Cardiff University

Heath Park,

Cardiff. CF14 4XW.

Tel 029 20687129

Email: godkinaj@cf.ac.uk

CONSENT FORM

The role of leukocytes in the colon and blood

Please initial boxes

Chief Investigator Prof Andrew Godkin (Consultant Gastroenterologist and Hepatologist)

1. I confirm that I have read and understand the information sheet Version 1.3 for the above study and have had the opportunity to ask questions. ☐
2. I understand that my participation is voluntary and that I am free to withdraw at any time, without giving any reason, without my medical care or legal rights being affected. ☐
3. I understand that relevant sections of my medical notes and data collected during the study, may be looked at by responsible individuals from regulatory bodies, Cardiff University or the Cardiff and Vale University Health Board. I give permission to these individuals to have access to my records. All information will remain confidential. ☐
4. I agree for blood and/or clinical waste samples to be collected and used for the purposes of this study (Groups 1-3) ☐
5. I agree for additional biopsies and a blood sample to be collected and used for the purposes of this study (Group 4 only) ☐
6. I consent for my anonymised results of this study to be published in scientific / medical journals. ☐
7. I consent for obtained samples to be stored for future research in the UK and abroad, I understand the research may involve DNA analysis and use by the commercial sector (Please cross out if you do not wish your samples to stored) ☐
8. I agree to take part in the above study ☐

Name of Patient	Signature	Date
Name of Person taking consent	Signature	Date

When completed make two copies: 1 offered to participant; 1 to be kept in medical notes. Original kept and filed by CI.